



UNIVERSITY OF  
**LEICESTER**

**Osteoimmunological investigations of  
bone mineral density in a mouse model:  
*in vivo* and *in vitro* study**

Thesis submitted for the degree of Doctor of Philosophy

By

***Zeayd Fadhil Saeed***

***(BSc, MSc)***

College of Medicine, Biological Sciences and Psychology

Department of Infection, Immunity and Inflammation

University of Leicester

June 2019

# ABSTRACT

---

## *Osteoimmunological investigations of bone mineral density in a mouse model: in vivo and in vitro study*

*Zeayd Fadhil Saeed*

Bone mineral density (BMD) is affected by complement system activation, excessive lipoproteins. One purpose of this project was to investigate the effect of complement properdin, the only positive complement regulator, on bone mineral density and the osteoclasts participation in alternative pathway component production. *In vivo* assays showed that there was no significant alteration in bone mineral density in properdin knockout (PKO) mice and wildtype at six months of age, and *in vitro*, the osteoclasts number and resorptive activity were the same in both genotypes, but there was a significant increase in BMD of PKO at an older age (10 months). Also, osteoclasts contribute to complement components production of CFD, CFB, CFP and C3 but not C5 and Vitamin D3 may have a role in curbing excessive complement component production by osteoclast induced by fatty acid.

Hereditary hypertriglyceridemia have an adverse effect on bone mineral density. Therefore, an additional aim of this project was to investigate the role of dietary supplementation of Vitamin D3 on BMD reduction induced by Low density lipoprotein receptor knockout (LDLR<sup>-/-</sup>) mice. The *in vivo* investigation showed that Vitamin D3 normalise the BMD reduction induced by LDLR<sup>-/-</sup> mice by enhancing osteoblast activity and reducing osteoclast activity. *In vitro* assays indicated that Vitamin D3 has an essential action on lowering osteoclast resorptive activity or enhancing osteoblast mineral deposition in LDLR<sup>-/-</sup> cell culture. In addition, Vitamin D3 has an anti-inflammatory action by normalising the secretion of tumour necrosis factor alpha (TNF- $\alpha$ ) and interleukin 6 (IL-6) cytokines *in vivo*.

In conclusion, these findings show that complement properdin could have a role in BMD at more advanced ages, and the osteoclasts may contribute in alternative complement components expression. Vitamin D3 normalise bone mineral density reduction in LDLR<sup>-/-</sup>.

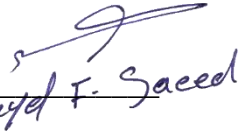
# STATEMENT

---

This accompanying thesis submitted for the degree of PhD entitled “**Osteoimmunological investigations of bone mineral density in a mouse model: *in vivo* and *in vitro* study**” based on work conducted by the author at the University of Leicester mainly during the period between July 2015 and June 2018.

All the work recorded in this thesis is original unless otherwise acknowledged in the text or by references.

None of the work has been submitted for another degree in this or any other University.

Signed:   
Zayed F. Saeed

Date: 13/06/2019

## DEDICATE

---

*To My....*

*Mother, Wife Hawraa, daughters,*

*Brothers and Sisters*

*&*

*To my Father's spirit*

*(God mercy be upon him)*

# ACKNOWLEDGMENT

---

Firstly, “*Thanks to Allah for all his mercy, blessing and help throughout my life*” then, I would like to express my sincere gratitude to my first supervisor **Dr Cordula Stover** for the continuous support of my PhD study and related research, for her patience, motivation, and immense knowledge. Her guidance helped me in all the time of research and writing of this thesis. I could not have imagined having a better advisor and mentor for my PhD study. Moreover, I would like to express my thanks to my second supervisor and **Prof. Jonathan Barratt** for his great advice along with my research.

Besides my advisors, I would like to thank the PRP committee: **Dr Michael Browning** and **Dr Yassine Amrani**, for their insightful comments and encouragement, but also for the hard question which incited me to widen my research from various perspectives.

My sincere thanks also go to **Dr Simon Byrne** for his support in the lab and his technical advice, and the thanks go to **Dr Michael Kelly** and **Justyna Janus**, who provided me with an opportunity to join their team in Imaging Facility Centre in Leicester University as intern, and who gave access to the laboratory and research facilities. Without their precious support it would not be possible to conduct this research.

I thank my lab mates **Dr Izzat Alryahi**, **Dr Ramiar Kamal Kheder** and **Hasanain Alaridhee**, also **Dr Alan Bevington** and **Dr Ahemed Merza** for the stimulating discussions, for working together before deadlines, and for all the fun we have had in the last four years. Also, I thank all my friends in Leicester and the University of Leicester.

Last but not the least, I would like to thank my family: my parents, brothers and sisters for supporting me spiritually throughout writing this thesis and my life in general.

With love,

**Zeayd Fadhil Saeed**

## PUBLICATIONS ARISING FROM THIS THESIS

---

- 1- Kheder, R., Hobkirk, J., Saeed, Z., Janus, J., Carroll, S., Browning, M.J. and Stover, C., 2017. Vitamin D3 supplementation of a high fat high sugar diet ameliorates prediabetic phenotype in female LDLR<sup>-/-</sup> and LDLR<sup>+/+</sup> mice. *Immunity, Inflammation and Disease*. A full version of the article can be found at the following link: <http://onlinelibrary.wiley.com/doi/10.1002/iid3.154/full>
- 2- Two papers are written now and they on way to publish.
  - Complement properdin is implicated in bone density.
  - Vitamin D3 ameliorates bone mineral density reduction associated with LDLR deficiency.

## Table of Contents

LIST OF TABLES .....	x
LIST OF FIGURES .....	xi
LIST OF ABBREVIATIONS.....	xiv
1 Chapter One-Introduction .....	19
1.1 Bone function and structure. ....	20
1.1.1 Cortical bone: .....	21
1.1.2 Cancellous bone:.....	21
1.1.3 Bone marrow: .....	22
1.2 Bone cells. ....	23
1.2.1 Osteoclasts (origin and function).....	23
1.2.2 Osteoblasts (origin and function). ....	24
1.3 Bone remodelling and bone mineral density. ....	26
1.4 The effect of the complement system on bone remodelling. ....	27
1.4.1 The osteoblast and complement system interaction. ....	28
1.4.2 Osteoclasts and complement system interaction. ....	30
1.5 LDLR <sup>-/-</sup> mice as a hyperlipidaemic model, the effect of LDL and LDLR on bone mineral density.....	31
1.6 Hypothesis.....	32
1.7 Aims and Objectives. ....	32
2 Chapter Two Methodology .....	35
2.1 <i>In vivo</i> methods: .....	36
2.1.1 The experimental animals and diets used in this project. ....	36
2.1.1.1 Mice used in this project:.....	36
2.1.1.2 Diet used in this project: .....	37
2.1.2 Measuring the bone mineral density by computed tomography (M-CT).....	37
2.1.3 Measuring osteoclast activity (Tartrate-resistant acid phosphatase, TRACP) by ELISA.....	51

2.1.4	Measuring osteoblast activity (Alkaline phosphatase activity) by ELISA.....	53
2.1.5	Osteocalcin level measurement as a bone formation marker: .....	54
2.1.6	Serum triglyceride level measurements.....	56
2.1.7	Measuring the functional activities of alternative and classical complement pathways by ELISA.....	58
2.1.8	TNF- $\alpha$ level measurements by ELISA as an indication of inflammatory cytokines.....	59
2.1.9	Murine IL-6 measurement as an inflammatory factor by ELISA: .....	61
2.1.10	Body weight measurement for 5 weeks.....	63
2.2	<i>In vitro</i> methodology:.....	63
2.2.1	Osteoclasts and Osteoblasts differentiation derived from mouse C57/BL6 bone marrow.....	63
2.2.2	J774 cell line:.....	64
2.2.3	Tartrate-resistant acid phosphatase (TRACP staining). .....	65
2.2.4	Alkaline phosphatase staining (ALP staining). .....	66
2.2.5	Osteoclast resorption activity assay.....	67
2.2.6	Evaluation of mineral deposition from differentiated osteoblasts derived from mouse bone marrow. ....	67
2.2.7	C5a protein detection by Western blotting in osteoclast cell culture. ....	68
2.2.8	C5a protein detection by ELISA in osteoclast cell cultures. ....	71
2.2.9	Reverse Transcriptase Polymerase Chain reaction (RT-PCR). ....	72
2.2.9.1	Total RNA extraction.....	72
2.2.9.2	Complementary Deoxyribonucleic Acid (cDNA) preparation. ....	73
2.2.9.3	Gradient PCR.....	74
2.2.9.4	Normal Polymerase chain reaction (PCR).....	75
2.2.9.5	Agarose Gel Electrophoresis: .....	76
2.2.10	Real Time- quantitative polymerase chain reaction (RT-qPCR).....	76
2.2.11	Preparation of Bovine Serum Albumin (BSA)-Conjugated Palmitate: .....	79

2.2.11.1	The prior setup of BSA and sodium palmitate solution preparation. ...	79
2.2.11.2	BSA solution preparation (0.34 mM). .....	79
2.2.11.3	Sodium palmitate solution preparation: .....	80
2.2.11.4	Conjugating Palmitate and BSA: .....	80
2.2.11.5	Thawing Palmitate-BSA: .....	80
2.2.12	Preparation of Bovine Serum Albumin (BSA)-Conjugated Oleate: .....	80
2.2.13	The optimal dose determination of fatty acid (FA) to stimulate osteoclast and osteoblast activities.....	81
2.2.14	Statistical analysis: .....	82
3	Chapter Three – The Results.....	83
3.1	The effect of complement properdin gene deletion on bone mineral density. ....	84
3.1.1	Results. ....	84
3.1.1.1	The effect of complement properdin deficiency on bone microarchitecture. ....	84
3.1.1.2	The effect of properdin deficiency on bone remodelling cells. ....	89
3.1.1.3	<i>In vitro</i> quantification of the effect of properdin deficiency on osteoclast activity... ..	90
3.1.1.4	The effect of properdin deficiency on bone mineral density in older age mice.....	93
3.2	Vitamin D3 or exercising normalise bone mineral density reduction associated with low-density lipoprotein receptor deficiency. ....	98
3.2.1	Results. ....	98
3.2.1.1	The effect of LDLR deficiency on serum triglyceride levels in mice. .	98
3.2.1.2	The effect of Low-density lipoprotein receptor (LDLR) deficiency on bone microarchitecture. ....	99
3.2.1.3	The effect of LDLR deficiency on bone remodelling activity.....	105
3.2.1.4	The effect of LDLR <sup>-/-</sup> on classical and alternative complement pathways activation.....	107

3.2.1.5	The effect of LDLR <sup>-/-</sup> on serum levels of proinflammatory cytokines TNF- $\alpha$ and IL-6.....	109
3.2.1.6	Suitability of 5-weeks protocol to study adaptation of vitamin D3 supplementation or voluntary wheel exercising in LDLR <sup>-/-</sup> mice.....	110
3.2.1.7	The effect of Vitamin D3 supplementation or access to exercise on bone mineral density reduction in LDLR <sup>-/-</sup> mice.....	111
3.2.1.8	Evaluation of the role of Vitamin D3 or Exercising on bone remodelling in LDLR <sup>-/-</sup> : .....	116
3.2.1.9	The effect of Vitamin D3 or exercising on serum inflammatory cytokines levels in LDLR <sup>-/-</sup> . .....	117
3.2.1.10	The <i>in vitro</i> effect of Vitamin D3 on osteoclast differentiation and resorptive activity derived from LDLR deficient mice. ....	118
3.2.1.11	The <i>in vitro</i> effect of Vitamin D3 on osteoblasts differentiation and mineral deposition activity derived from LDLR deficient mice.....	123
3.3	Vitamin D3 normalises long chain fatty acid-induced expression of alternative pathway complement components in osteoclasts ( <i>In vitro</i> study). .....	126
3.3.1	Introduction. ....	126
3.3.2	Results. ....	127
3.3.2.1	The role of murine osteoclasts in C5 Cleavage to C5a.....	127
3.3.2.2	The alternative complement component expression by differentiated murine osteoclasts.....	131
3.3.2.3	The effect of Vitamin D3 on the excessive gene expression of alternative pathway components induced by fatty acid.....	136
4	Chapter Four – The General Discussion .....	140
4.1	The effect of properdin deficiency on bone mineral density: .....	141
4.2	The effect of vitamin D3 or exercising on bone mineral density reduction induced by low-density lipoprotein receptor deficiency (LDLR <sup>-/-</sup> ).....	144
4.3	The effect of vitamin D3 and fatty acid on complement component production of the alternative pathway in murine osteoclasts. ....	148

5 Conclusion. ....	154
6 Future Plan: .....	156
7 Appendices.....	157
8 References .....	166

## LIST OF TABLES

Table 2-1: The components of different diets.....	37
Table 2-2: Preparation of Triglyceride Standards.....	57
Table 2-3: Preparation 10ml of 2X Laemmli sample buffer. ....	68
Table 2-4: Preparation 15% sodium dodecyl sulfate-polyacrylamide gel for western blotting. ....	69
Table 2-5: Preparation of 1x running buffer for western blotting .....	69
Table 2-6: Preparation of 1x Transfer buffer for western blotting .....	69
Table 2-7: Preparation of 1x washing buffer for western blotting .....	70
Table 2-8: The temperature cycling conditions of qRT-PCR.....	77
Table 2-9: Primer sequences with TA and product sizes used in this study.....	78
Table 3-5: The percent of alternative pathway activity related to commercial mouse serum in serum of LDLR deficient mice .....	108
Table 3-6: The percent of classical pathway activity related to commercial mouse serum in serum of LDLR deficient mice .....	108

# LIST OF FIGURES

Figure 1-1: The anatomical structure of normal bone: .....	22
Figure 1-2: The osteoclasts differentiation and activation: .....	24
Figure 1-3: A representative scheme showing the osteoblast differentiation and bone formation.....	25
Figure 1-4: A representative scheme is showing the bone remodelling cycle.....	27
Figure 1-5: The interaction between the complement system and bone remodelling. ....	30
Figure 1-6: the effect of low-density lipoprotein receptor on bone mineral density. ....	32
Figure 2-1: The 3 <sup>rd</sup> lumbar vertebrae harvesting and fixation preparation:.....	38
Figure 2-2: The Calipare Micro tomography machine and the solid resin-embedded hydroxyapatite phantom that was used to convert the BMD grayscale.....	39
Figure 2-3: Plot of grayscale values vs mineral density of phantom:.....	40
Figure 2-4: Data processing and pre-segmentation: .....	42
Figure 2-5: bone cortical segmentation: .....	44
Figure 2-6: Bone Cortex refinement:.....	46
Figure 2-7: The segmented trabecula refinement: .....	48
Figure 2-8: Bone morphometric indices: .....	48
Figure 2-9: Examples of bone mineral density parameters: .....	50
Figure 2-10: The general experimental flow for measuring bone mineral density. ....	51
Figure 2-11: Example standard curve showing the absorbance of different concentrations of mouse C-terminal of bone alkaline phosphatase (ALP).....	54
Figure 2-12: Example for the standard curve showing the absorbance of different concentrations of mouse Osteocalcin. ....	56
Figure 2-13: Example for the standard curve showing the absorbance of different concentrations of Triglyceride (the optical density is 450nm). ....	58
Figure 2-14: Example for the standard curve showing the absorbance of different concentrations of Tumour necrosis factor alpha (the optical density is 450nm). ....	61
Figure 2-15: Example for the standard curve showing the absorbance of different concentrations of Interleukin 6 (the optical density is 450nm). ....	63
Figure 2-16: A scheme represented the order layers of blotting gel of western blot.....	70
Figure 2-17: Program used for cDNA synthesis.....	74
Figure 2-18: Program used in Gradient PCR.....	75
Figure 2-19: An example of a program used for normal PCR.....	76

Figure 3-1: The impact of properdin gene deficiency on bone microarchitecture: .....	87
Figure 3-2: The effect of properdin deficiency on bone microarchitecture in male and female mice:.....	88
Figure 3-3: The osteoclast and osteoblast activities measurements in properdin knockout mice:.....	90
Figure 3-4: The in vitro analysis of differentiated osteoclast activity derived from WT and PKO mice:.....	93
Figure 3-5: The impact of properdin gene deficiency on bone mineral density at older ages: .....	96
Figure 3-6: The effect of properdin absence on bone mineral density in female mice at 10 months old: .....	97
Figure 3-7: The effect of LDLR deficiency on Triglyceride level in mouse serum:.....	99
Figure 3-8: The experimental flow for quantifying the effect of LDLR gene deletion on bone mineral density.....	99
Figure 3-9: The effect of LDLR gene deletion on bone microarchitecture:.....	102
Figure 3-10: 3D rendering images of the effect of LDLR absence on bone mineral density in male and female mice: .....	104
Figure 3-11: The LDLR deficiency on osteoclast and osteoblast activities in mice: ...	106
Figure 3-12: The effect of LDLR absence on classical and alternative complement pathways activation: .....	108
Figure 3-13: inflammatory cytokines (IL-6 and TNF- $\alpha$ ) levels in LDLR deficient mice: .....	109
Figure 3-14: The effect of Vitamin D3 or exercising on body weight or triglyceride levels in LDLR <sup>-/-</sup> : .....	111
Figure 3-15: The influence of Vitamin D3 or exercising on bone microarchitecture induced by LDLR <sup>-/-</sup> whilst on normal diet for 5 weeks. ....	114
Figure 3-16: The 3D rendering images represent the BMD corrections by vitamin D3 or Exercising in LDLR <sup>-/-</sup> for one mouse in each group.....	115
Figure 3-17: The effect of Vitamin D3 or exercising on bone remodelling in LDLR <sup>-/-</sup> for 5 weeks: .....	117
Figure 3-18: The effect of Vitamin D3 or exercising on serum levels of IL-6 and TNF- $\alpha$ in LDLR <sup>-/-</sup> : .....	118
Figure 3-19: the effect of vitamin D3 addition on the activity of osteoclasts derived from LDLR <sup>-/-</sup> : .....	122

Figure 3-20: The effect of Vitamin D3 addition <i>in vitro</i> on osteoblasts activity derived from LDLR <sup>-/-</sup> mice bone marrow: .....	125
Figure 3-21: Identification of complement C5/C5a production by murine osteoclasts: .....	128
Figure 3-22: The complement C5 detection in osteoclast and J774 macrophage cell line supernatant: .....	129
Figure 3-23: The complement C5 gene expression in murine osteoclasts: .....	130
Figure 3-24: The effect of RANKL on complement C5 gene expression: .....	131
Figure 3-25: complement factor D expression by murine osteoclasts:.....	132
Figure 3-26: the complement factor B expression by murine osteoclasts: .....	133
Figure 3-27: Complement C3 expression by murine osteoclasts: .....	134
Figure 3-28: Complement properdin expression by murine osteoclasts: .....	135
Figure 3-29: The qPCR analysis for the level of B2M gene expression as a housekeeping gene in osteoclasts stimulated by fatty acid with or without Vitamin D3. The experiment was performed three times in duplicates.....	137
Figure 3-30: Vitamin D3 normalises the excessive complement factor D expression induced by free fatty acid.....	138
Figure 3-31: Vitamin D3 normalises the over complement factor B expression induced by free fatty acid. ....	138
Figure 3-32: Vitamin D3 normalises the excessive complement C3 expression induced by free fatty acid. ....	139
Figure 3-33: Vitamin D3 normalises the excessive complement properdin expression induced by free fatty acid.....	139
Figure 4-1: The representative scheme is showing the effect of age on female properdin-deficient mice bone mineral density. ....	143
Figure 4-2: The effect of vitamin D3 on bone remodelling in LDLR deficient mice. .	148
Figure 4-3: The interaction between Vitamin D3 and fatty acid stimulation of gene expression in osteoclasts.....	153

# LIST OF ABBREVIATIONS

%: Percent

°C: Degree Celsius

μ-CT: Micro-computed tomography

μg: microgram

μl: microliter

μmol: Micromole

58R1: Low-fat diet (normal diet)

58R3: high-fat-high sugar diet

5LF2: normal diet

5TJN: Western diet (high-fat diet)

ALP: Alkaline phosphatase

AP: alternative pathway

APS: Ammonium Persulfate

B2M: Beta-2 microglobulin

BM: Bone marrow

BMA: Bone microarchitecture

BMD: Bone mineral density

BMU: Basic multicellular unit

bp: base pair

BSA: Bovine Serum Albumin

BV/TV: Bone volume fraction

C1: Complement component 1

C3<sup>-/-</sup>: Complement component 3 knockout

C3: Complement component 3

C3aR: C3a receptors

C4: Complement component 4

C5: Complement component 5

C5aR: C5a receptors

C9: Complement component 9

cDNA: complementary Deoxyribonucleic acid

CFB: Complement factor B

CFD: Complement factor D

c-fms: colony stimulating factor 1 receptor

CFP: Complement factor P or complement properdin

CMS: Commercial mouse serum

Conn.D: Connectivity density

CP: Classical pathway

dH<sub>2</sub>O: Distilled water

DTT: Dithiothreitol

DW: Distilled water

EDTA: Ethylenediaminetetraacetic acid

ELISA: Enzyme-Linked Immunosorbent Assay

EX: Exercising

F: female

FCS: Fetal calf serum

FFA: Free Fatty acid

FOV: fold of view

g: Gram

GAPDH: Glyceraldehyde 3-phosphate dehydrogenase

HA: hydroxyapatite

HFD: high-fat diet

HPLC: high performance (or high pressure) liquid chromatography

hr.: Hour

HRP: Horse reddish peroxidase

IL-1 $\beta$ : Interleukin-1 beta

IL-6: Interleukin 6

IMS: Industrial methylated spirit

IU: International Unit

J774: Murine Macrophage cell line

kDa: Kilo Dalton

KO: knockout

LDLR<sup>-/-</sup>: Low-density lipoprotein receptor knockout

LDL-R: Low-Density Lipoprotein Receptor

LPS: Lipopolysaccharide

M: Male

MAPKs: Mitogen-Activated Protein kinase

MCP-1: Monocyte Chemoattractant Protein-1

M-CSF: Macrophage Colony-Stimulating Factor

mg: milligram

min: minutes

ml: millilitre

mM: millimolar

MMP-9: Matrix MetalloProteinase-9

mRNA: messenger Ribonucleic Acid

NFATc1: nuclear factor of activated t cells, cytoplasmic, calcineurin-dependent 1

ng: nanogram

nm: nanometer

ns: no significant difference

OB: osteoblasts

OC: osteoclast

OCL: Osteocalcin

OD: Optical Density

OPG: Osteoprotegerin

Ox-LDL: oxidative Low-density lipoprotein

PBS: Phosphate buffered saline

PCR: polymerase chain reaction

PE<sub>2</sub>: Prostaglandin E<sub>2</sub>

pg: Picogram

PKO: Properdin knockout

pNPP: para-nitrophenyl phosphate

qRT-PCR: quantitative Real-Time polymerase chain reaction

RANK: Receptor activator of nuclear factor kappa-B

RANKL: Receptor activator of nuclear factor kappa-B ligand

RT: Room temperature

SD: standard deviation

SDS: sodium dodecyl sulphate

TA: Annealing temperature

Tb. Sp: Trabecular separation

Tb. Th: Trabecular Thickness

TBS: Tris-buffered saline

TEMED: N, N, N', N'-tetramethyl ethylenediamine

TG: Triglyceride

TMB: 3,3',5,5'-Tetramethylbenzidine

TNF- $\alpha$ : Tumour Necrosis Factor-alpha

Tr. N: Trabecular number

TRACP or TRACP: Tartrate-Resistant Acid Phosphatase

v/v: Volume/Volume

VD: Vitamin D

VDR: Vitamin D receptor

w/v: Weight/Volume

WB: western blot

WT: wildtype

$\kappa$ : Kappa

# **1 Chapter One-Introduction**

## **1.1 Bone function and structure.**

A bone is an inflexible organ that constitutes most of the vertebrate skeleton. Bones support and protect the different organs of the body like brain, spinal cord, heart and lungs in the thoracic cage, and viscera in the pelvic cavity. In addition, bones can deliver red and white blood cells, platelets, store minerals, give structure and support to the body, and empower versatility. Bones occur in an assortment of shapes, sizes and have a complex inner and outside structure. They are lightweight yet solid and hard and serve various functions.

Bone tissue is a hard tissue, a kind of thick connective tissue. It has a honeycomb-like framework inside, which gives the bone its unbending nature. Bone tissue is comprised of several types of bone cells. Osteoblasts and osteocytes engage with the arrangement and mineralisation of bone; osteoclasts are associated with the resorption of bone tissue. The osteoblast in turn forming a protective frame layer on the bone surface. The mineralised lattice of bone tissue consists of collagen called ossein and an inorganic bone mineral made up of different salts like  $\text{Ca}^+$  and phosphates. Bone tissue is a mineralised tissue of two kinds, cortical bone and cancellous bone. Other different sorts of tissue found in bones incorporate bone marrow, endosteum, periosteum, nerves, veins and ligament (Steele and Bramblett, 1988).

The bony matrix makes up around 30% of the bone, and the other 70% is of salts that offer bone strength. The matrix is comprised of 90-95% collagen fibres, and the rest is a ground substance (J. Hall, 2011). Bone matrix consists of a composite material consolidating the inorganic mineral calcium phosphate named calcium hydroxyapatite (this is the bone mineral that gives bones their unbending nature) and collagen, a flexible protein which enhances fracture resistance (Schmidt-Nielsen, 1984). Bone is shaped by the solidifying of this matrix around embedded cells.

Mainly, two kinds of tissue might be found in bones, thick or cortical bone, which covers the surface shell of bone, and spongy cancellous or Trabecular bone, which is encased by the cortical bone. The external layer of bones is made of cortical bone additionally called compact bone, being significantly denser than cancellous bone. It frames the hard outside (Cortex) of bones.

### **1.1.1 Cortical bone:**

It gives bone its smooth, white, and strong appearance, and accounts for 80% of the aggregate bone mass of a grown-up human skeleton. It encourages bone's fundamental capacities: to help the protect organs, give strength and store and discharge components like calcium. It comprises multiple microscopic columns, called an osteon. Every column is numerous layers of osteoblasts and osteocytes around a focal trench called the Haversian channel. Volkmann's canals at right angles connect the osteons. Cortical bone is secured by a periosteum on its external surface and an endosteum on its internal surface. The endosteum is the limit between the cortical bone and the cancellous bone (Figure 1-1). The essential anatomical and functional unit of cortical bone is the osteon (Young, 2006).

### **1.1.2 Cancellous bone:**

The words cancellous and Trabecular refer to the small cross-section units (trabeculae) that frame the tissue (Gomez, 2002). Cancellous bone otherwise called Trabecular or elastic bone tissue is the inside tissue of the skeletal bone, and it is an open porous network (Young, 2006). Cancellous bone has a higher surface-area-to-volume ratio than cortical bone since it is less thick. The greater surface region likewise makes it ideal tissue for metabolic activities in bones such as the exchange of calcium ions. Cancellous bone is found at the ends of long bones, close to joints and within the interior of vertebrae. Cancellous bone is vascular and contains red bone marrow where haematopoiesis happens. The essential anatomical and functional unit of cancellous bone is the trabecula. The trabeculae are responsible for the mechanical load dispersion that a bone encounters inside long bones, for example, the femur. As far as short bones are concerned, the Trabecular arrangement occurs in the vertebral pedicle (Gdyczynski *et al*, 2014). Trabecular bone makes an irregular network of spaces called intra-Trabecular spacing. Inside these spaces, the bone marrow, hematopoietic cells, platelet formation and white blood cell generation can occur (Young, 2006). Trabecular marrow is made of a system of bar and plate-like components that make the organ lighter and permit space for veins and marrow (Figure 1-1). In general, Trabecular bone consists of 20% of aggregate bone mass (S. J. Hall, 2007).

### 1.1.3 Bone marrow:

Bone marrow is a semi-strong tissue inside the light or cancellous bits of bones (Farhi, 2009). It is found in the focal point of numerous bones especially in the ribs, vertebrae, sternum, and bones of the pelvis (Figure 1-1). In mammals, bone marrow is the essential site of new blood cell generation or hematopoiesis (Birbrair and Frenette, 2016). It consists of hematopoietic cells, adipose tissue and mesenchymal stromal cells. Human marrow delivers around 500 billion platelets each day, which join the blood circulation by permeable vasculature sinusoids inside the medullary cavity (R. Rubin, Strayer and Rubin, 2008). All sorts of hematopoietic cells, including both myeloid and lymphoid lineages, are made in bone marrow; nonetheless, lymphoid cells like T-cells, B-cells must move to other lymphoid organs (e.g. thymus and lymph nodes) to finish their development.

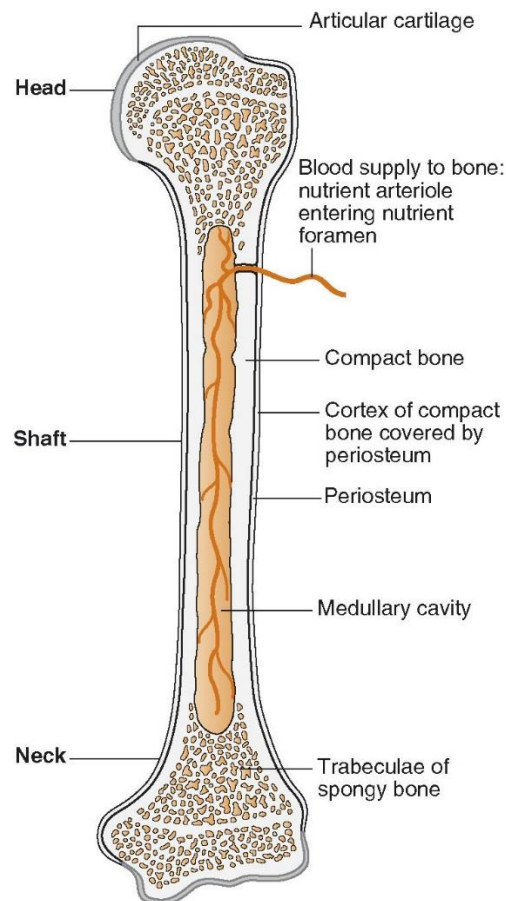


**Figure 1-1: The anatomical structure of normal bone:**

Showing the compact bone, spongy bone and medullary marrow structures (Aspinall and O'Reilly, 2004).

## 1.2 Bone cells.

Osteoblasts are associated with mineralisation of bone tissue. Osteocytes, and osteoclasts, are engaged with the reabsorption of bone tissue. Osteoblasts and osteocytes are derived from osteoprogenitor cells. However, osteoclasts are derived from cells that also differentiate to form macrophages and monocytes (Young, 2006).

### 1.2.1 Osteoclasts (origin and function).

The osteoclast dismantles and processes the composite of hydrated protein and mineral at a molecular level by emitting corrosive acids and a collagenase, a procedure known as bone resorption. This procedure likewise manages the level of blood calcium. Osteoclasts are derived from macrophage fusion to form multinucleated cells (Teitelbaum, 2000). Osteoclast development requires the presence of two central cytokines: RANKL (receptor activator of nuclear factor  $\kappa\beta$  ligand) and M-CSF (Macrophage colony-stimulating factor). These cytokines are produced by stromal cells and osteoblasts, providing direct contact between these cells and osteoclast precursors. Both M-CSF and RANKL are essential to osteoclast differentiation. The binding of M-CSF via its receptor on osteoclasts, colony-stimulating factor 1 receptor (c-fms) induces a tyrosine kinase activation which is vital to osteoclastogenesis from monocyte-macrophage lineage. The RANKL-RANK interaction on osteoclasts activates NF- $\kappa\beta$  (nuclear factor- $\kappa\beta$ ) and NFATc1 (nuclear factor of activated t cells, cytoplasmic, calcineurin-dependent 1) essential for osteoclast differentiation (Okayasu *et al*, 2012). Osteoprotegerin plays a role in osteoclastogenesis regulation, it is secreted by osteoblasts and acts as a decoy protein for RANKL and prevents it from binding to its receptor on osteoclasts (Numan *et al*, 2015). In bone, osteoclasts are found in pits in the bone surface which are called resorption bays, or Howship's lacunae (Holtrop and King, 1977). A large cytoplasm characterises osteoclasts with a homogeneous, "frothy" appearance. This appearance is because of a high centralisation of vesicles and vacuoles. These vacuoles incorporate lysosomes filled with acid phosphatase (Vaananen *et al*, 2000). The acid phosphatase allows identification of osteoclasts by their stain for high expression of tartrate-resistant acid phosphatase (TRACP), and cathepsin K. Osteoclast irregular endoplasmic reticulum is scanty, and the Golgi complex occupies a large area (Vaananen *et al*, 2000). At the resorption site, the osteoclasts form a unique cell membrane fold called the ruffled border,

by which the osteoclast adheres to the surface area of the bone, which is degraded by bone resorption components secreted by the osteoclast (Standing and Wigley, 2005). Once osteoclasts are activated by chemotactic factors, they start to migrate to the target resorbing area and attach to the bone via the sealing zone by podosomes. Then, they start to secrete hydrogen ions by the action of carbonic anhydrase ( $\text{H}_2\text{O} + \text{CO}_2 \rightarrow \text{HCO}_3^- + \text{H}^+$ ) through the ruffled border into the resorptive cavity; the acidity environment contributes to the dissolution of the bone matrix into  $\text{Ca}^{2+}$ ,  $\text{H}_3\text{PO}_4$ ,  $\text{H}_2\text{CO}_3$ ,  $\text{H}_2\text{O}$  and other components. Additionally, several enzymes released by osteoclasts contribute to bone resorption, such as Cathepsin K and matrix metalloprotease (MMP) groups (Vaananen *et al*, 2000). See (Figure 1-2).

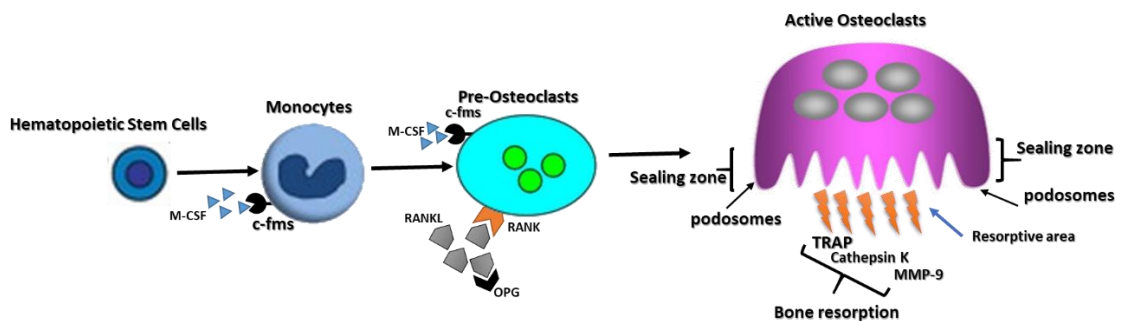


**Figure 1-2: The osteoclasts differentiation and activation:**

The macrophage colony stimulating factor (M-CSF) produced by mesenchymal stem cells activates the monocytes by c-fms receptor to differentiate them from monocytes/macrophages. The RANKL via RANK induces macrophage fusion to form pre-osteoclasts and then active osteoclasts. OPG is the decoy protein released by osteoblasts to block RANKL action.

## 1.2.2 Osteoblasts (origin and function).

Osteoblasts originate from mesenchymal stem cells (Pittenger *et al*, 1999). The osteoblast is the cell that structures bone and is required, alongside the chondrocyte of the development plate, for longitudinal bone development. Osteoblasts cover the surface of the bone and pack firmly together against nearby osteoblasts by producing type I collagen and bone matrix proteins for bone mineralisation. Mature osteoblasts may migrate to the surface of the bone where they stop moving and end up as bone coating cells, or they might be encompassed by bone matrix and progress toward becoming osteocytes (Bostrom and Mikos, 1997).

Bone mineralisation happens continuously during the life. It starts at places on the collagen fibrils separated by unmineralised areas. As mineralisation develops minerals

fill all the available space inside the collagen fibrils then mineralisation continues quickly with roughly 60% of the mass accounted for by minerals. Then, the water and non-collagenous protein are reduced, but the collagen concentration stays unaltered. The increased mineralisation and changing of the Trabecular bone into compact bone leads to increased bone strength (Bostrom and Mikos, 1997).

Briefly, the mechanism of mineralisation by osteoblasts depends on enzymatic osteoblast activity. Osteoblasts synthesise collagen and bone matrix proteins and secrete phosphate which precipitates the hydroxyapatite mineral. Alkaline phosphatase, a membrane-anchored protein that is a marker expressed in large amounts on active osteoblasts from a mineralisation front by making a high phosphate concentration (Blair, Zaidi and Schlesinger, 2002) see (Figure 1-3).

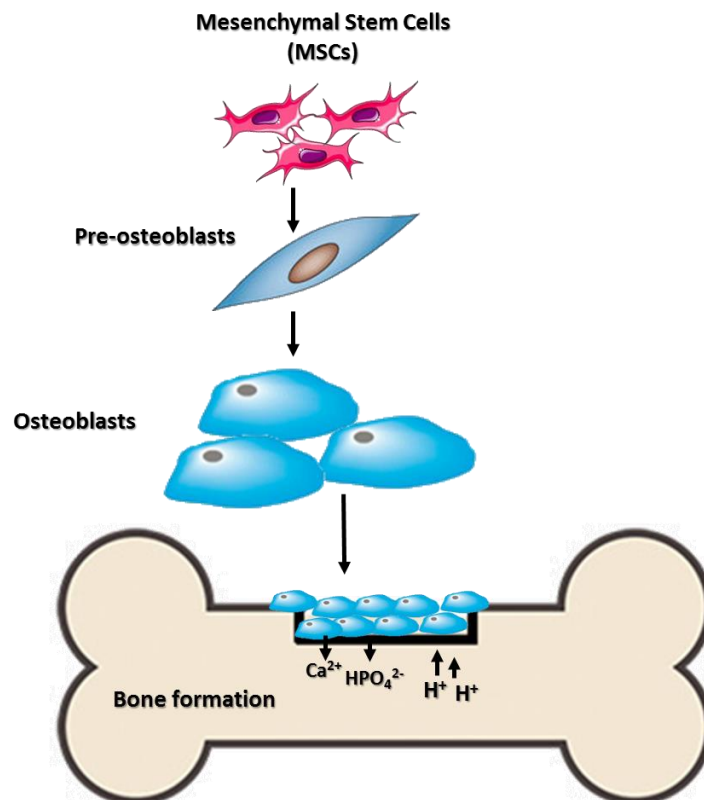


Figure 1-3: A representative scheme showing the osteoblast differentiation and bone formation.

### **1.3 Bone remodelling and bone mineral density.**

Bone remodelling (or bone metabolism) is a bone reshaping process whereby bone tissue is degraded from the skeleton by a procedure called bone resorption by osteoclasts. However, the new bone tissue is shaped by a procedure called ossification or new bone formation induced by osteoblasts (Raggatt and Partridge, 2010). The bone remodelling process plays a significant role in regulating bone mineral density. It depends on the balance of both osteoblast and osteoclast activities, and the changes in one or both of these activities could induce either bone mineral density reduction (Osteoporosis) or increased bone mineral density (Osteopetrosis).

The mechanism of bone remodelling occurs by migration of the mature osteoclasts to resorb the surface of the target bone. Then, the mature osteoblasts start to be attracted and osteoclasts are dispatched from the degraded bone. Bone mineralisation starts by activation of osteoblasts by increasing bone mineral deposition. Then, osteoblasts line and cover the bone surface see (Figure 1-4). Together, osteoclasts and osteoblasts involved in bone remodelling are known as the basic multicellular unit (BMU), and the life expectancy of the BMU is referring to as the bone rebuilding time frame (Pietrzak, 2008). Bone remodelling depends on different signalling pathways to accomplish bone shaping that can be controlled by different factors like Vitamin D, Parathyroid hormone, growth hormone, steroids, and calcitonin, also soluble cytokines and growth factors (like M-CSF, RANKL, TNF- $\alpha$ , IL-6 family). Although bone remodelling is considered to be essential for bone repair, it is a source of calcium supply for different physiological processes. Bone structure and supply of calcium require close collaboration between osteoclast, osteoblast and other cell populations introduced at the bone remodelling locales like immune cells (Sims and Martin, 2014).

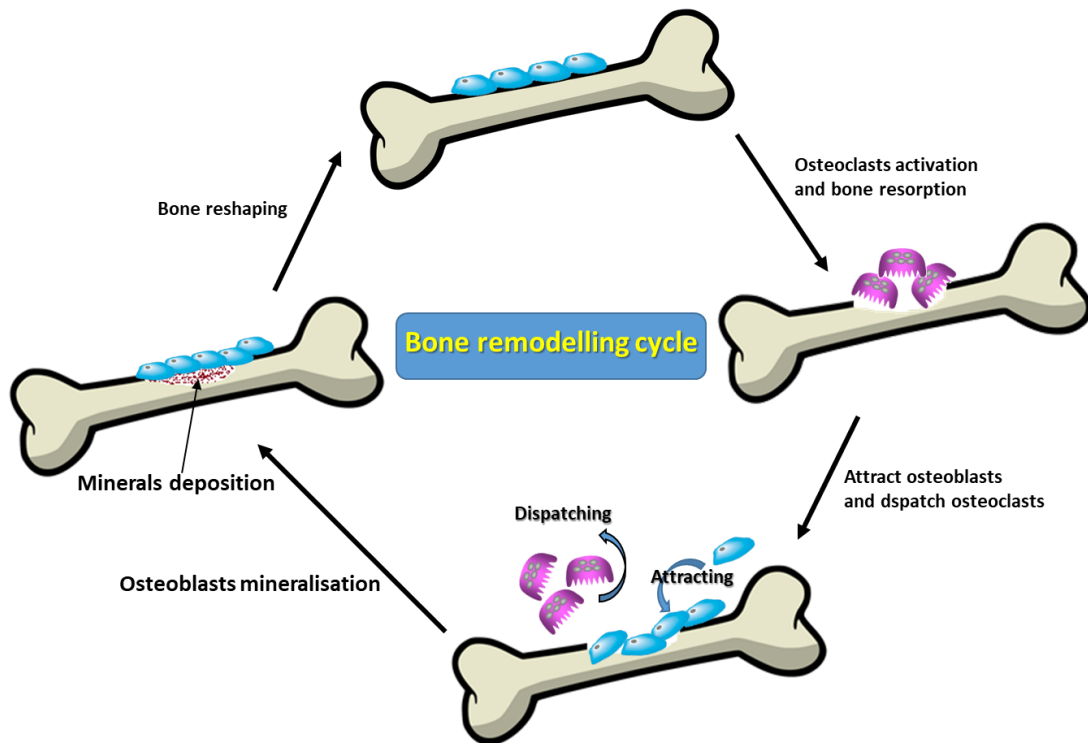


Figure 1-4: A representative scheme is showing the bone remodelling cycle.

## 1.4 The effect of the complement system on bone remodelling.

In recent decades, it has been shown that there is a strong interaction between the complement system and bone development. Various complement components have a role in bone cell activation and differentiation. In the zones of resting, proliferating, and pre-hypertrophic chondrocytes, the endochondral cell proliferation in the bridge zones of bone are replaced by bone formation by osteoblast function. This process is associated with either stimulatory or inhibitory different growth factors (Wuelling and Vortkamp, 2010). Using immunofluorescence to study the localisation of different complement proteins in Tibias or femurs of rat, Andrades *et al* (1996) showed that different complement proteins were found in the proliferation bone zone, the area of bone growth resulting from cellular division. Complement C3, factor B, and properdin were found in the resting zone, which is responsible for the organization of the growth plate into distinct zones of proliferation and hypertrophy. The factor B and complement properdin were present in the proliferating zone; C5 and C9 were found in the hypertrophic zone in which

the chondrocytes grow greatly, and their surrounding matrix becomes calcified (Andrades *et al*, 1996). Therefore, the alternative complement pathway could have a role in bone proliferation and ossification.

The classical complement pathway may contribute to bone turnover. The first component of the classical pathway (C1s) was found in the epiphyseal cartilage, a hyaline cartilage plate in the metaphysis at each end of a long bone, and in hamsters at the fracture callus area, bony and cartilaginous material forming a connecting bridge across a bone fracture during repair (Toyoguchi *et al*, 1996). In human, C1s was found in the region of calcification. Also it was found in the hamster tibia in the secondary ossification centre, where bone formation continues after beginning in the long shaft or body of the bone, usually in an epiphysis (Sakiyama *et al*, 1994). The C1s was found in the digested bone matrix near the damaged vessels (Sakiyama *et al*, 1997). Yamaguchi *et al*. (1990) illustrated that C1s has a significant role in bone matrix degradation. It was able to cleave collagen type I and II and gelatine by the activity of its serine protease (Yamaguchi *et al*, 1990). Moreover, it was shown that C1s can activate the matrix metalloproteinase (MMP)-9, which has a role in bone degradation, in the primary ossification centre (Sakiyama *et al*, 1994). These studies represent the role of the complement system in bone development, and the complement proteins may mediate the bone generation and growth, although, the described activity is outside the typical complement activity sequence.

#### **1.4.1 The osteoblast and complement system interaction.**

The essential action of the complement system in bone homeostasis is summarised by the expression of several complement proteins and receptors in various types of bone cells. C5aR is expressed in osteoblasts and osteocytes in normal bone in human and also on osteoblasts, osteoclasts, and chondrocytes during bone fracture callus formation in rats (Ignatius *et al*, 2011b). The complement regulators Membrane Cofactor Protein (MCP or CD46), Complement decay-accelerating factor (DAF or CD55), MAC-inhibitory protein (MAC-IP or CD59), the C3aR and C5aR, C3 and C5 were found to be expressed by mesenchymal stem cells (MSC) and osteoblasts, but C5 in osteoclasts was not expressed. The expression of these factors is increased during osteogenic differentiation (Ignatius *et al*, 2011a). Although Ignatius *et al* (2011b) show that the presence of C3a and C5a did not affect the osteogenic differentiation of osteoblasts, their anaphylatoxin receptors were

up-regulated during osteogenic differentiation, showing that the osteoblast is a target of complement system activation. The anaphylatoxins may have a chemotactic effect on osteoblasts. It is likely to have an essential effect on osteoblasts and Mesenchymal stem cell (MSC) migration. Schraufstatter *et al* (2009) and Ignatius *et al.* (2011a) showed that C5a through its C5aR chemo-attracts the MSC and osteoblasts to the target area and this might occur during the expression of C5aR on osteoblast (Schraufstatter *et al.*, 2009; Ignatius *et al.*, 2011b). The inflammatory function of anaphylatoxins in bone cells could be indicated by cytokine release mainly from immune cells. Pobanz *et al.* (2000) showed that C5a binding to its receptor on osteoblast induces a significant increase in the IL-1 $\beta$ -induced release of IL-6 (Pobanz *et al.*, 2000). It was found that osteoblast stimulation with IL-1 $\beta$  and C3a or C5a increased the pro-inflammatory interleukins IL-6 and IL-8 release by osteoblasts (Ignatius *et al.*, 2011b). Even though of the mechanisms of interleukin and anaphylatoxin interactions are still unknown, it was shown that ERK1/2 and NF- $\kappa$ B are likely to be activated by the C3aR signalling pathway (K. Li *et al.*, 2008). Also, ERK1/2, AKT, and MAPK p38 may be activated by C5aR binding to its anaphylatoxins (Rousseau *et al.*, 2006). These observations may suggest that anaphylatoxins and their receptors and inflammatory cytokines have a role in osteoblasts activation, or osteoblasts modulate an inflammatory response during inflammation.

The complement zymogens also could be expressed and activated by bone cells. Ignatius *et al.* (2011b) found that complement C3 and C5 were expressed by mesenchymal stem cells and osteoblasts, while in osteoclastogenesis, C3 was expressed but not C5 by osteoclasts (Ignatius *et al.*, 2011a). Ignatius *et al.* (2011a) agreed with Hong *et al.* (1991) and Sato *et al.* (1991) when they found that the C3 expression was up-regulated by Vitamin D3 supplementation *in vitro* by osteoblasts (Hong *et al.*, 1991; Sato *et al.*, 1991). Therefore, it was evident that there is a strong association between the complement system and osteoblasts activity by expressing different complement component receptors like C3aR and C5aR that could interact with their anaphylatoxins to enhance or release some of the pro-inflammatory cytokines to induce an inflammatory response by osteoblasts. Also, the osteoblasts were able to produce the main complement proteins such as C3 and C5 that contribute to complement activation. Therefore, possibly the complement system has a role in bone formation and in regulating the bone mineral density (Figure 1-5).

## 1.4.2 Osteoclasts and complement system interaction.

Osteoclasts, like mesenchymal stem cells and osteoblasts, express most of the complement components. The complement regulators like MAC-inhibitory protein (MACIF or CD59), C3aR and C5aR, and C3 are expressed by osteoclasts (Ignatius *et al*, 2011a). The third complement component has a vital role in osteoclastogenesis. It has been reported that osteoclast formation derived from mouse bone marrow was suppressed by blocking the C3 using anti-C3 antibody in osteoclast differentiation culture (Sato *et al*, 1993). Also, C3aR and C5aR blocking by anti- C3aR and C5aR antibodies showed significant inhibition of osteoclast formation (Tu *et al*, 2010). Further study revealed that osteoclast formation differentiated from C3<sup>-/-</sup> mice was less than WT mice (Sato *et al*, 1991). These studies suggested that C3, C3a, C5a and their receptors are essential for osteoclast formation.

M-CSF and RANKL are needed for efficient osteoclast differentiation, and the expression of M-CSF and RANKL were significantly less in C3<sup>-/-</sup> bone marrow cells treated with vitamin D3 than in cells from WT mice (Tu *et al*, 2010). The complement anaphylotoxins and their receptors (C3a, C5a, C3aR and C5aR) are essential for osteoclastogenesis (Tu *et al*, 2010). The osteoblast stimulation by IL-1 $\beta$  and C3a or C5a induce osteoclast-differentiating cytokine (RANKL) production by osteoblast to enhance osteoclast differentiation (Ignatius *et al*, 2011a). These studies show that the complement system components significantly interact with osteoclast formation and activation and therefore the complement system possibly contributes to the bone resorption process and affects the bone mineral density (Figure 1-5).

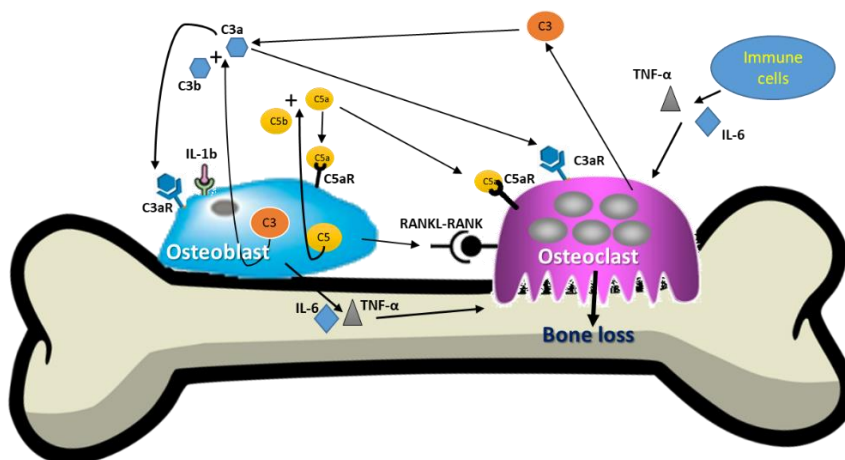


Figure 1-5: The interaction between the complement system and bone remodelling.

## **1.5 LDLR<sup>-/-</sup> mice as a hyperlipidaemic model, the effect of LDL and LDLR on bone mineral density.**

Bone loss is distinguished by decreasing bone formation (osteoblast number) and increased bone resorption. Recent evidence suggests that hyperlipidaemia may contribute to bone loss (osteoporosis), and lipid oxidation may be the mechanism underlying this process: it was suggested that oxidised lipoproteins inhibit the osteoblast formation and enhance osteoclast differentiation (Gharavi, 2002).

Since the LDLR is responsible for lipoprotein endocytosis, in the case of LDLR deficiency, the lipoproteins accumulate in extracellular space of vascular tissue (Sage *et al*, 2011). The extracellular lipoproteins are exposed to oxidative reactions to form oxidised lipoprotein by metabolic actions of smooth muscle, macrophages and osteoblasts. Since the bone and its marrow are vascularised, a similar process could happen in osteoporotic bones (Sage *et al*, 2011). Because the immature osteoblasts are located immediately adjacent to the sub-endothelial matrix of bone vessels, lipid accumulation in the sub-endothelial matrix would be expected to inhibit differentiation of the bone-forming cells (osteoblasts) by inhibiting different osteoblast differentiation factors such as alkaline phosphatase, collagen I and osteocalcin (Gharavi, 2002).

In addition, the oxidised lipids induce endothelial expression of monocyte chemotactic factors and M-CSF, a potent inducer of osteoblast differentiation released by lymphocytes, monocytes, fibroblasts, endothelial cells, myoblasts and osteoblasts. Oxidized lipids would be expected to promote bone resorption by recruitment and differentiation of osteoclast precursor cells (Parhami, Garfinkel and Demer, 2000).

There are several studies that have demonstrated that the decrease in bone mineral density (BMD) relates to bone loss mediated hyperlipidaemia. *In vitro* studies showed that lipoprotein oxidation inhibits osteoblast differentiation progenitor cells in mice (L. Wang *et al*, 2018; Ali *et al*, 2005). In addition, oxidised lipoproteins stimulate adipocyte differentiation markers like lipoprotein lipase (Moseti, Regassa and Kim, 2016). The accumulation of fat droplets in the cytoplasm of the cells decreases bone mineral density because oxidised lipid inhibits osteoblast differentiation (Parhami *et al*, 2001). Furthermore, an *in vivo* study has shown that in a mouse strain which loses a more

significant amount of bone mass in response to hyperlipidaemia, at the same time, plasma lipoproteins levels were increased (Parhami *et al*, 2001). It can be concluded that the absence of low-density lipoprotein receptor increased the lipoprotein (LDL) accumulation in bone tissue and conversion to oxidised-LDL by the oxidation reactions. The ox-LDL affects the bone remodelling process and induces bone reduction (Figure 1-6).

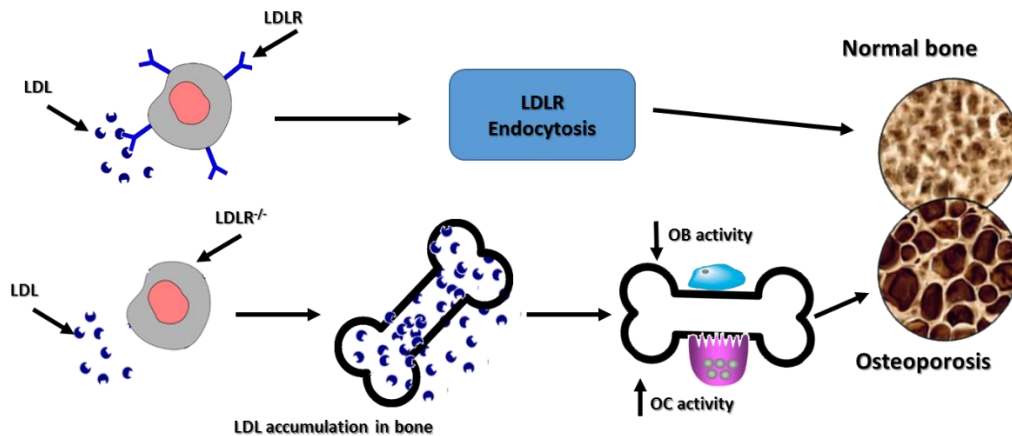


Figure 1-6: the effect of low-density lipoprotein receptor on bone mineral density.

## 1.6 Hypothesis.

Bone mineral density responds to changes in systemic inflammation.

## 1.7 Aims and Objectives.

1. Investigation of whether complement properdin could play an immunological role in the regulation of osteoclast activity which may induce bone microarchitecture change by maintaining bone mass (bone mineral density), this can be done by: -

❖ *In vivo*:

- Evaluation of bone mineral density using microcomputed tomography in properdin-deficient mice compared to wildtype at 6 or 10 months old.
- Evaluation of the bone remodelling activity by measuring the levels of serum osteoclast biomarker (TRACP activity) and serum osteoblast biomarker (ALP activity) in both genotypes.

❖ *In vitro*

- Quantify the osteoclast TRACP<sup>+</sup> numbers, resorption activity by differentiation of murine osteoclasts from WT and properdin knockout using the osteo-resorption assay.
2. To quantify whether lack of LDLR has an adverse effect on bone mineral density and Vitamin D3 dietary supplementation or voluntary exercising could influence the BMD in LDLR deficient mice, this can be done by: -

❖ *In vivo:*

- Quantifying the bone mineral density using  $\mu$ -CT in LDLR<sup>-/-</sup> mice compared to wildtype at six months old. Then, evaluation whether 11IU/g diet of Vitamin D3 or voluntary exercising for five weeks affects bone mineral density in LDLR<sup>-/-</sup> mice.
- Evaluation of bone remodelling activity in LDLR<sup>-/-</sup> mice fed a normal diet with or without Vitamin D3 supplementation or voluntary exercising by measuring the serum levels of osteoclast and osteoblast biomarkers.
- Quantifying the inflammatory response, (the alternative and classical pathway activation) by measuring the formation of C9 in mice serum. In addition, the serum proinflammatory cytokines TNF-alpha and IL-6 can be measured in LDLR<sup>-/-</sup> mice fed a normal diet with or without Vitamin D3 supplementation or voluntary exercising for five weeks.

❖ *In vitro:*

- To evaluate whether LDLR deficiency with or without Vitamin D3 addition could influence the osteoclast and osteoblast differentiation. This aim can be achieved by differentiating osteoclast and osteoblast treated with or without (4 $\mu$ g/ml of Vitamin D3) and derived from bone marrow from LDLR<sup>-/-</sup> compared to WT mice.
- To quantify whether LDLR deficiency could affect the osteoclast resorption activity and whether Vitamin D3 could affect this activity in LDLR<sup>-/-</sup> osteoclast cultures. The resorption area can be measured in osteoclast derived from LDLR<sup>-/-</sup> mice treated with or without Vitamin D3, in addition to measuring the TRACP activity in osteoclasts supernatants.
- To quantify whether LDLR deficiency could affect the osteoblast mineral deposition activity and whether Vitamin D3 could affect this activity in

LDLR<sup>-/-</sup> osteoblast cultures. This aim can be achieved by measuring the mineral deposition area of osteoclasts derived from LDLR<sup>-/-</sup> treated with or without Vitamin D3 using Von Kossa stain, in addition to measuring the ALP activity in osteoblasts supernatants.

3. To investigate whether murine osteoclasts contribute to alternative complement component expression. This can be done by: -

❖ *In vitro*:

- To investigate whether murine osteoclasts could cleave C5 to C5a, the osteoclasts could be differentiated and stimulated with purified C5 to find out the production of the C5/C5a protein using Western blotting and ELISA.
- To investigate the alternative complement component gene expression by murine osteoclasts, the gene expression of CFD, CFB, C3 and complement properdin can be investigated by qPCR.

4. To investigate whether Vitamin D3 addition could normalise the excessive alternative pathway component expression induced by fatty acid in osteoclasts. This aim can be by qPCR quantification of the gene expression of CFD, CFB, C3 and complement properdin in differentiated osteoclasts stimulated by fatty acid (FA) with or without Vitamin D3.

## **2 Chapter Two Methodology**

## **2.1 *In vivo* methods:**

### **2.1.1 The experimental animals and diets used in this project.**

#### **2.1.1.1 Mice used in this project:**

The mouse strains of C57BL/6 mice for all animal experimentation was performed in accordance with UK Home Office regulations and institutional guidelines. The mouse studies were periodically reviewed by the ethical review body of the institution. Mice were housed in a specific pathogen-free barrier facility in groups in ventilated cages at 21°C, 50% humidity, with 12/12 h light/dark cycle, and had *ad libitum* access to food and water.

For investigating the effect of properdin gene deletion on bone mineral density, two groups of males and females of wildtype and properdin-deficient mice six months old were used to measure the BMD and osteoclast activity *in vivo* and *in vitro*. The mice were maintained on 58R1 or normal diet (ND).

For investigating the effect of LDLR gene deletion on bone mineral density, two groups of males and females of wildtype and LDLR deficient mice six months old were maintained on 58R1 or normal diet. The LDLR deficient mice are homozygous for the *Ldlr*<sup>tm1Her</sup> mutation and have an elevated serum cholesterol level of 200-400 mg/dl, while the normal serum cholesterol in the mouse is 80-100 mg/dl.

The wildtype C57BL/6 mice were used to investigate the effect of 11IU/g chow of Vitamin D3 dietary supplementation or access to voluntary wheel exercise on bone mineral density whilst on high-fat diet feeding for five weeks. At the end, the revolutions of the wheel were recorded (6126276 revolution for males and 4555408 revolution for females).

At the end of each study, mice were bled under terminal anaesthesia, serum prepared, and organs saved for further measurements. Analyses were conducted blinded to the genotypes and treatment.

### 2.1.1.2 Diet used in this project:

The following table shows the components of diets.

**Table 2-1: The components of different diets.**

	Type of Diets						
	Normal Diet or Maintenance Diet (ND)		High-fat diet (HFD)		ND with Vitamin D3	HFD with Vitamin D3	HFD with exercise
Diet components	<b>58R1</b>	<b>5LF2</b>	<b>58R3</b>	<b>5TJN</b>	<b>MH516</b>	<b>58R3+VD</b>	<b>5TJN</b>
Proteins %	14.8%	14.3%	20.2%	18.0%	14.8%	20.2%	18.0%
Fat %	4.8%	2.5%	35.8%	19.8%	4.8%	35.8%	19.8%
Carbohydrate %	73.9%	65.2%	35.0%	51.3%	73.7%	35.0%	51.3%
Vitamin D3 IU/g chow	0.7 IU/g chow	1 IU/g chow	1 IU/g chow	1.2IU/g chow	11IU/g chow	11IU/g chow	1.2IU/g chow

### 2.1.2 Measuring the bone mineral density by computed tomography (M-CT).

#### A- Sample Fixation stage:

The lumbar spine of mice was harvested and preparing for  $\mu$ -CT scanning. After culling the animals, the skin was peeled, and all the viscera were removed from the abdominal and thoracic cavity as shown in (Figure 2-1A), the upper extremities and the head were removed as well. Then, the mice were labelled and attached to the flat thermacol board, and the ventral side was kept up uppermost fixing the samples by pins through the ribcage and feet. It is very important to keep the vertebrae as straight as possible when fixing to make the  $\mu$ -CT scanning easier and get the right anatomical position for image data (Figure 2-1 B).

Once the samples were fixed on the thermacol board, they were submerged in a container containing 10% formalin as a fixative solution overnight as shown in (Figure 2-1 C). Next day, the samples were washed twice by tap water. The lumbar vertebrae L1 - L5 were harvested using a scalpel or straight scissors: the cutting included the tops of the iliac bones to be used as a guide reference later during the scanning stage (Figure 2-1D).

The muscles and soft tissue were removed from the vertebral column make vertebral bones more visible: it is not necessary to remove all muscles. Then the vertebral samples were put in a 50ml falcon tube containing 70% IMS and kept at 4<sup>0</sup>C till scanning by  $\mu$ -CT machine.

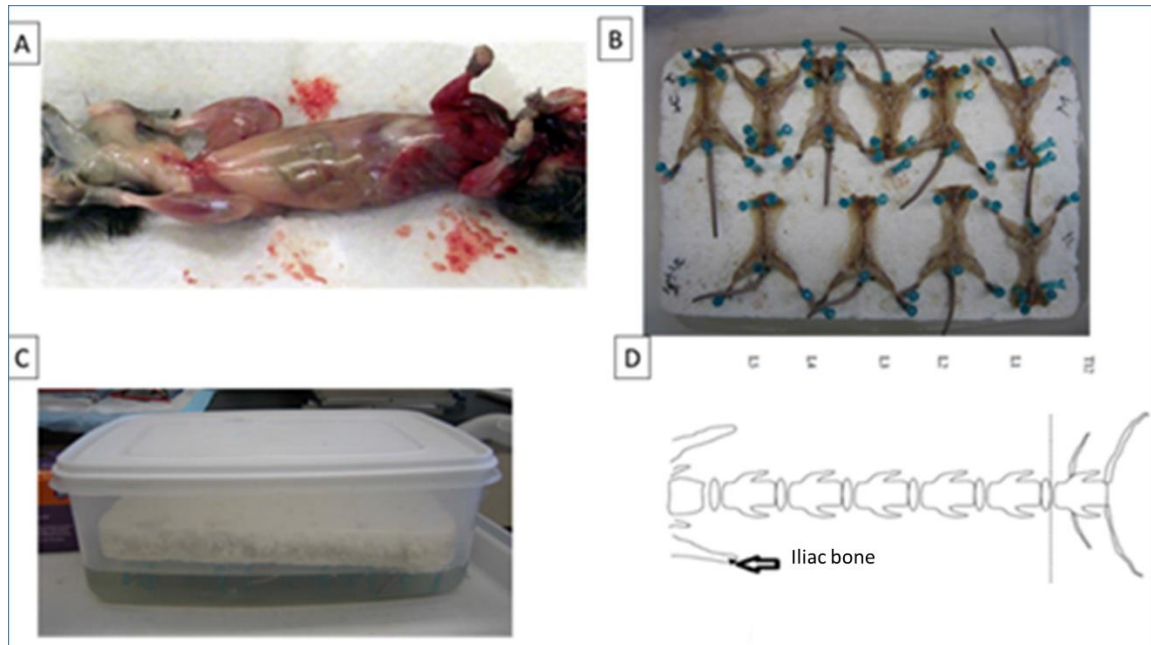


**Figure 2-1: The 3<sup>rd</sup> lumbar vertebrae harvesting and fixation preparation:**

Skin and viscera removing from a culled animal (A); lumbar spine fixation on thermacol board (B), Spine fixation by 10% formalin overnight (C), then lumbar vertebrae were cut as shown in (D).

### **B- Scanning stage:**

The scanning of vertebrae was the next stage of bone mineral density measurements. It was done using a Caliper Micro-CT machine in the Central Research Facility- University of Leicester (Figure 2-2A). One day before doing the scanning, the samples were put in 1x PBS overnight instead of 70%IMS. Then the samples were transferred to the CRF for data image scanning.

The spine was fixed in 1.5ml centrifuge tube filled by PBS avoiding bubbles (**before opening the Caliper Micro-CT machine gate, it is essential to make sure that the X-ray lamp is off, to be safe from the X-rays**). The sample was fixed onto the scanning table of the Micro-CT machine using blue tack sticker. Then, using PerkinElmer software, the samples were named or labelled using create sample tool.

The required vertebra (3<sup>rd</sup> lumbar vertebra) was centralised in the scanning square using the right, left, up and down controls on the Micro-CT machine and then fitted to the home position and the 90° position. The samples were scanned using 90 Voltage Peak (VPK),

80 $\mu$ A, fold of view (FOV 5) for 3 minutes. Then the scanning was saved as a DICOM file to analyse using Analyze 12.0 software (AnalyzeDirect.com) for BMA measurements.

**At this stage,** it is important to scan the phantom to create a standard curve of bone mineral density. The phantom was used to convert the grayscale numbers to BMD units (mg/cc). This conversion is accomplished by using a phantom of solid resin-embedded hydroxyapatite of known densities to generate a calibration line with concentrations (0, 50, 200, 800, 1200 mg/cc) of one rod for each concentration as shown in (Figure 2-2B). These densities were used to create a linear regression of measured grayscale value versus BMD as shown in (Figure 2-3). Then, the slope (Sigma-CT= 3.855) and offset (Beta-CT=935.1) values were recorded which were inserted into Analyze 12.0 software to generate the BMA values.

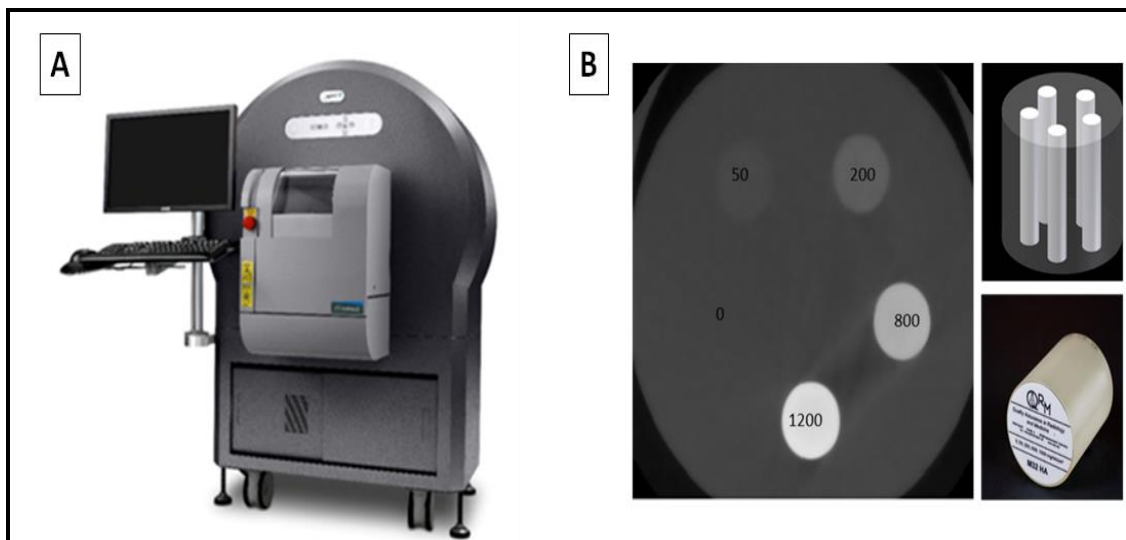


**Figure 2-2: The Calipare Micro tomography machine and the solid resin-embedded hydroxyapatite phantom that was used to convert the BMD grayscale.**

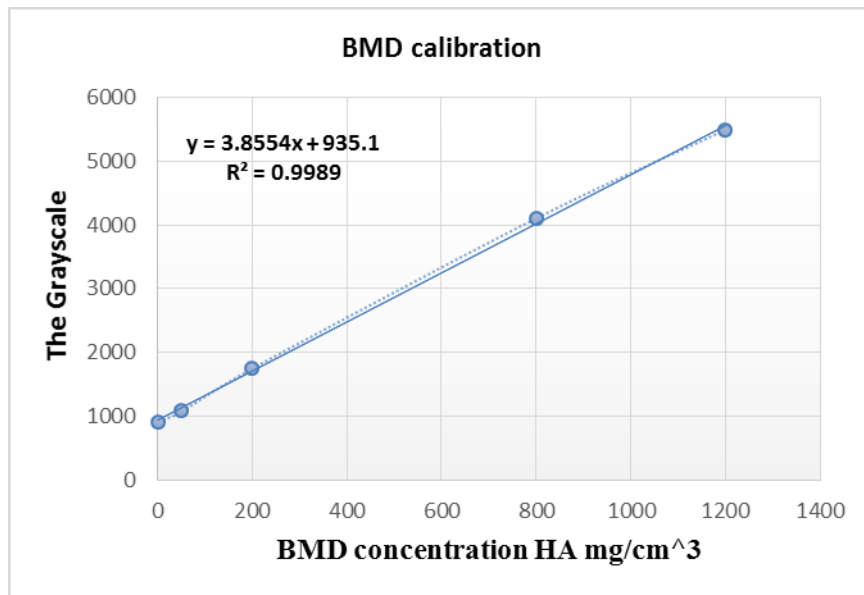


**Figure 2-3: Plot of grayscale values vs mineral density of phantom:**

The BMD scaling parameters (Sigma CT and Beta CT) were calculated for the proper conversion of CT or grayscale numbers to BMD units (mg/CC). The slope in the linear regression equation represents the Sigma CT value while the intercept in the Y equation represents Beta CT. These values are important to calibrate the BMD values to analyse image data of samples.

### **B- Bone Microarchitecture measurement stage: -**

Bone Microarchitecture (BMA) is the third stage of bone parameter measurement. It was done using specially developed software Analyze 12.0 (AnalyzeDirect.com) which is a powerful pre-clinical research application designed for the evaluation of micro-CT image data. This data generates an extensive set of bone-morphometric indices such as Bone mineral density, volumes, surface areas, ratios, Cortex indices, 3D Trabecular Thickness and its structure, connectivity, Trabecular separation and bone volume fraction (BV/TV). The BMA workflow was subdivided into two sections: Data Pre-processing and Bone Microarchitecture Analysis.

During the pre-processing data overview, the image data was uploaded on the workflow using the file option. Then, using the volume edit option, the body of the 3<sup>rd</sup> lumbar vertebra was extracted from accessory bones, cropped and filtered into the correct anatomical orientation to reduce data size and enhance initial object segmentation and saved as a pre-segmentation object map (Figure 2-4A-D).



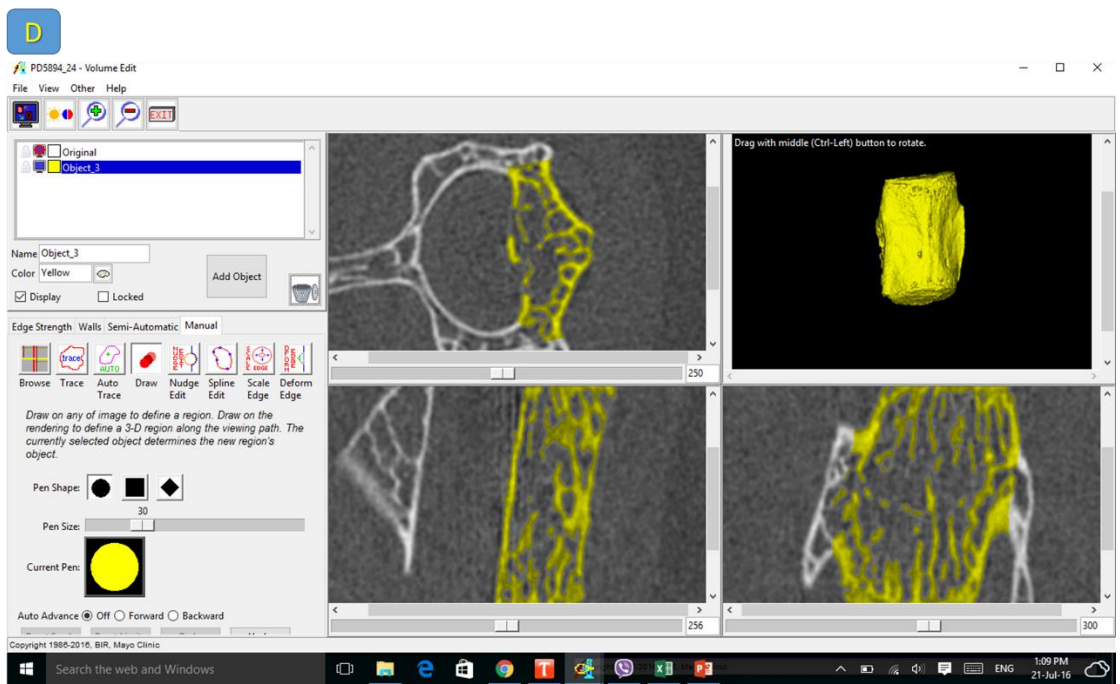
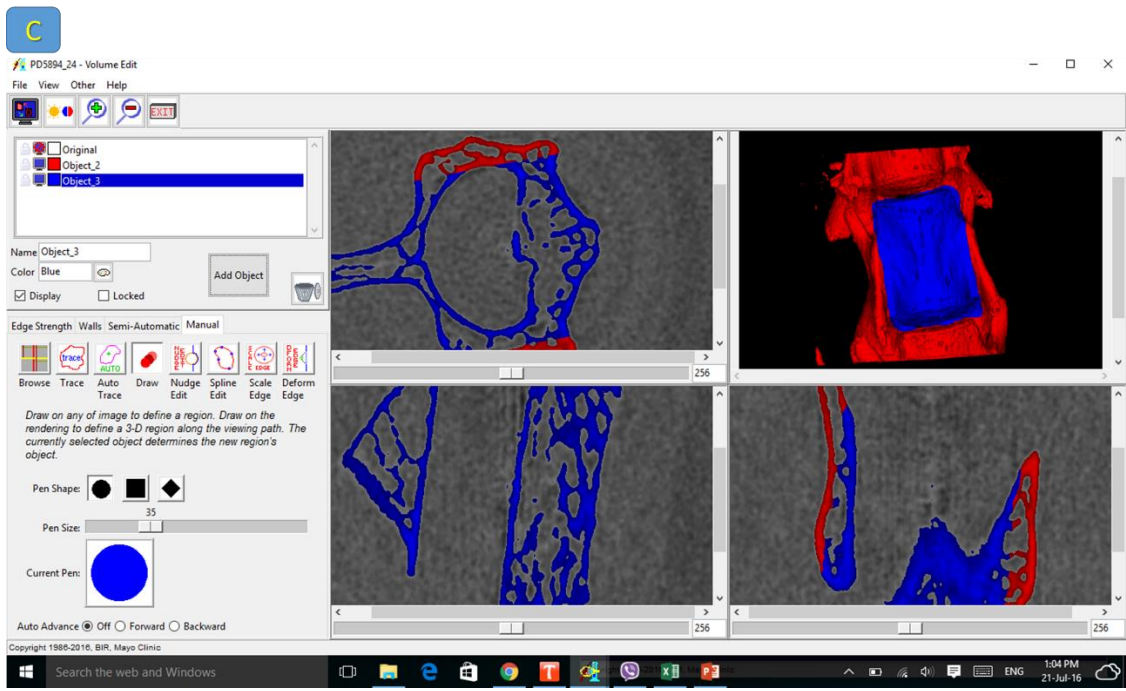
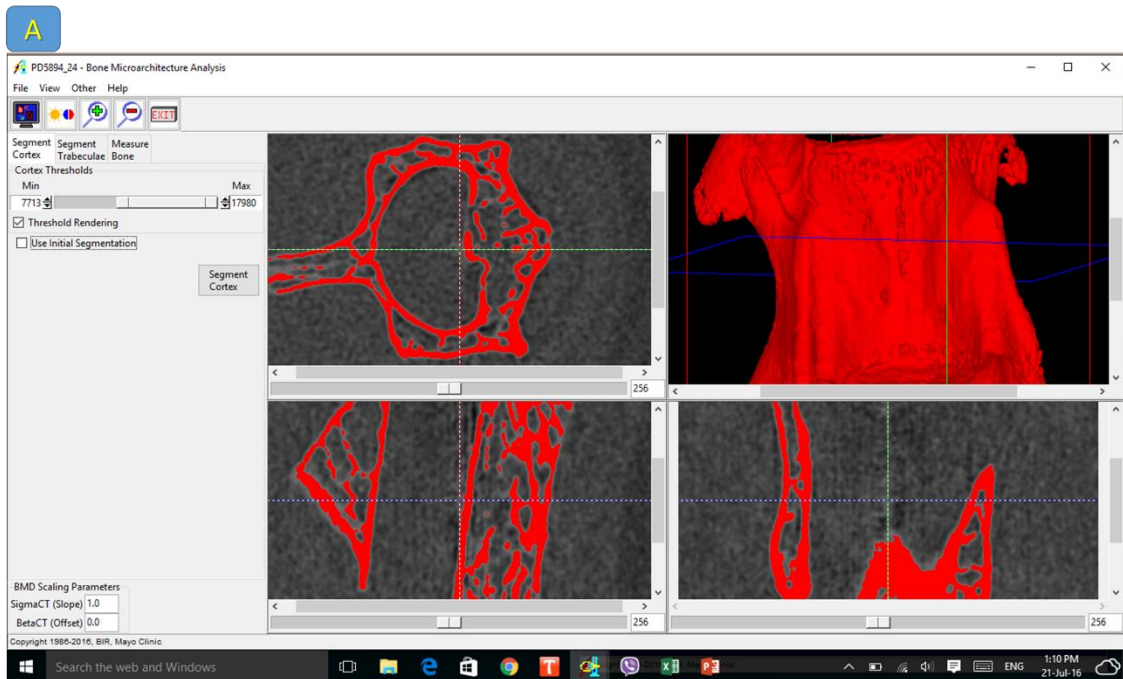


**Figure 2-4: Data processing and pre-segmentation:**

The image data were uploaded to the Analyze 12.0 add-on (A); image-data thresholding (B), the body of third lumbar vertebra determination (C). The 3rd lumbar vertebra body extraction from accessory bones (D).

The second part of the Bone Microarchitecture Analysis workflow is conducted within the BMA add-on module, and it is separated into three steps: Cortical Bone Segmentation, Trabecular Bone Segmentation, and Calculation of Bone Morphometric Indices.

1. **Cortical Bone Segmentation:** Once the image data is loaded, the BMA add-on conducted a preliminary segmentation which allowed the module to identify the cortical shell, cortical pores and Trabecular tissue regions. The initial object segmentation of the vertebral body was uploaded to the BMA add-on module indicating the bone of interest. This pre-segmentation was only used to avoid segmenting and measuring the other bones in the data image. It was thresholded with range 6500 min and 17980 maxima (Figure 2-5 A&B). The Cortex segmentation was done using the segment Cortex option on the BMA add-on model (Figure 2-5C). This step of data analysing is the longest step, and it could take one hour to segment the Cortex per mouse or sample.



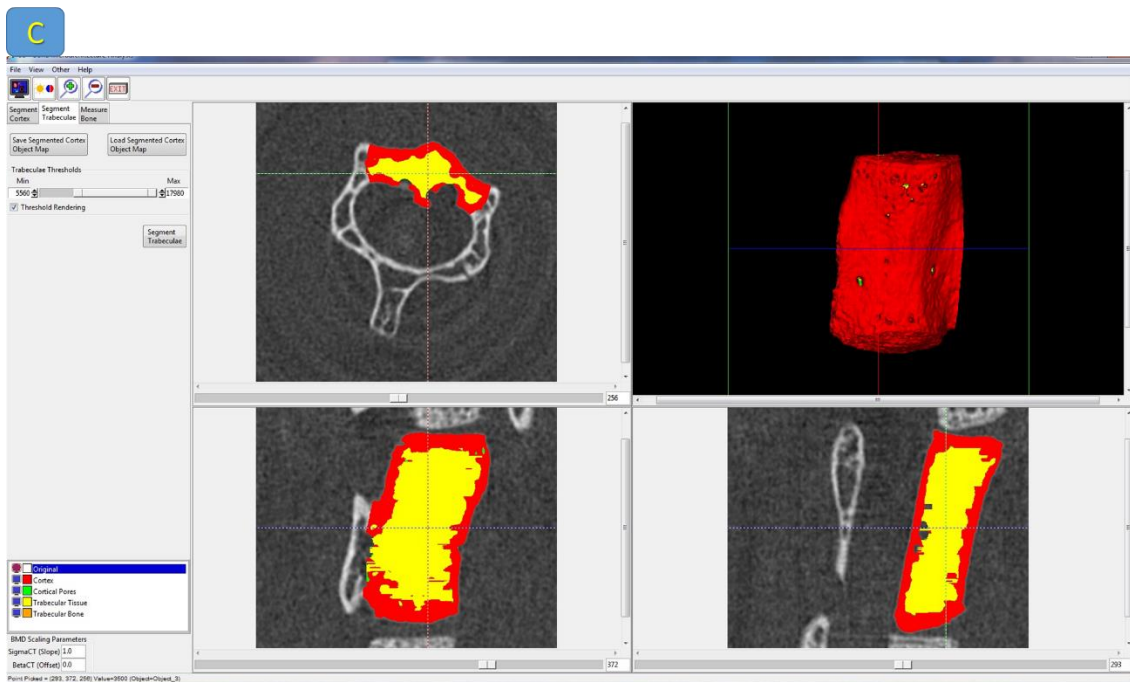
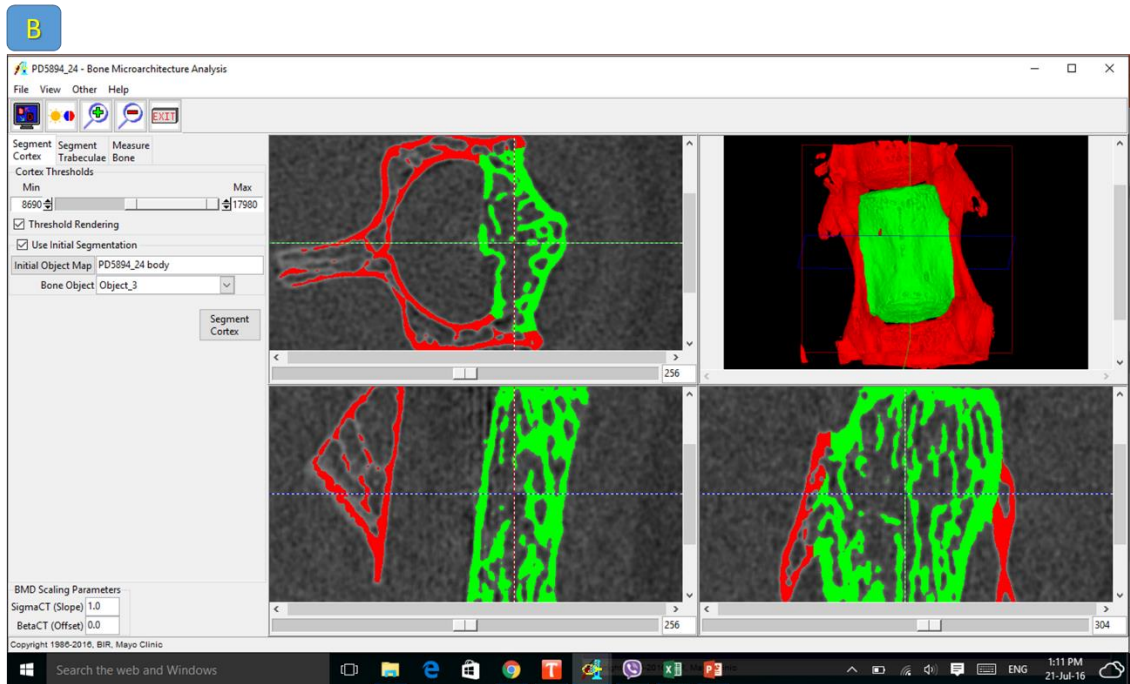


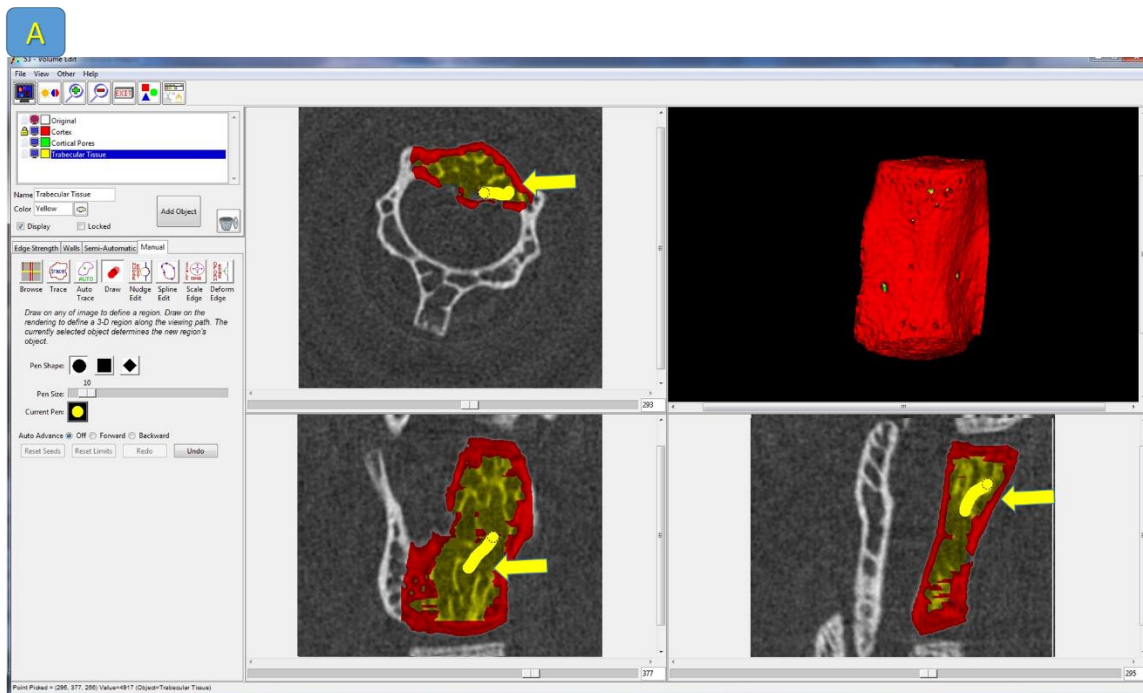
**Figure 2-5: bone cortical segmentation:**

The initial object map of the 3rd lumbar vertebra was uploaded (A), it was thresholded to segment just the bone of interest (vertebral body) (B), the Cortex was segmented (red colour), and the yellow colour refers to Trabecular tissue (C).

Once the Cortex segmentation was done; it is essential to navigate through image slices (512 slices) to visually review the segmentation result to evaluate the quality. If the result is acceptable, then processing can continue to the second step in the BMA processing workflow, Segment Trabeculae. However, if the segmentation result requires manual refinement, then this can be done by refining the object map using Volume Edit, available

within Analyze 12.0. After the cortex segmentation, 1-3% of slices had to be corrected in this way.

The manual refinement means the reassignment of incorrectly labelled bone structures as a Cortex in the Trabecular tissue region (Figure 2-6A&B). This can be done by using the draw tool of the Trabecular tissue (yellow colour pointed by arrows) and pass through all slices on transverse, sagittal and coronal sections to reassign the Trabecular tissue in each slice. Again, this process takes a long time because each section needs to be refined.



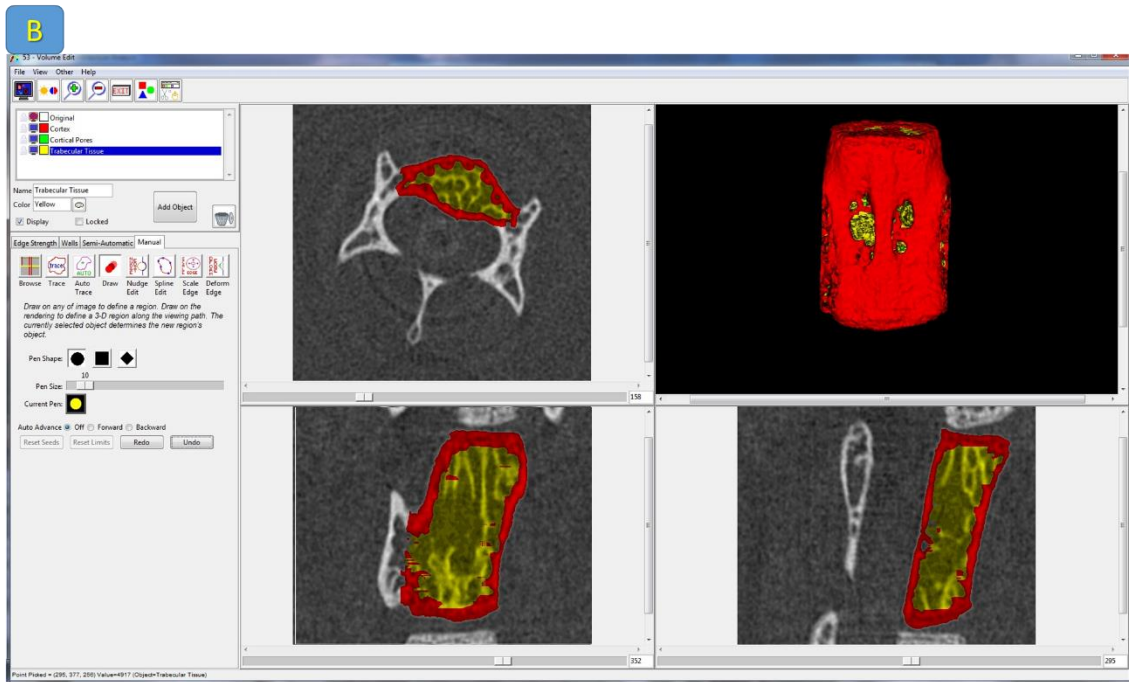
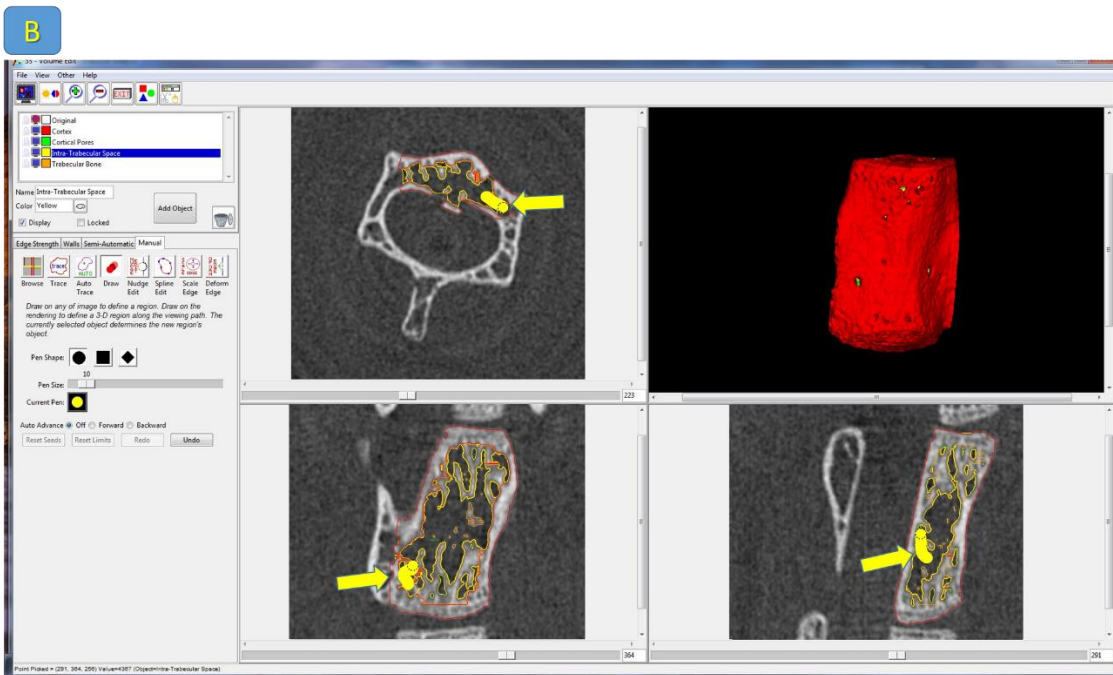
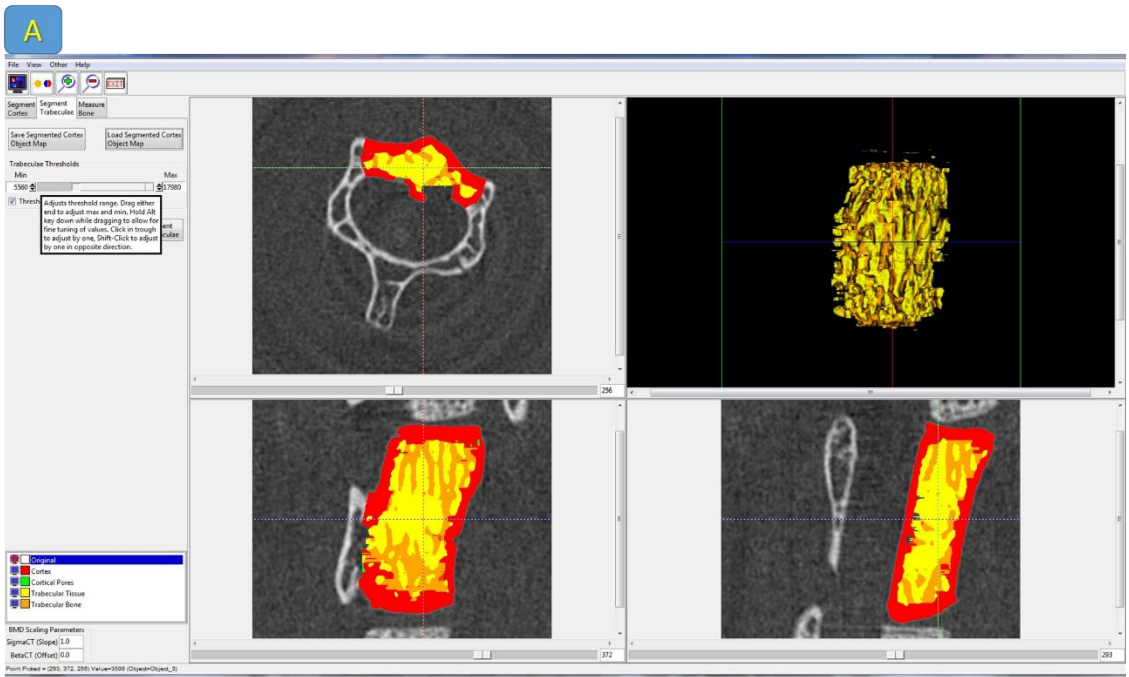


**Figure 2-6: Bone Cortex refinement:**

The panel (A) refers to the reassignment of incorrectly labelled bone structures as a Cortex in the Trabecular tissue region (yellow arrow), this can be done using the circle draw tool to correct Trabecular tissue. (B) Refers to refined Trabecular tissue in each slice.

2. **Trabecular Bone Segmentation:** This is the second step of the BMA process provide for segmentation of the Trabecular region into Trabecular Bone and Intra-Trabecular Space. After the Cortex segmentation or its correction, the vertebral body was thresholded again. The same range of Cortex thresholding was used. The Trabecular bone segmentation was done using segment trabecula option (Figure 2-7 A).

At this point, it is necessary to visually review the segmentation result to determine if the Trabecular bone segmentation is acceptable or it needs to manual corrections and refinement. The manual correction of small regions of Trabecular bone identified as Cortex will improve the accuracy of the measurements generated by the BMA add-on module (Figure 2-7 B&C).



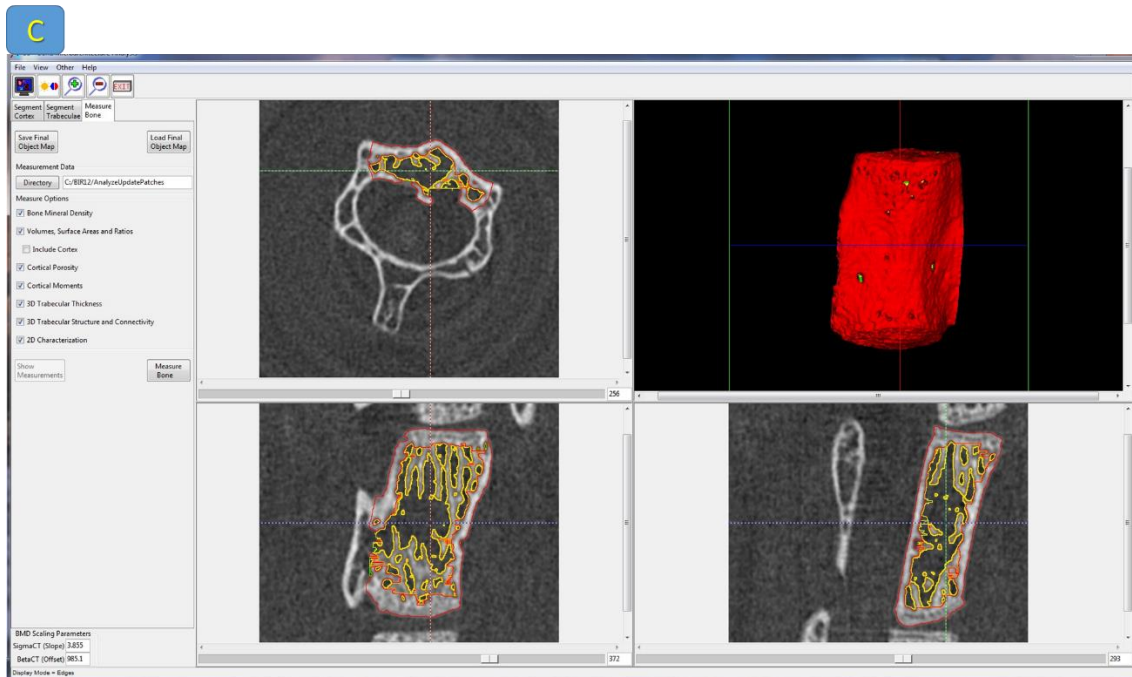


**Figure 2-7: The segmented trabecula refinement:**

The segmented trabecula of the vertebral body after Cortex segmentation (A), the manual correction of small regions of Trabecular bone identified as Cortex will improve the accuracy of the measurements (B&C).

3. **Calculation of Bone Morphometric Indices:** This is the third and final step of the BMA processing workflow. It is the generation of the bone-morphometric indices. The measurements are automatically calculated for the Trabecular and cortical bone and output in several values including the BMD (Figure 2-8).

File	slice	angle	measurement	value	units
PD5893_23	all	all	BoneMean BMD	2569.60	mg/cc
PD5893_23	all	all	BoneStd BMD	236.38	mg/cc
PD5893_23	all	all	BoneVolume	1.86	mm <sup>3</sup>
PD5893_23	all	all	CortexMean BMD	2786.07	mg/cc
PD5893_23	all	all	CortexStd BMD	250.91	mg/cc
PD5893_23	all	all	CortexVolume	0.69	mm <sup>3</sup>
PD5893_23	all	all	IntraTrabecularMean BMD	1307.79	mg/cc
PD5893_23	all	all	IntraTrabecularStd BMD	179.34	mg/cc
PD5893_23	all	all	IntraTrabecularVolume	2.74	mm <sup>3</sup>
PD5893_23	all	all	TrabeculaeMean BMD	2441.14	mg/cc
PD5893_23	all	all	TrabeculaeStd BMD	85.82	mg/cc
PD5893_23	all	all	TrabeculaeVolume	1.17	mm <sup>3</sup>
PD5893_23	all	all	TrabecularTissueMean BMD	1646.66	mg/cc
PD5893_23	all	all	TrabecularTissueStd BMD	410.31	mg/cc
PD5893_23	all	all	TrabecularTissueVolume	3.91	mm <sup>3</sup>
PD5893_23	all	all	WholeMean BMD	1818.37	mg/cc
PD5893_23	all	all	WholeStd BMD	421.33	mg/cc
PD5893_23	all	all	WholeVolume	4.61	mm <sup>3</sup>
PD5893_23	all	all	TV	4.65	mm <sup>3</sup>
PD5893_23	all	all	BV	1.86	mm <sup>3</sup>
PD5893_23	all	all	BS	62.35	mm <sup>2</sup>
PD5893_23	all	all	BV/TV	40.08	%
PD5893_23	all	all	BS/TV	13.40	mm <sup>-1</sup>
PD5893_23	all	all	BS/BV	33.43	mm <sup>-1</sup>
PD5893_23	1	all	/ap	0.0000	mm <sup>-4</sup>
PD5893_23	1	all	/ml	0.0000	mm <sup>-4</sup>
PD5893_23	1	all	/max	0.0000	mm <sup>-4</sup>
PD5893_23	1	all	/min	0.0000	mm <sup>-4</sup>
PD5893_23	1	all	J	0.0000	mm <sup>-4</sup>
PD5893_23	2	all	/ap	0.0000	mm <sup>-4</sup>
PD5893_23	2	all	/ml	0.0000	mm <sup>-4</sup>
PD5893_23	2	all	/max	0.0000	mm <sup>-4</sup>
PD5893_23	2	all	/min	0.0000	mm <sup>-4</sup>
PD5893_23	2	all	J	0.0000	mm <sup>-4</sup>
PD5893_23	3	all	/ap	0.0000	mm <sup>-4</sup>
PD5893_23	3	all	/ml	0.0000	mm <sup>-4</sup>
PD5893_23	3	all	/max	0.0000	mm <sup>-4</sup>
PD5893_23	3	all	/min	0.0000	mm <sup>-4</sup>
PD5893_23	3	all	J	0.0000	mm <sup>-4</sup>
PD5893_23	4	all	/ap	0.0000	mm <sup>-4</sup>

**Figure 2-8: Bone morphometric indices:**

After the cortex and trabecular segmentation have been finished, the bone microarchitecture parameters have been generated and each tab refers to different sets of measurements.

The Bone density or bone mineral density (BMD) is the amount of bone mineral in bone tissue especially Calcium salt and phosphate components. Bone density measurement is used in clinical medicine as a method for the detection of osteoporosis (bone density loss). It is measured by a procedure called densitometry, often performed in Radiology using X-ray, generating cross-sections of bone that can be used to recreate a virtual model (3D model). The lumbar spine and femur are most generally used to measure bone mineral density (Mautalen *et al*, 2016). The following parameters contribute to diagnosing bone density loss or osteoporosis in addition to bone mineral density (BMD):

-

- 1-Whole Bone mineral density (BMD) which include: Bone Mean BMD, Cortex Mean BMD, Trabecular Mean BMD, Intra Trabeculae BMD (Figure 2-9).
- 2-Trabecular Thickness (Tb.Th. mm): It is the mean thickness of one trabecula. A decrease in the strength of Trabecular bone with ageing in men is usually associated with a decrease in Tb.Th.
- 3-Trabecular separation (Tb.Sp. mm): It is the mean distance between trabeculae as determined by a 3D sphere-fitting method. Tb.Sp. is sometimes called Trabecular spacing. Higher Tb.Sp. is associated with vertebral fracture and bone density loss.
- 4-Connectivity density (Conn.D  $1/\text{mm}^3$ ) is a measure of the degree of connectivity of trabeculae, normalised to the total volume. Conn.D contributes to bone strength and decreases significantly with age in the femoral neck and vertebra.
- 5-Bone volume fraction (BV/TV %) is the ratio of the segmented bone volume to the total volume of the region of interest. Trabecular BV/TV has been found to be lower in patients who have sustained a vertebral fracture. BV/TV decrease is a diagnostic parameter of osteoporosis with age in both women and men.

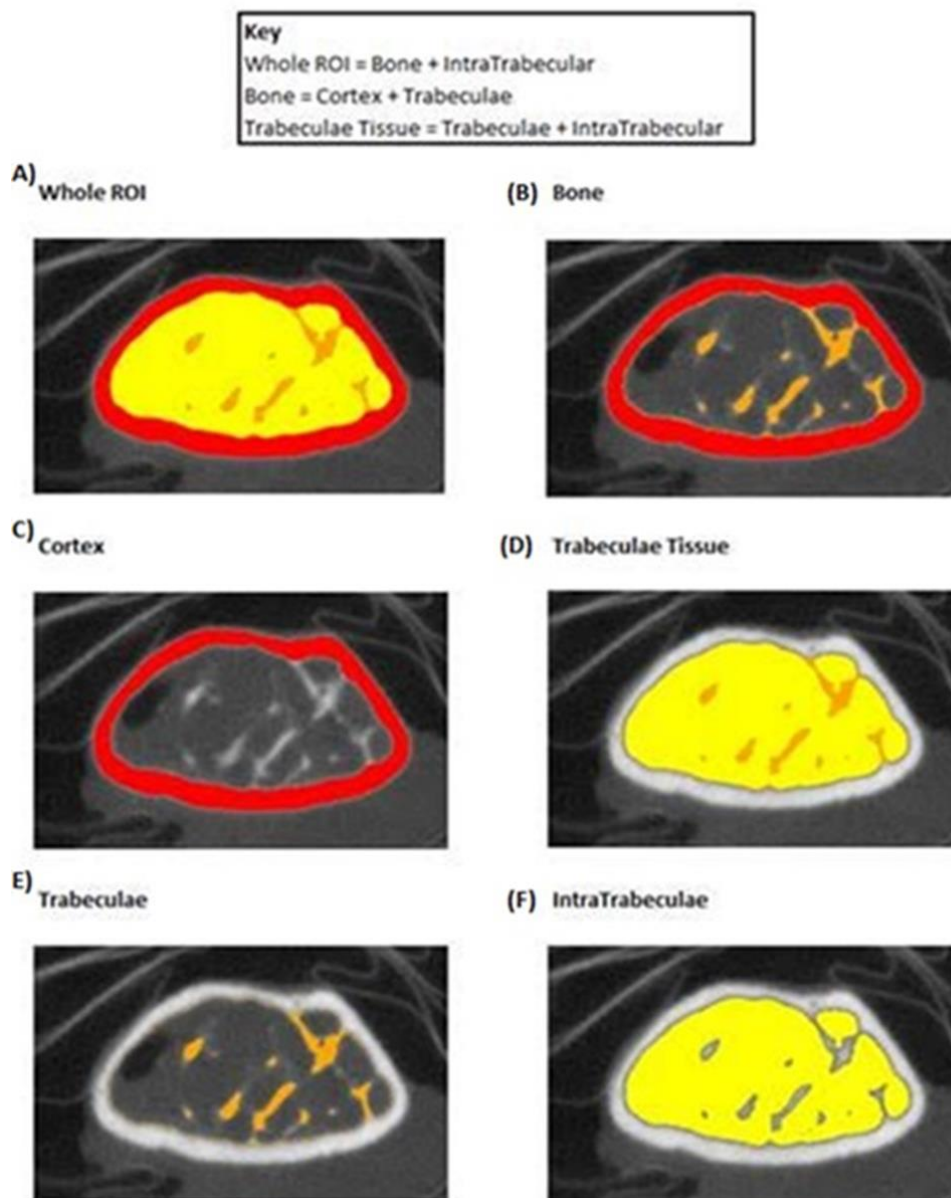


**Figure 2-9: Examples of bone mineral density parameters:**

(A)-Whole mean bone mineral density (red and yellow in colour), (B) Bone mean mineral density (Cortex and trabeculae), (C) the bone Cortex mineral density (red colour), (D) the Trabecular tissue (trabecula and Intra-Trabecular (yellow colour), (E) Trabecula (Orange colour), (F) Intra-Trabecular mean density.

The Figure 2-10 represents the experimental flow for measuring the bone mineral density of different experiments.

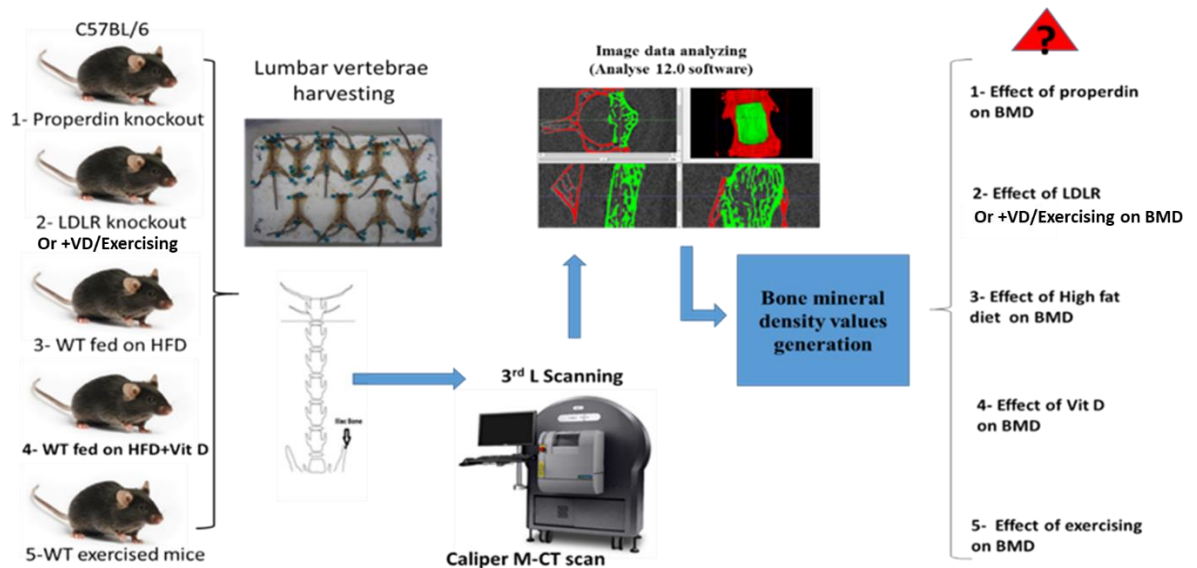


Figure 2-10: The general experimental flow for measuring bone mineral density.

### 2.1.3 Measuring osteoclast activity (Tartrate-resistant acid phosphatase, TRACP) by ELISA.

The level of TRACP was measured in serum or supernatant to quantify the osteoclast activity. TRACP or acid phosphatase (AP) is a specific biochemical marker for osteoclast activity, TRACP is a member of the hydrolase class of enzymes, and it can be found in both plant and animal species. The assay was performed using the Acid Phosphatase Colorimetric Assay Kit (Caymanchem, 10008051).

The serum samples were prepared by collecting blood from the mice without using an anticoagulant tube. The blood was left to clot for 30 minutes on ice; then blood was centrifuged at 2,000 g for 15 minutes at 4°C. The top yellow serum layer was pipetted off without disturbing the white buffy layer, and serum was stored on ice.

The supernatants of differentiated osteoclasts were collected and centrifuged at 200g for 5 minutes; then the supernatant was transferred into a new tube and stored at -80 till use.

The principle of this assay depends on utilising para-nitrophenyl phosphate (pNPP) as a chromogenic substrate for the enzyme. In the first step, TRACP dephosphorylates pNPP. In the second step, the phenolic OH-group is deprotonated under alkaline conditions

resulting in p-nitrophenolate that yields an intense yellow colour which can be measured at 405-414 nm.

The reagents were prepared following kit manufacturer's instructions. Acid phosphatase assay buffer (1X) (100mM HEPES, pH 5.0) was prepared from acid phosphatase assay buffer (10X) by diluting 5 ml of Assay Buffer with 45 ml of HPLC-grade water. This buffer was used for the dilution of samples and dissolving the acid phosphatase substrate. The acid phosphatase substrate was prepared by dissolving two tablets in 3 ml of diluted Assay Buffer. The acid Phosphatase Stop Solution of 500mM sodium hydroxide was prepared by diluting 15 ml of acid Phosphatase Stop Solution 2M with 45 ml (dilution 1:3) of HPLC-grade water. A lyophilised powder of wheat germ acid phosphatase (AP) was used as a positive control for acid phosphatase: the powder was dissolved with 2 ml of diluted Assay Buffer and was stored on ice.

The 96-assay plate was set up with blank wells by adding 30  $\mu$ l of assay buffer to two wells, serum blank wells by adding 10 $\mu$ l of assay buffer and 20 $\mu$ l of serum or supernatant to two wells per sample. The positive control wells (Acid Phosphatase) was set up by adding 10 $\mu$ l of assay buffer and 20 $\mu$ l of acid phosphatase (control) to at least two wells. Then, the sample wells were set up by adding 10 $\mu$ l of assay buffer and 20 $\mu$ l of the sample to each well being used. Then, the reaction was initiated by adding 20 $\mu$ l of TRACP substrate solution to each well which was being assayed except serum blank wells. The plate was covered with the plate cover and incubated for 20 minutes at 37°C. Then, the plate cover was removed, and 100  $\mu$ l of diluted stop solution was added to each well and 10  $\mu$ l of TRACP Substrate Solution was added to the serum blank wells. Finally, the absorbance of the assay plate was read at 405 nm using a plate reader.

The average absorbance of the blanks, positive control, and each sample was calculated. The average absorbance was subtracted from the blank from all samples and the positive control; the adjusted absorbance was used in the equation below. The serum blanks were used for correcting serum samples. One unit is the amount of the acid phosphatase required to release 1  $\mu$ mol of phosphate from pNPP in one minute at 37°C. The acid phosphatase activity of the samples was calculated using the following equation.

$$AP \text{ activity } (\mu\text{mol}/\text{min}/\text{ml}) = \frac{\Delta A_{405}}{[20\text{min} * 10.68\text{mM}]} * \frac{0.15\text{ml}}{0.02\text{ml}} * \text{Sample Dilution}$$

#### **2.1.4 Measuring osteoblast activity (Alkaline phosphatase activity) by ELISA.**

The level of the C-terminal peptide of bone-specific alkaline phosphatase was measured to quantify osteoblast activity using Mouse C-terminal peptide of bone-specific alkaline phosphatase ELISA kit (NeoBiotech, NB-34-016069).

Bone alkaline phosphatase (ALP) is the bone-specific isoform of alkaline phosphatase, a glycoprotein that is found on the surface of osteoblasts; ALP reflects the biosynthetic activity of these bone-forming cells. ALP has been shown to be a sensitive and reliable indicator of bone metabolism (Kress, 1998). The serum samples and the osteoblast supernatants were prepared as shown in [section 2.1.3](#).

The ELISA kit reagents were prepared following the manual instructions. 100-fold dilution of Biotin-antibody (1x) was prepared from Biotin-antibody (100x) as a detecting antibody [10µl of Biotin-antibody (100x) + 990µl of Biotin-antibody Diluent]. HRP-avidin (1x) was prepared for detecting biotinylated antibodies [100-fold dilution is 10µl of HRP-avidin + 990µl of HRP-avidin Diluent]. 20ml of Wash Buffer Concentrate (25x) was diluted into deionized or distilled water to prepare 500ml of Wash Buffer (1x) [1:25 dilution].

The standard vial was centrifuged at 6000-10000 rpm for 30 seconds then the standard was reconstituted with 1.0ml of Sample Diluent: this reconstitution produces a stock solution of 50mU/ml. The standard was mixed to ensure complete reconstitution and it was left to sit for a minimum of 15 minutes with gentle agitation prior to making dilutions. Then, 250µl of Sample Diluent was pipetted into each tube (S0-S6). The stock solution was used to produce a 2-fold dilution series. Each tube was mixed thoroughly before the next transfer. The undiluted Standard serves as the high standard (50mU/ml) and the Sample Diluent serves as the zero standard (0mU/ml).

The sandwich ELISA assay was performed following the manufacturer instructions. Serum samples were objected to 4-fold dilution into Sample Diluent,

A 100µl/well aliquot of standard and sample were added to the microplate wells, after a specific antibody for a C-terminal peptide of bone-specific alkaline phosphatase had been pre-coated onto a microplate as a capture antibody. The plate was covered with the adhesive strip provided by the kit and incubated for 2 hours at 37°C. Then the liquid was

removed from each well (not washed). A 100µl aliquot of Biotin-antibody (1x) was added to each well and covered with a new adhesive strip and incubated for 1 hour at 37°C.

The liquid was aspirated from each well and washed by filling each well with Wash Buffer (200µl) using a multi-channel pipette and it was stood for 5 minutes: the process was repeated two times for a total of three washes. The complete removal of liquid at each step is essential to good performance. After the last wash, the remaining wash Buffer was removed by aspirating or decanting. Then, the plate was inverted and blotted against clean paper towels. A 100µl aliquot of HRP-avidin (1x) was added to each well and the microtiter plate was covered with a new adhesive strip and incubated for 1 hour at 37°C. Then, the aspiration/wash process was repeated for five times as before. A 90µl TMB Substrate was added to each well and incubated for 15-30 minutes at 37°C (protecting from light). A 50µl Stop Solution was added to each well and the plate was gently mixed. The optical density was determined of each well within 5 minutes, using a microplate reader set to 450 nm.

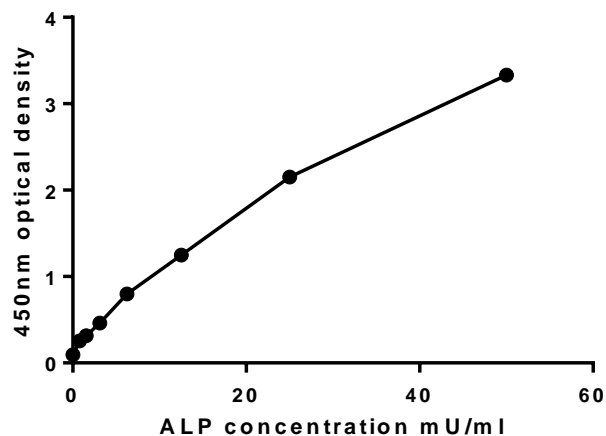


**Figure 2-11: Example standard curve showing the absorbance of different concentrations of mouse C-terminal of bone alkaline phosphatase (ALP).**

### **2.1.5 Osteocalcin level measurement as a bone formation marker:**

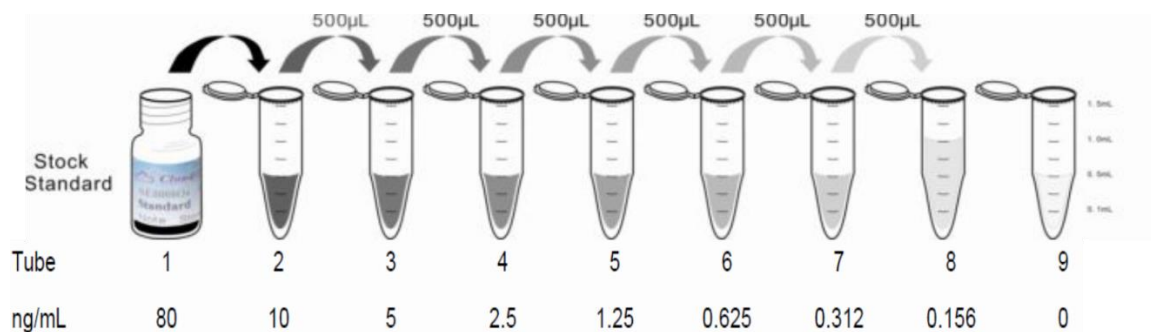
Osteocalcin, a bone gamma-carboxyglutamic acid protein (BGLAP), is a noncollagenous protein hormone in bone and dentin. Osteocalcin is produced solely by osteoblasts and plays a part in bone mineralization and calcium ion homeostasis. As osteocalcin is produced by osteoblasts, it is often used as a biomarker for the bone formation process.

It has been observed that higher serum-osteocalcin levels are relatively well correlated with increased bone mineral density (BMD) (Bharadwaj *et al*, 2009; Lee *et al*, 2007).

The level of osteocalcin in mouse serum was measured to quantify osteoblast functional activity in bone mineral deposition using Enzyme-linked Immunosorbent Assay Kit for Osteocalcin (OC) (Cloud-Clone Crop, SEA471Mu).

The serum was prepared as shown in [section 2.1.3](#). Then, the Enzyme-linked Immunosorbent Assay for Osteocalcin (OC) was performed following the manufacturer's instructions.

The stock standard solution (80ng/mL) was prepared by reconstituting the standard with 1.0mL of standard diluent and kept for 10 minutes at room temperature, shaken gently (not to foam). Then, 7 points of diluted standard such as 10ng/mL the highest standard, was prepared, then a double dilution series (5ng/mL, 2.5ng/mL, 1.25ng/mL, 0.625ng/mL, 0.312ng/mL, and 0.156ng/mL) in standard diluent were mixed thoroughly before the next transfer. The last EP tube with Standard Diluent is the blank as 0ng/ml.



The microplate provided in this kit had been pre-coated with an antibody specific to osteocalcin.

Wells for diluted standard, blank and sample were set up (7 wells for standard, 1 well for blank were prepared). Then, 100µl aliquot each of dilutions of standard, blank and samples were added into the appropriate wells, the plate was covered with sealer and incubated for 1 hour at 37°C. The liquid of each well was removed (washing not needed). Then, 100µl aliquot of Detection Reagent A working solution (1:100-fold dilution) was added to each well, the wells were covered with new plate sealer and incubated for 1 hour at 37°C. The solution was aspirated and washed with 350µL of 1× wash solution to each well using a multi-channel pipette and left to sit for ~5 minutes. The remaining liquid was removed from all wells completely by snapping the plate onto absorbent paper. In

total wash 3 times. After the last wash, any remaining wash buffer was removed by inverting the plate against absorbent paper. Then, 100µl aliquot of Detection Reagent B with working solution (1:100-fold dilution) was added to each well; the wells were covered with the plate sealer and incubated for 1 hour at 37°C. The aspiration/wash process was repeated in total 5 times as before. Then, 90µL of Substrate Solution (TMB) was added to each well and covered with a new plate sealer, incubated for 10 - 20 minutes at 37°C (no more than 30 minutes). Then, 50µL of Stop Solution was added to each well for stopping the reaction. Then, the plate was run through the microplate reader at 450nm immediately.

Average of triplicate readings for each standard, control, and samples were made after subtracting the average zero standard optical density. A standard curve was constructed by plotting the mean of optical densities and concentration for each standard and drawing a best fit curve through the points on the graph GraphPad Prism 7.

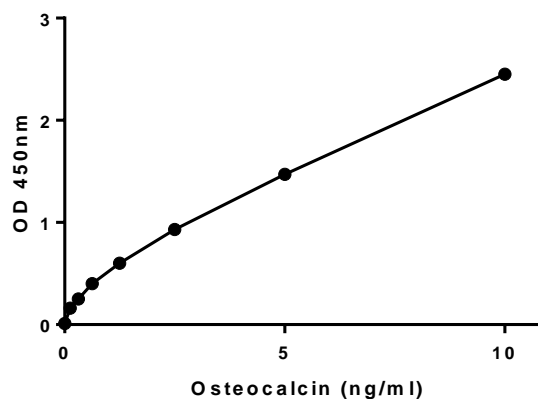


**Figure 2-12: Example for the standard curve showing the absorbance of different concentrations of mouse Osteocalcin.**

### **2.1.6 Serum triglyceride level measurements.**

The principle of this method to determine triglyceride concentrations is an enzymatic hydrolysis of triglyceride to glycerol and free fatty acid followed by colorimetric assay measurement of the glycerol released. Therefore, the level of triglyceride using Triglyceride colorimetric assay kit (Cayman, 10010303) was measured in mouse serum.

The standard curve dilutions were prepared by labelling eight clean test tubes A-H. 200 µl of (1X) diluted Standard Diluent was added to tubes B-H. Then, 400 µl of diluted Standard Diluent was added to tube A, then, 100 µl of Triglyceride Standard

was added to tube A and mixed thoroughly. The concentration of tube A is 200 mg/dl (2.26 mmol/L). Serially, the standard was diluted by removing 200  $\mu$ l from tube A and added it to tube B; and mixed thoroughly. Next, 200  $\mu$ l was removed from tube B and placed it into tube C; and mixed thoroughly. This process was repeated for tubes D-G. Tube H only has diluted Standard Diluent and is used as the blank (Table 2-2).

**Table 2-2: Preparation of Triglyceride Standards**

Tube	Triglyceride Concentration (mg/dl)
A	200
B	100
C	50
D	25
E	12.5
F	6.25
G	3.125
H	0

The assay was performed by adding 10 $\mu$ l serum samples or standard (tubes A-H) to the designated wells for the standard curve on the 96 well-plate, in triplicates. The reaction was initiated by adding 150 $\mu$ l of diluted Enzyme Mixture solution to each well (the vial contains a lyophilized enzyme mixture which was reconstituted with 14 ml of the diluted Assay Buffer, a 50mM sodium phosphate, pH 7.2). The plate was carefully shaken for a few seconds to mix and then it was covered with the plate cover and incubated for 15 minutes at room temperature. Then, the absorbance was measured at 530-550 nm using a plate reader.

The average absorbance of each standard and sample was calculated. The absorbance value of the standard H (0 mg/dl) was subtracted from itself and all other values (both standards and samples): this is the corrected absorbance. The corrected absorbance values were graphed as a function of the final triglyceride concentration (mg/dl) (Table 2-2) using GraphPad Prism 7.0 software.

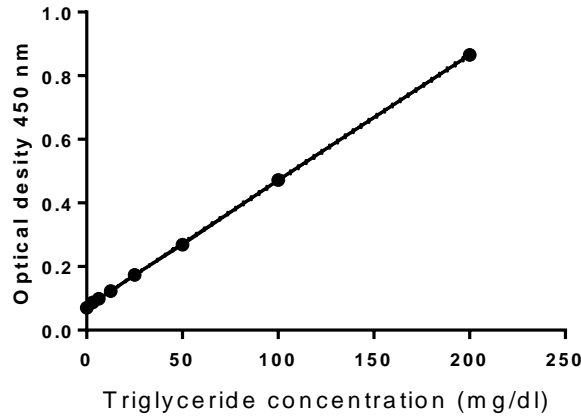


**Figure 2-13: Example for the standard curve showing the absorbance of different concentrations of Triglyceride (the optical density is 450nm).**

### **2.1.7 Measuring the functional activities of alternative and classical complement pathways by ELISA.**

To quantify the levels of classical complement and alternative pathway activation in mouse serum, the level of complement C9 formation was measured as in a recently published paper on mice (Kotimaa *et al*, 2015).

For measuring the CP pathway, the human IgM purified immunoglobulin was coated at 1µg/ml in coating buffer (100mM Na<sub>2</sub>CO<sub>3</sub>, pH 9.6) (diluted 1:1000). For measuring the AP pathway, LPS was coated at 1µg/ml in PBS/10mM MgCl<sub>2</sub> (diluted 1:1000).

For the classical pathway, the samples were diluted in BVB++ buffer (1x veronal buffer, 0.5mM MgCl<sub>2</sub>, 2mM CaCl<sub>2</sub>, 0.05% tween 20, 1% BSA, pH 7.5). For the Alternative pathway, the samples were diluted in BVB++/MgEGTA (BVB++, 10mM EGTA, 5mM MgCl<sub>2</sub>). The final sample volume was 100µl per well in triplicate.

The Maxisorp plates were incubated as needed regarding the pathway measurement for 16h at 4°C overnight. Then, the wells were washed with 200µl of 0.05% Tween-20 in PBS washing buffer (3 times, 5 minutes). The wells were blocked with 150µl of blocking buffer (1% BSA in PBS) per well for 90 minutes at 37°C. Then, the wells were washed with 200µl of 0.05% Tween-20 in PBS washing buffer per well (3 times, 5 minutes). Aliquots of 20% dilution of serum samples and normal mouse serum (NMS) were added (100µl per well) in triplicates on the Maxisorp plates and incubated for 1h at 37°C. Then, the wells were washed with 200µl of 0.05% Tween-20 in PBS washing buffer per well

(3 times, 5 minutes). After washing, 100µl aliquot of polyclonal rabbit complement component 9 antibody (concentration 0.2 mg/ml; diluted 1:200 with D.W.) was added per well and incubated at 37°C for 1h. Then, the wells were washed with 200µl of 0.05% Tween-20 in PBS washing buffer per well (3 times, 5 minutes). After washing, 100µl aliquot of polyclonal swine anti-rabbit HRP antibody (0.3mg/ml) (Dako P 0399) (at final concentration 1.5µg/ml, diluted 1:200 with D.W.) was added per well and incubated at 37°C for 1h. Then, the wells were washed with 200µl of 0.05% Tween-20 in PBS washing buffer per well (3 times, 5 minutes). Later, 100µl of the coloured substrate (TMB) was added per well and left at room temperature for 5-10 minutes, and then 50µl of the stop solution was added per well to stop the reaction. Finally, the result was read immediately using an ELISA reader TECAN Magellan for 405nm. Then, the percent of residual C9 of complement activation was correlated to the classical pathway activation or alternative pathway activation in commercial mouse serum as a 100% activation standard.

### **2.1.8 TNF- $\alpha$ level measurements by ELISA as an indication of inflammatory cytokines.**

Tumour necrosis factor alpha (TNF- $\alpha$ ) is a cell signalling protein (cytokine) involved in systemic inflammation. It is one of the cytokines that makes up the acute phase reaction. It is produced chiefly by activated macrophages. Since the osteoclasts derived from the monocytes/macrophage's lineage, it was hypothesised that the decline of the bone mineral density might be caused by inflammation leading to an increase in the osteoclasts' activity.

The Murine TNF- $\alpha$  ELISA development kit (PeproTech 900-TM54) was used to quantify the level of TNF-alpha in mouse serum or cell culture supernatant. The quantitative measurement of natural murine TNF- $\alpha$  was performed in a sandwich ELISA format within the range of 10–2500pg/ml.

Following the manufacturer's protocol, the capture antibody containing 11µg of Rabbit Anti-Murine TNF- $\alpha$  + 0.5mg D-mannitol was reconstituted in 110µl sterile water for a concentration of 100µg/ml. Then the capture antibody was diluted with PBS to a concentration of 0.50µg/ml (1:200 dilution). Immediately, 100µl aliquot of capture antibody was added to each well and sealed and incubated overnight at room temperature.

Next day, the well liquid was aspirated and removed then the plate was washed 4 times using 300µl of wash buffer per well (washing buffer: 0.05% Tween-20 in PBS). After the last wash, the plate was inverted to remove residual buffer and blotted on paper towel. Then, 300µl block buffer (Blocking Buffer: 1% BSA in PBS) was added to each well and incubated for at least 1 hour at room temperature. Then, the plate was aspirated and washed 4 times by washing buffer.

The Murine TNF- $\alpha$  Standard containing 1µg of Recombinant Murine TNF- $\alpha$  + 2.2mg BSA + 11.0mg D-mannitol was reconstituted in 1ml sterile water for a concentration of 1µg/ml. Then, the standard was diluted from 2500pg/ml to zero (1:400 dilution) in diluent (Diluent: 0.05% Tween-20, 0.1% BSA in PBS). Immediately 100µl aliquot of standard or samples were added to each well in triplicate and incubated at room temperature for at least 2 hours.

The plate was aspirated and washed 4 times by washing buffer. Then, the detection antibody containing 6µg of Biotinylated Rabbit Anti-Murine TNF- $\alpha$  + 0.5mg D-mannitol was reconstituted in 60µl sterile water for a concentration of 100µg/ml. The detection antibody was diluted in diluent to a concentration of 0.25µg/ml (1:400 dilution) and 100µl aliquot was added per well and incubated at room temperature for 2 hours, then the plate was aspirated and washed 4 times using washing buffer.

Streptavidin-HRP conjugate 4µl/vial was diluted using 36µl of 1xPBS for a total of 40µl at a concentration of 100µg/ml. Then, it was diluted in diluent to a concentration of 0.025µg/ml (1:4000 dilution) and then 100µl aliquot was added per well and incubated for 30 minutes at room temperature. Then the plate was aspirated and washed 4 times using a washing buffer.

The substrate solution (100µl) was added to each well and incubated at room temperature for colour development for 20 minutes and then, 100µl of 1M HCl stop solution was added. The colour development was monitored with an ELISA plate reader at 450nm.

The average absorbance of each standard and sample was calculated. The absorbance values were graphed for each standard as a function of the final TNF-alpha concentration (pg/ml) using GraphPad Prism 7.0 software.

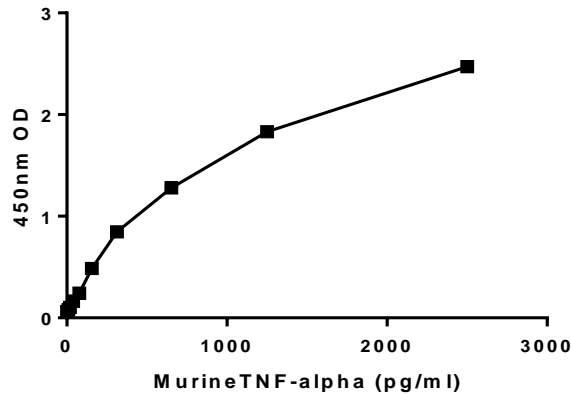


**Figure 2-14:** Example for the standard curve showing the absorbance of different concentrations of Tumour necrosis factor alpha (the optical density is 450nm).

### **2.1.9 Murine IL-6 measurement as an inflammatory factor by ELISA:**

Interleukin 6 (IL-6) is an interleukin that acts as both a pro-inflammatory cytokine and an anti-inflammatory myokine. Interleukin 6 is secreted by T cells and macrophages to stimulate an immune response, during infection and after trauma and other tissue damage leading to inflammation. In addition, osteoblasts secrete IL-6 to stimulate osteoclast formation and this may lead to reducing the bone mineral density (Ishimi *et al*, 1990).

The murine IL-6 ELISA development kit (PeproTech, 900-TM50) was used to quantify the level of IL-6 in mouse serum or cell culture supernatant. The quantitative measurement of natural murine IL-6 was performed in a sandwich ELISA format within the range of 32-4000pg/ml.

Following the manufacturer's protocol, the capture antibody containing 21µg of Rabbit Anti-Murine IL-6 + 0.5mg D-mannitol was reconstituted in 210µl sterile water for a concentration of 100µg/ml. then the capture antibody was diluted with PBS to a concentration of 1µg/ml (1:100 dilution) and immediately, 100µl aliquot was added to each well, the plate was sealed and incubated overnight at room temperature.

Next day, the liquid was aspirated and removed from the wells. The plate was washed 4 times using 300µl of wash buffer per well (Washing Buffer: 0.05% Tween-20 in PBS). After the last wash, the plate was inverted to remove residual buffer and blotted on paper towel. Then, 300µl block buffer (Blocking Buffer: 1% BSA in PBS) was added to each well and incubated for at least 1 hour at room temperature. Then, the plate was aspirated and washed 4 times by washing buffer.

The Murine IL-6 Standard containing 1µg of Recombinant Murine IL-6 + 2.2mg BSA + 11.0 mg D-mannitol was reconstituted in 1ml sterile water for a concentration of 1µg/ml. Then, the standard was diluted from 4000pg/ml to 16 µg/ml (1:250 dilution) in diluent (Diluent: 0.05% Tween-20, 0.1% BSA in PBS). Immediately, 100µl aliquot of standard or samples were added to each well in triplicate and incubated at room temperature for at least 2 hours.

The liquid was aspirated, and plate wells washed 4 times by washing buffer and then the detection antibody containing 3µg of Biotinylated Rabbit Anti-Murine IL-6 + 0.5mg D-mannitol was reconstituted in 30µl sterile water for a concentration of 100µg/ml. The detection antibody was diluted in diluent to a concentration of 0.1µg/ml (1:1000 dilution) and 100µl aliquot was added per well and incubated at room temperature for 2 hours, then the plate was aspirated and washed 4 times using washing buffer.

Streptavidin-HRP Conjugate containing 4µl vial was diluted using 36µl of 1xPBS for a total of 40µl at a concentration of 100µg/ml. Then, it was diluted in diluent to a concentration of 0.15ug/ml (1:600 dilution) and 100µl aliquot was added per well and incubated for 30 minutes at room temperature. Then the liquid was aspirated, and the well plate washed 4 times using a washing buffer.

100µl of substrate solution was added to each well and incubated at room temperature for colour development for 20 minutes and then, 100µl of 1M HCl stop solution was added. The colour development was monitored with an ELISA plate reader at 620nm.

The average absorbance of each standard and sample was calculated. The absorbance values were graphed for each standard as a function of the final IL-6 concentration (pg/ml) using GraphPad Prism 7.0 software.

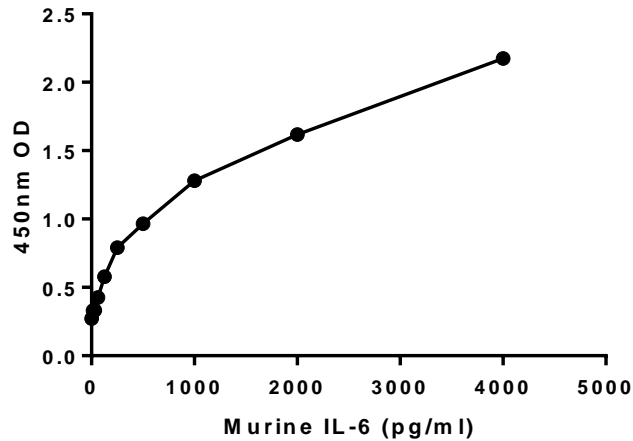


Figure 2-15: Example for the standard curve showing the absorbance of different concentrations of Interleukin 6 (the optical density is 450nm).

### 2.1.10 Body weight measurement for 5 weeks.

The body weight measurement is an important indication for following the body weight development (increase or decrease). The body weight of all experimental animals was determined and recorded by a technician in the animal unit at the beginning of the experiment and then the weight was measured every week for each group. The body weight was compared after 5 weeks of high-fat diet supplemented with or without 11IU/g chow of Vitamin D3, or after 5 weeks high-fat diet with or without access to voluntary wheel exercise.

## 2.2 *In vitro* methodology:

### 2.2.1 Osteoclasts and Osteoblasts differentiation derived from mouse C57/BL6 bone marrow.

Osteoclast or osteoblast differentiation was performed by femur and tibia dissection of C57BL/6 mice. Bones were cleared of soft tissue by tissue paper; then the bones were put in a Petri dish containing 70% IMS for 5 minutes for sterilising the bones before transferring them to 50 ml conical tube containing 3 ml of FACS buffer kept on ice (Tevlin *et al*, 2014).

The clean bones were placed into a mortar and pestle and gently crushed with 3 ml of FACS buffer, and the blood-stained fluid was aspirated off and passed through a 70µm strainer into a new 50 ml conical tube. (This step was repeated 3 times until the fluid did

not stain red). The bone marrow (BM) fluid was centrifuged at 200g for 5 min at 4 °C to obtain a cell pellet, which was re-suspended in 10 ml of FACS buffer (maintained at RT). The BM solution was layered onto the density gradient cell separation media (Histopaque-1077, Gibco) to give a clear separation between the two solutions. Then, the samples were centrifuged at RT 200xg for 15 min (acceleration and deceleration were set to zero on a centrifuge). Then, the cloudy middle layer which contains the bone marrow cells of interest were aspirated off and transferred into a new conical tube with 20 ml of additional FACS buffer (kept on ice) to wash cells and centrifuged at 200xg for 5 min at 4 °C yielding a cell pellet. Finally, the pellet was re-suspended in 1ml of minimal essential media containing 20ng/ml of MCSF and  $10^{-7}$ M of PE2 for cell counting using a haemocytometer (Tevlin *et al*, 2014).

For osteoclast differentiation, the isolated cells were adjusted to 200000 cells/well into 24-well plate and cultured with macrophage simulating media (10ml) containing Minimal essential media (MEM) without phenol red (Gibco.com) supplemented with, glutamate (1%), FCS (10%), 10,000 units/ml penicillin and streptomycin, 20 ng/ml recombinant M-CSF (R&D system), Prostaglandin E2 (Sigma.com) at  $10^{-7}$  M final concentration, for three days. On day 3, the osteoclast stimulating media was added containing minimal essential media without phenol red (Gibco.com) supplemented with, glutamine (2mM), FCS (10%), 10,000 units /ml penicillin (1%), 20 ng/ml M-CSF (R&D System) and 20ng/ml RANKL (R&D System), Prostaglandin E2 at  $10^{-7}$  M final concentration. The media was changed every day until day 7. The cells obtained should be large and fused together and multinucleated (Tevlin *et al*, 2014).

For osteoblast differentiation, the cells were adjusted at 60000 cells/well of a 6 well plate. A fresh medium containing 80ng/ml of MCSF and other components, but not RANKL was changed every 3 days. After 21 days of culture, mononuclear spindle shaped, and alkaline phosphatase positive cells were obtained and considered as osteoblasts.

### **2.2.2 J774 cell line:**

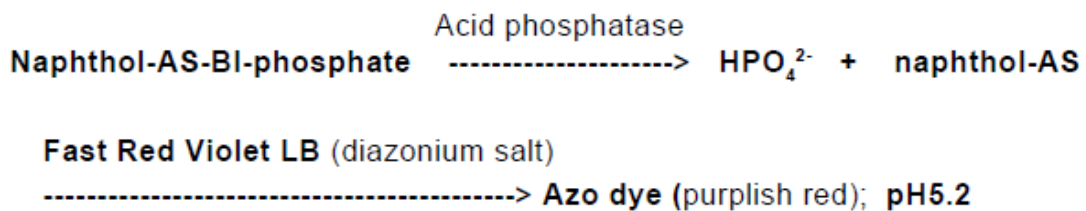
This is a Mouse BALB/c monocyte macrophage cell line (Sigma) that was used as a positive control. Minimum Essential Medium (MEM) (Gibco) with 10% fetal calf serum, glutamine 2mM and 10,000 units/ml penicillin and streptomycin were used to maintain the J774 cell line. Incubation was at 37°C with 5% CO<sub>2</sub> in a humidified chamber. Cells

were counted and adjusted to 180,000/ml for J774, in 75cm<sup>2</sup> flasks (10ml) and treated or split when 70% confluent.

### 2.2.3 Tartrate-resistant acid phosphatase (TRACP staining).

A phosphatase is an enzyme that acts on aliphatic and aromatic phosphate esters and hydrolyses them to release phosphate. It was reported that potent acid phosphatase activity is found in osteoclasts. The acid phosphatase activity of osteoclasts was shown to be of the type that retains phosphatase activity in the presence of tartrate (tartrate-resistant acid phosphatase: TRACP) (Burstone, 1958).

The principle for tartrate-resistant acid phosphatase (TRACP) staining was performed by using the Naphthol-AS-BL-Phosphate (NABP/FRVLB) as a substrate solution for acid phosphatase supplemented with tartrate. The tartrate-resistant acid phosphatase (TRACP) activity can be detected as shown below. The formation of azoic dye with purplish red colour is generated in each sample in the presence of the enzyme.



The reaction was performed following the manufacturer's instructions using TRACP & ALP double-stain Kit (TAKARA BIO INC.). After osteoclast differentiation as shown in [section 2.2.1](#), the osteoclast medium was discarded, and the cells were washed once with sterilized PBS. Then, 250 µl of fixation solution was added to each well at room temperature for 5 minutes, allowing the cells to be fixed in the well (the fixation solution of citrate buffer (pH 5.4) containing 60% acetone and 10% methanol). Then, about 2 ml of sterilized distilled water was added to each well to dilute the fixation solution, and then it was aspirated, the process being repeated twice. The solution was removed from the wells.

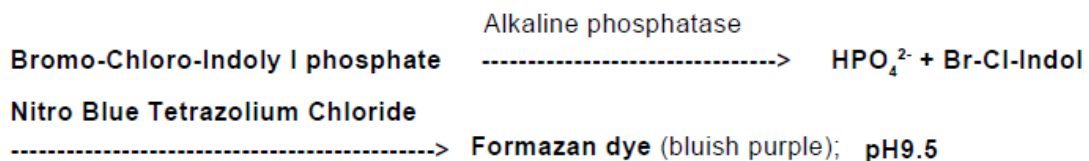
The substrate for acid phosphatase (NABP/FRVLB) was prepared by dissolving the material in a vial with 10 ml of sterilized distilled water. For detection of the tartrate-resistant enzyme, 0.1 volume of sodium tartrate (0.5M sodium tartrate buffer (pH 5.2)) was added to this solution. Then, 250µl of substrate solution was added to the wells on which the cells were fixed. The plate was incubated at 37°C for 15-45 minutes for a

reaction. The solution was discarded and the well was washed three times with sterilized distilled water to terminate the reaction. The samples were examined microscopically (Sterilized distilled water can be added for microscopic examination). This method was used to confirm the osteoclast differentiation in all *in vitro* work.

#### 2.2.4 Alkaline phosphatase staining (ALP staining).

The bone-specific isozyme also called bone type alkaline phosphatase is an enzyme bound to the membrane of osteoblasts (Karaca and Ugar, 1999). ALP functions to enhance osteogenesis by degrading pyrophosphate that inhibits crystallization at the calcification site and by degrading organic phosphate esters to increase the inorganic phosphate concentration (Orimo, 2010). Therefore, bone type alkaline phosphatase is particularly known as a marker of osteogenesis in the cycle of bone metabolism.

The principle for staining of alkaline phosphatase is that the Bromo-Chloro-Indoly I Phosphate (BCIP/NBT) was used as a substrate solution for alkaline phosphatase to form formazan dye with bluish purple colour that was generated in the presence of alkaline phosphatase as shown below.



The osteoblasts were differentiated from mouse bone marrow as shown in [section 2.2.1](#), and then the cells were fixed and washed as shown in [section 2.2.3](#). The (BCIP/NBT) substrate for ALP was made by dissolving one tablet of this component in 10 ml of sterilized distilled water to be used as a substrate solution for the reaction of alkaline phosphatase. Then, 250µl of substrate solution was added to the wells on which the cells were fixed then the plate was incubated at 37°C for 15-45 minutes for a reaction. The solution was discarded, and the cells were washed three times with sterilized distilled water to terminate the reaction. The samples were examined microscopically (Sterilized distilled water can be added for microscopic examination). This method was used to confirm the osteoblasts differentiation in all *in vitro* work.

### **2.2.5 Osteoclast resorption activity assay.**

To assess osteoclast functional activity, the osteoclast resorption activity was evaluated by measuring the resorption area of the osteoclast. The osteoclast precursors were seeded and adjusted to (200000 cells/well) in duplicate for 14 days on Corning osteo assay surface 24 well plates (corning.com) coated with a thin hydroxyapatite material for bone cell growth and functional assay. This provides a uniform and reliable substrate that can be easily used for assessment of osteoclast resorption activity.

At day 14, the media were discarded, and the wells were washed with PBS to remove non-adherent cells. The cells were stained with Tartrate resistance acid phosphatase stain (TRACP) using TRACP & ALP double-stain Kit (Takara Bio Inc.) to confirm the osteoclast TRACP+ cell differentiation. Then, the wells were stained with **Von Kossa** stain, a calcium stain used for visualization of calcium deposits in tissues, to detect the non-degraded hydroxyapatite. The cells were fixed by methanol for 2 minutes then washed 3 times by dH<sub>2</sub>O. Then, 1.5% (w/v) silver Nitrate (AgNO<sub>3</sub>) was added to each well for 15 minutes and incubated in the dark. Then, the wells were washed with dH<sub>2</sub>O at least 10 times. The developer with hydroquinone (photographic developer) was added to wells for 5 minutes. Then, the wells were rinsed with water 10 times. Then, the wells were fixed with 2.5% sodium thiosulfate for 5 minutes (photographic fixer) then the wells were washed with distilled water.

The osteoclast resorptive area was detected by microscope (20x magnification) then pictures were taken of each well. Then, the percent of osteoclast resorption area was measured per well using ImageJ software and the result was analysed using GraphPad Prism 7.

### **2.2.6 Evaluation of mineral deposition from differentiated osteoblasts derived from mouse bone marrow.**

The mineralisation activity of bone matrix is essentially induced by osteoblasts. To quantify mineralisation activity of differentiated osteoblasts derived from mouse bone marrow, the mineral deposition was measured using Von Kossa stain. The osteoblasts were differentiated as shown in [section 2.2.1](#); then the cells were washed and stained by **Von Kossa** as shown in [section 2.2.5](#). The pictures taken were quantified using ImageJ software by measuring the optical density (the grey value) of osteoblast mineral

deposition. The grey values of the background were subtracted from the grey value of the deposition area for each image.

### **2.2.7 C5a protein detection by Western blotting in osteoclast cell culture.**

To detect the fifth complement component (C5) and anaphylatoxin C5a production by differentiated osteoclast derived from bone marrow, the osteoclast supernatant was run in electrophoresis.

To prove that the osteoclast has an ability to cleave the complement protein C5 to C5a anaphylatoxin, the differentiated osteoclast supernatant on day seven was aspirated and replaced by serum-free minimal essential media. Then, the purified human C5 protein 5µg/ml was incubated for 4 hours with each osteoclast culture; then the supernatant was collected to identify the C5a that could be produced by osteoclast derived activity. Stimulated human plasma with LPS at 37 °C for 1hr. was used as a positive control. The positive control was kindly provided by Dr Alharbi, Azza (2018).

Then, 20µg of total protein was subjected to the western blotting under reducing conditions by mixing 2X Laemmli sample buffer (Table 2-3) in a ratio 1:1 with the sample. For the reducing conditions 50 µl of dithiothreitol (DTT) per 950 µl of sample buffer was added for a final concentration of 5% dithiothreitol (DTT), then the mixture was boiled at 95-100°C for 5 minutes then it was ready to run on the SDS-PAGE.

**Table 2-3: Preparation 10ml of 2X Laemmli sample buffer.**

<b>Reagent</b>	<b>Amount to add</b>	<b>Final concentration (2X)</b>
10% (w/v) SDS	4 mL	4%
Glycerol	2 mL	20%
1 M Tris-Cl (pH 6.8)	1.2 mL	120 mM
H <sub>2</sub> O	2.8 mL	---
Bromophenol blue was added to a final concentration of 0.02% (w/v) and the 2X Laemmli sample buffer was stored at room temperature.		

The electrophoresis under reducing conditions was done by 15% sodium dodecyl sulfate-polyacrylamide gel electrophoresis as mentioned in (Table 2-4). The 15% SDS-PAGE was used to increase the chance of C5a detection which is a small polypeptide protein of 16 kDa. The samples were loaded in running buffer (also called standard migration

buffer) 1x Tris-glycine (Table 2-5) for 1 hour at 90 V. Then, the gel was blotted overnight at 30V as shown in (Figure 2-16) for protein transfer onto a nitrocellulose membrane (Thermo Fisher.com) using 1x transfer buffer (Table 2-6). Then, the membrane was blocked with blocking buffer (5% skimmed milk in PBS) for 1 hour at room temperature. Then, the membrane was washed 3 times, 15 minutes each with 1X Tris Buffered Saline-Tween-20 (TBST) buffer (Table 2-7).

**Table 2-4: Preparation 15% sodium dodecyl sulfate-polyacrylamide gel for western blotting.**

<b>Resolving Gel (15% Acrylamide)</b>	
40% Acrylamide	3ml
ddH <sub>2</sub> O	2.8ml
1.5M Tris pH 8.8	2ml
10% SDS	80μl
10% APS	80μl
TEMED	8μl
Total volume	8ml
<b>Stacking Gel (6% Acrylamide)</b>	
40% Acrylamide	0.75ml
ddH <sub>2</sub> O	2.9ml
0.5M Tris pH 6.8	1.25ml
10% SDS	50μl
10% APS	50μl
TEMED	5μl
Total volume	5ml

**Table 2-5: Preparation of 1x running buffer for western blotting**

<b>1X Running buffer pH 8.3</b>
25 mM Tris base
190 mM glycine
0.1% SDS

**Table 2-6: Preparation of 1x Transfer buffer for western blotting**

<b>1X Transfer buffer pH 8.3</b>
25 mM Tris base
190 mM glycine
20% methanol

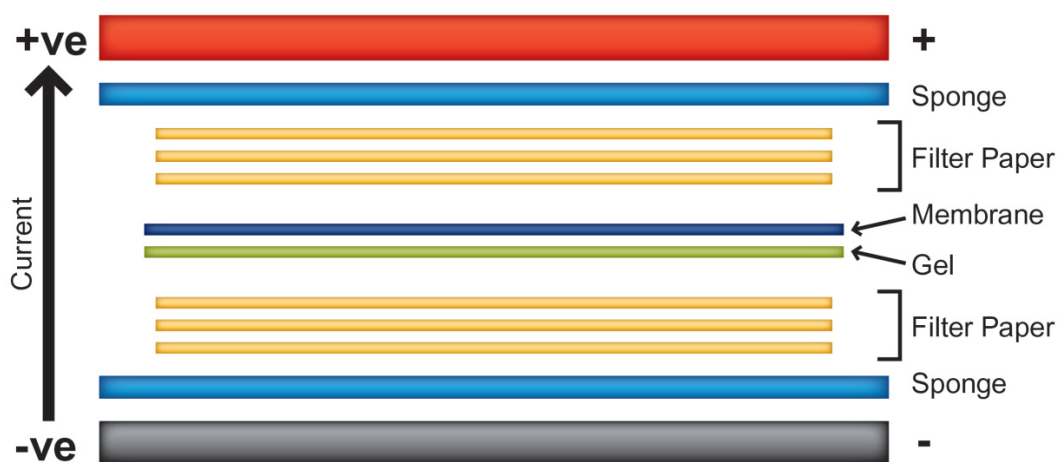


Figure 2-16: A scheme represented the order layers of blotting gel of western blot.

Table 2-7: Preparation of 1x washing buffer for western blotting

1X Tris Buffered Saline-Tween-20 (TBST) pH (7.6)
2.42 g Tris base
8 g NaCl
0.1% Tween-20
Complete to 1L dH <sub>2</sub> O

Then, the membrane was incubated with the rabbit polyclonal anti-human C5a IgG (GeneTex.com) (at a final concentration of 1µg/ml) overnight at 4°C. After washing 3 times 15 minutes each by washing step (with TBS buffer containing 0.05% Tween 20), a HRP conjugated goat anti-rabbit IgG Ab (BioRad.com) was used as a secondary Antibody at a final concentration of 0.5 µg/ml (1:5000 dilution) at room temperature for 1 hour, followed by an additional washing step (3 times 15 minutes each with TBS buffer containing 0.05% Tween 20). Immunoreactive proteins were visualized using Western blot chemiluminescence reagents (Amersham Biosciences) in accordance with the instructions of the manufacturer. The protein bands on the blot membrane were detected using a Bio-Rad ChemDoc Touch imager.

### **2.2.8 C5a protein detection by ELISA in osteoclast cell cultures.**

To measure the level of C5a production in osteoclast cell cultures, the osteoclasts were differentiated as shown in [section 2.2.1](#), then at day 7 the supernatant was aspirated and assayed using a mouse complement component C5a sandwich ELISA kit (R&D system). In parallel, the J774 macrophage murine cell line was cultured in 6 well-plates in triplicate. The cells were treated with or without MCSF and RANKL cytokines like the differentiated osteoclasts. Then the C5a was investigated using the ELISA test.

The complement component C5 protein consists of an alpha chain (C5a) and a beta chain (C5b). Therefore, the capture mouse C5a antibody of the ELISA kit could capture the whole C5 from the alpha chain and the cleaved C5a fragment

Rat anti-mouse C5a (720 µg/mL) was used as a capture antibody when reconstituted with 1.0 mL of PBS. Then 100 µl/well of 4.0 µg/mL in PBS (1:180 dilution) was used as a working concentration of capture antibody for coating a 96-well microplate. The plate was sealed and incubated overnight at room temperature.

Next day, each well was aspirated and washed with 300 µl of washing buffer (0.05% Tween-20 in PBS): the process was repeated three times 5 minutes each. After the last wash, the remaining washing buffer was removed by inverting the plate and blotting it against clean paper towels, which is essential for good performance. Then, the plate was blocked by adding 300 µL of Reagent Diluent (1% BSA in PBS) to each well and incubated at room temperature for 1 hour. The washing step was repeated as mentioned previously. A recombinant mouse C5a was used as a standard which was reconstituted with 0.5 mL of Reagent Diluent to get 130 ng/ml. Then, a 7-point standard curve was used in 2-fold serial dilutions in reagent diluent, the highest standard was 1000 pg/mL and the lowest 0 pg/ml. Both of sample and standard were added in triplicate 100 µl per well. The plate was covered with an adhesive strip and incubated 2 hours at room temperature. Then the washing step was repeated as mentioned above. A biotinylated goat anti-mouse C5a (36 µg/mL) was used as a detection antibody when reconstituted with 1.0 mL of reagent diluent. Then, 100 µl/well of 200 ng/ml in reagent diluent (1:180 dilution) was used as a working concentration of detection antibody following the kit manual instructions. The plate was covered with a new adhesive strip and incubated 2 hours at room temperature. Then, the washing step was repeated as mentioned above. Streptavidin conjugated to horseradish-peroxidase was added at 100 µl/well (1:200

dilution using reagent diluent). The plate was covered and incubated for 20 minutes at room temperature avoiding direct light. Then, the washing step was repeated as mentioned above. A 100µl aliquot of Substrate Solution (1:1 mixture of Colour Reagent A (H<sub>2</sub>O<sub>2</sub>) and Colour Reagent B (Tetramethylbenzidine)) was added to each well and incubated for 20 minutes at room temperature avoiding direct light. 50 µl of Stop Solution (H<sub>2</sub>SO<sub>4</sub> 1.11ml + dH<sub>2</sub>O 8.89ml) was added to each well and the plate gently tapped to ensure thorough mixing. Then, the optical density of each well was determined immediately, using a microplate reader set to 450 nm. Finally, the C5a concentrations were measured regarding the standard curve for each sample.

## **2.2.9 Reverse Transcriptase Polymerase Chain reaction (RT-PCR).**

### **2.2.9.1 Total RNA extraction.**

Total RNA was extracted from osteoclast cell cultures or mouse tissue using Trizol Reagent (Invitrogen, Paisley, UK) following the manufacturer's instructions. The differentiated OC and J774 were cultured in 3 wells of a 6 well plate. The supernatant was discarded and 300µl of Trizol Reagent was added to each well and incubated for 5 minutes to detach cells. Then, cells were scraped and collected in a 1.5ml tube. Then, 200 µl of chloroform (Fisher Scientific, Loughborough, UK) was added and the tubes were shaken for 5 seconds and incubated for 5 minutes. After centrifugation for 15 minutes at 12,000g, the aqueous phase (top) containing the RNA was collected in new 1.5ml tubes. Then, 500 µl of Isopropanol (Fisher Scientific) was added to the aqueous phase to precipitate the nucleic acids and incubated for 5 minutes at room temperature. The samples were centrifuged for 10 minutes at 12,000g and the supernatant was discarded. The RNA pellet was washed using 1 ml of 75% (v/v) ethanol in H<sub>2</sub>O (Fisher Scientific) and centrifuged at 7,500g for 5 minutes. The ethanol was removed, and the RNA pellet was dried by air for 10 minutes. The RNA pellet was dissolved in (25µl) Diethylpyrocarbonate 0.2% (v/v)-treated water. The isolated RNA was digested with DNase I (5 U for 10µg RNA preparation, 37 °C, and 30 min). This step removes contaminating genomic DNA. The total RNA concentration was measured by using a NanoDrop spectrophotometer ND-1000 (Thermo Scientific) according to the manufacturer's protocol.

### 2.2.9.2 Complementary Deoxyribonucleic Acid (cDNA) preparation.

First strand cDNA was synthesized from total RNA using RevertAid H Minus Kit (Thermo scientific K1632) for RT-PCR (Invitrogen) following the manufacturer's instructions. 0.1ng-5000ng of poly (A) total RNA was used to generate first strand cDNA as the initial step of a two-step RT-PCR protocol. The RNA volume needed can be calculated by the following equation ( $RNA\ quantity = \frac{5000ng}{total\ RNA}$ ). Tube A mix was prepared using 5 µg of total RNA, 1 µl Oligo dT 18 primer (0.5 µg/µL), then the total volume was made up to till 12 µl with water (nuclease free). Tube B of the MasterMix was prepared containing 4 µl of 5x reaction buffer (250 mM Tris-HCl (pH 8.3), 250 mM KCl, 20 mM MgCl<sub>2</sub>, 50 mM DTT), 1 µl of Ribolock RNase inhibitor (20 U/µL), and 2 µl of dNTP Mix (10mM) and 1 µl of Revert Aid H Minus M-bMul reverse transcriptase (200 U/µL). The tube A was run for 3 minutes for initial denaturation at 65.0°C. Then, 8 µl of tube B Master Mix was added to tube A for a total volume of 20 µl then, samples were initially denatured at 65.0°C for a further 5 minutes. The mixture was heated at 42°C for 1hr., and the final extension was carried out for 5min at 70°C. At the end the cDNA was kept at -20°C until further use. See (Figure 2-17).

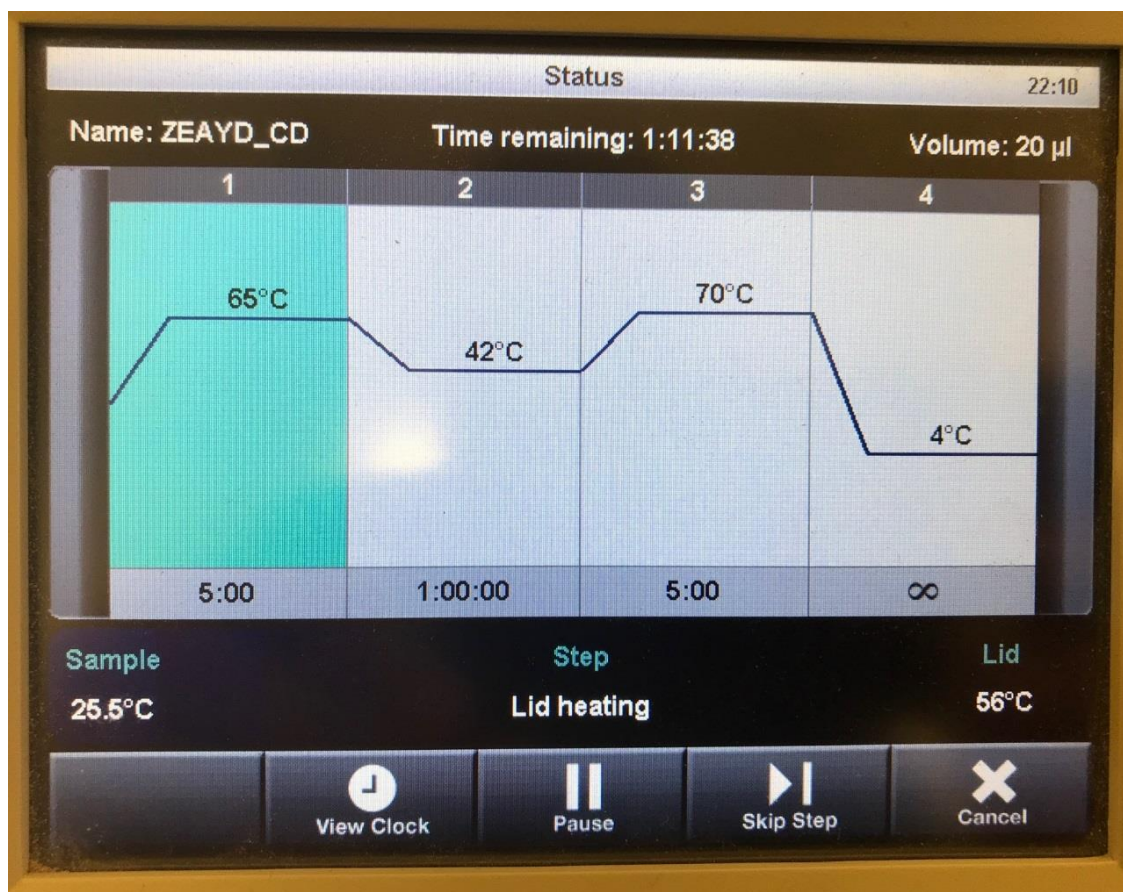


**Figure 2-17: Program used for cDNA synthesis.**

### 2.2.9.3 Gradient PCR.

Gradient PCR was used for detecting the optimum annealing temperature for different primer sets. The reaction was performed by preparing 8 PCR tubes for the same cDNA at total volume 25µl containing 10.8 µl PCR-grade dH<sub>2</sub>O, 2.5 µl (10x) reaction buffer, 2.5 µl MgCl<sub>2</sub> (25mM), 4µl dNTP mix (1.25 mM), 0.2µl Taq polymerase (5 U/µL), 2µl forward primer (5µmol), 2µl reverse primer (5µmol) and 1µl cDNA in PCR Eppendorf tubes. The PCR tubes were loaded in the (Bio-Rad Thermocycler) Gradient PCR machine. The program started at 94°C for 3min. Next, the reaction was cycled up to 30 times including denaturation (94°C for 30sec), annealing (55-64°C for 30sec), and elongation (72°C for 45sec) steps. The reaction was performed for 30 cycles. Finally, the temperature was kept at 72°C for 5min for the final extension and then the reaction stopped and stabilized at 4°C (Figure 2-18). This method was used to detect the optimal annealing temperature of the primers used in this thesis.

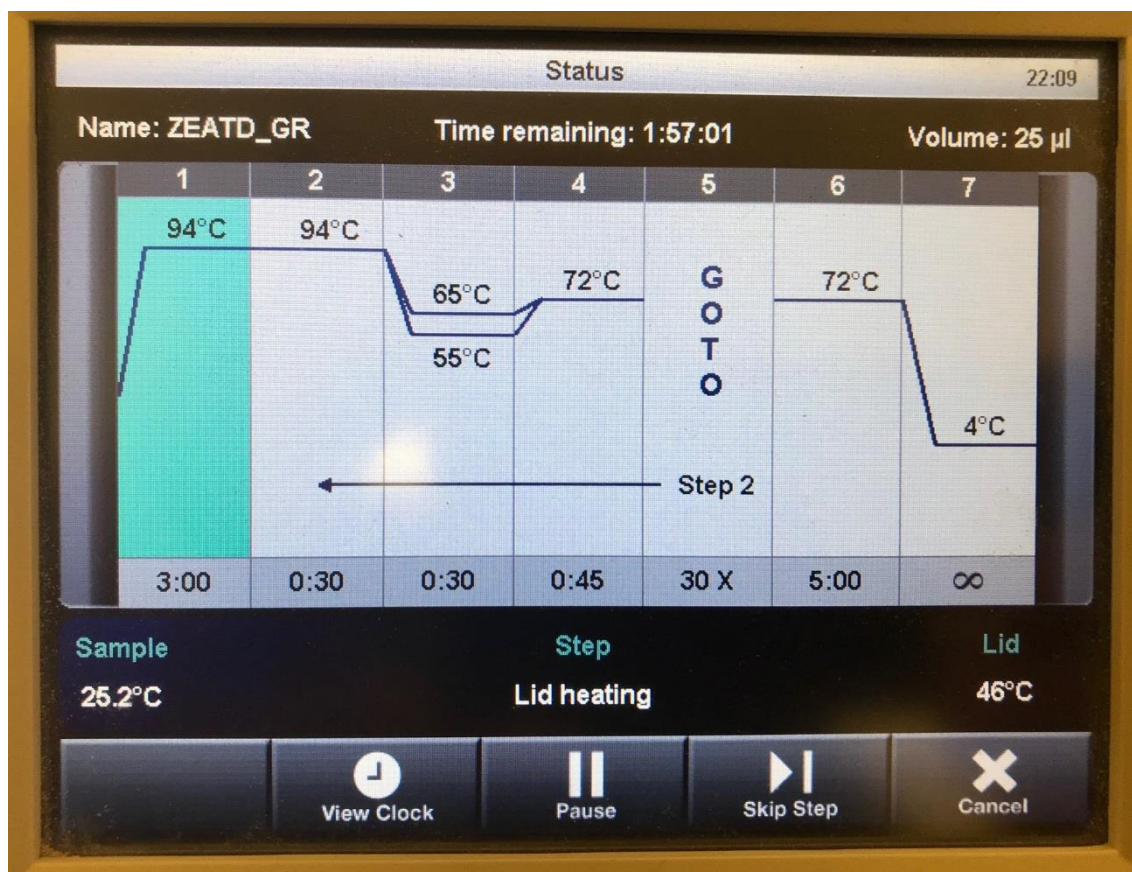


Figure 2-18: Program used in Gradient PCR.

#### 2.2.9.4 Normal Polymerase chain reaction (PCR)

Polymerase chain reaction (PCR) was used for amplification of different target genes. The reaction was performed in a total volume of 25  $\mu$ l containing 10.8  $\mu$ l PCR-grade dH<sub>2</sub>O, 2.5 $\mu$ l (10x) reaction buffer, 2.5 $\mu$ l MgCl<sub>2</sub> (25mM), 4 $\mu$ l dNTP mix (1.25 mM), 0.2 $\mu$ l Taq polymerase (5 U/ $\mu$ L), 2 $\mu$ l of forward primer (5  $\mu$ mol), 2 $\mu$ l of reverse primer (5  $\mu$ mol) and 1 $\mu$ l cDNA in PCR Eppendorf tubes. The PCR tubes were loaded in the (Bio-Rad Thermocycler) PCR machine and the program started at 94°C for 3 min. Next, the reaction was cycled up to 30 times including denaturation (94°C for 30sec), annealing (55-64°C depending on primers annealing temperature for 30sec), and elongation (72°C for 45sec) steps, the reaction was performed for 30 cycles. Finally, the temperature was kept at 72°C for 5min for the final extension and then the reaction stopped and stabilized at 4°C. (Figure 2-19).

This method was used to detect the DNA products of the alternative complement components (CFD, CFB, CFP and C3) in murine osteoclasts.

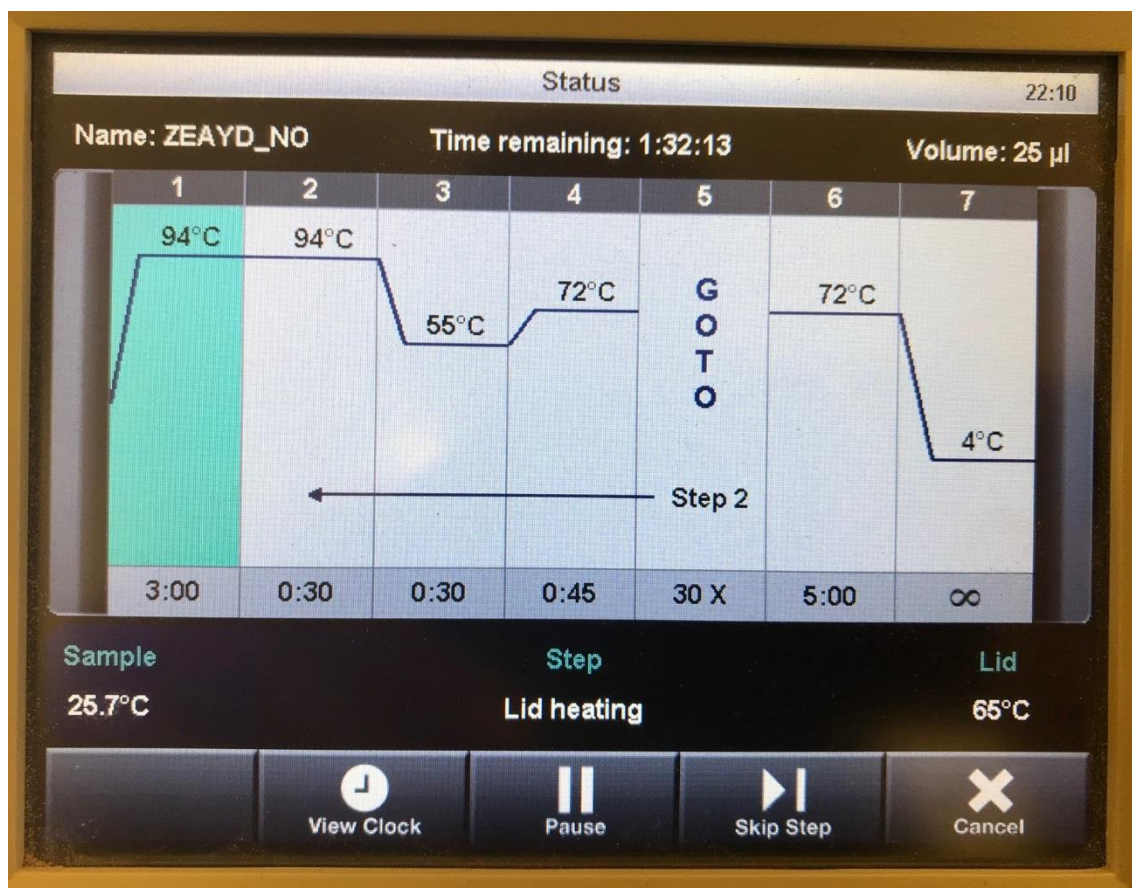


Figure 2-19: An example of a program used for normal PCR.

### 2.2.9.5 Agarose Gel Electrophoresis:

The 1% agarose Gel was prepared [1g agarose in 100 ml of 0.5M Tris-Borate-EDTA buffer], the solution was heated in a microwave for 3min, and then the mixture was cooled to 60°C and 5µl of ethidium bromide were added. Then, 2µl of loading dye (10x DNA gel loading dye, 15% (w/v) BP blue, 50% (v/v) glycerol and 0.5mM EDTA) was added to the PCR product. Then, 7µl of each sample and 5µl of GeneRuler 50bp DNA Ladder, (0.5µg/µL) were loaded on the gel. The electrophoresis was performed at a constant voltage of 90V for 60 minutes. Finally, DNA on the gel was visualized using a ChemiDoc™ Touch Imaging System from Bio-Rad.

### 2.2.10 Real Time- quantitative polymerase chain reaction (RT-qPCR).

The RT-qPCR technique using SYBR Green I dye (SensiMix™ SYBR Kit, Cat.QT605) was used to quantify gene expression. SYBR Green I dye is a high-performance reagent designed for superior sensitivity and specificity on various real-time instruments.

The qPCR reactions were performed using 20µl total volume strip tubes and caps. Each tube contains 3µl of cDNA (previously diluted 1:4 in dH<sub>2</sub>O), 10µl SYBRGreen (containing MgCl<sub>2</sub>) and 2µl of diluted forward primer (5µM), 2µl of diluted reverse primer (5µM) for genes of interest (1µl of stock primer (100µM) in 19µl dH<sub>2</sub>O for each forward and reverse primer) and made up to 20µl by adding 3µl dH<sub>2</sub>O. In parallel, water rather than cDNA template was used as a negative control (NTC). The gene expression was quantified and normalised to GAPDH expression.

The samples of 20µl total volume qPCR reaction were run on the Corbett: Rotor-Gene<sup>TM</sup> 6000 machines and software using the RT-qPCR reaction program in (Table 2-8). The temperature cycling conditions and primers sequences are shown in (Table 2-9).

**Table 2-8: The temperature cycling conditions of qRT-PCR.**

The X is shown as TA I table 2-9

Cycle	Cycle Point for X gene expression
Hold	Hold @ 95°C, 10min 0s
Cycling (40 repeats)	Step 1: Hold @ 95°C, 15s
	Step 2: Hold @ X°C, 60s, acquiring to Cycling A
	Step 3: Hold @ 72°C, 15s
Melt	Ramp from 55°C to 95°C
	Hold for 90s on the 1st step
	Hold for 5s on next steps, Melt A

At the end of each extension step, the fluorescence signal was measured. The occurrence of one distinct peak for each sample for each gene in a melting curve was checked to ensure that one product was amplified and absence of contaminants or primer dimer products.

The amplification of each sample is tracked in real time and the machine calculates the cycle threshold (CT) value for each sample. In RT-qPCR, a positive reaction is detected by the accumulation of a fluorescent signal. The CT is defined as the number of cycles required for the fluorescent signal to cross the threshold. The relative position of the crossing of this CT line with the threshold against the cycle numbers (on the x-axis) gives an indication of the abundance of gene expression. So, when CT < 29, that means on abundant amount of the target cDNA; CT between 30-37 means indicative of moderate amounts of target, however, if CT is 38-40 there are likely to be negligible amounts of

target and that the amplification may have occurred because of some environmental contamination. The threshold of each target gene product was set manually and CT under the threshold through all 40 cycles means a negative result or that the expression of the target gene is very low or undetectable.

The  $\Delta$ CT method was used to calculate the relative expression target gene in each sample.

$$\Delta\text{CT (test)} = \text{CT (target gene)} - \text{CT (ref gene)}$$

$$\Delta\text{CT (calibrator)} = \text{CT (target gene)} - \text{CT (ref gene)}$$

$$2^{-\Delta\text{CT}} = \text{the level of the gene expression}$$

CT: Cycle number at which detectable signal is achieved.

Calibrator: The control sample, meaning an untreated sample.

Test: Test sample means treated.

Reference gene (ref): The reference gene is one that is expressed at a constant level in all test and control samples without being affected by the experimental treatment in the study.

**Table 2-9: Primer sequences with TA and product sizes used in this study.**

Primers		Sequence (5'-3')	Product size	Annealing TA	NCBI
Mouse C5	Forward	5'-AGGGTACTTTGCCTGCTGAA-3'	172bp	58°C	NM_010406.2
	Reverse	5'-TGTGAAGGTGCTCTTGGATG-3'			
Mouse GAPDH	Forward	5'-CCCTTAAGAGGGATGCTGCC-3'	124bp	55°C	NM_001289726.1
	Reverse	5'-TACGGCCAAATCCGTTCA-3'			
Mouse CFD	Forward	5'-ACCTGAAGGCGGGTGTTC-3'	200bp	64°C	NM_001329541.1
	Reverse	5'-TCTTGTTTCATGGCCGCTG-3'			
Mouse CFB	Forward	5'-GCT ACA GTC CCC AAA GTG TT-3'	800bp	65°C	NM_001142706
	Reverse	5'-CAT GCT ATA CAC AGC CTG GA-3'			
Mouse C3	Forward	5'-CCCCTTCATTTCCTCCACCTT-3'	213bp	65°C	NM_009778.3
	Reverse	5'-AGTGACTGTGACTGGGATGTC-3'			
Mouse Properdin	Forward	5'-TTCACCCAGTATGAGGAGTCC-3'	149bp	62°C	NM_008823.3
	Reverse	5'-GCTGACCATTGTGGAGACCT-3'			
Mus B2M	Forward	5'-GACCGCCTGTATGCTATCC-3'	300bp	55°C	NM_009735.3
	Reverse	5'-CAGTAGACGGTCTTGGGCTC-3'			

## 2.2.11 Preparation of Bovine Serum Albumin (BSA)-Conjugated Palmitate:

Palmitic acid  $\text{CH}_3(\text{CH}_2)_{14}\text{COOH}$  is the most prominent saturated fatty acid utilized in the body. However, the utilization of Palmitate in cell-based assays is challenging due to its low solubility in aqueous solutions. Bovine Serum Albumin (BSA) has been used as a carrier, and stabilizing agent, for insoluble fatty acid. Because Palmitate conjugation to BSA creates an aqueous-soluble reagent that can be absorbed and utilized by cells, it is well-suited for use in cell-based-assays. BSA exists as a single polypeptide with 59 lysine residues, 30 to 35 of which have primary amines that are capable to binding to a conjugation reagent.

To prepare 1 mM Sodium Palmitate /0.17 mM BSA Solution (6:1 Palmitic acid: BSA) (Patkova, J. *et al.* 2014).

### 2.2.11.1 The prior setup of BSA and sodium palmitate solution preparation.

1. Warm about 200 mL of tap water in each of 2 and 1 L beakers in 37°C water bath.
2. Warm 250 mL beaker with a stir bar in 37°C incubator.
3. Make 300 mL 150 mM NaCl by adding 9 mL 5 M NaCl stock to 291 mL dH<sub>2</sub>O.

### 2.2.11.2 BSA solution preparation (0.34 mM).

To prepare 0.34 mM of ultra-fatty acid-free (FAF) BSA (Fisher BP9702), 2.267g was weighed out and added to 100 mL of 150 mM NaCl in 250 mL glass beaker while stirring on a stir plate. Then, the beaker was covered with parafilm and placed in one of the 1L water baths pre-warmed to 37°C on a heated stir plate; the heat was adjusted as needed to maintain temperature near 37°C but never more than 40°C (a thermometer was kept in the water bath) and the BSA was stirred until completely dissolved. Then, the BSA solution was transferred and filtered into a new beaker using a 0.22μ filter. Then, the BSA was transferred to a pre-warmed 250 mL beaker, covered with parafilm, and returned to a 37°C water bath and stirring resume.

$$BSA \text{ mM} = \frac{w}{mw} * 100\text{ml (150mM NaCl)} = \frac{2.267 \text{ g}}{66.463 \text{ g}} * 100 \text{ ml} = 0.341 \text{ mM}$$

$$BSA \text{ Dilution Factor} = \frac{0.341\text{mM}}{0.17\text{mM}} = 1:2$$

### **2.2.11.3 Sodium palmitate solution preparation:**

For preparing 2mM sodium palmitate, 15.3 mg of sodium palmitate (Sigma P9767) was weighed and added to 25 ml of 150 mM NaCl solution in a 50 mL Erlenmeyer flask. The flask was covered with parafilm and placed in the other pre-warmed 1 L water bath on a heated stir plate; heated to 70°C while stirring with a thermometer in the water bath. The palmitate solution may appear increasingly cloudy as the temperature reaches 50- 60°C but will clarify near 70°C.

### **2.2.11.4 Conjugating Palmitate and BSA:**

Parafilm was removed from both beaker and flask and 20 mL of hot palmitate solution were transferred to the 25 mL of BSA solution stirring at 37°C. Palmitate will precipitate if it is allowed to sit in a pipette – thus 5 mL was transferred at a time, 4 times, in 10 mL pipette, taking up and expelling quickly. The beaker was re-covered with parafilm and stirred at 37°C for 1 hour, the temperature was monitored in of the water bath to keep it between 35 and 40°C and the ice was added to the water bath to lower temperature if it reached 40°C. The volume was measured in a 100 mL glass graduated cylinder and adjusted to 50 ml with 150 mM NaCl for a 1 mM palmitate solution. The pH was checked with a pH meter and adjusted to 7.4. (Should take 0.5-1 µL of 1 M NaOH.). Then the solution was aliquoted in a glass vial and frozen at -20°C.

### **2.2.11.5 Thawing Palmitate-BSA:**

Palmitate-BSA was thawed in a 37°C water bath for about 7-10 minutes before loading. Palmitate and BSA are known to be stable at -20°C for at least two weeks and thought to be stable for up to one month.

The Palmitate-BSA solution is 1 mM palmitic acid and BSA 0.17 mM in a 6 to 1 molar ratio with BSA, and to get 200 µM palmitate and BSA 33.3 µM as a final working stock concentration for stimulating the differentiated osteoblasts and osteoclasts, the solution was diluted (5x).

## **2.2.12 Preparation of Bovine Serum Albumin (BSA)-Conjugated Oleate:**

Oleic acid is a fatty acid that occurs naturally in various animal and vegetable fats and oils. It is an odourless, colourless oil, though commercial samples may be yellowish. In

chemical terms, oleic acid is classified as a monounsaturated omega-9 fatty acid. It has the formula  $(\text{CH}_3(\text{CH}_2)_7\text{CH}=\text{CH}(\text{CH}_2)_7\text{COOH})$ .

The BSA (0.34mM) was prepared as shown in [section 2.2.11](#). Then, 4mM Oleic acid (Sigma O3880) was prepared by weighing out 30.4 mg Oleic acid and dissolved in 25ml of 150 mM NaCl solution in a 50 mL Erlenmeyer flask. The flask was covered with parafilm and placed in the pre-warmed 1 L water bath on a heated stir plate; heated to 95°C while stirring (thermometer in a water bath) and the solution was left until clarifying near 95°C.

For bovine serum albumin (BSA)- Oleate Conjugation, 20 ml of Oleic acid solution (4mM) was added to 25ml of BSA solution (0.34mM) to get a final stock concentration 0.17mM BSA and 2mM oleic acid at a ratio (1:12) respectively. The solution was heated to 37°C degree with stirring and once the complete solution is clear, then it is conjugated and can be used as a stock solution to stimulate the differentiated osteoclasts and osteoblasts.

The palmitate-BSA and Oleate-BSA conjugates were used to treat the differentiated osteoblasts and osteoclasts cell cultures, as an *in vitro* model of a high-fat diet.

### **2.2.13 The optimal dose determination of fatty acid (FA) to stimulate osteoclast and osteoblast activities.**

The osteoblasts and osteoclasts were differentiated from mouse bone marrow as shown in [section 2.2.1](#) and then the primary cell cultures were treated with different concentrations of free fatty acid to detect the optimal concentration to work with.

The palmitic acid (1mM)-BSA (0.17mM) at ratio (6:1), and Oleic acid (2mM)-BSA (0.17mM) at ratio (12:1) were prepared as shown in [sections 2.2.11](#) and [2.2.12](#) and then both solutions were mixed at ratio (palmitic acid 1:2 Oleic acid) at different concentrations (10µmol/ml, 20µmol/ml, 40µmol/ml, 60µmol/ml) and added to osteoclast and osteoblast cultures for 24 hr stimulation. The 40 µmol/ml was found to be the best concentration to work with.

#### **2.2.14 Statistical analysis:**

Data were expressed as Means  $\pm$  SD for some experiments or Mean  $\pm$  SEM for others, (n= the total number of independent experiments, biological replicates). Statistical analysis was performed using Graph Pad Prism 7 (Graph Pad, San Diego California, USA). For a comparison of one data set with a control data set, an unpaired t-test was performed. To compare more than one treated group to their control, an ordinary one-way ANOVA test or the two-way ANOVA was used to assess the main effect of each independent variable with the interaction between them. Tukey multiple comparison test was run as post hoc test to find the differences between groups. The values \*p<0.05, \*\*P<0.01, \*\*\*P<0.001, \*\*\*\*P<0.0001 were deemed as significant differences.

## **3 Chapter Three – The Results**

## **3.1 The effect of complement properdin gene deletion on bone mineral density.**

The complement system is tightly associated with bone homeostasis. The presence of some complement regulators and receptors on bone cells possibly have a significant role in osteoclastogenesis derived from mesenchymal stem cells (MSC). The complement C3 and C5 zymogens are produced from osteoblasts, while the osteoclasts produce only C3 (Ignatius *et al*, 2011a). In addition, it was shown that osteoclasts and osteoblasts derived from human mesenchymal stem cells express C3a and C5a receptors (Schraufstatter *et al*, 2009; Tu *et al*, 2010); therefore, C3a and C5a anaphylatoxins could directly induce osteoclast activation. Both C3a and C5a in cooperation with IL-1 and IL-6 induce RANKL production and its competitor OPG from osteoblasts and subsequently increase osteoclast formation (Ignatius *et al*, 2011a). The C3 component has a crucial role in osteoclast formation and differentiation derived from mouse bone marrow by potentiating M-CSF from bone marrow cells (Sato *et al*, 1993). In addition, C3 deposits and binds to hydroxyapatite then attracts mononuclear cells which fuse to form multinuclear osteoclasts and resorption occurs (Mangham, Scoones and Drayson, 1993). Taken together, the complement system has a crucial role in the activation of osteoblast-osteoclast interaction.

Properdin is the only known naturally positive regulator of complement activation (Schwaeble and Reid, 1999; Fearon and Austen, 1975). Properdin-deficient mice had a skewing in macrophage activity deviant from wildtype mouse (Dupont *et al*, 2014), and since osteoclasts are derived from macrophages lineage (Miron and Bosshardt, 2016), this section will evaluate whether properdin deficiency may have a direct or indirect effect on osteoclast activity and hence influence bone resorption and bone density.

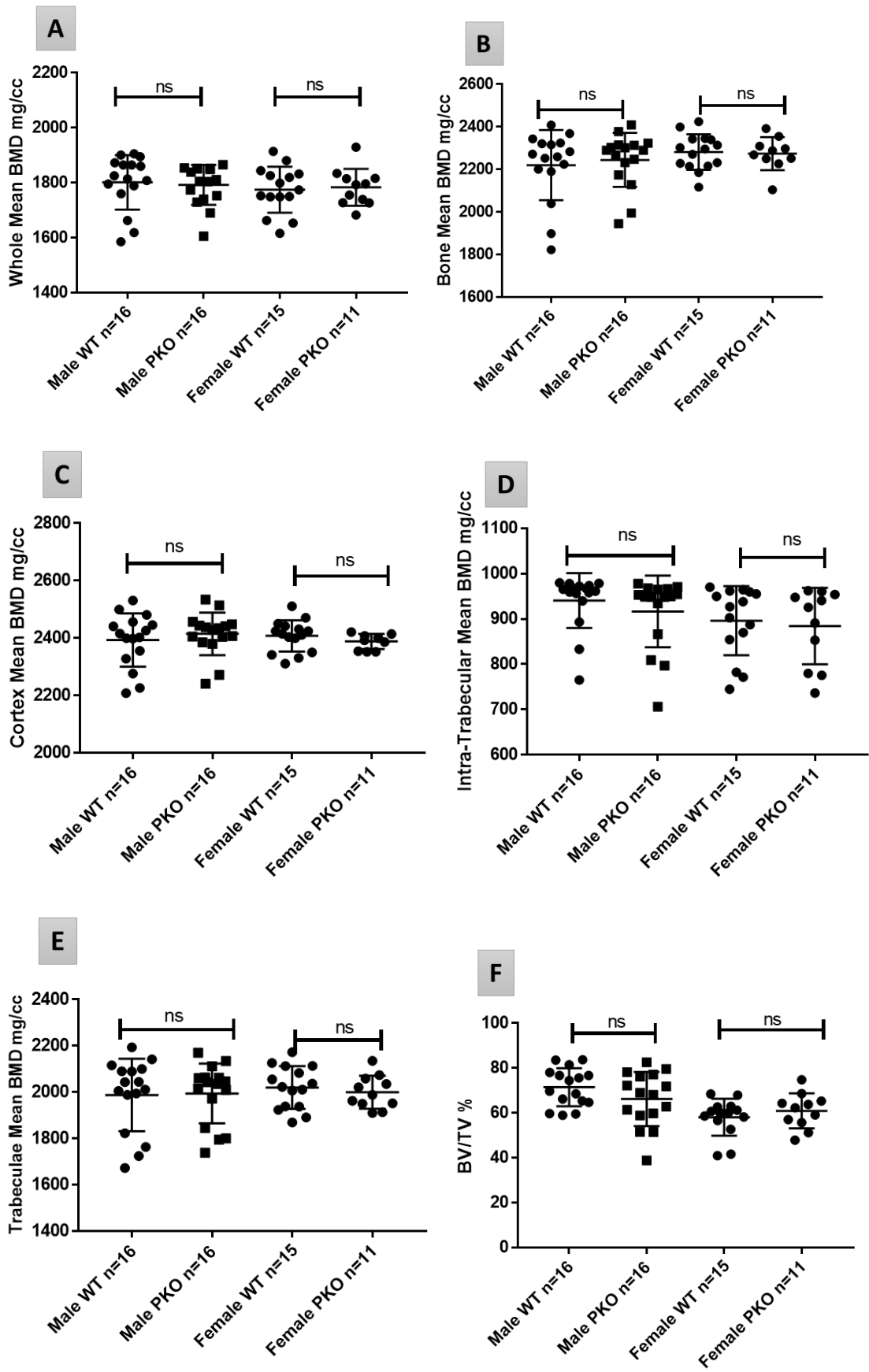
### **3.1.1 Results.**

#### **3.1.1.1 The effect of complement properdin deficiency on bone microarchitecture.**

Wildtype and properdin deficient (PKO) C57BL/6 mice at 6 months old mice were used to assess the effect of properdin deficiency on bone mineral density. The BMD was measured in males (WT n=16; PKO=16) and females (WT n=15; PKO=11), the experimental animal were fed a normal diet (58R1).

The Whole Bone mineral densities were not significantly different in both of male and female in response to properdin absence (Figure 3-1 A). There was no significant difference in bone mean and Cortex densities and this indicates that the compact bone was not influenced by properdin gene absence (Figure 3-1 B and C). The Trabecular bone was not affected by properdin gene deletion possibly because the Trabecular bone mineral density, BT/TV, Intra-Trabecular bone mineral density, Trabecular thickness and separation were not significantly different in both males and females which are genetically modified for properdin gene deletion comparing to their control wildtype (Figure 3-1 G-H). Therefore, the degree of the bone strength or the degree of connectivity in both genders was not changed in properdin gene deletion comparing to wildtype mice (Figure 3-1 I). The number of trabeculae was the same in WT and PKO of both sexes (Figure 3-1 J).

The 3D rendering segmentation showed that there was no significant difference in Cortex and Trabecular segmentation in both males and females of WT and PKO mice (Figure 3-2 A&B). Finally, it can be concluded that the complement properdin had no effect on bone mineral density.



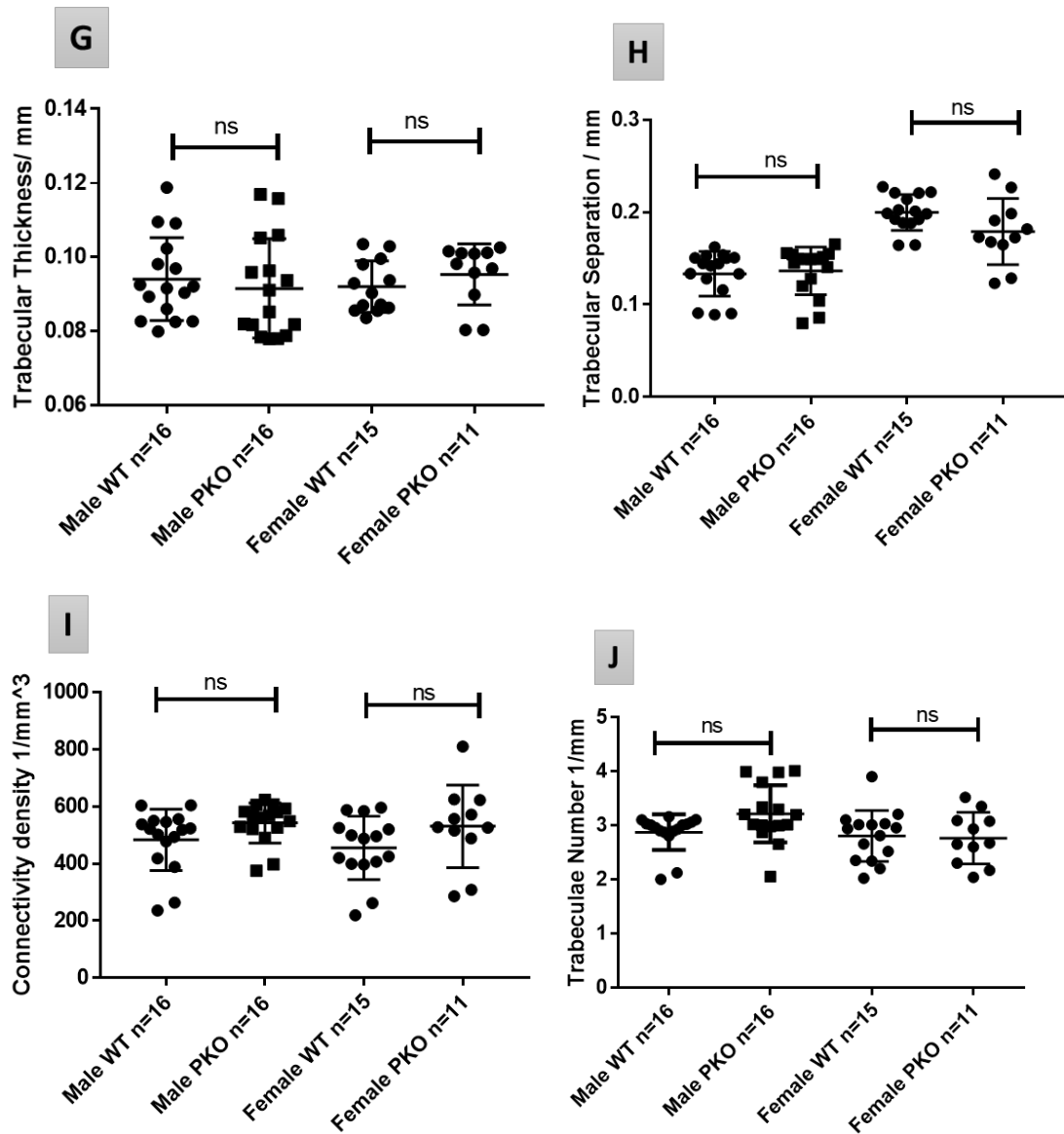


**Figure 3-1: The impact of properdin gene deficiency on bone microarchitecture:**

(A); The Bone Mean (B); Cortex Mean (C); Intra-trabeculae tissue (D); trabeculae Mean BMD (E); BV/TV (F); Trabecular thickness (G); Trabecular separation (H); degree of connectivity (I) and Trabecular number (J). The data are represented as means  $\pm$  SEM (Unpaired t-test ns= no significant differences), the experiment repeated three times.

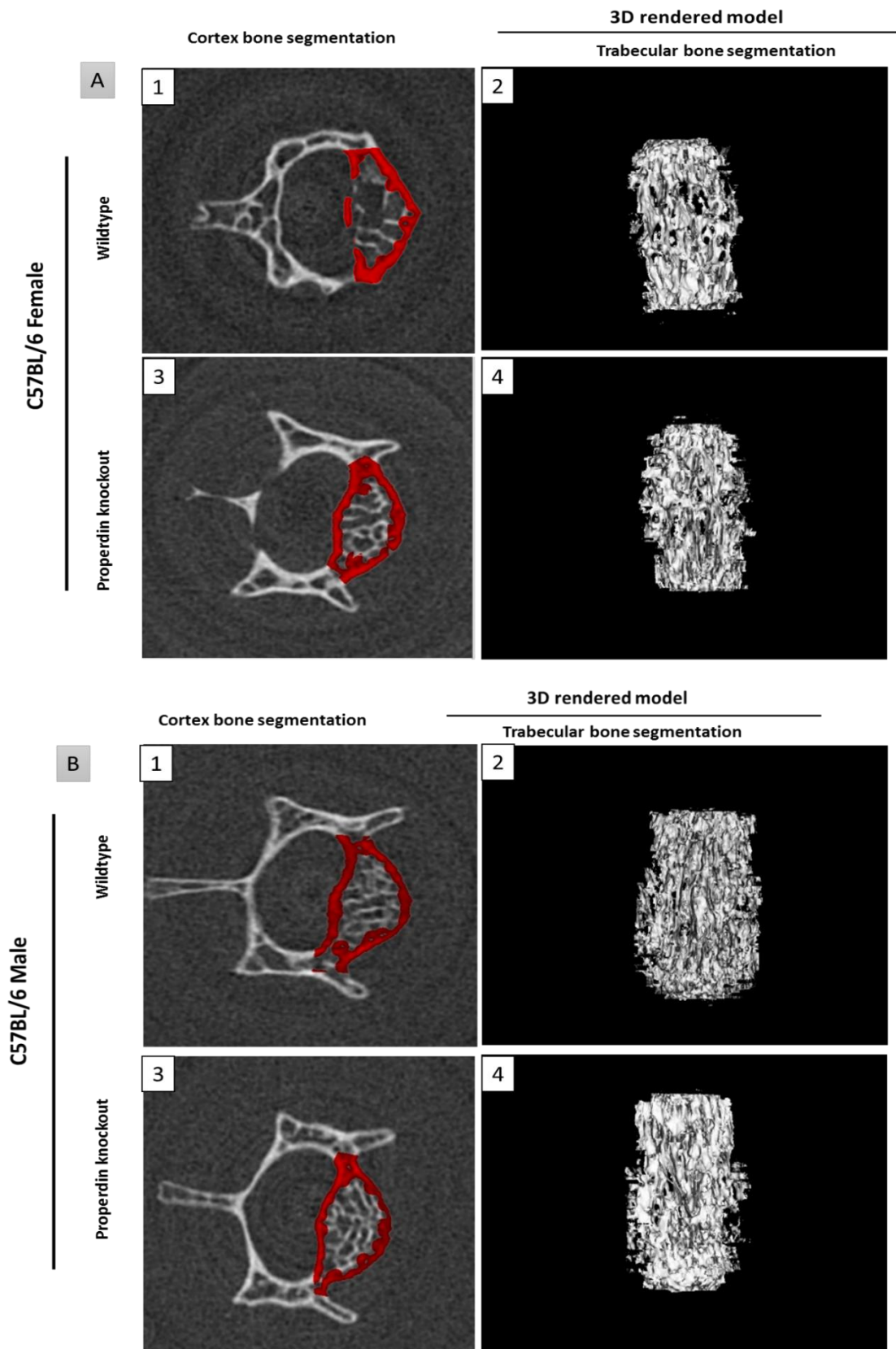


**Figure 3-2: The effect of properdin deficiency on bone microarchitecture in male and female mice:** Three-dimensional reconstruction of Micro-computed tomography was done for female (A) and male (B) of Wildtype and PKO. The panels A 1 and 3, B 1 and 3 refer to cortex segmentation (red colour), the panels A 2 and 4, B 2 and 4 refer to Trabecular segmentation.

### **3.1.1.2 The effect of properdin deficiency on bone remodelling cells.**

It has been proposed that complement components have an important role in osteoclast and osteoblast activities (Schraufstatter *et al*, 2009; Tu *et al*, 2010) but the effect of properdin deficiency on osteoblast and osteoclast activities has been not studied. Therefore, the serum TRACP and ALP were measured in wildtypes and PKO mice to quantify the effect of properdin absence on osteoclasts and osteoblasts activities.

The result shows that there was no difference in serum TRACP level, a serum osteoclasts activity biomarker, in PKO and WT mice of both males and females (Figure 3-3A&B). In addition, there was no significant difference in the serum level of ALP, a serum osteoblast activity biomarker, in WT and PKO mice of both male and female (Figure 3-3 C&D). These results could indicate that the absence of complement properdin has no effect on osteoclast or osteoblast activities *in vivo*.

These results may confirm that properdin deficiency has no effect on bone mineral density because there was no effect of properdin absence on osteoclasts or osteoblasts activities *in vivo*.

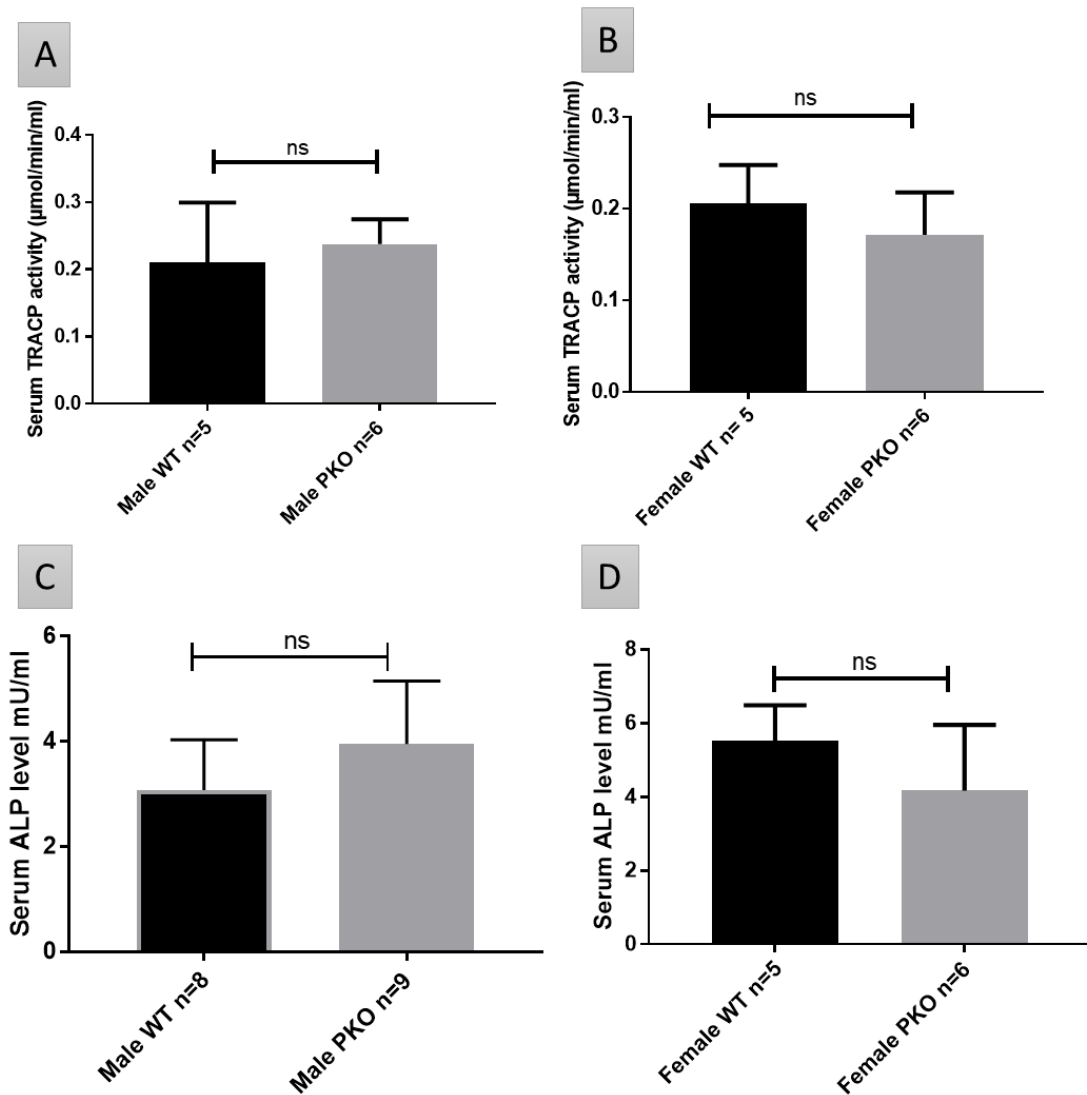


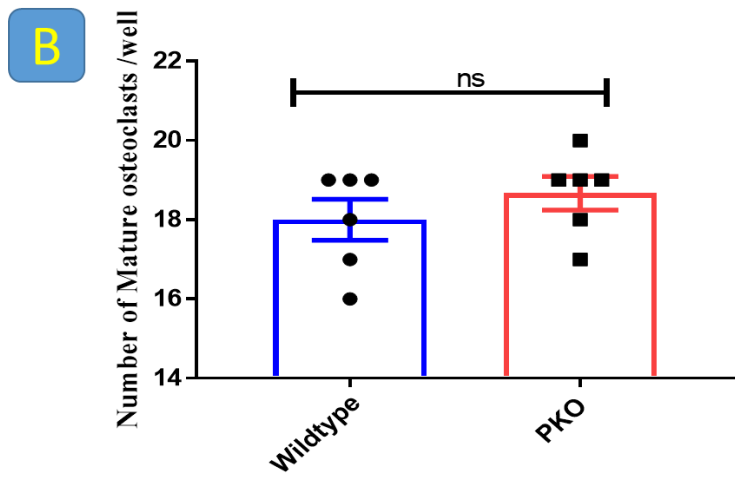
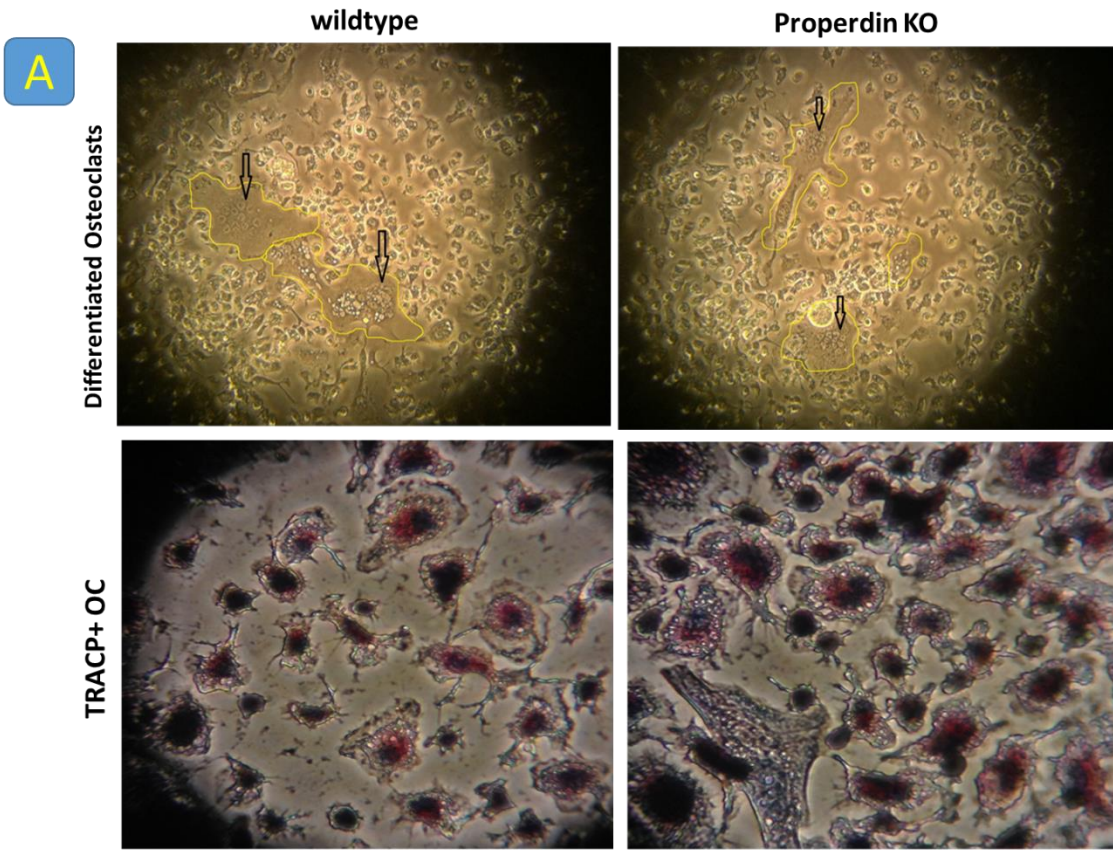
**Figure 3-3: The osteoclast and osteoblast activities measurements in properdin knockout mice:** The bone remodelling was measured by estimating the osteoclast and osteoblast activities in terms of properdin gene deletion. The serum TRACP levels in male (A) and female (B); the serum ALP levels in male (C) and female (D). The data are presented as means  $\pm$  SD of analytical triplicates (Unpaired t-test ns= no significant differences).

### 3.1.1.3 *In vitro* quantification of the effect of properdin deficiency on osteoclast activity.

The complement components have an important role on osteoclasts differentiation and activation (Andrades *et al*, 1996; Tu *et al*, 2010; Sato *et al*, 1993; Sato *et al*, 1991), but the effect of properdin deficiency on osteoclast activation has been not studied. Therefore, osteoclasts were differentiated from WT and PKO to quantify the osteoclast TRACP+ cell number and their resorptive activity.

The osteoclasts were identified morphologically by having a large size with a large cytoplasm and multinucleated cell and they about 30% of the cultured cells (Figure 3-4 A). The results showed that there was no significant difference in osteoclast morphology between both genotypes. In addition, the number of mature osteoclasts (TRACP+) differentiated from wildtype and properdin knockout mice were counted in each well after adjusting the cultured cell number. There was no significant difference in TRACP+ osteoclasts number between both genotypes (Figure 3-4 B). The percent of osteoclast resorptive area on the hydroxyapatite-coated well plate was quantified by ImageJ software. The results showed that there were no significant differences in osteoclast resorptive area in wildtype and properdin-deficient mice (Figure 3-4 C).

Overall, it could be concluded that the bone mineral density has not been affected by properdin absence. The *in vivo* work shows that bone mineral density in properdin knockout mice and wildtype was the same in males and females at 6 months old. In addition, the bone remodelling process was not changed in properdin knockout mice versus wildtype mice, because the osteoblasts and osteoclasts activities *in vivo* didn't change in both genotypes. Moreover, the *in vitro* osteoclast activity derived from properdin knockout and wildtype mice have no differences between genotypes especially in the number and morphology of TRACP+ osteoclasts and resorptive activity; this could explain why the bone remodelling and bone mineral density are the same in properdin-deficient and wild-type mice.



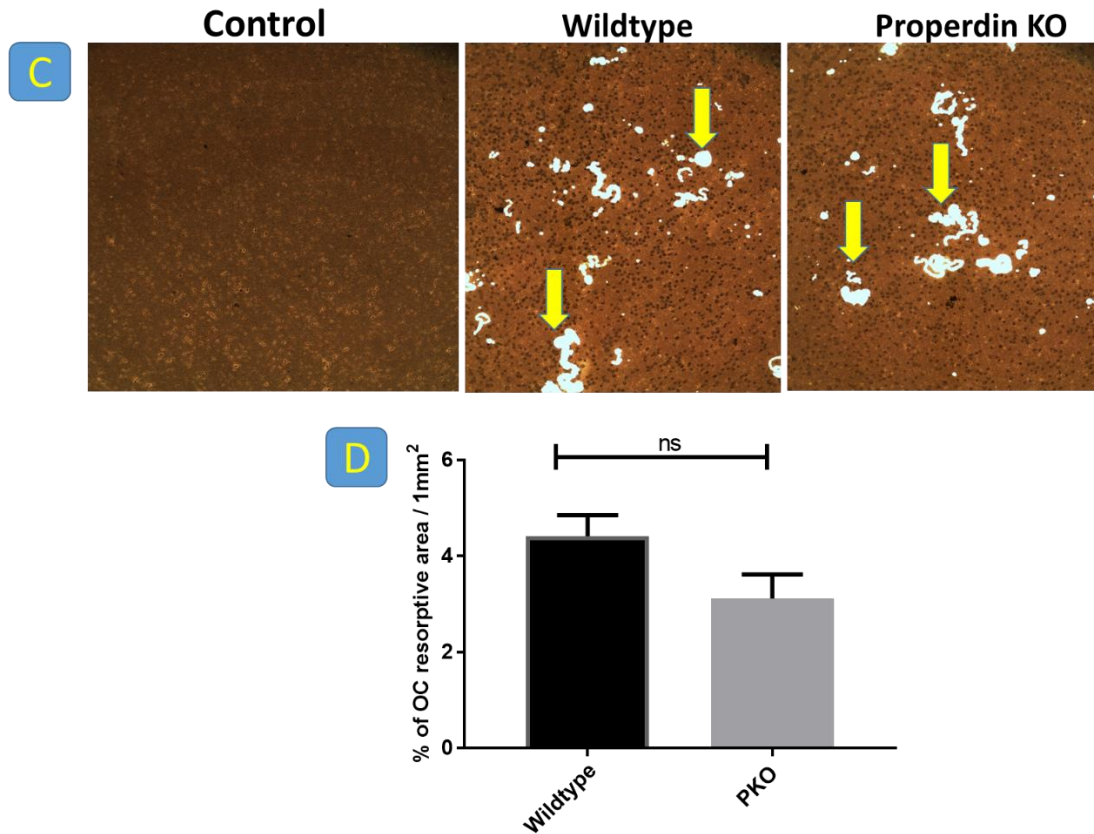
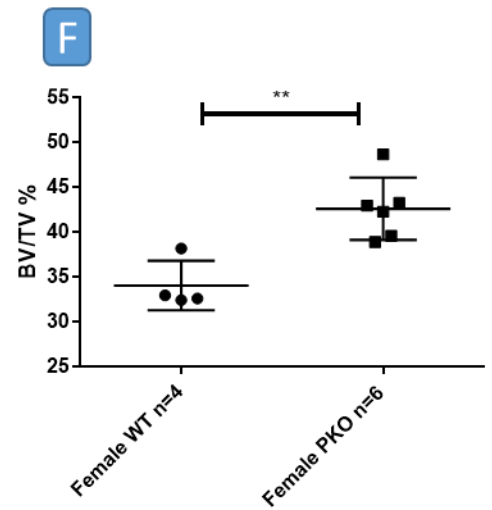
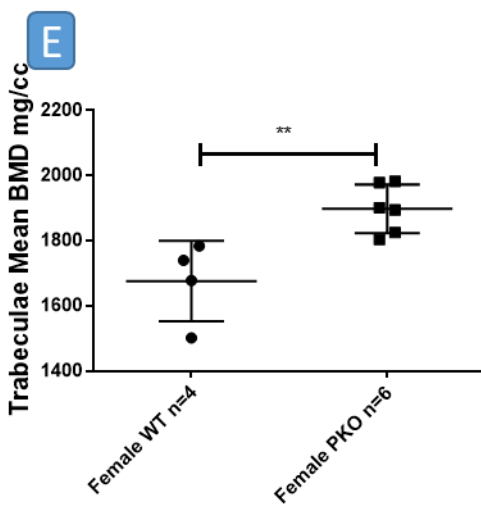
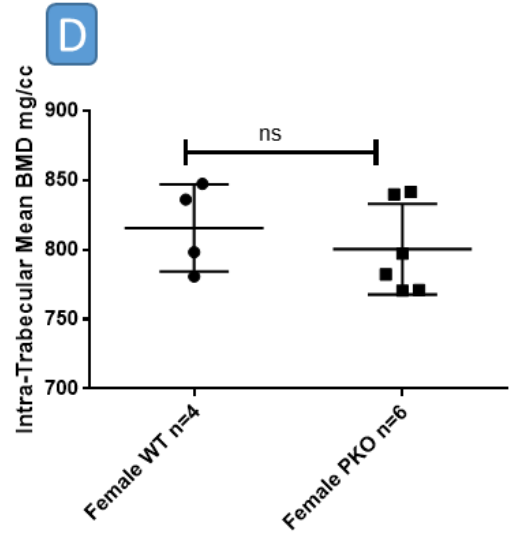
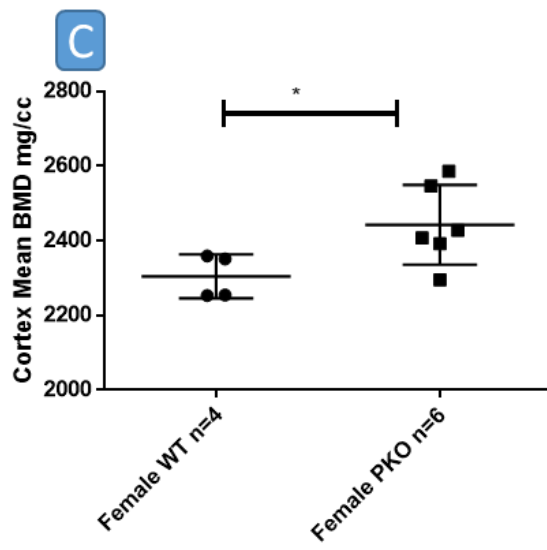
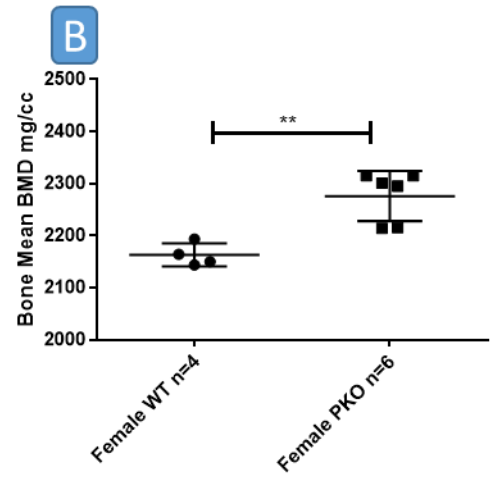
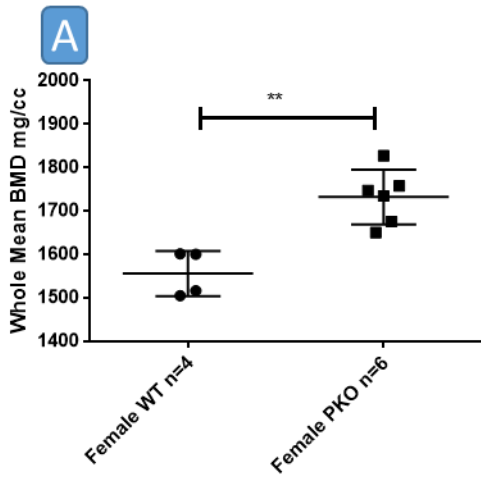


**Figure 3-4: The in vitro analysis of differentiated osteoclast activity derived from WT and PKO mice:** Osteoclast differentiation and TRACP+ positive osteoclasts from WT and PKO, black arrows refer to mature multinucleated osteoclasts (A); the number of mature osteoclasts per well (B); osteoclast resorptive pits of WT and PKO, yellow arrows refer to resorptive pits (C); percent of osteoclasts resorptive area (D). The data represent the mean  $\pm$  SEM of two experiments of analytical quadruplicates assessed by unpaired t-test, ns= no significant differences.

### 3.1.1.4 The effect of properdin deficiency on bone mineral density in older age mice.

The previous findings found in male and female at 6 months old that there was no significant difference in bone mineral density *in vivo*. In addition, there were no significant differences arising from properdin absence on osteoclasts derived from properdin-deficient mice versus with at 6 months old. Therefore, to quantify the effect of properdin deficiency at an older age on bone mineral density, the BMD was measured in the female of properdin-deficient mice at 10 months old that had been fed on the same normal diet containing the same dose of vitamin D3 and calcium. The 10-month-old mice are comparable to about 40 years old in human (Dutta and Sengupta, 2016). At this age, the bone mineral density starts to decline in human.

The Whole Bone mineral density in properdin knockout was significantly higher than wildtype. The reduction in Whole Bone mineral density of wildtype mice maybe because the significant decrease in Bone Mean density in WT compared to PKO mice. This could lead to a significant decrease in Cortex and Trabecular bone mineral densities in WT but not in PKO mice (Figure 3-5 A, B, C and E). The percent of minerals in the region of interest or the bone volume fraction (BV/TV) in properdin-deficient mice was higher than wildtype (Figure 3-5 F). In addition, the Trabecular Thickness in properdin-deficient mice was higher than wild-type mice, but Trabecular separation was less than wildtype, this led to significant increase in the degree of connectivity in properdin knockout versus wildtype (Figure 3-5 G, H and I). The Intra-Trabecular and Trabecular number were not changed in both genotypes (Figure 3-5 D, J). The 3D rendering imaging representing the Cortex and Trabecular segmentation showed that the Cortex and Trabecular bone mineral densities in properdin knockout mice were significantly higher than in WT mice (Figure 3-6). These findings showed that the absence of properdin could enhance the bone mineral density or might affect the osteoclast activity.



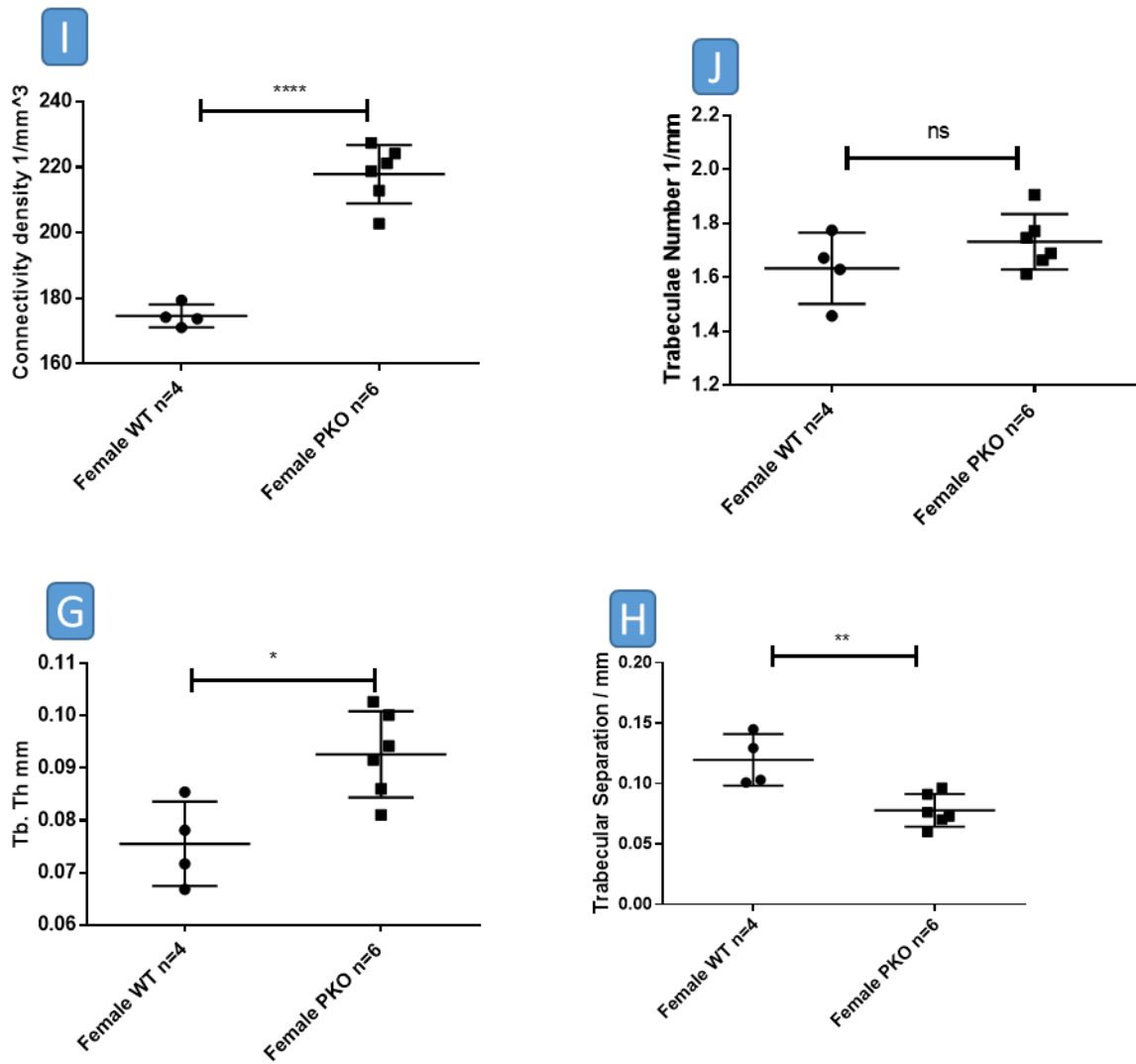


**Figure 3-5: The impact of properdin gene deficiency on bone mineral density at older ages:**

(A); The Bone Mean (B); Cortex Mean (C); Intra-trabeculae tissue (D); Trabeculae Mean BMD (E); BV/TV (F); Trabecular Thickness (G); Trabecular separation (H); Degree of connectivity (I) and Trabecular number (J). The data are represented as means of  $\pm$  SD (Unpaired t-test \* $P < 0.05$ ; \*\* $P < 0.01$  and \*\*\*\* $P < 0.0001$ ; ns= no significant differences).

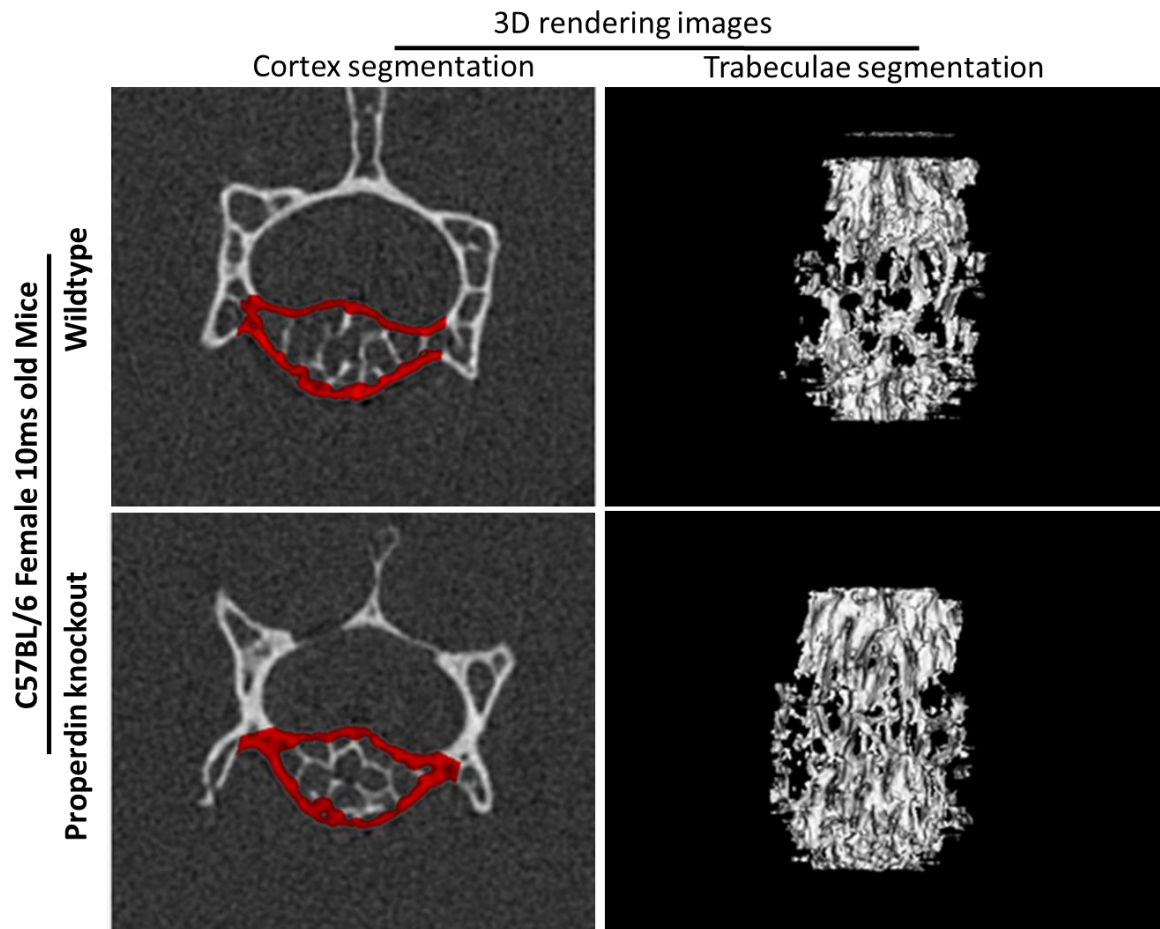


**Figure 3-6: The effect of properdin absence on bone mineral density in female mice at 10 months old:**

Three-dimensional reconstruction of Micro-computed tomography was done for female (A) and male (B) of Wildtype and PKO each at 10 months old. The panels A 1 and 3, B 1 and 3 refer to cortex segmentation (red colour), the panels A 2 and 4, B 2 and 4 refer to Trabecular segmentation.

## **3.2 Vitamin D3 or exercising normalise bone mineral density reduction associated with low-density lipoprotein receptor deficiency.**

The Low-Density Lipoprotein (LDL) Receptor (LDLR) is a cell surface receptor that mediates the endocytosis of low-density lipoprotein (LDL) (Peterson, 2005). LDLR gene deletion increases LDL cholesterol that has adverse implications for bone mineral density (osteoporosis) by oxidised lipoproteins, which inhibit the osteoblast formation and enhance osteoclast differentiation (Tintut, Morony and Demer, 2004; Gharavi, 2002). Vitamin D3 plays a critical role in skeletal homeostasis and its supplementation is used to maintain optimal bone health through its action as a regulator of minerals. The daily administration of Vitamin D3 increases bone mineral density (BMD) by suppressing bone resorption and/or enhancing bone formation (Harada *et al*, 2012). In addition, regular exercise has a significant role in enhancing bone mineral density (Ehrlich and Lanyon, 2002). Therefore, it was hypothesised that deletion of low-density lipoprotein receptor (LDLR<sup>-/-</sup>) in mice could reduce bone mineral density and that Vitamin D3 dietary supplementation or voluntary exercising could ameliorate bone mineral density reduction induced by LDLR gene deletion.

### **3.2.1 Results.**

#### **3.2.1.1 The effect of LDLR deficiency on serum triglyceride levels in mice.**

Low-density lipoprotein receptor deficiency may induce significant changes in levels of lipids in serum. Mice deficient in LDLR exhibit a rise in serum triglyceride, which may be associated with bone loss (Bieghs *et al*, 2012; Pirih *et al*, 2012). Therefore, to assess whether mice lacking LDLR have a hyperlipidaemia, the serum level of triglyceride was measured in serum. The results showed that the serum level of triglyceride was significantly elevated in both males and females lacking the LDLR gene, due to lipids accumulation in the serum resulting from LDLR absence (Figure 3-7). This experiment confirmed that lacking LDLR induced hyperlipidemia that can be a risk factor for bone health.

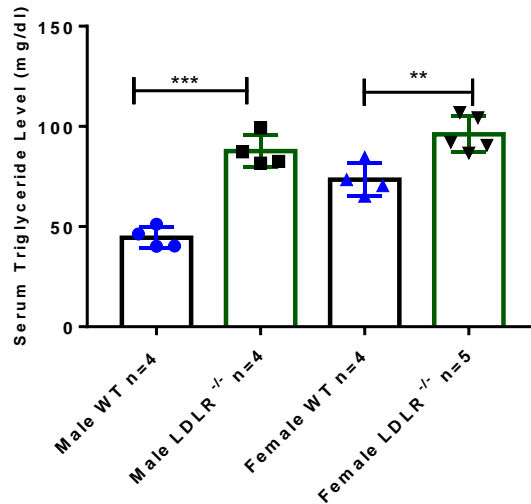
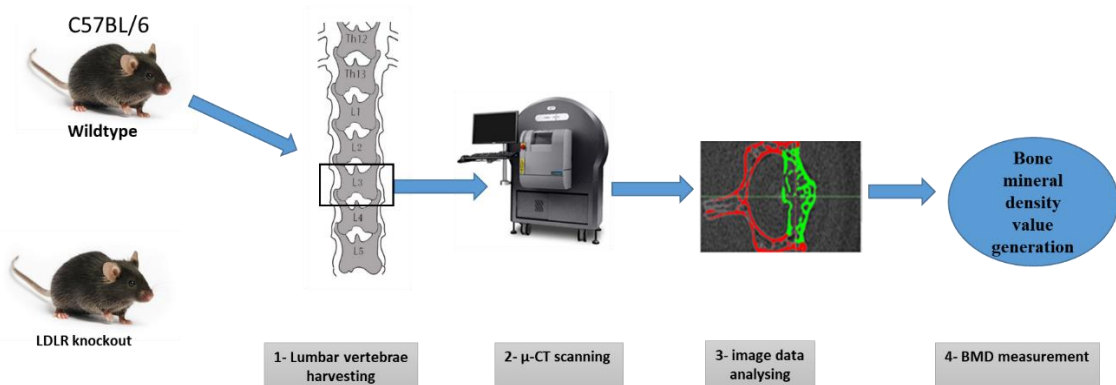


**Figure 3-7: The effect of LDLR deficiency on Triglyceride level in mouse serum:**

Quantification of triglyceride level in the serum of mice lacking LDLR. The data are presented as means  $\pm$  SD and Unpaired t-test was performed, \*\*P < 0.01; \*\*\*P < 0.001).

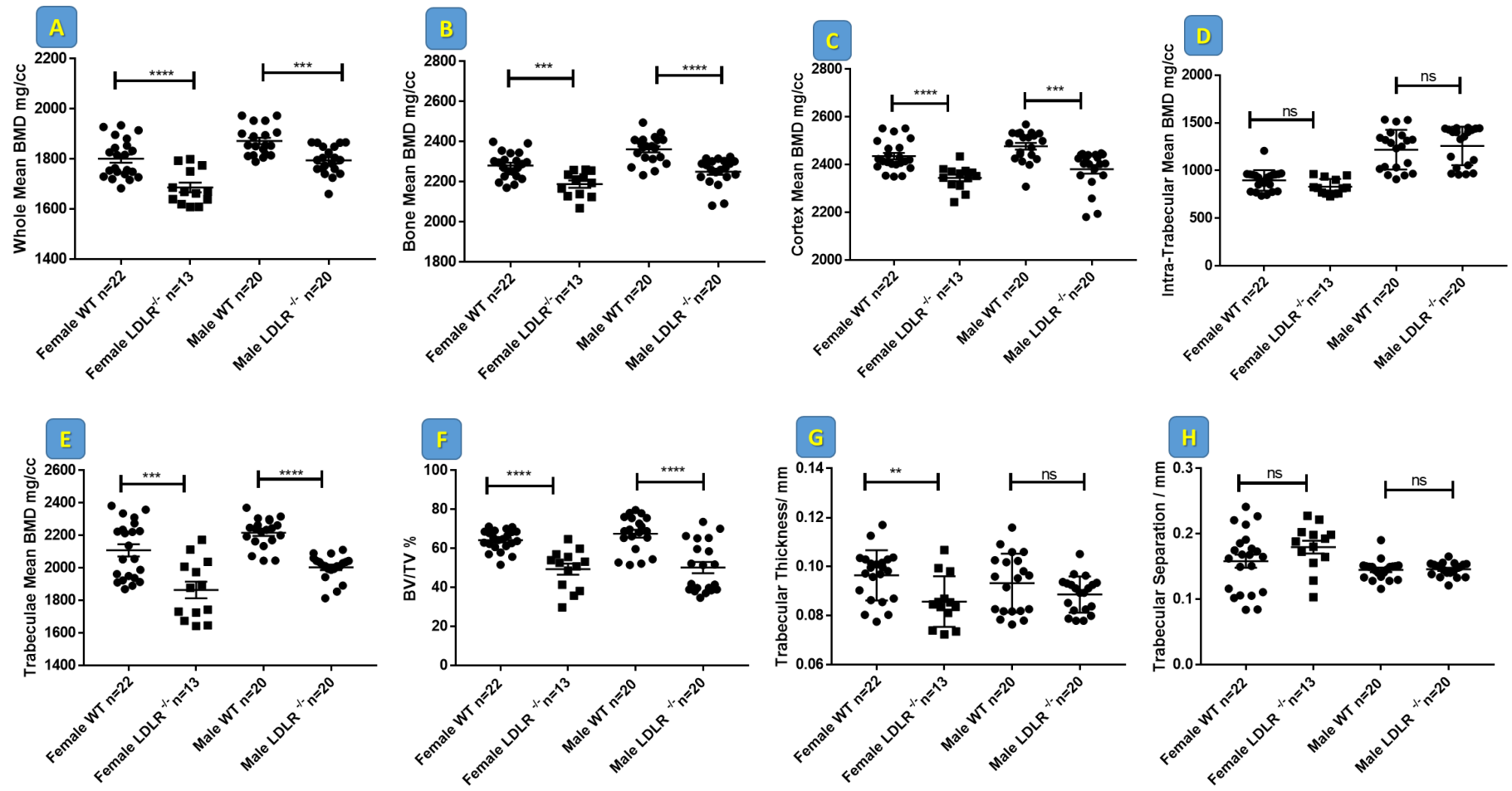
### 3.2.1.2 The effect of Low-density lipoprotein receptor (LDLR) deficiency on bone microarchitecture.

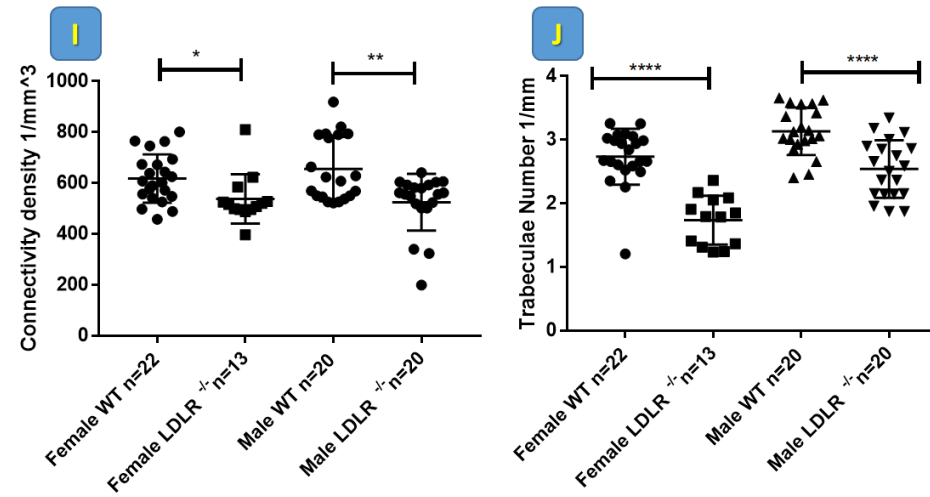
The low-density lipoprotein receptor (LDLR) plays an essential role in osteoclastogenesis. LDLR gene deletion may have a role in the bone loss by reducing lipoproteins uptake by endocytosis (Okayasu *et al*, 2012). Therefore, to quantify whether low-density lipoprotein receptor (LDLR) gene deletion has an effect on bone mineral density, the 3<sup>rd</sup> lumbar vertebrae of wildtype and LDLR<sup>-/-</sup> male and female C57BL/6 mice 6 months old were subjected to microcomputed tomography for measuring the bone mineral density (Figure 3-8).



**Figure 3-8: The experimental flow for quantifying the effect of LDLR gene deletion on bone mineral density.**

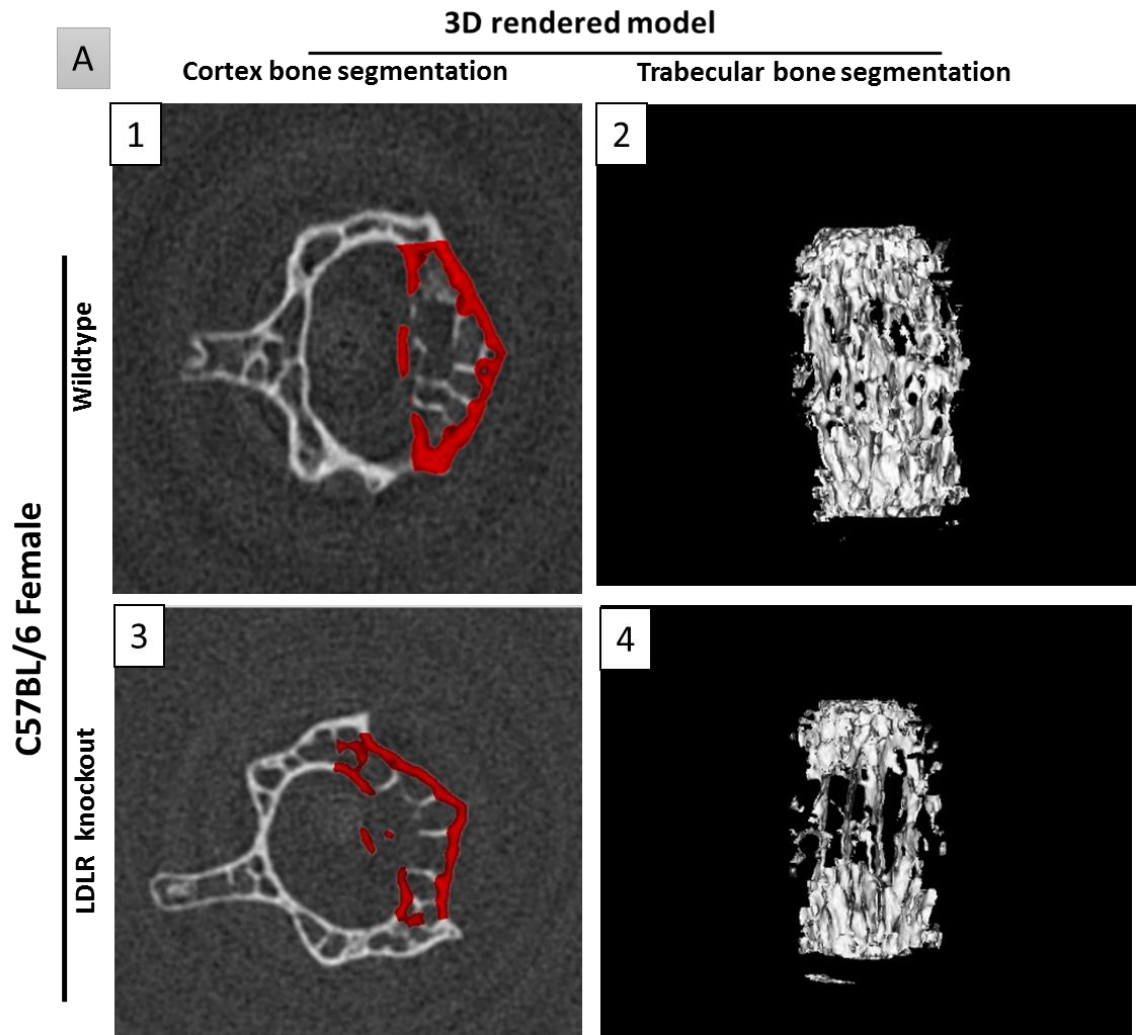
Two large groups of LDLR<sup>-/-</sup> mice (female n=13, male n=20) comparing to wildtype mice (female n=22 and male n=20) were used to quantify the effect of the LDLR gene deletion on the bone mineral density. In general, male and female mice lacking LDLR in male and female had low mineral density especially in whole mean bone mineral density compared to their respective wild-type counterparts (Figure 3-9A). The whole mean mineral density reduction was decreased in female and male LDLR<sup>-/-</sup> comparing to wildtype mice maybe due to the significant reduction in the mean of bone density (Figure 3-9 B). These findings also show that the Cortex mean bone mineral density highly reduced in LDLR<sup>-/-</sup> males and female compared to wildtype (Figure 3-9 C). The Trabecular Bone Means density was declined in LDLR<sup>-/-</sup> of males and females in comparison to wildtype mice (Figure 3-9E). Consequently, the degree of connectivity was sharply declined in knockout mice a companied by a significant reduction in BV/TV % and Trabecular number (Figure 3-9 F, I&J). However, the intra-Trabecular tissue, Trabecular Thickness (in female but not in male) and Trabecular separation parameters were not significantly changed in both males and females (Figure 3-9 D, G&H).





**Figure 3-9: The effect of LDLR gene deletion on bone microarchitecture:**

The 3<sup>rd</sup> lumbar vertebra of C57BL/6 mice WT (female n=22; male n=20) and LDLR knockout mice (female n=13; male n=20) were subjected to Micro-CT for measuring bone mineral density. The whole BMD (A); Bone Mean (B); Cortex Mean (C); Intra-trabeculae tissue (D); trabeculae Mean BMD (E); BV/TV (F); Trabecular Thickness (G); Trabecular separation (H); degree of connectivity (I) and Trabecular number (J). The experiment was repeated three times and the data were represented as means  $\pm$  SEM (Unpaired t-test \*P < 0.05; \*\*P<0.01; \*\*\*P<0.001; \*\*\*\*P<0.0001).



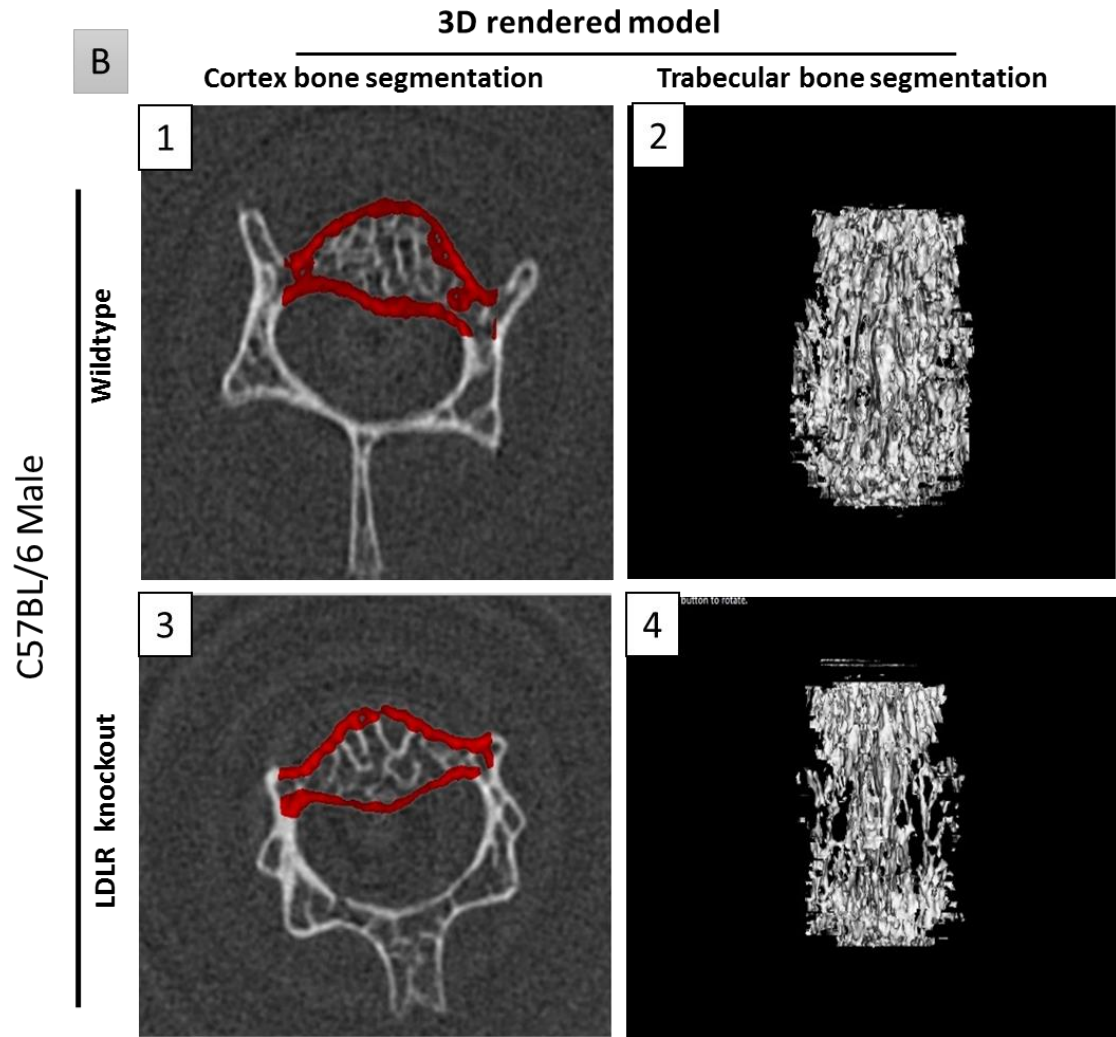


**Figure 3-10: 3D rendering images of the effect of LDLR absence on bone mineral density in male and female mice:**  
 Three-dimensional reconstruction of Micro-computed tomography analysis shows the Cortex and Trabecular segmentation of one representative mouse of WT and LDLR<sup>-/-</sup> of female mice (A) and male (B).

### **3.2.1.3 The effect of LDLR deficiency on bone remodelling activity.**

Low-density lipoprotein receptor deficiency may induce hyperlipidaemia that could affect the osteoclast and osteoblast activities. LDLR<sup>-/-</sup> mice exhibit low levels of osteoblast differentiation factors such as alkaline phosphatase, collagen I and osteocalcin, in addition, to promoting bone resorption by recruitment and differentiation of osteoclast precursor cells (Parhami, Garfinkel and Demer, 2000; Gharavi, 2002). Therefore, to quantify the activity of the bone remodelling in Low-density lipoprotein receptor (LDLR) knockout mice, tartrate-resistant acid phosphates (TRACP), a specific serum biomarker for bone resorption, and Alkaline serum phosphatase, a serum biomarker for bone formation, were measured in LDLR<sup>-/-</sup> mice compared to WT control.

There was no significant difference in serum level of TRACP in LDLR<sup>-/-</sup> in males, but the TRACP level was significantly elevated in females (Figure 3-11 A&B). This may indicate that LDLR absence could affect the osteoclasts activity in females but not in males. In addition, there was a significant decrease in the level of alkaline phosphatase level of LDLR<sup>-/-</sup> compared to WT control mice in both males and females (Figure 3-11 C&D). This could show that osteoblasts activity may be influenced by LDLR absence. These results support the bone mineral density findings regarding LDLR gene deletion. There was a significant decrease in BMD of LDLR deficient mice possibly due to an alteration of osteoclast and/or osteoblast activities.

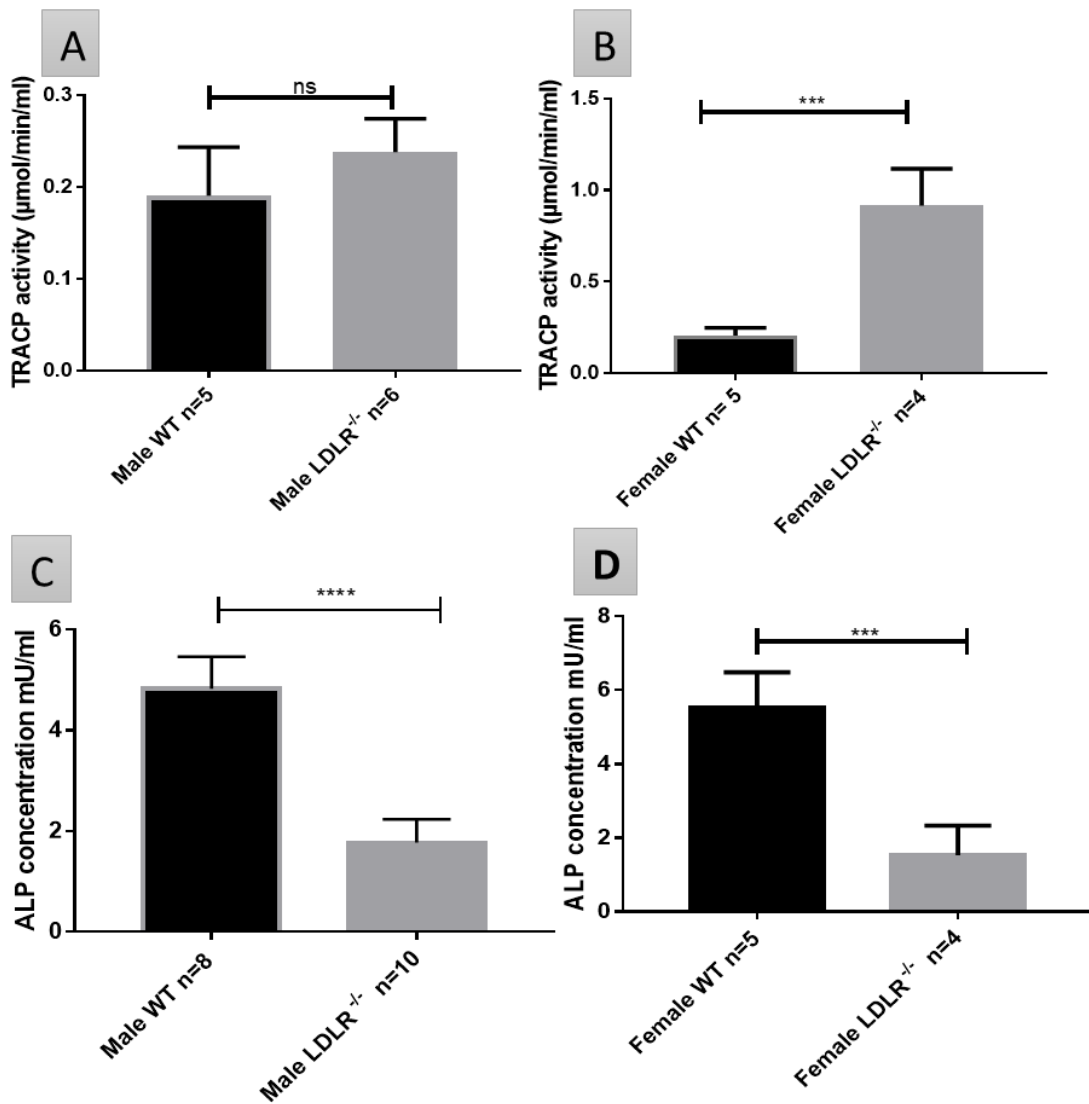


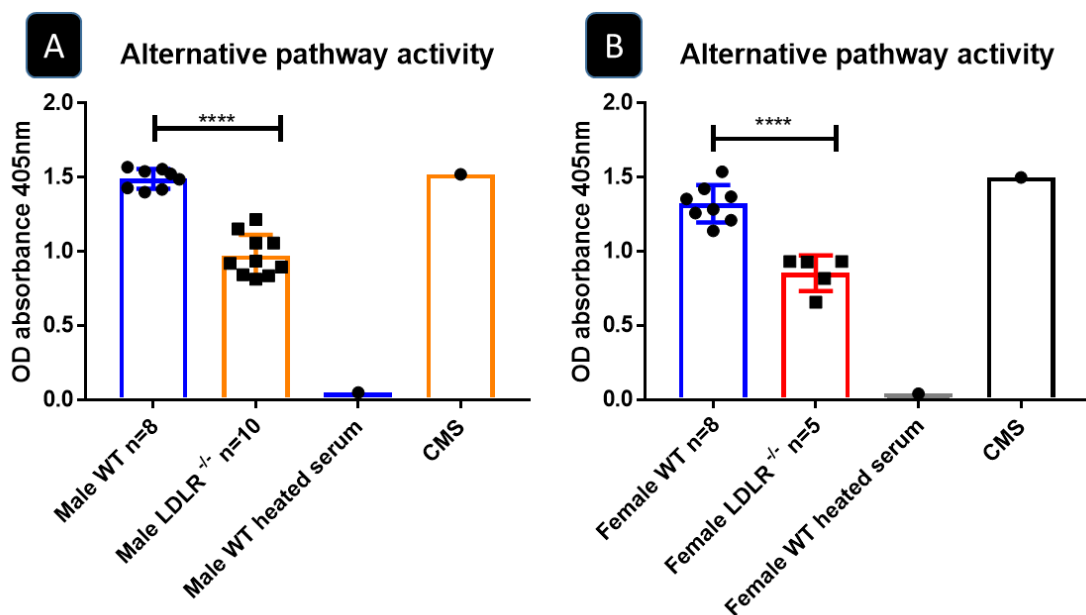
**Figure 3-11: The LDLR deficiency on osteoclast and osteoblast activities in mice:**

The level of serum TRACP and ALP were measured in LDLR<sup>-/-</sup> to estimate the osteoclast activity and osteoblast activity. The serum TRACP (A) for male and (B) for female; the level of ALP (C) for male and (D) for female. The experiment was repeated twice in analytical quadruplicates and the data were represented as means of triplicates ± SD (Unpaired t-test \*\*\*P<0.001; \*\*\*\*P<0.0001).

### 3.2.1.4 The effect of LDLR<sup>-/-</sup> on classical and alternative complement pathways activation.

Hyperlipidaemia induced by lacking LDLR may have a role in complement activation including the alternative and classical complement pathways activation. It was shown in human and in mice that the plasma level increase of LDL or severe hypercholesterolemia induced mRNA upregulation of C3, C4, C1s, and C1q in addition to protein expression of C3 and C4 (Verdeguer *et al*, 2007; Hillian *et al*, 2013). Therefore, to evaluate whether hyperlipidaemia induced by LDLR absence may contribute to complement activation, the alternative and classical pathways activation were measured by the formation of C9 in mice serum in mice lacking LDLR and wildtype at 6 months old. Later, the residual activities of classical and alternative pathways were correlated to the activities in commercial mouse serum.

The residual activity (remaining activity) of alternative and classical pathways in LDLR<sup>-/-</sup> mice of both sexes was significantly reduced in their serum comparing to their control wildtype (Figure 3-12; Table 3-1; Table 3-2). This means that consumption of complement compounds was higher in LDLR<sup>-/-</sup> than WT.



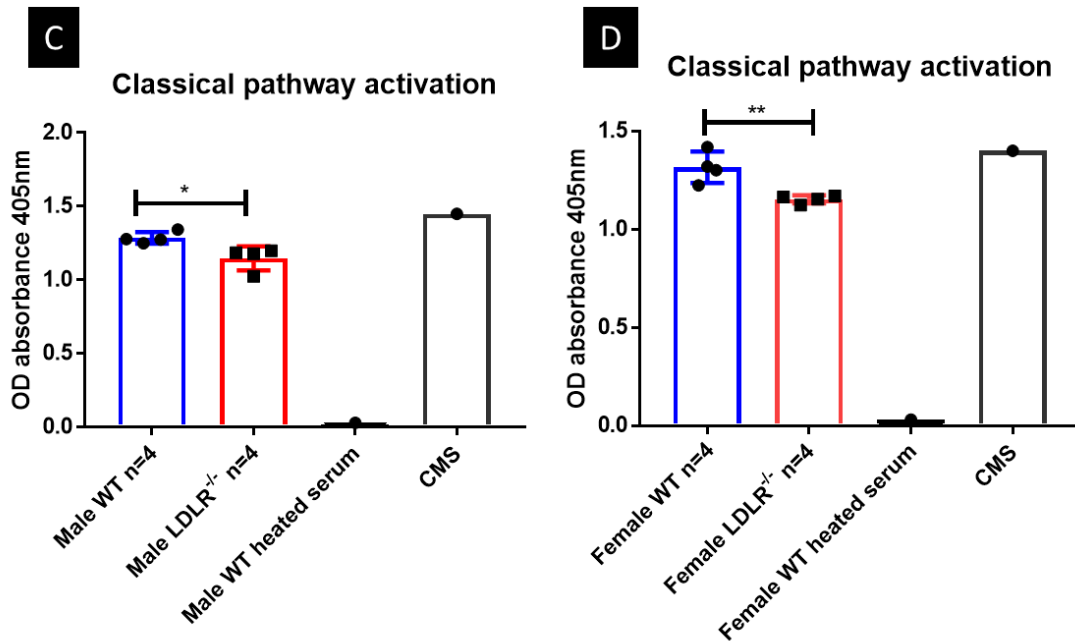


**Figure 3-12: The effect of LDLR absence on classical and alternative complement pathways activation:**

The classical and alternative pathways activities were measured using functional ELISA by measuring the final product of complement C9 in the serum of mice lacking LDLR compared to WT. The alternative pathway activation in male (A) and female (B); the classical pathway activation in male (C); female (D). The unpaired t test of the mean  $\pm$ SD of three analytical triplicates, \*P<0.05, \*\*P<0.001.

**Table 3-1: The percent of alternative pathway activity related to commercial mouse serum in serum of LDLR deficient mice**

	Wildtype	LDLR <sup>-/-</sup>
Males	98%	64%
Females	88%	56%

**Table 3-2: The percent of classical pathway activity related to commercial mouse serum in serum of LDLR deficient mice**

	Wildtype	LDLR ko
Males	88%	79%
Females	94%	82%

### 3.2.1.5 The effect of LDLR<sup>-/-</sup> on serum levels of proinflammatory cytokines TNF- $\alpha$ and IL-6.

The inflammatory cytokines (IL-6 and TNF- $\alpha$ ) levels increase associated with LDLR<sup>-/-</sup> mice (Tanaka *et al*, 2016). To investigate whether LDLR absence may influence serum proinflammatory cytokine levels that could affect bone mineral density, the levels of serum TNF-alpha and IL-6 were measured in serum of LDLR deficient mice compared to WT.

The serum tumour necrosis factor alpha and IL-6 were significantly increased in mouse serum lacking low-density lipoprotein receptor (LDLR<sup>-/-</sup>) in both male and female comparing to their control mice (Figure 3-13). This indicates that the LDLR absence could induce a significant increase of serum TNF-alpha and IL-6 that have a role in bone mineral density reduction.

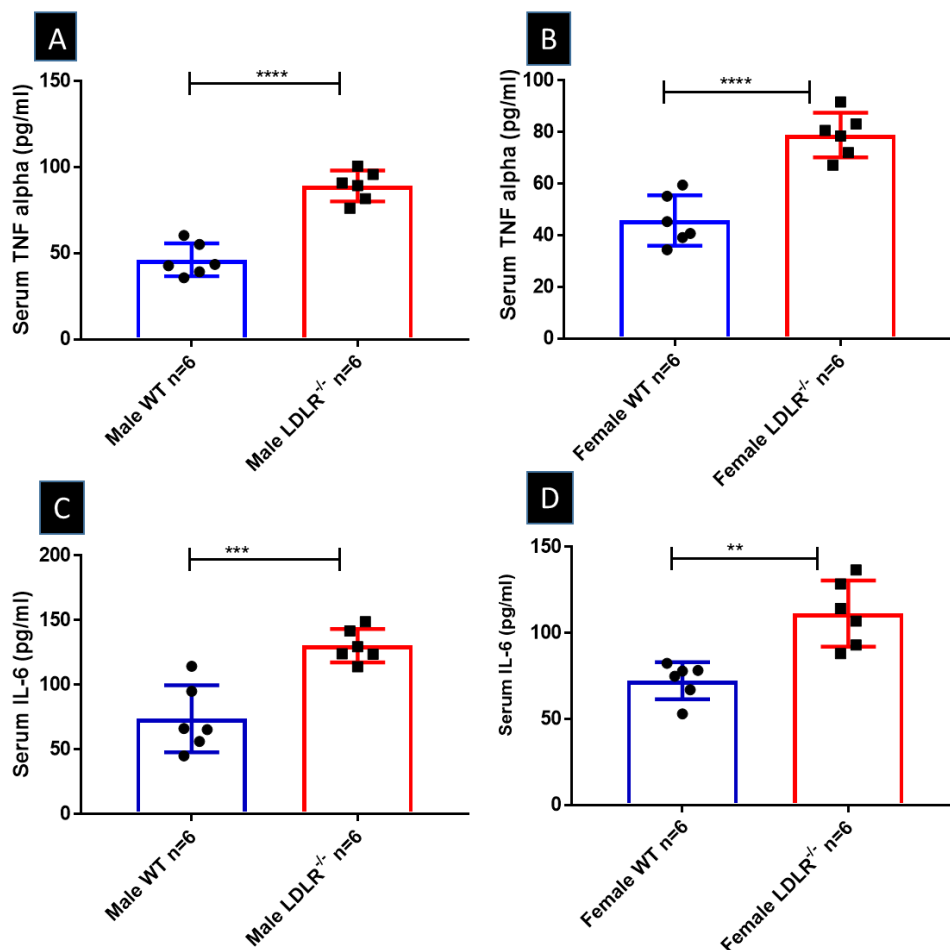


**Figure 3-13: inflammatory cytokines (IL-6 and TNF- $\alpha$ ) levels in LDLR deficient mice:**

The serum inflammatory cytokines were measured in LDLR<sup>-/-</sup> mice serum. The serum TNF-alpha (A) for males and (B) for females; the serum IL-6 (C) for males and (D) for females. The experiment was repeated twice in analytical triplicates and the data represent the mean  $\pm$ SEM of the unpaired t-test, \*\*\*\*P<0.0001.

### **3.2.1.6 Suitability of 5-weeks protocol to study adaptation of vitamin D3 supplementation or voluntary wheel exercising in LDLR<sup>-/-</sup> mice.**

There is a significant effect of vitamin D3 supplementation on body weight loss and serum triglyceride level reduction (R. Kheder *et al*, 2017a; R. K. Kheder, 2017b). In addition, voluntary exercising plays a significant role in body weight loss and reduced triglyceride serum level (Meissner *et al*, 2011). Therefore, to investigate whether 5 weeks of vitamin D3 supplementation or voluntary exercising could control the body mass and levels of triglyceride, the body weight and serum triglyceride were measured in LDLR<sup>-/-</sup> mice with or without 11IU/g diet of vitamin D3 or access to voluntary exercising for 5 weeks.

There was a significant increase in the body weight of LDLR<sup>-/-</sup> mice after 5 weeks compared to their WT mice. However, the body weight in LDLR<sup>-/-</sup> fed a normal diet with Vitamin D3 supplementation or access to wheel exercise was normalised to their control group (Figure 3-14 A). In addition, the triglyceride level was significantly higher in LDLR<sup>-/-</sup> than the control group, but Vitamin D3 supplementation and exercising reduced the TG levels in LDLR<sup>-/-</sup> or normalised to their WT control (Figure 3-14 B). This means that vitamin D3 or exercising are likely to contribute to reducing the triglyceride levels in LDLR<sup>-/-</sup> mice serum.

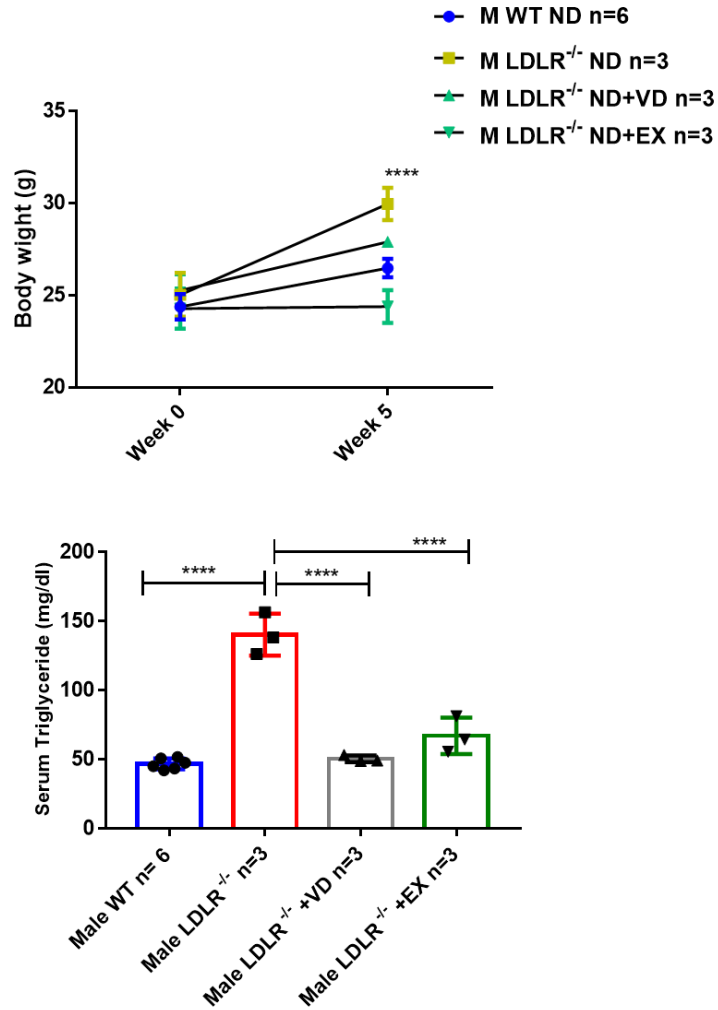
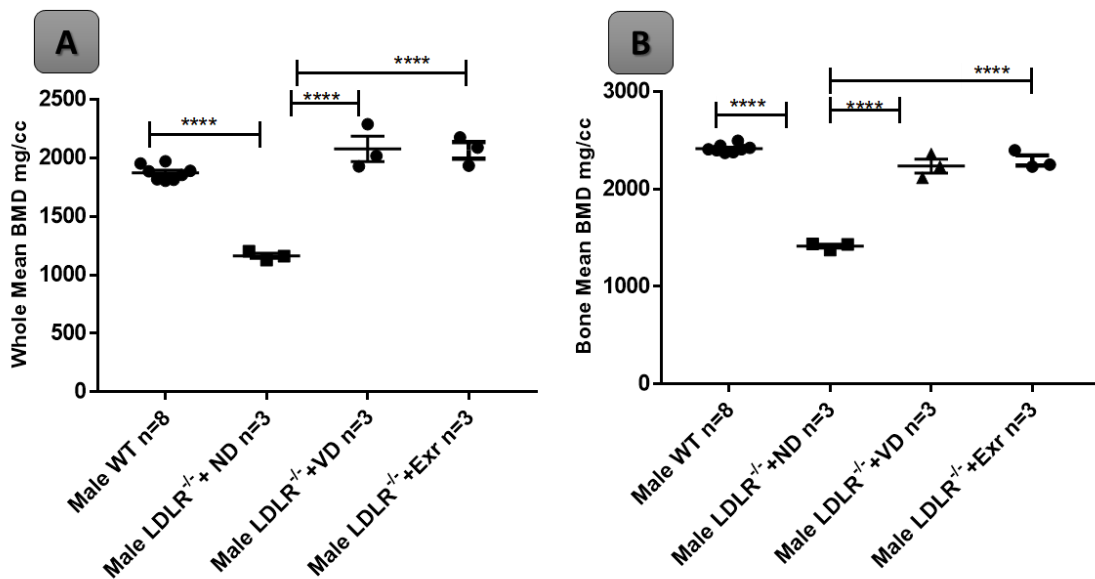


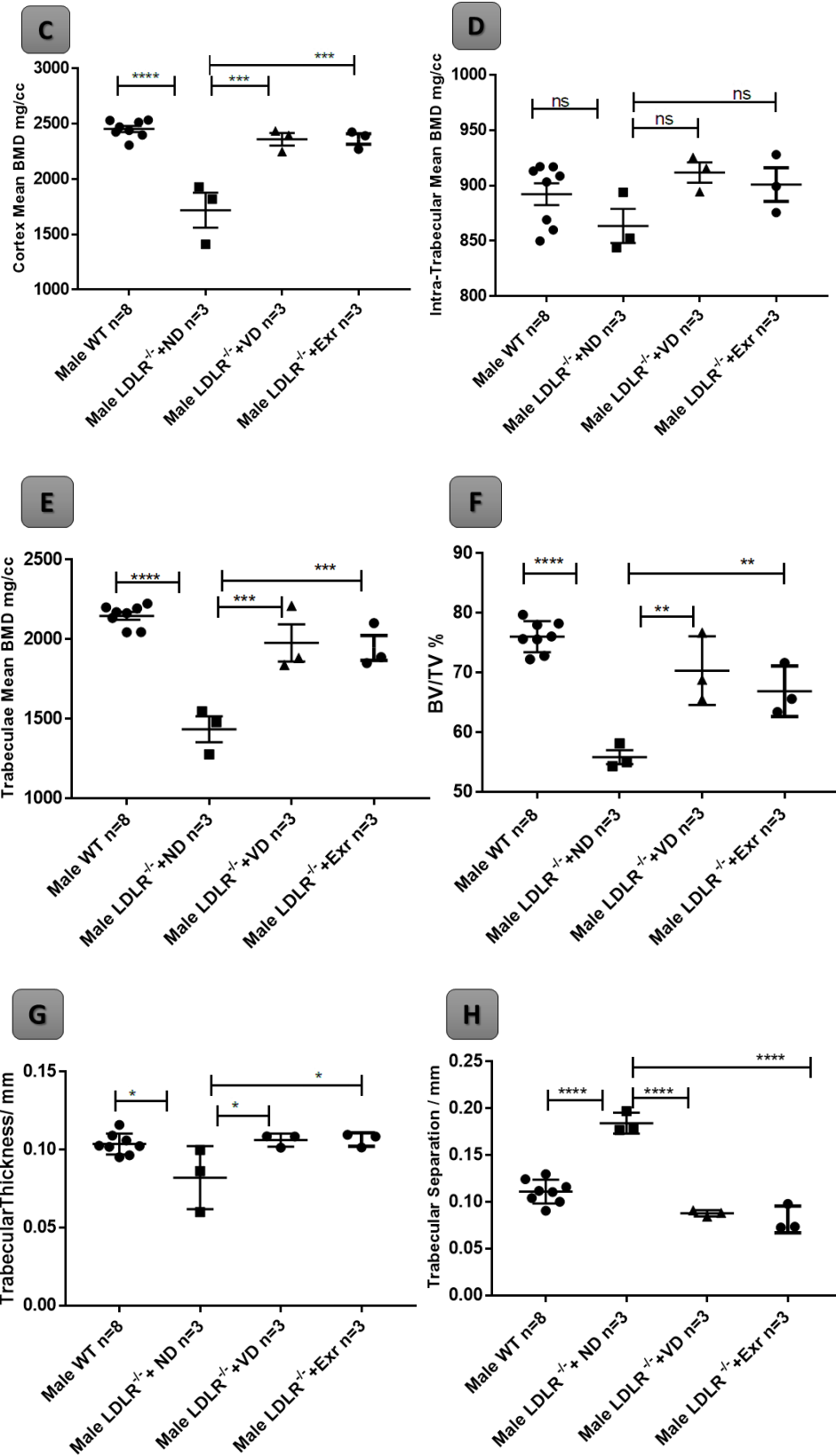
**Figure 3-14: The effect of Vitamin D3 or exercising on body weight or triglyceride levels in LDLR<sup>-/-</sup> :**  
 (A) Represent the body weight; (B) level of serum Triglyceride. The data represent the mean  $\pm$ SD of Tukey multiple comparison of one-way ANOVA \*\*\*\*P<0.0001.

### 3.2.1.7 The effect of Vitamin D3 supplementation or access to exercise on bone mineral density reduction in LDLR<sup>-/-</sup> mice.

It was found in this project that Vitamin D3 supplementation or access to voluntary exercising normalised bone mineral density reduction induced by a high-fat diet. Therefore, to investigate whether Vitamin D3 supplementation or access to voluntary exercising influence bone mineral density reduction induced by LDLR<sup>-/-</sup>, the BMD was assessed in 3<sup>rd</sup> lumbar vertebrae of LDLR<sup>-/-</sup> mice fed a normal diet with or without vitamin D3 supplementation or access to voluntary wheel exercising for 5 weeks.

The Whole Bone mineral and Bone mean densities were significantly reduced in LDLR<sup>-/-</sup>, but the Whole Bone mineral density was elevated in both of LDLR<sup>-/-</sup> with VD or LDLR<sup>-/-</sup> with exercising comparing to LDLR<sup>-/-</sup> or it was normalised to their control wildtype (Figure 3-15 A, B&C). The reduction of Bone Mean density induced a sharp decline in Cortex Mean density, Trabeculae Mean density, BV/TV, Trabecular Thickness, the degree of connectivity and Trabecular number of LDLR<sup>-/-</sup> mice. At the same time, these parameters were significantly increased in LDLR<sup>-/-</sup> fed a normal diet with Vitamin D3 or access to voluntary exercising for 5 weeks compared to LDLR<sup>-/-</sup> (Figure 3-15 C, E, F, H, I&J). The intra-Trabeculae Mean density was not affected in all groups (Figure 3-15 D). The 3D rendering image representing the Cortex and Trabecular segmentations and showing the reduction in BMD of LDLR<sup>-/-</sup> mice was corrected to the WT in LDLR<sup>-/-</sup> with VD or LDLR<sup>-/-</sup> with exercising (Figure 3-16). These results could indicate that vitamin D3 or exercising strongly contribute to enhancing bone mineral density in LDLR<sup>-/-</sup> mice.





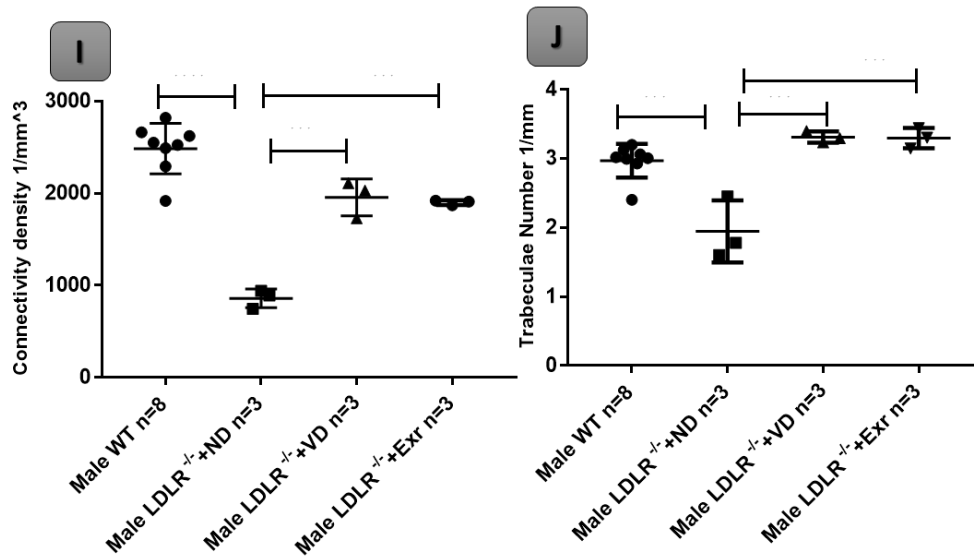


**Figure 3-15: The influence of Vitamin D3 or exercising on bone microarchitecture induced by LDLR<sup>-/-</sup> whilst on normal diet for 5 weeks.**

The 3<sup>rd</sup> vertebrae of LDLR<sup>-/-</sup> with or without dietary vitamin D3 supplementation or access to exercise subjected to  $\mu$ -CT to quantify the effect of VD or exercising on BMD reduction in LDLR<sup>-/-</sup>. Whole BMD (A); The Bone Mean (B); Cortex Mean (C); Intra-trabeculae tissue (D); trabeculae Mean BMD (E); BV/TV (F); Trabecular Thickness (G); Trabecular separation (H); degree of connectivity (I) and Trabecular number (J.) The data are represented as means  $\pm$  SD of Tukey multiple comparison of one way ANOVA (\*P < 0.05; \*\*P < 0.01; \*\*\*P < 0.001; \*\*\*\*P < 0.0001; ns = not significant).

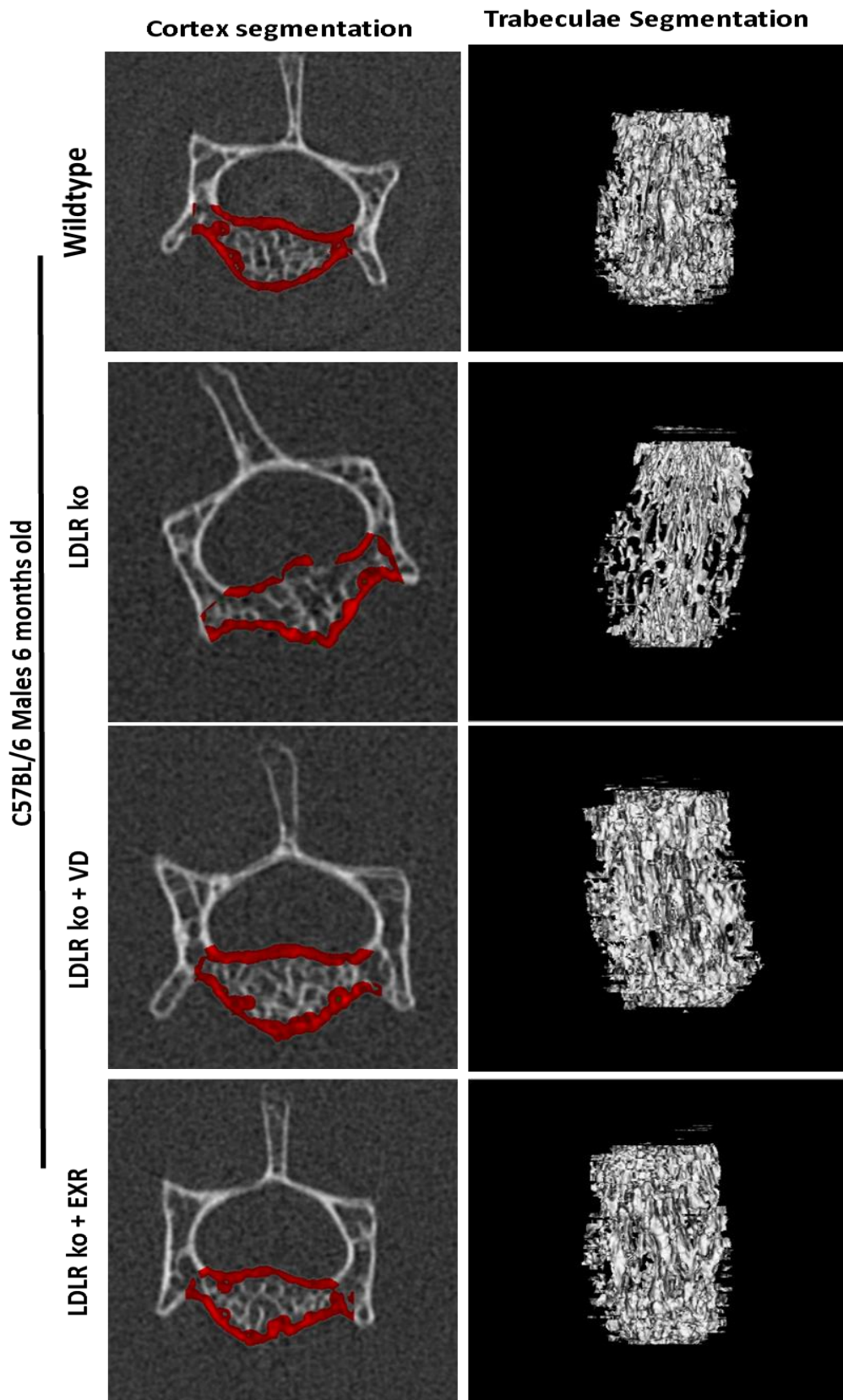
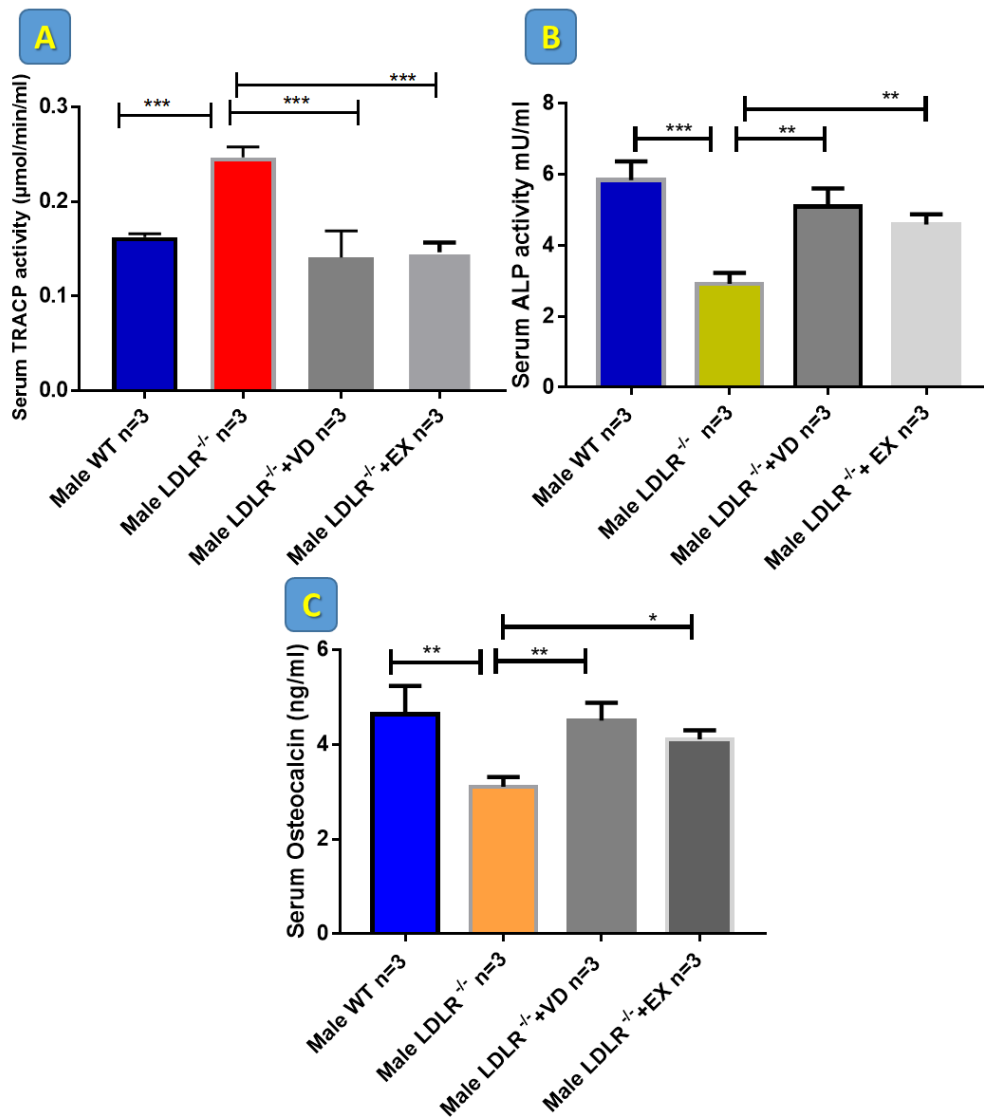


Figure 3-16: The 3D rendering images represent the BMD corrections by vitamin D3 or Exercising in LDLR<sup>-/-</sup> for one mouse in each group.

### **3.2.1.8 Evaluation of the role of Vitamin D3 or Exercising on bone remodelling in LDLR<sup>-/-</sup>:**

The findings showed that there was a significant BMD reduction in LDLR<sup>-/-</sup> mice as shown in [section 3.2.1.2](#). In addition, our findings showed that 11 IU/g diet of vitamin D3 dietary supplementation or access to voluntary wheel exercising for 5 weeks normalised the osteoclast and osteoblast activities during high-fat diet as shown in [section 3.2.2.3](#) and [section 3.3.2.3](#). Therefore, to quantify whether vitamin D3 supplementation or access to voluntary exercise for 5 weeks influence osteoclast and/or osteoblast activities of LDLR<sup>-/-</sup> mice, the serum TRACP, an osteoclasts activity marker, serum ALP and osteocalcin, osteoblast activity markers, were measured in serum of LDLR<sup>-/-</sup> mice fed a normal diet for 5 weeks with or without vitamin D3 dietary supplementation or access to wheel exercising.

The serum level of TRACP in LDLR<sup>-/-</sup> was significantly elevated compared to WT. Vitamin D3 supplementation or wheel exercising for 5 weeks significantly reduced serum TRACP level compared to LDLR<sup>-/-</sup> or normalised to the level in WT mice ([Figure 3-17 A](#)). This may indicate that Vitamin D3 or exercising strongly suppressed osteoclast activity in LDLR<sup>-/-</sup> and then enhanced bone mineral density in LDLR<sup>-/-</sup>. Serum ALP and osteocalcin sharply declined in the LDLR<sup>-/-</sup> group compared to WT mice. Vitamin D3 or exercising ameliorated the levels of ALP and osteocalcin levels in their serum ([Figure 3-17 B&C](#)). These results indicate that osteoblasts become more active in response to Vitamin D3 or exercising compared to LDLR<sup>-/-</sup> untreated mice.



**Figure 3-17: The effect of Vitamin D3 or exercising on bone remodelling in LDLR<sup>-/-</sup> for 5 weeks:** The TRACP activity as osteoclast marker and alkaline phosphatase, osteocalcin as osteoblast markers were measured in serum of LDLR<sup>-/-</sup> with or without Vitamin D3 or wheel exercising for 5 weeks. The serum TRACP activity (A); Serum ALP activity (B); Serum osteocalcin level (C). The data represent the mean  $\pm$ SD of Tukey multiple comparison of one-way ANOVA (\*P < 0.05; \*\*P < 0.01; \*\*\*P < 0.001).

### 3.2.1.9 The effect of Vitamin D3 or exercising on serum inflammatory cytokines levels in LDLR<sup>-/-</sup>.

The serum levels of TNF-alpha and IL-6 were significantly increased in LDLR<sup>-/-</sup> mice compared to their control group as shown in [section 3.2.1.5](#). In addition, the complement activity was significantly increased in LDLR<sup>-/-</sup> mice as shown in [section 3.2.1.4](#). However, our results showed that vitamin D3 dietary supplementation or exercising normalised the excessive level of production in mice serum fed a high-fat diet for five weeks as shown in [sections 3.2.2.5](#) and [3.3.2.5](#). Therefore, to quantify whether Vitamin

D3 or exercising could affect inflammatory cytokines levels in LDLR<sup>-/-</sup>, the serum levels of IL-6 and TNF- $\alpha$  were measured in LDLR<sup>-/-</sup> fed on normal diet with vitamin D3 supplementation or access to exercising for 5 weeks.

Vitamin D3 or access to exercising were associated with a significant reduction in IL-6 and TNF- $\alpha$  serum level of LDLR<sup>-/-</sup> fed on normal diet with vitamin D3 supplementation or exercising compared to LDLR<sup>-/-</sup> (Figure 3-18).

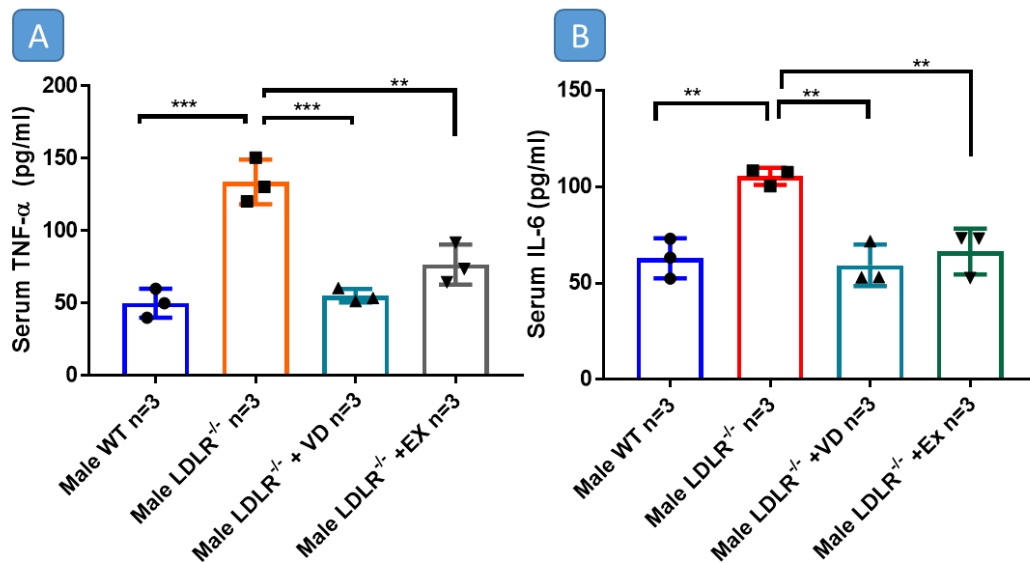


**Figure 3-18: The effect of Vitamin D3 or exercising on serum levels of IL-6 and TNF- $\alpha$  in LDLR<sup>-/-</sup>:** The serum IL-6 and TNF- $\alpha$  levels were measured in LDLR<sup>-/-</sup> mice fed a normal diet for 5 weeks supplemented with Vitamin D3 or accessing to exercising. Serum TNF-alpha (A); Serum IL-6 (B). Each individual point represents the mean  $\pm$ SD of Tukey multiple comparison of one-way ANOVA test triplicates for one animal, \*\*P<0.01; \*\*\*P<0.001.

### 3.2.1.10 The *in vitro* effect of Vitamin D3 on osteoclast differentiation and resorptive activity derived from LDLR deficient mice.

Low-density lipoprotein receptor deficiency may have a role in osteoclast activation and differentiation by influencing the RANKL expression (Bartelt *et al*, 2018). As shown in section 3.2.2.10; Vitamin D3 addition to osteoclast cultures stimulated with fatty acid reduced osteoclast differentiation. Therefore, to quantify whether Vitamin D3 addition could influence osteoclast activity derived from LDLR<sup>-/-</sup>, the TRACP + osteoclast number, resorption activity and TRACP activity were measured in osteoclast cultures with or without 4 $\mu$ g/ml of vitamin D3.

The number of differentiated TRACP+ osteoclasts was increased in LDLR<sup>-/-</sup> but it was decreased in osteoclasts treated with Vitamin D3 (Figure 3-19 A, B&F). The resorption

activity of differentiated osteoclasts was significantly increased in LDLR<sup>-/-</sup> compared to WT, while vitamin D3 addition to osteoclasts cultured from LDLR<sup>-/-</sup> reduced the resorption area (Figure 3-19 C&D). The TRACP activity in osteoclast supernatants was increased in LDLR<sup>-/-</sup> but it significantly decreased or normalised to WT in LDLR<sup>-/-</sup> with vitamin D3 supplementation (Figure 3-19 E). This indicates that vitamin D3 addition *in vitro* controlled the osteoclast differentiation and activation.

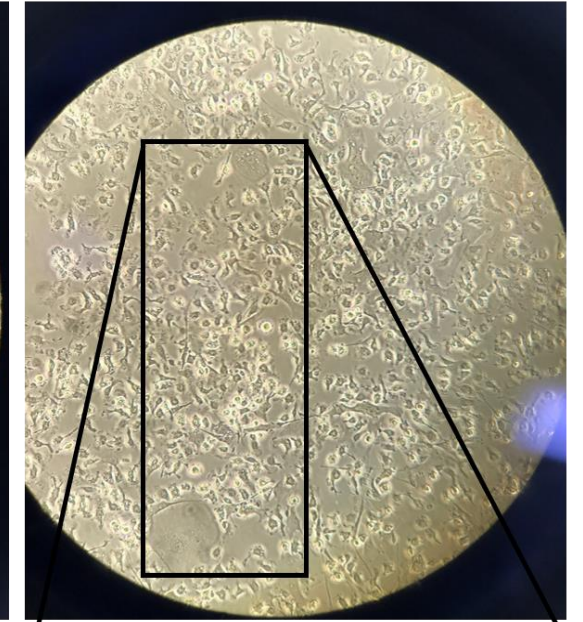
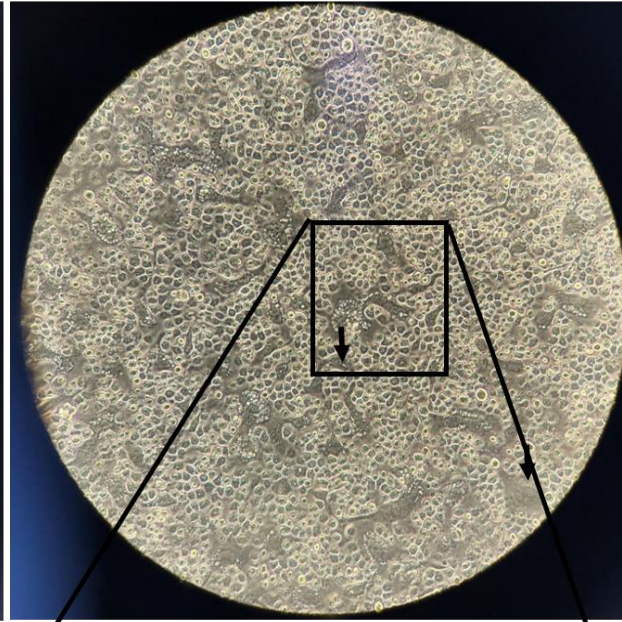
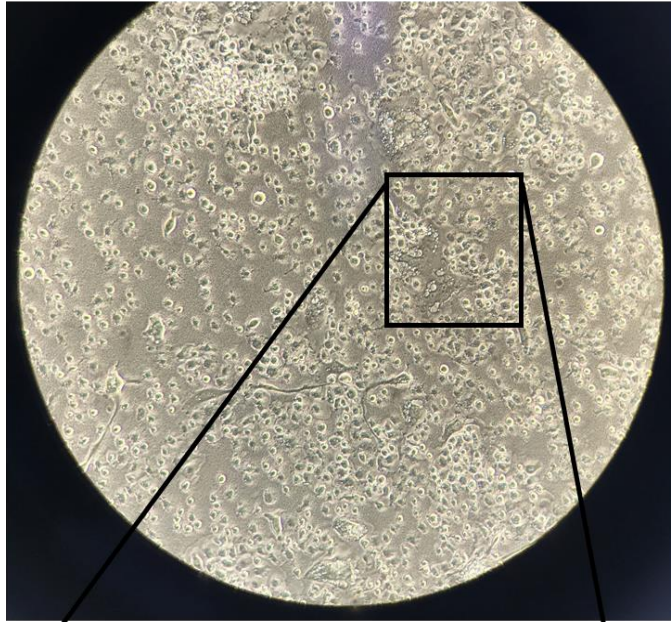
A

Mature osteoclasts  
WT

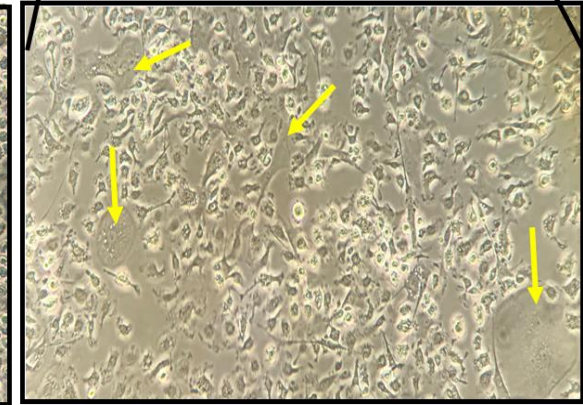
Mature osteoclasts  
LDLR<sup>-/-</sup>

Mature osteoclasts  
LDLR<sup>-/-</sup> + VD

10x magnification



40x magnification



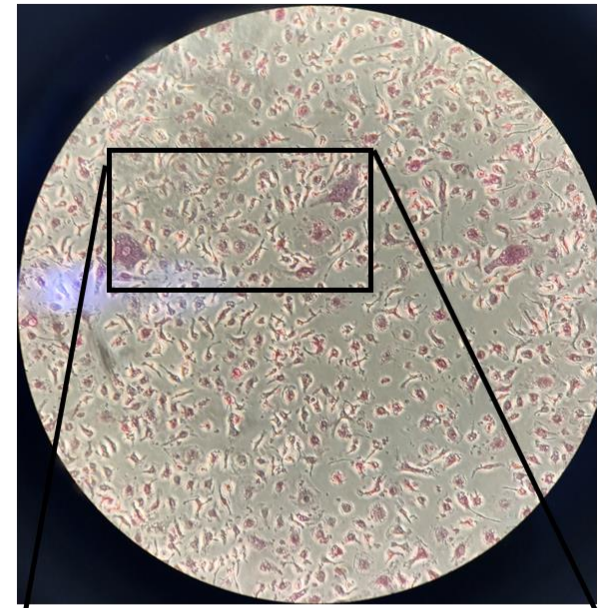
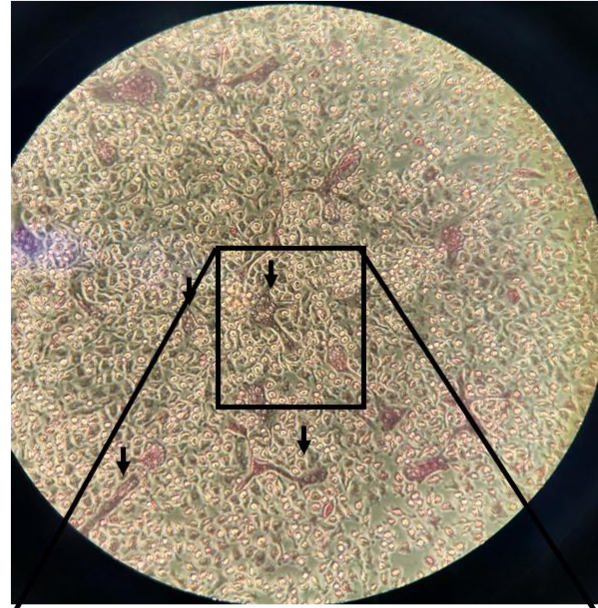
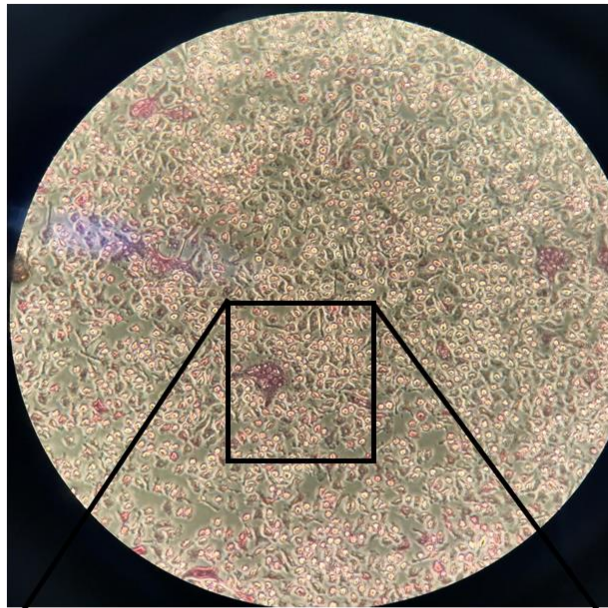
**B**

TRACP + Mature osteoclasts  
WT

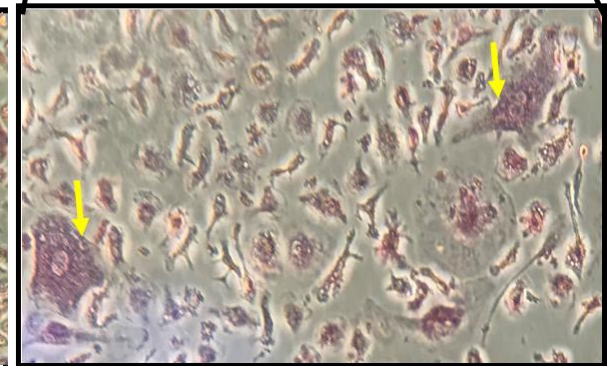
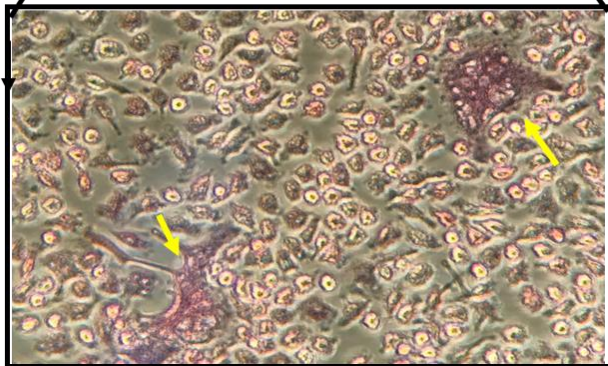
TRACP + Mature osteoclasts  
LDLR<sup>-/-</sup>

TRACP + Mature osteoclasts  
LDLR<sup>-/-</sup>+VD

10x magnification



40x magnification



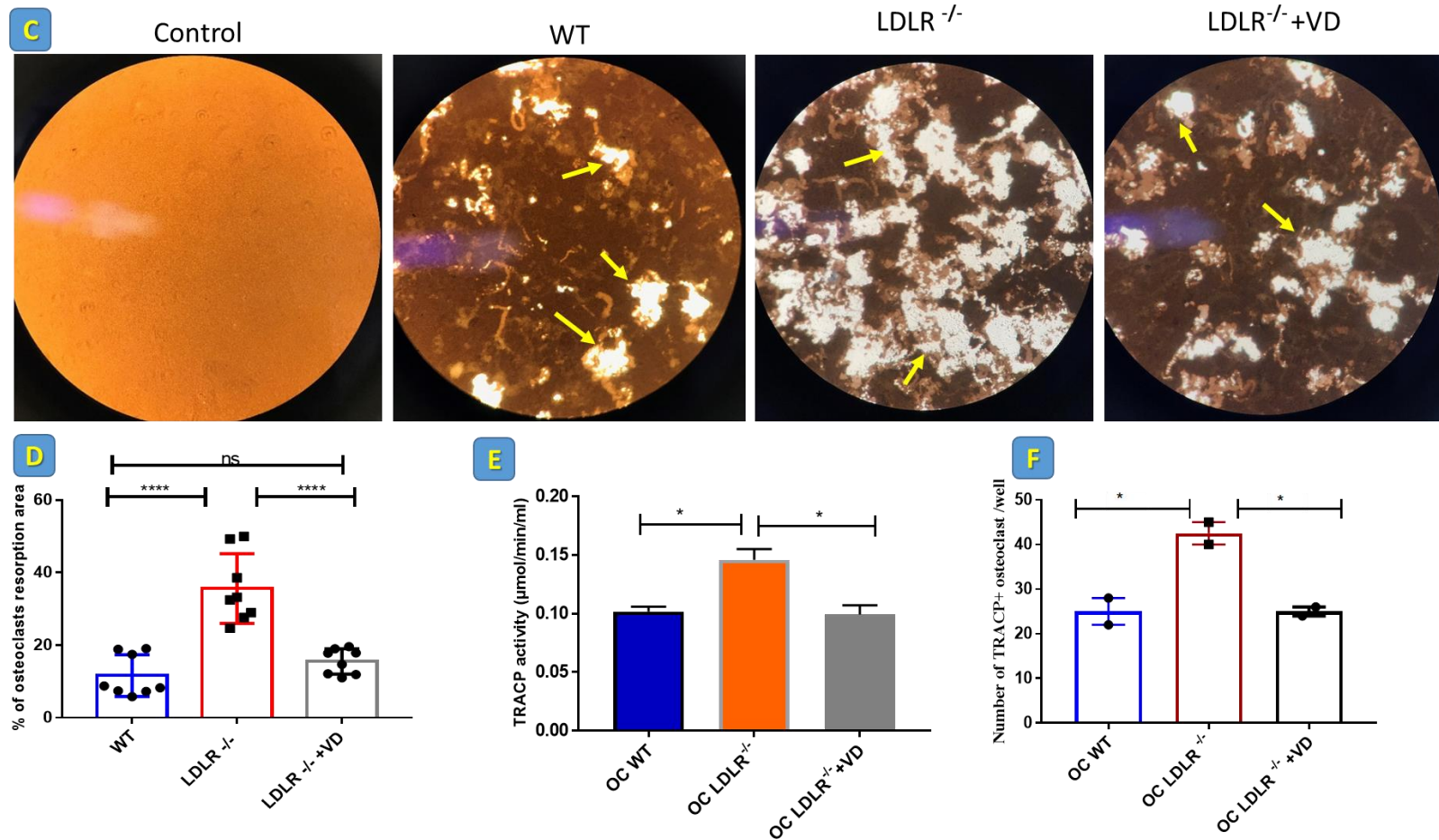


**Figure 3-19: the effect of vitamin D3 addition on the activity of osteoclasts derived from LDLR<sup>-/-</sup>:**

(A) differentiated osteoclasts; (B) the yellow arrows refer to mature TRACP<sup>+</sup> osteoclasts; (C) the yellow arrows refer to osteoclasts resorptive activity; (D) osteoclasts resorptive area; (E) TRACP activity; (F) number of TRACP<sup>+</sup> osteoclasts. The experiment was repeated twice in analytical quadruplicates and represented as means of  $\pm$  SEM (one-way Anova test \*P < 0.05; \*\*P < 0.01; \*\*\*P < 0.001; \*\*\*\*P < 0.0001).

### **3.2.1.11 The *in vitro* effect of Vitamin D3 on osteoblasts differentiation and mineral deposition activity derived from LDLR deficient mice.**

Low-density lipoprotein receptor deficiency may influence osteoblast activity and differentiation (N. Zhang *et al*, 2017). Vitamin D3 has a significant role in osteoblast activation and bone formation increase (Harada *et al*, 2012). Therefore, to investigate whether vitamin D3 influences osteoblast activity *in vitro*, the osteoblast differentiation, bone mineral deposition and ALP activity were measured in osteoblast cultures derived from LDLR<sup>-/-</sup> mice by stimulating with or without 4µg/ml of vitamin D3.

The findings showed there was a significant reduction in ALP+ osteoblast formation in LDLR<sup>-/-</sup> cell cultures compared to WT, but vitamin D3 addition significantly enhanced osteoblast differentiation and proliferation derived from LDLR<sup>-/-</sup> (Figure 3-20 A). The density of osteoblast mineral deposition in LDLR<sup>-/-</sup> cell cultures was significantly less compared to control WT cultures, and vitamin D3 addition to LDLR<sup>-/-</sup> culture increased the density of osteoblast from LDLR<sup>-/-</sup> (Figure 3-20 B&C). Vitamin D3 treatment increased the ALP activity in osteoblast supernatants of LDLR<sup>-/-</sup> or vitamin D3 addition normalised osteoblast ALP activity to the level WT control cultures, the negative control had no cells (Figure 3-20 D). These results indicate that Vitamin D3 has a positive effect on bone formation in LDLR<sup>-/-</sup> by enhancing osteoblast activity.

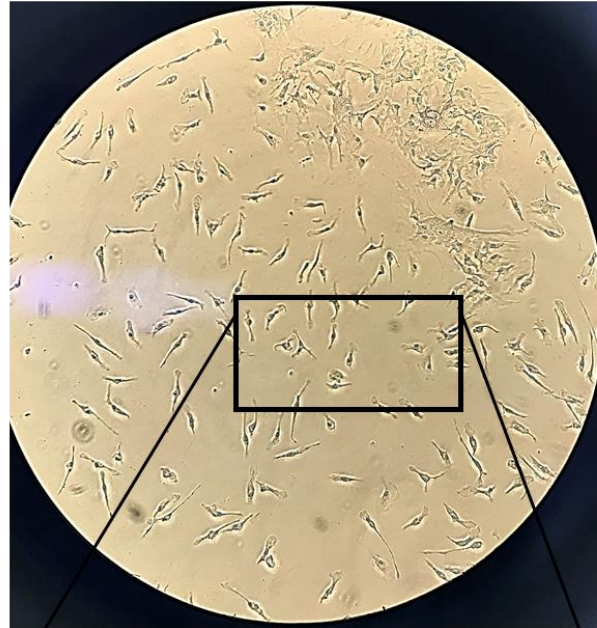
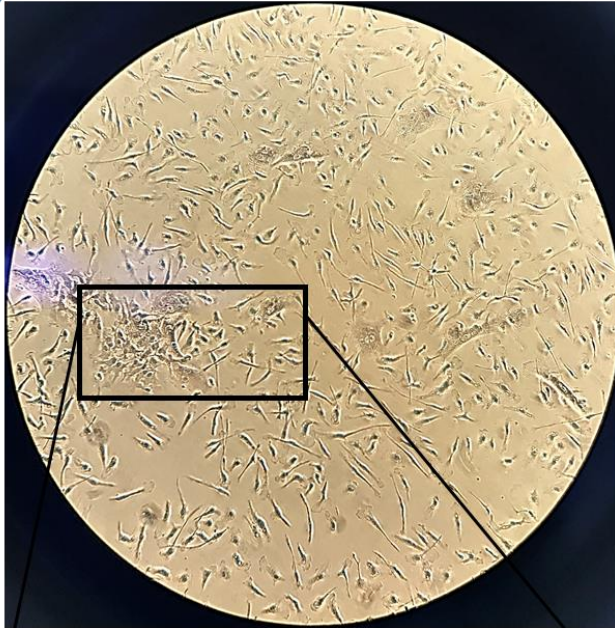
**A**

Osteoblasts (ALP+) WT

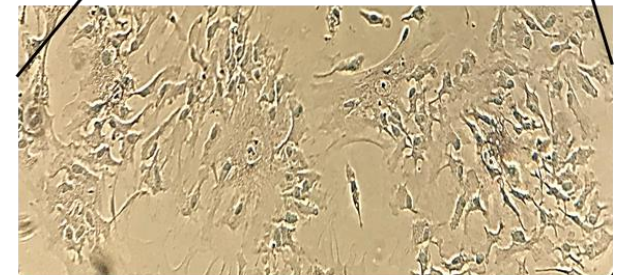
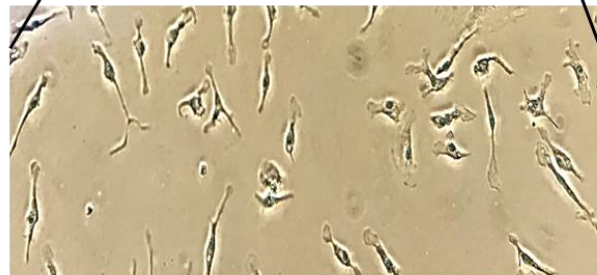
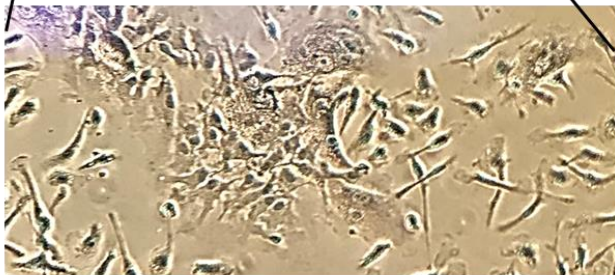
Osteoblasts (ALP+) LDLR<sup>-/-</sup>

Osteoblasts (ALP+) LDLR<sup>-/-</sup> +VD

10x magnification



40x magnification



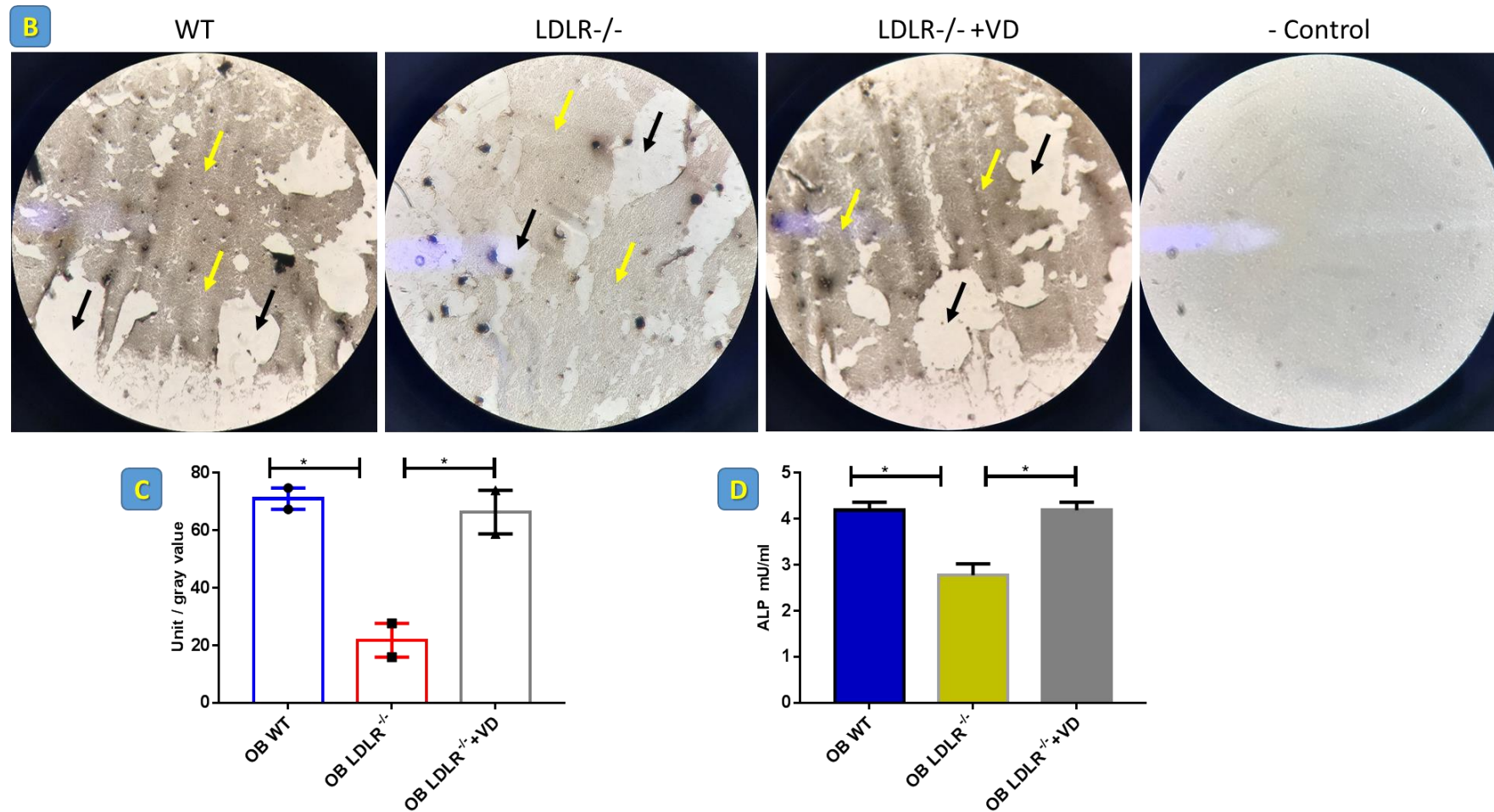


**Figure 3-20: The effect of Vitamin D3 addition *in vitro* on osteoblasts activity derived from LDLR<sup>-/-</sup> mice bone marrow:**

(A) Osteoblasts ALP<sup>+</sup> cells; (B&C) quantification of osteoblasts mineral deposition (yellow arrows) (black arrows refer to background); (D) ALP activity in osteoblasts supernatant, the negative control had not cells. The experiment was repeated twice in quadruplicates and represent the mean  $\pm$  SEM analysed by Tukey multiple comparison of one-way ANOVA test; \*P<0.05.

### **3.3 Vitamin D3 normalises long chain fatty acid-induced expression of alternative pathway complement components in osteoclasts (In vitro study).**

#### **3.3.1 Introduction.**

Different complement proteins are engaged in the bone formation during bone development: alternative complement proteins like C3, CFB, properdin, C5 and C9 exist in the proliferation area of bone development (Andrades *et al*, 1996). The osteoclast differentiation was actively suppressed by C3 blocking at the early period of osteoclast formation, and this indicated that C3 was essential for osteoclast precursors to progress to osteoclasts formation (Sato *et al*, 1993). C3<sup>-/-</sup> mice had less *in vitro* differentiated osteoclasts than wildtype (Tu *et al*, 2010). In humans, it was claimed that osteoclasts could cleave C5 to produce C5a by a membrane protease (Ignatius *et al*, 2011a). These studies showed the role of the complement system on osteoclast activity.

The fatty acid could be related to reducing bone density by activating the osteoclast activity and increasing bone resorption. It was shown that osteoclast differentiation gene expression (RANKL/OPG ratio) and inflammatory cytokines (IL-6 and IL-8) were significantly increased by fatty acid stimulation (Cornish *et al*, 2008). Additionally, fatty acids have an influence on osteoclast survival by reducing their apoptosis through signalling via TLR4, Myeloid differentiation primary response 88 (MYD88), and NF-κB expression (Oh *et al*, 2010). However, Kheder, *et al* (2017a) showed that Vitamin D3 has a significant role in normalising the excessive activation of alternative and classical complement pathways induced by a high-fat diet by measuring both pathway's activation by the C9 formation in serum of mice fed a high-fat diet with or without vitamin D3 supplementation for 5 weeks. Therefore, it was hypothesised that:

- Murine osteoclasts could cleave complement C5 to its anaphylatoxin C5a.
- Murine osteoclasts could express alternative pathway complement components.
- *In vitro* addition of Vitamin D3 normalises the complement component expression from differentiated osteoclasts stimulated by fatty acid.

### 3.3.2 Results.

#### 3.3.2.1 The role of murine osteoclasts in C5 Cleavage to C5a.

The fifth component of complement C5 plays a significant role in inflammation and host defence against pathogens. It was claimed that human osteoclasts could cleave C5 to C5a by a protease on osteoclast membranes (Ignatius *et al*, 2011a). Therefore, to investigate whether murine osteoclasts may play a role in C5 cleavage to C5a, the murine osteoclasts were differentiated and incubated with purified human C5 to detect the C5a production by Western blotting and ELISA.

The mouse-differentiated osteoclasts were incubated with or without purified human C5 protein (5µg/ml) for 4 hours as in Ignatius *et al* (2011a) methods. According to the NCBI website, there is about 77-78% of identity and 88-89% of similarity between murine complement C5 and human complement C5 protein. Then, C5a was detected in the supernatant using rabbit polyclonal anti-human C5a IgG (Gene Tex.com) by Western blotting to detect the C5a produced from the added purified human C5. The murine macrophage cell line J774 supernatant and human plasma activated with Salmonella LPS were used as positive controls to detect C5 and C5a. The complement C5 was detected in serum-free media of differentiated osteoclasts incubated with purified C5, but it was not detected in osteoclasts supernatant without C5 incubation, although, C5 was detected in J774 macrophage supernatants incubated with or without C5. Moreover, the anaphylatoxin C5a was detected in human plasma stimulated with LPS, but not in osteoclast supernatant (Figure 3-21 A). In addition, the cellulose membrane was submerged under the Ponceau S stain to confirm that there were different proteins run in all samples (Figure 3-21 B). These results indicate the murine osteoclasts did not produce C5 and they could not cleave the incubated C5 to its C5a.

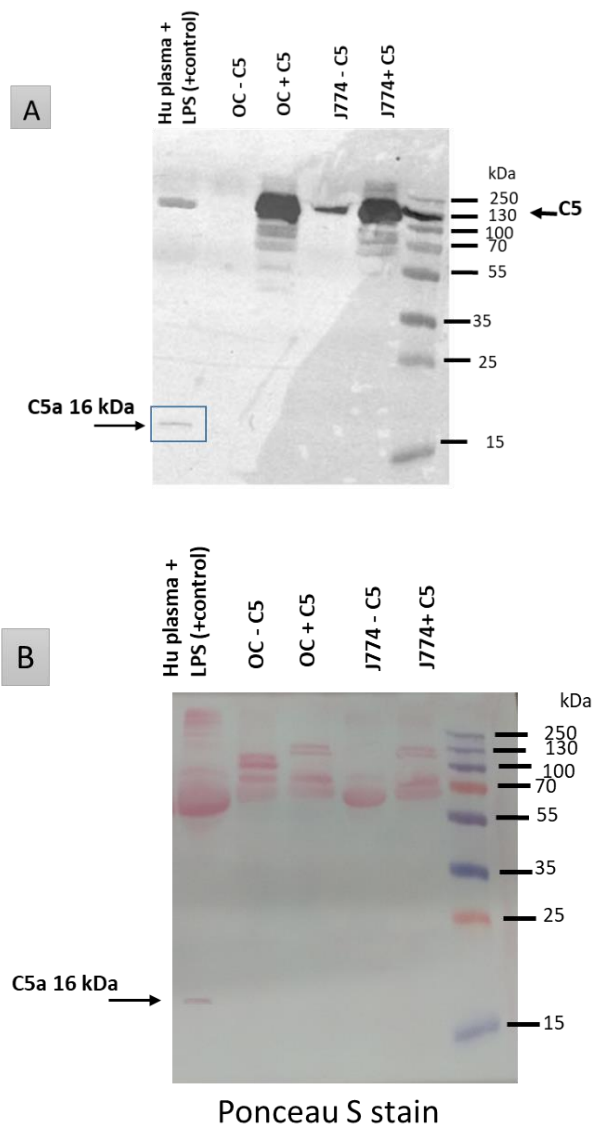


**Figure 3-21: Identification of complement C5/C5a production by murine osteoclasts:**

(A) C5 and C5a detection by Western blotting in osteoclasts and J774 supernatants. (B) Ponceau stain shows different proteins running in each sample. The experiment was performed twice.

RANKL has been identified to affect the immune system and control bone regeneration and remodelling by activating osteoclast formation (Wada *et al*, 2006; Mueller and Hess, 2012). Therefore, to investigate whether RANKL influences the complement C5 protein production by murine osteoclast, the C5 concentration using ELISA was measured in cell culture supernatants of differentiated osteoclasts, J774 macrophage murine cell line treated with or without 20ng/ml RANKL along with osteoclasts. The 1:20 diluted mouse serum was used as a positive control. In addition, minimal essential media MEM was used as negative control (Figure 3-22). The complement C5 detection in differentiated osteoclast supernatant was under the detection limit. Interestingly, there was no C5

detection in J774 supernatant cell culture treated with RANKL comparing to J774 untreated by RANKL (Figure 3-22). This may lead to a new understanding that RANKL may suppress the complement C5 protein production. Potentially, this could be cause of inhibition of the C5 produced by osteoclasts derived from murine bone marrow. Therefore, an attempt was made to investigate the complement C5 gene expression in differentiated osteoclasts and J774 macrophage cell line ( $\pm$  RANKL) using qPCR technique.

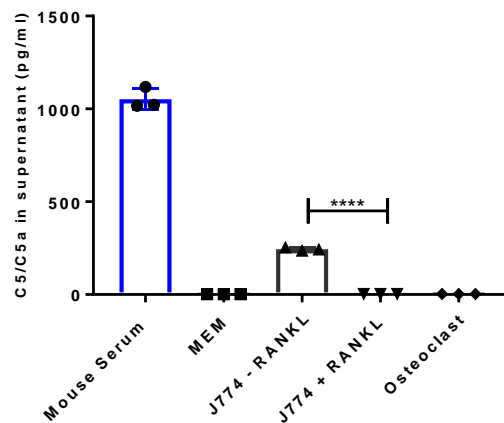


**Figure 3-22: The complement C5 detection in osteoclast and J774 macrophage cell line supernatant:**

The effect of RANKL on C5 protein expression in the supernatants of J774 treated with or without RANKL and osteoclasts supernatant. The experiment was performed three times in triplicates and presented as mean  $\pm$ SEM of unpaired of t test, \*\*\*\*P<000.1.

For quantifying complement C5 gene expression in osteoclasts derived from murine bone marrow, the gene expression was done using the qPCR technique using SYBR Green I dye (SensiMix<sup>TM</sup> SYBR). The J774 macrophage cell line or liver were used as positive controls.

The GAPDH gene expression by qPCR was done as a reference gene expression. The result shows that there was one amplification peak of the product for each sample regarding GAPDH expression (Figure 3-23 A, B&C).

The results show that there was amplification product for C5 gene expression in the positive control (mouse liver mRNA), while it showed that there was no C5 gene expression in osteoclast mRNA (Figure 3-23 D&E). Then, to confirm this result, a normal PCR was run, and it showed there was a C5 expression in liver and J774 mRNAs, but not in osteoclast mRNA (Figure 3-23 F). This result could be consistent with the absence of C5 protein in osteoclast supernatant, and this may be due to lack of C5 gene suppression.

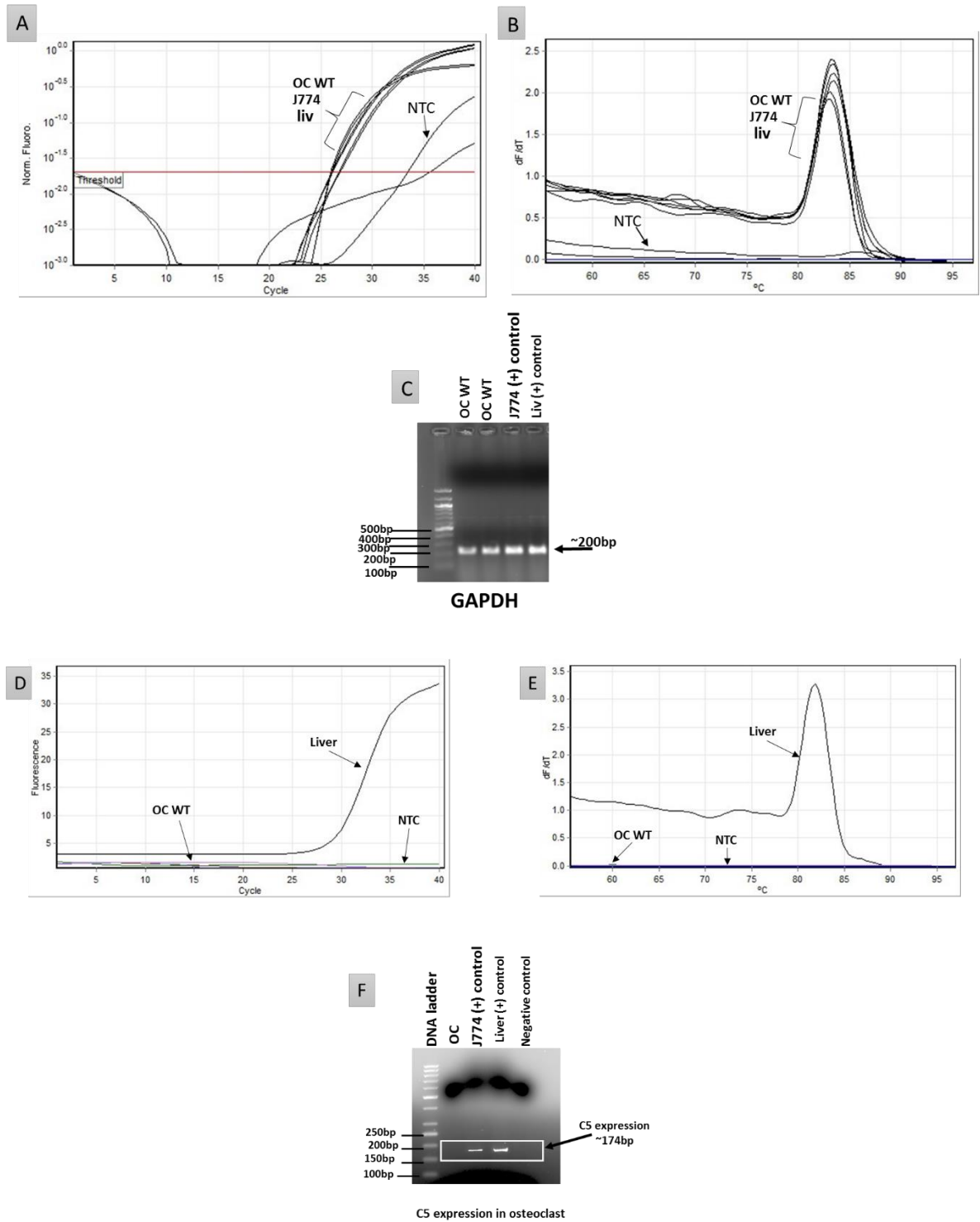


**Figure 3-23: The complement C5 gene expression in murine osteoclasts:**

(A&B) the qPCR analysis for GAPDH as a housekeeping gene expression; (C) the PCR analysis for GAPDH; (D&E) the qPCR analysis for C5 gene expression in murine osteoclast, liver; (F) the PCR analysis for C5 gene expression in murine osteoclast, liver and J774, the experiment performed twice.

Next, a pilot study was done to seek whether RANKL has an effect on complement C5 gene expression. Therefore, the J774 cell line was cultured with or without 20ng/ml RANKL for 7 days, then the total RNA was extracted, and cDNA was synthesised.

The GAPDH gene expression was done as a housekeeping gene for cDNAs of J774  $\pm$  RANKL and mouse liver as a positive control. The results showed that there was one amplification peak of the product for each sample regarding GAPDH expression (Figure 3-24 A&B). Interestingly, the C5 expression was suppressed in J774 cell line cultured with RANKL comparing to the J774 cell line that cultured without RANKL, which amplified in parallel to mouse liver as a positive control (Figure 3-24 C).

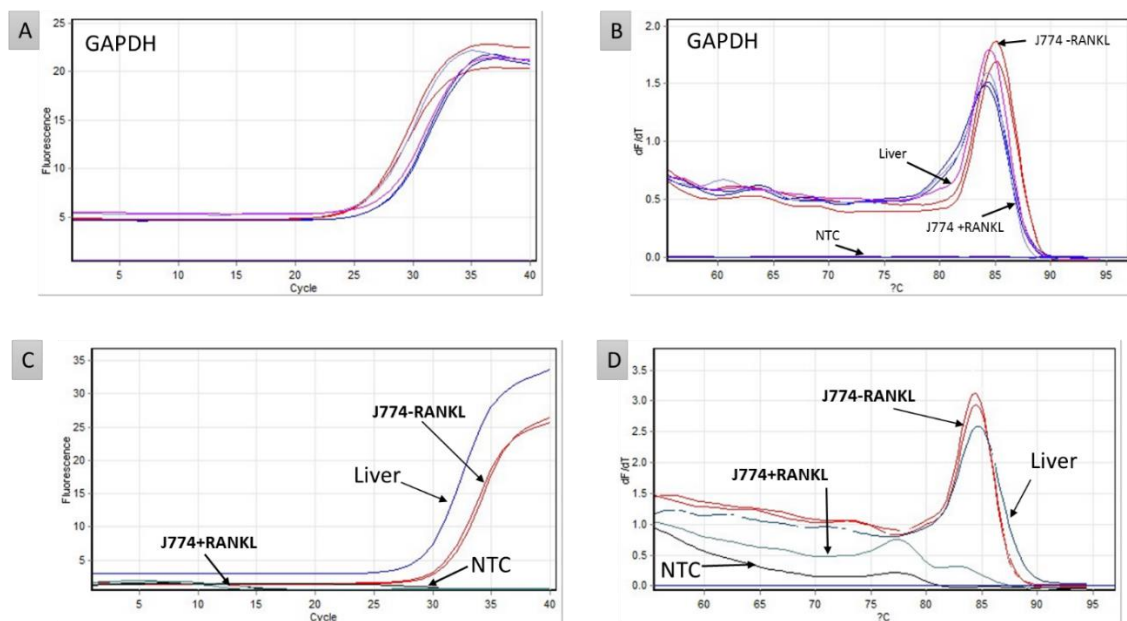


**Figure 3-24: The effect of RANKL on complement C5 gene expression:**

A pilot study to investigate the effect of RANKL on C5 gene expression. GAPDH was done for all samples as a normaliser (A&B). The complement C5 gene expression in J774 cell line treated with or without 20ng/ml of RANKL(C&D). The experiment was performed three times in duplicates.

### 3.3.2.2 The alternative complement component expression by differentiated murine osteoclasts.

Different studies showed that the complement system is associated with bone turnover especially the effect of complement components on osteoclast activation and differentiation (Sato *et al*, 1991; Sato *et al*, 1993; Tu *et al*, 2010). However, the role of murine osteoclasts in the expression of alternative complement components has been not studied. Therefore, the gene expression of the CFD, CFB, CFP, C3 and C5 were investigated in differentiated murine osteoclasts.

The annealing temperatures of CFD, CFB and C3 were determined by gradient PCR which showed that 65°C degree was the best temperature of single product amplification of CFD, CFB and C3 genes (Figure 3-25 A; Figure 3-26 A; Figure 3-27 A). The GAPDH expression was used as a normaliser for cDNA amplification as shown in (Figure 3-23 A). In addition, the qPCR GAPDH was done as shown in (Figure 3-23 B&C).

The major source of plasma CFD is adipose tissue in which it is secreted by both mature adipocytes and macrophages, suggesting a role for adipose tissue in immune system biology (White *et al.*, 1992; Barnum and Volanakis, 1985). However, the CFD expression in bone cells especially the osteoclasts have not been studied. Therefore, the complement factor D gene expression was quantified in osteoclasts derived from murine bone marrow using the qPCR technique using SYBR Green I dye (SensiMix™ SYBR). The results show that there was amplification for CFD gene expression in osteoclast mRNA and the positive control (mouse J774 mRNA) (Figure 3-25 B&D), then to confirm this result, a normal PCR was run and it showed the CFD was expressed in J774 and in osteoclast mRNAs (Figure 3-25 C).

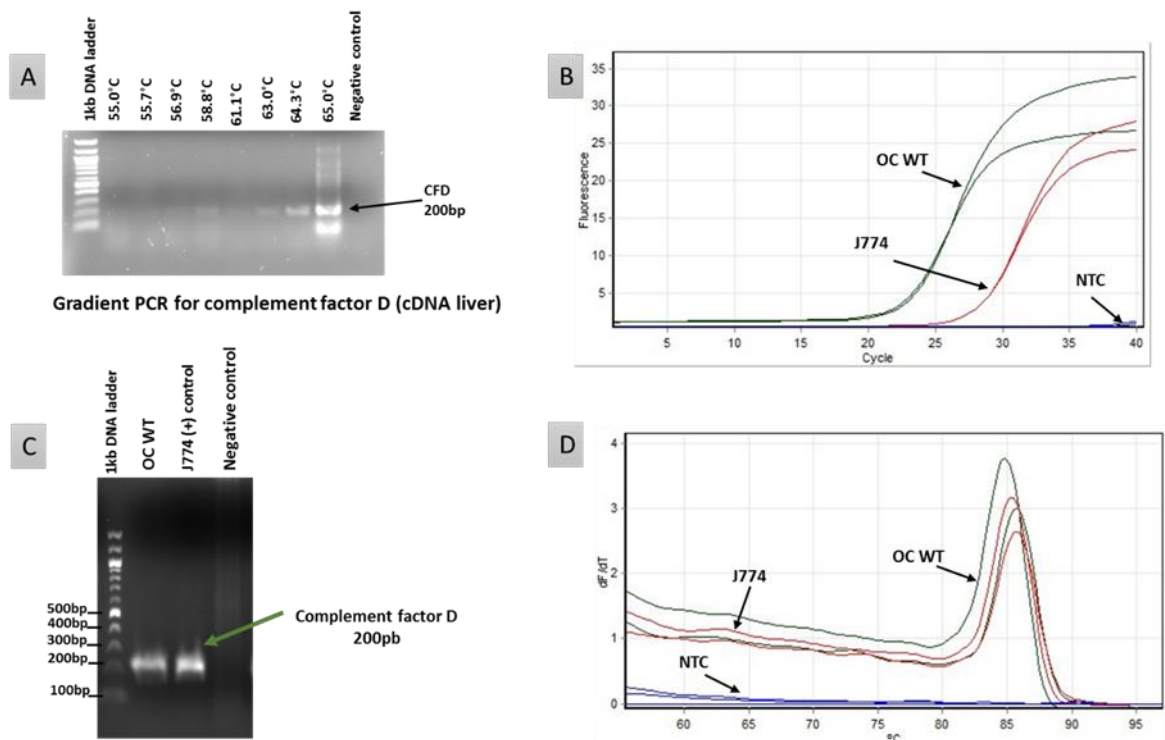


**Figure 3-25: complement factor D expression by murine osteoclasts:**

The expression of complement factor D in differentiated osteoclast and J774 macrophages. (A) Gradient PCR analysis shows the optimal annealing temperature for CFD; (C) the PCR analysis for CFD expression in murine osteoclasts; (B&D) the qPCR analysis for CFD expression in murine osteoclasts. The experiment was performed three times in duplicates.

The complement factor B is produced from different cells like fibroblasts, mononuclear phagocytes, epithelial and endothelial cells, alveolar type II cells, kidney and hepatocytes (D. Li *et al*, 2016); however, its expression in bone cells especially the osteoclasts has not been studied. Therefore, the complement factor B gene expression was quantified in osteoclasts derived from murine bone marrow using normal PCR and qPCR technique using SYBR Green I dye (SensiMix™ SYBR). The result show that the CFB gene was expressed in osteoclast mRNA and the positive control (mouse J774 mRNA) (Figure 3-26 B&D). Then, to confirm this result, a normal PCR was run, and it showed the FB expression in J774 and in osteoclast mRNAs (Figure 3-26 C).

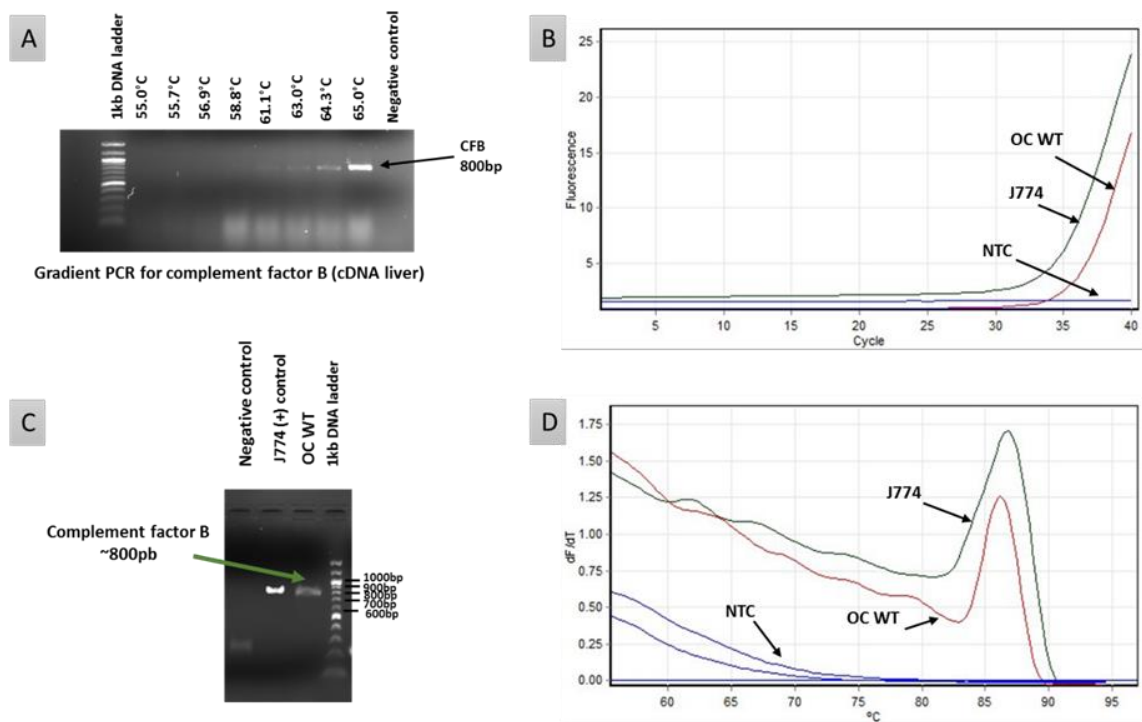


**Figure 3-26: the complement factor B expression by murine osteoclasts:**

The expression of complement factor B in differentiated osteoclasts and J774 macrophages. (A) Gradient PCR analysis shows the optimal annealing temperature for CFB; (C) the PCR analysis for CFB expression in murine osteoclasts; (B&D) the qPCR analysis for CFB expression in murine osteoclasts. The experiment was performed three times in duplicates

Complement component 3 plays a central role in complement system activation and its activation is required for both classical and alternative complement activation pathways (Sahu and Lambris, 2001). The production of C3 has been reported in different cell types, such as hepatocytes, mononuclear, phagocytes, polymorphonuclear leucocytes, fibroblasts, endothelial cells, glioma cell lines and renal Glomerular endothelial cells (Alper *et al*, 1969; Tsukamoto *et al*, 1990; Daha and van Kooten, 2000). Complement C3

is required for bone cell differentiation especially osteoclasts (Ignatius *et al*, 2011a). However, the third complement component expression by murine osteoclasts has not reported yet. Therefore, the normal PCR and qPCR technique using SYBR Green I dye (SensiMix™ SYBR) were used to quantify the complement C3 gene expression in osteoclasts derived from murine bone marrow. There was an amplification or expression for the C3 gene in osteoclast mRNA and the positive controls (mouse J774 mRNA and mouse liver) (Figure 3-27 B&D). Then to confirm this result, a normal PCR showed the C3 expression in J774, mouse liver and osteoclast mRNAs (Figure 3-27 C).

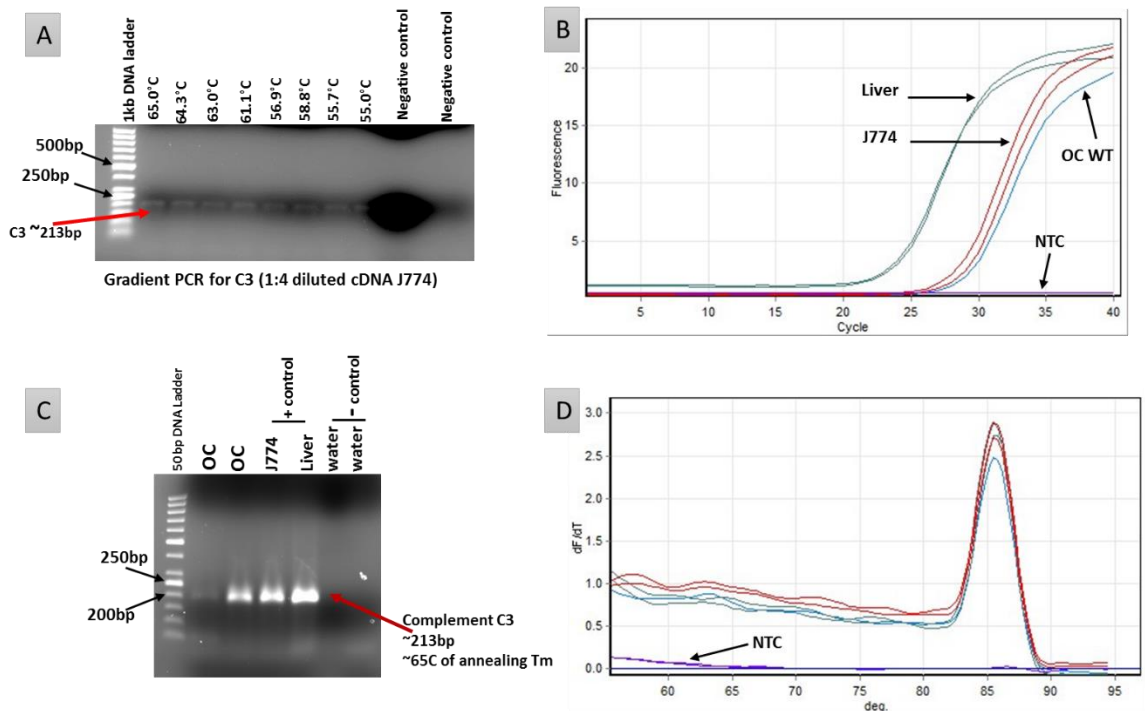


**Figure 3-27: Complement C3 expression by murine osteoclasts:**

The expression of complement C3 in differentiated osteoclast and J774 macrophages and liver. (A) Gradient PCR analysis shows the optimal annealing temperature for C3; (C) the PCR analysis for C3 expression in murine osteoclasts; (B&D) the qPCR analysis for C3 expression in murine osteoclasts. The experiment was performed three times in duplicates.

Complement properdin or Factor P is the only known positive plasma glycoprotein regulator of complement activation that stabilizes the alternative pathway convertases of the innate immune system (Schwaeble and Reid, 1999; Hourcade, 2006). The complement properdin expressed by different cells like liver, neutrophils, macrophages, might have an essential role in osteocyte activity. However, the properdin expression by the osteoclast itself has not investigated. Therefore, the qPCR technique using SYBR Green I dye (SensiMix™ SYBR) was used to quantify the complement properdin

component gene expression in osteoclasts derived from murine bone marrow. In the qPCR analysis, there was amplification or expression for the CFP gene in osteoclast mRNA and the positive controls (mouse J774 mRNA and mouse liver) (Figure 3-28 A&B). Then, to confirm this result, the normal PCR showed the CFP expression in J774, mouse liver and osteoclasts mRNAs (Figure 3-28 C). Therefore, this data shows that the osteoclasts may produce the complement properdin component and might have an essential role in complement activation in bone turnover.

In conclusion, these results revealed for the first time that the osteoclasts could take a role in complement FD, FB, FP, C3 production, but not complement C5. Therefore, murine osteoclasts might have a significant role in complement alternative pathway activation.

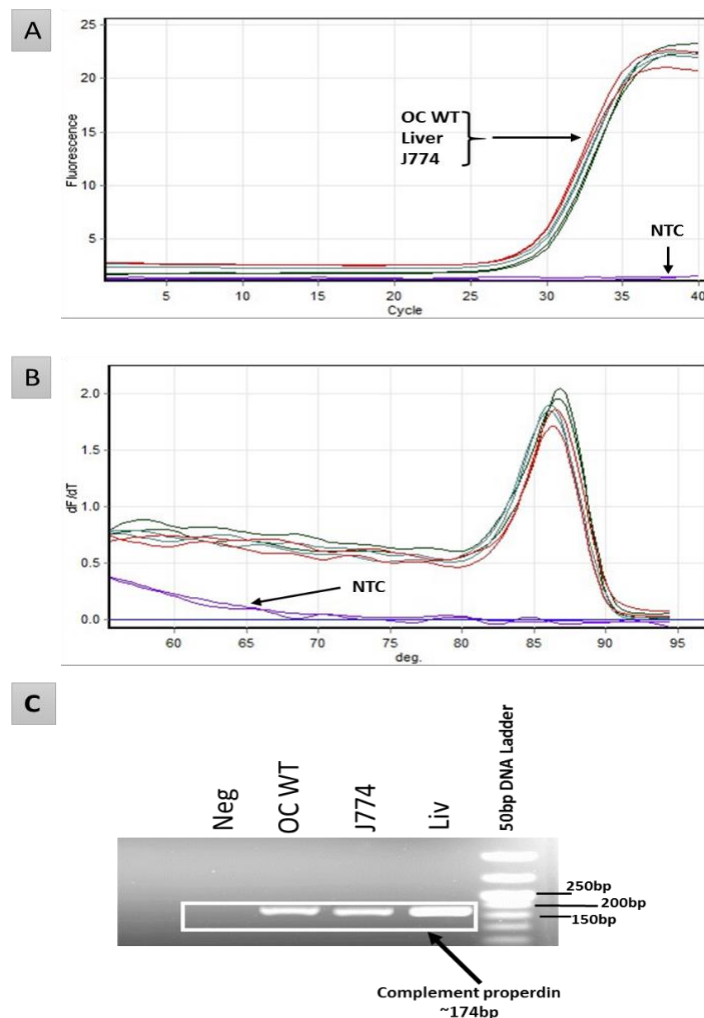


**Figure 3-28: Complement properdin expression by murine osteoclasts:**

Complement properdin expression in differentiated osteoclasts and J774 macrophages and liver. (A&B) the qPCR analysis shows the complement properdin gene expression in murine osteoclasts; (C) the PCR analysis for complement properdin expression in murine osteoclasts. The experiment was performed three times in duplicates.

### **3.3.2.3 The effect of Vitamin D3 on the excessive gene expression of alternative pathway components induced by fatty acid.**

Briefly, the previous data revealed that vitamin D3 *in vivo* has a significant role in normalising the alternative and classical pathways activation in mice fed a high-fat diet for 5 weeks as shown in [section 3.2.1.4](#). Additionally, it normalised the proinflammatory cytokine levels induced responding to high-fat diet intake for 5 weeks as shown in [section 3.2.1.5](#). *In vitro*, Vitamin D3 played an essential role in reducing the resorptive activity of differentiated osteoclasts during free fatty acid stimulation by normalising their TRACP activity as shown in [section 3.2.1.9](#) also it normalised the TNF- $\alpha$  and IL-6 secretion in osteoclast cultures as shown in [section 3.2.1.11](#). Therefore, the gene expression of alternative pathway components was quantified by PCR and qPCR to estimate whether *in vitro* addition of Vitamin D3 normalises the excessive alternative pathway components expression induced by fatty acid in murine osteoclasts.

The  $\beta_2$  microglobulin was used as a housekeeping gene for normalising the levels of other components' expression, and the results showed one amplification peak of the product as shown in ([Figure 3-29 A&B](#)).

The results showed that the level of complement factor D gene expression was significantly increased in osteoclasts stimulated with fatty acid (palmitic and oleic) compared to the WT osteoclasts untreated, while the CFD gene expression was normalised in osteoclasts stimulated by fatty acid with vitamin D3 ([Figure 3-30 A, B&D](#)). The normal PCR showed that the CFD product was significantly more than WT and Vitamin D3 treated group normalised to the level seen in untreated osteoclasts ([Figure 3-30 C](#)).

The level of complement factor B was dramatically increased in osteoclasts stimulated by fatty acid compared to untreated osteoclasts, but using the vitamin D3 treatment with fatty acid (FA) may suppress the excessive CFB expression induced by FA ([Figure 3-31 A, B&D](#)). Then, the normal PCR showed that the osteoclasts stimulated with FA expressed a higher level of CFB than WT, but Vitamin D3 addition with FA to osteoclast cultures could reduce the excessive expression of CFB in osteoclasts ([Figure 3-31 C](#)).

The complement C3 gene was highly expressed in osteoclasts stimulated by FA compared to untreated osteoclasts. The C3 expression in osteoclasts stimulated by FA with Vitamin D3 was normalised to the untreated osteoclasts C3 gene expression ([Figure 3-32 A,](#)

B&D). The normal PCR revealed that the level in osteoclasts stimulated with FA expressed more C3 product than WT and osteoclasts stimulated with Vitamin D3 (Figure 3-32 C).

The complement properdin was increasingly expressed by FA stimulation in osteoclasts, but the level of CFP in osteoclasts treated with Vitamin D3 was significantly less than osteoclasts treated with FA only. The CFP gene expression in osteoclasts treated by FA with Vitamin D3 was comparable to the control without FA (Figure 3-33 A, B&D). The normal PCR revealed that the FA group has more CFP product expression than WT and Vitamin D3 group (Figure 3-33 C).

These results revealed for the first time that murine osteoclasts are likely to contribute to complement component production CFD, CFB, CFP and C3. Vitamin D3 may have a role in curbing excessive complement component production by osteoclasts induced by fatty acid.

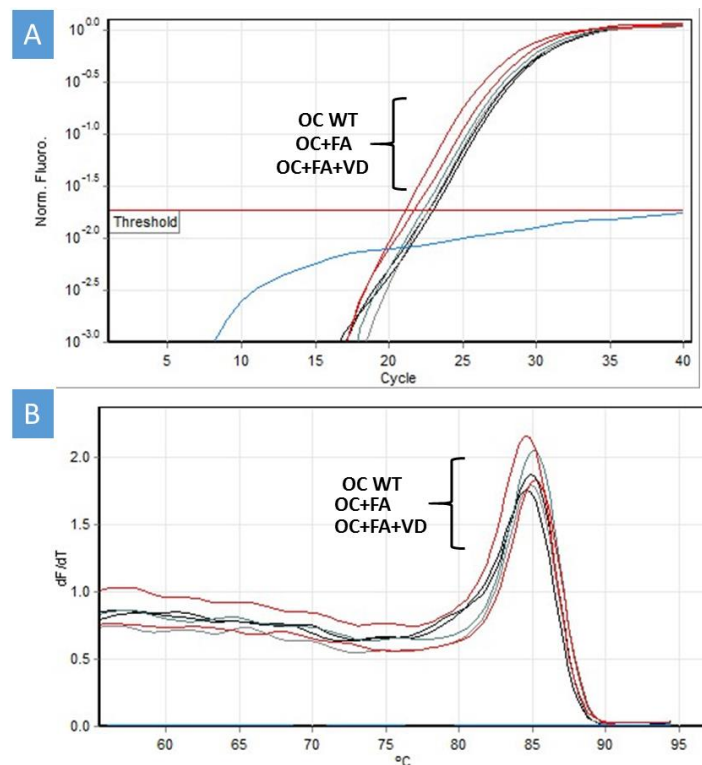


**Figure 3-29:** The qPCR analysis for the level of B2M gene expression as a housekeeping gene in osteoclasts stimulated by fatty acid with or without Vitamin D3. The experiment was performed three times in duplicates.

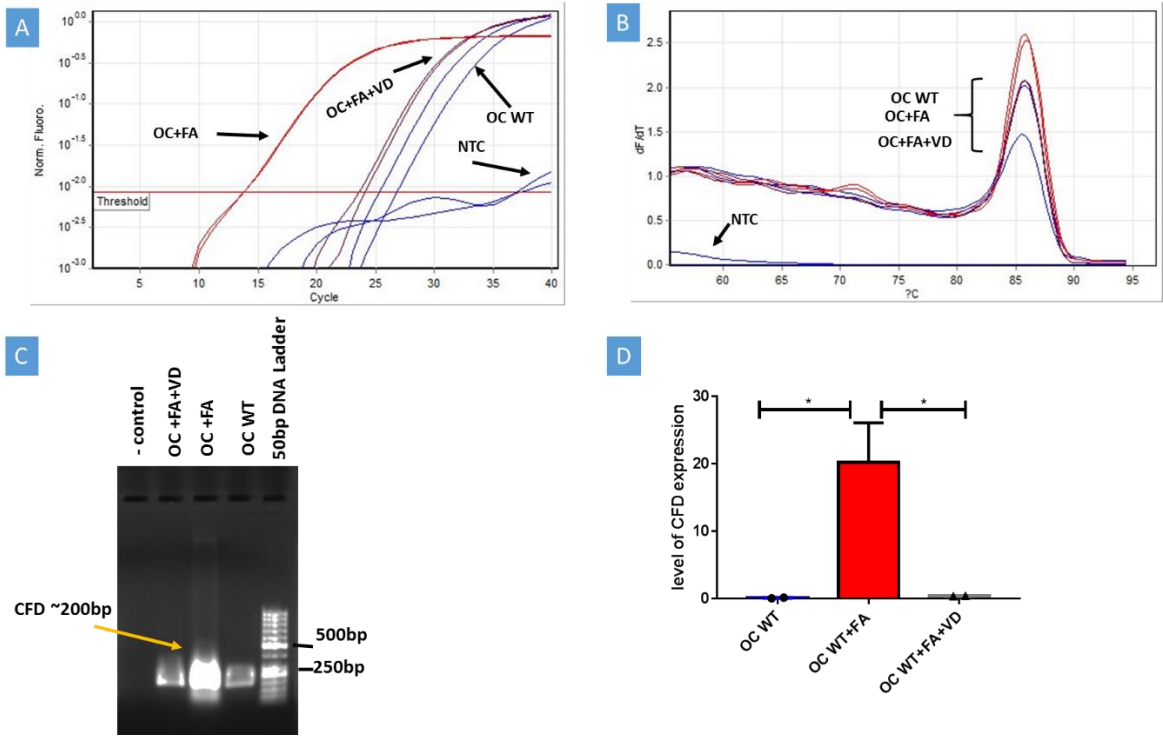


**Figure 3-30: Vitamin D3 normalises the excessive complement factor D expression induced by free fatty acid.**

The experiment was performed three times in duplicates and represent the mean  $\pm$  SEM analysed by Tukey multiple comparison of one-way ANOVA test; \* $P < 0.05$ .

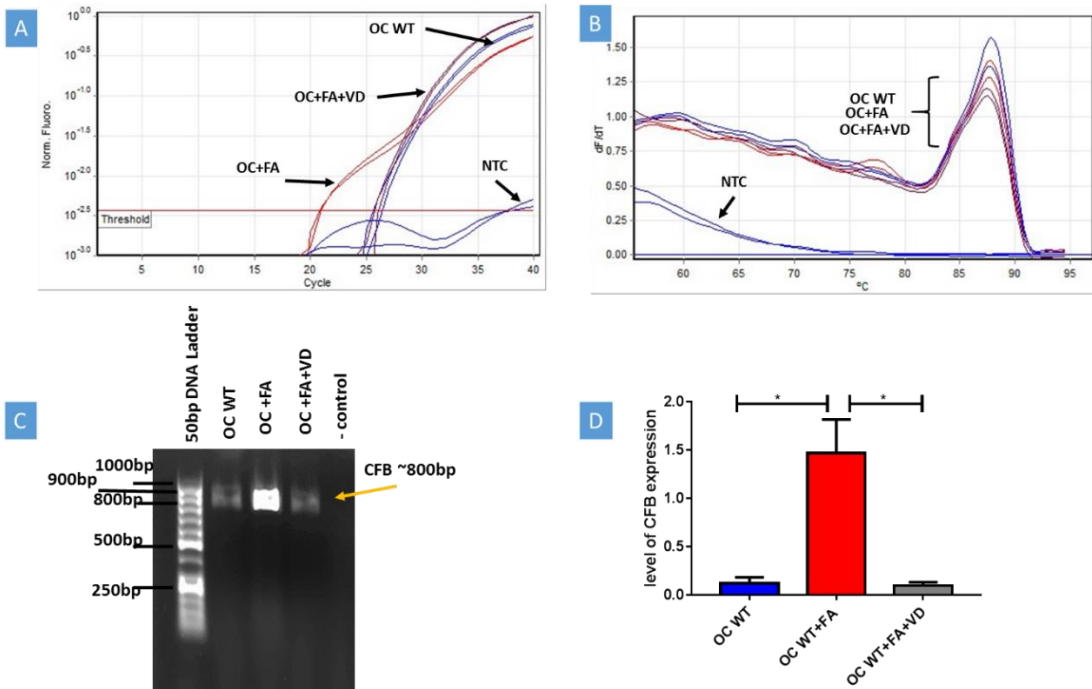


**Figure 3-31: Vitamin D3 normalises the over complement factor B expression induced by free fatty acid.**

The experiment was performed three times in duplicates and represent the mean  $\pm$  SEM analysed by Tukey multiple comparison of one-way ANOVA test; \* $P < 0.05$ .

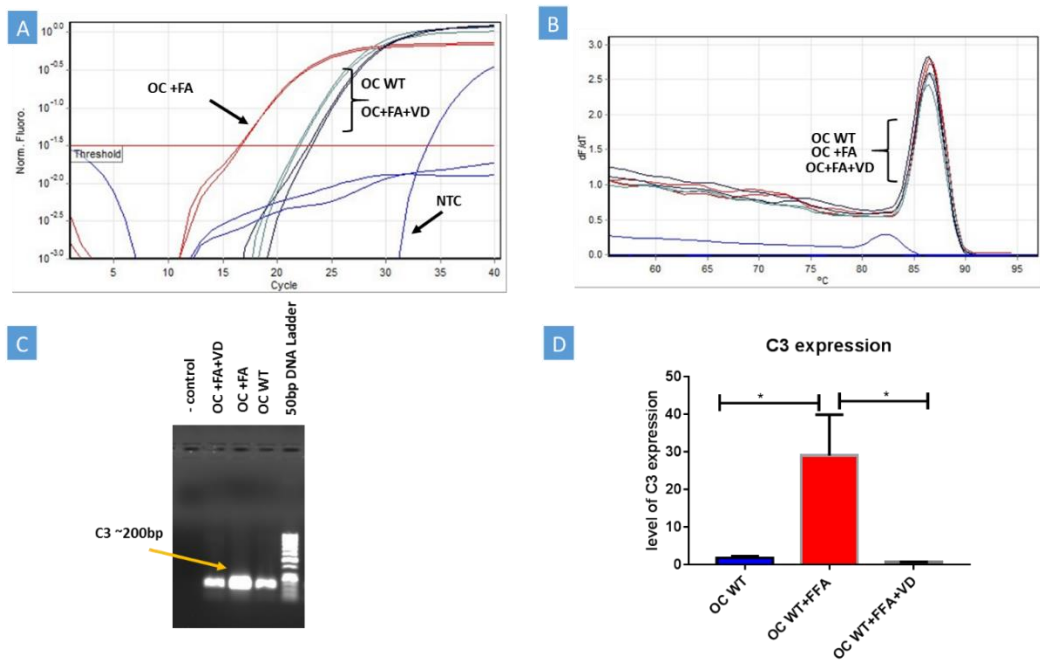


**Figure 3-32: Vitamin D3 normalises the excessive complement C3 expression induced by free fatty acid.**

The experiment was performed three times in duplicates and represent the mean  $\pm$  SEM analysed by Tukey multiple comparison of one-way ANOVA test; \*P<0.05.

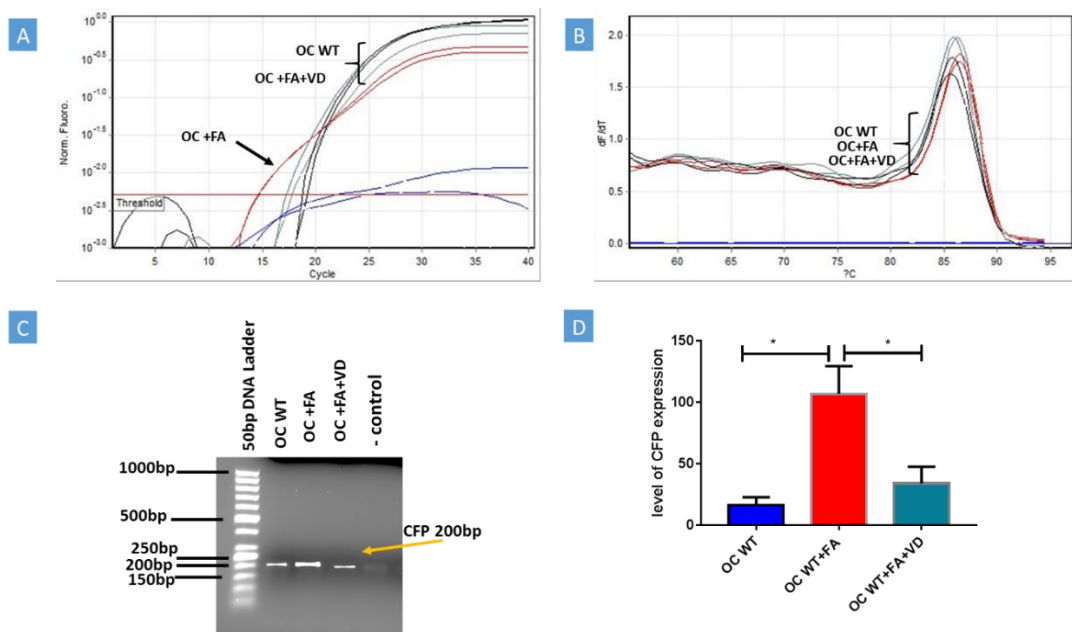


**Figure 3-33: Vitamin D3 normalises the excessive complement properdin expression induced by free fatty acid.**

The experiment was performed three times in duplicates and represent the mean  $\pm$  SEM analysed by Tukey multiple comparison of one-way ANOVA test; \*P<0.05.

## **4 Chapter Four – The General Discussion**

## **4.1 The effect of properdin deficiency on bone mineral density:**

The complement system has a presumed role in bone remodelling because of the expression of complement proteins and their receptors on bone cells, namely osteoclasts and osteoblasts. Osteoclasts and osteoblasts express different components of the complement system. Osteoblasts produce the complement components C3 and C5, and osteoclasts can produce complement component C3 (Ignatius *et al*, 2011a). Osteoclast and osteoblasts express C3a and C5a receptors (Schraufstatter *et al*, 2009; Tu *et al*, 2010). This evidence indicates that the complement system tightly overlaps with bone homeostasis, but the effect of properdin deficiency on bone mineral density has been not investigated. The effect of properdin deficiency on osteoclast activity or bone mineral density did not exist in the literature, so our results presented novel findings in this field. Therefore, this section will discuss the effect of the absence of properdin on bone mineral density and activity of osteoclasts derived from properdin-deficient mice.

The complement system components are strongly associated with maintaining the optimal bone mineral density. The third complement component has an essential role in bone remodelling. It was found that osteoclast formation was less in C3 blocked cultures (Sato *et al*, 1991; Sato *et al*, 1993). In addition, complement C5 plays a part in maintaining bone mineral density. It was found that complement C3 and complement C5 deficient mice have a higher bone mineral density than WT mice (Ehrnthaller *et al*, 2013). In addition, the complement components could have a significant effect on bone growth and osteocytes proliferation. It was demonstrated that alternative pathway proteins like C3, C5, factor B and C9 and complement properdin were found in the proliferation area of bone (Andrades *et al*, 1996). In addition, the anaphylatoxin receptors could have an important role in bone mineral density. It was found that absence of C5aR in mice could reduce the bone mineral density possibly due to significantly increased osteoclast numbers by increased the expression of IL-6 and RANKL from osteoblasts derived from C5aR1 deficient mice (Bergdolt *et al*, 2017). However, in a different study, it was shown that the Trabecular compartment was not significantly altered in C5aR1<sup>-/-</sup> mice, but both C5aR1<sup>-/-</sup> and C5aR2<sup>-/-</sup> mice displayed an increased bone mass compared to wild-type controls due to reduced osteoclast formation and increased osteoblast numbers, respectively (Kovtun *et al*, 2017). The studies by Bergdolt *et al* (2017) and Kovtun *et al*

(2017) vary in their outcomes for C5aR<sup>-/-</sup> mice possibly due to the different fracture models used with and without additional trauma. In human, it was found that C3a and C5a anaphylatoxins could have a direct effect on osteoclast differentiation even with the absence of RANKL, via their interaction with C3aR and C5aR expressed on osteoclasts and osteoblasts (Ignatius *et al*, 2011a). Most of these studies demonstrated that the complement system components and their anaphylatoxins have significant actions on bone mineral density, but there was no study presented the effect of properdin deficiency on BMD. Our findings found for the first time that there was no significant difference in bone mineral density of properdin-deficient mice compared to their control mice at 6 months of age (Figure 3-1; Figure 3-2), and that the bone mineral density was significantly higher in female properdin-deficient mice at 10 months of age (Figure 3-5; Figure 3-6). In the previous work in this laboratory, it was found that properdin-deficient mice had a skewing in macrophage activities (Dupont *et al*, 2014). Since the osteoclasts are giant, multinucleated cells and they are derived from cells of monocyte/macrophage lineage (Miron and Bosshardt, 2016), the absence of complement properdin could skew the activity of osteoclasts. On the other hand, the murine skeleton continues to grow slowly after puberty and lacks osteonal remodelling of cortical bone. In advancing mouse age, it is like human deterioration of bone mineral density with old age especially in cancellous bone and increases in cortical porosity (Jilka, 2013). Another study showed that using dual-energy X-ray absorptiometry; the BMD tends to be reduced in C57BL/6 mice between 10 and 25 months of age after their median lifespan of 29 months of age (Almeida *et al*, 2007; Hui, Slemenda and Johnston, 1988; Yuan *et al*, 2009). This evidence shows that mice like a human could lose bone density with advanced age. In humans, the reduction of oestrogen level after menopause is one of the possible reasons for bone mineral density reduction (Väänänen and Härkönen, 1996), therefore, our result showed that there is a possibility of affecting the osteoclast activity at ages of 10 months old by properdin deficiency, and thus the bone mineral density is increased or maintained at the normal level in case of properdin deficiency, suggesting that properdin absence could reduce the complement system activation which then reduces the osteoclasts activity.

*In vitro*, the complement components have a direct or indirect effect on osteoclast activation and differentiation. Therefore, it was proposed that properdin absence could alter the osteoclast differentiation and activation in mice. Therefore, our findings for the

first time revealed that the *in vivo* activities of osteoblasts and osteoclasts were not changed in properdin-deficient mice of both male and females at 6 months of age (Figure 3-3). In addition, the *in vitro* investigation found that the number of mature differentiated osteoclasts were the same in properdin-deficient mice and WT mice. Moreover, it was found that the resorptive activity was the same in mice lacking to properdin compared to WT mice (Figure 3-4). Therefore, the properdin deficiency may have no effect on osteoclast activity *in vitro* and *in vivo* at 6 months of age.

In conclusion, the complement system components could have a significant effect on osteoclast activity and bone mineral density. The bone mineral density was investigated in properdin deficient mice at 6 months old and 10 months old. Our findings found that the complement properdin deficiency could increase the BMD in older ages but not in young individuals may be due to the menopause changes (Figure 4-1). These results could indicate that the absence of properdin could be beneficial for maintaining the optimal bone mineral density at an older age in mice.

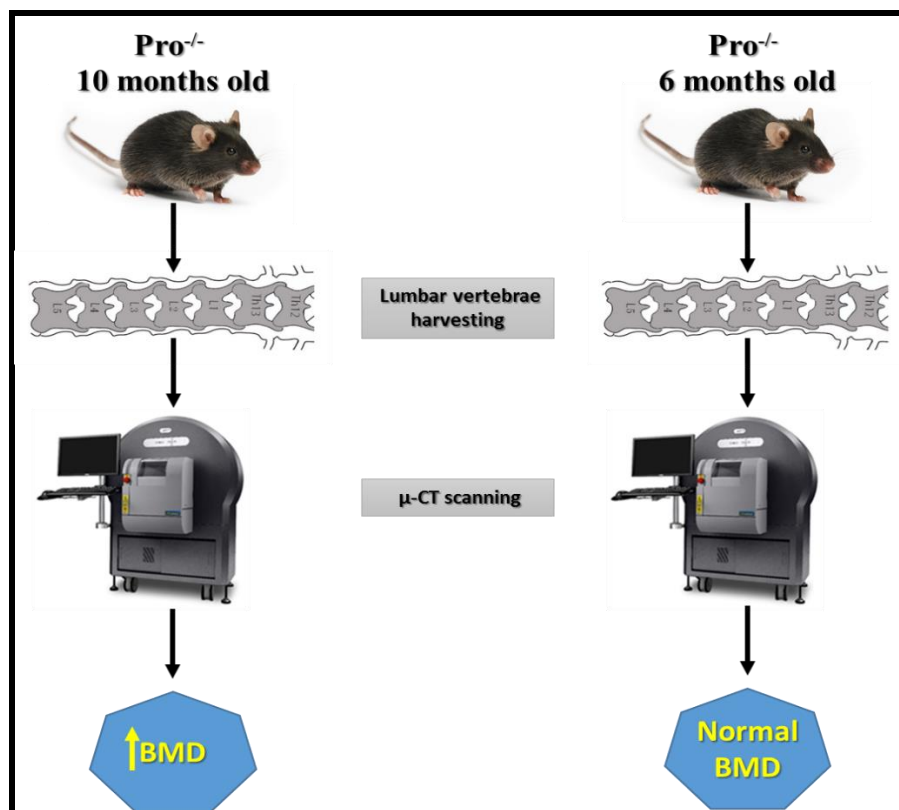


Figure 4-1: The representative scheme is showing the effect of age on female properdin-deficient mice bone mineral density.

## **4.2 The effect of vitamin D3 or exercising on bone mineral density reduction induced by low-density lipoprotein receptor deficiency (LDLR<sup>-/-</sup>).**

Oxidized lipids have a recognised role in the pathogenesis of atherosclerosis, but their impacts on bone are less known. In human, the National Health and Nutrition Examination Survey (NHANES III) found that (63%) of patients have osteoporosis associated with hyperlipidaemia. In the animal, the elevation of plasma lipoprotein levels was highly associated with bone loss and bone mineral density reduction (Hirasawa *et al*, 2007). Consistent exercising plays an important factor to maintain the optimal bone mineral density (C. Rubin *et al*, 2002). In addition, Vitamin D3 has a crucial role in preventing bone loss (Sergeev and Song, 2014). It was found in this project that vitamin D3 or exercising had a significant role to correct the bone mineral density reduction induced by high-fat diet intake for 5 weeks. In this section, I will discuss the effect of LDLR deficiency on bone mineral density, and whether Vitamin D3 or exercising as interventions affect bone mineral density in low-density lipoprotein receptor-deficient mice.

Low-density lipoprotein receptor deficiency may influence the body weight increase. It was reported that LDLR deficient mice exhibit a significant increase in the body gain compared to WT mice (Constantinou *et al*, 2014). Vitamin D3 could have a role in body weight loss and fat mass in mice (Sergeev and Song, 2014). Access to physical exercise reduced the body weight increase in mice fed a high-fat diet (R. K. Kheder, 2017b). Our findings showed that the body weight increase in LDLR<sup>-/-</sup> mice was significantly decreased in mice fed a normal diet with Vitamin D3 supplementation or accessed to voluntary wheel exercising for 5 weeks (Figure 3-14A). These findings show that dietary supplementation of vitamin D3 or voluntary exercising is likely to control the body weight increase in LDLR deficient mice.

The low-density lipoprotein receptor is responsible for LDL endocytosis and its absence induces hyperlipidaemia, exhibiting a high level of serum triglyceride (Okayasu *et al*, 2012). It was reported that high level of plasma-low-density lipoprotein (LDL) is considered to be a risk factor for bone loss, suggesting that LDL accumulation in subendothelial matrix bone marrow could be exposed to nonenzymatic oxidative reaction

to inflammatory lipids and upregulate the proinflammatory cytokines (Navab *et al*, 2004). Vitamin D3 intake may have an important role to reduce the triglyceride level in serum on a high-fat diet (Sergeev and Song, 2014). It was shown that exercising reduced the serum triglyceride in mice fed a high-fat diet (Dall'Aglia *et al*, 1983). The findings showed that Vitamin D3 intake or access to wheel exercising for 5 weeks decreased the serum triglyceride level in LDLR<sup>-/-</sup> mice (Figure 3-14 B). This could indicate that Vitamin D3 supplementation or access to voluntary exercising controlled the serum triglyceride level in LDLR<sup>-/-</sup> mice.

The low-density lipoprotein receptor deficiency could have a negative effect on bone mineral density, but Vitamin D3 or exercise may enhance the BMD in LDLR<sup>-/-</sup> mice. It was shown that hyperlipidaemia induced by LDLR gene deletion induces osteoclast activation that in turn reduces bone formation and strength by decreasing the BV/TV and increasing the cortical porosity (Pirih *et al*, 2012). Vitamin D3 presented a positive effect on bone mineral density by enhancing the bone remodelling (Chapuy *et al*, 1992; Ornoy *et al*, 1978). In addition, the mechanical loading could enhance bone mineral density by activating bone formation (C. Rubin *et al*, 2002). Our findings revealed that most of the bone microarchitecture parameters were significantly reduced in LDLR<sup>-/-</sup> mice compared to WT (Figure 3-9). However, the bone mineral density parameters were increased in LDLR<sup>-/-</sup> mice fed a normal diet with Vitamin D3 supplementation or access to wheel exercise (Figure 3-15). Therefore, it was apparent that Vitamin D3 dietary supplementation or exercising reduced bone mineral density reduction induced by LDLR deficiency.

The LDLR deficiency may have significant action on osteoclast and osteoblast activities. The *in vitro* studies reported that Low-density lipoprotein receptor on osteoblasts takes an essential role in osteoclasts activity regulation through a PDGF–RANKL signalling axis by increasing the RANKL expression and enhancing osteoclast differentiation and then bone loss (Bartelt *et al*, 2018). In addition, LDLR deficiency may inhibit osteoblastogenesis by reducing the alkaline phosphatase activity, mineral deposit formation was delayed, the gene expression levels of runt-related transcription factor 2 (Runx2) and transcription factor Sp7 (Osterix), transcription factors associated with osteoblast differentiation, were dramatically reduced in LDLR<sup>-/-</sup> mice (N. Zhang *et al*, 2017). In contrast, Vitamin D3 has an essential role in osteoblast activity through its interaction with Vitamin D receptor on osteoblasts enhancing bone formation (Gardiner

*et al*, 2000). In addition, it was demonstrated that the physical activities could activate the osteocytes and increase osteoblasts differentiation and proliferation (Ehrlich and Lanyon, 2002). Therefore, it was suggested that Vitamin D3 or exercising have an effect on osteoblasts and osteoclast derived from LDLR<sup>-/-</sup> mice. Our findings revealed that LDLR deficiency showed an increase in serum TRACP activity and decreased serum ALP and osteocalcin levels (Figure 3-11), but Vitamin D3 or exercising normalised TRACP, ALP and osteocalcin levels to those measured in control WT mice. These results indicate that the osteoclasts activity was higher in LDLR<sup>-/-</sup> mice and they have lower osteoblast activity than their control mice. However, Vitamin D3 or exercising for 5 weeks were likely to have a positive effect on normalising the osteoblasts and osteoclasts activities in LDLR<sup>-/-</sup> mice. In addition, our *in vitro* work found that the TRACP<sup>+</sup> osteoclasts and their resorption and TRACP activities were higher in LDLR<sup>-/-</sup> cell culture, but Vitamin D3 addition reduced their activities and their number (Figure 3-19). In addition, the differentiated osteoblasts and their mineral deposition and ALP activities were less than control WT cell culture, Vitamin D3 addition normalised osteoblasts activity (Figure 3-20). These results were consistent with *in vivo* work showing that LDLR<sup>-/-</sup> mice have high osteoclasts activity and fewer osteoblasts activity while Vitamin D3 normalised both activities.

The oxidative lipids in LDLR deficient mice may induce an inflammatory response in bone matrix that increases bone loss. A study demonstrated recently that LDLR<sup>-/-</sup> mice developed an inflammatory response in the liver because of the increase in oxidative LDL intake (Bieghs *et al*, 2012). A different study showed that the transmembrane receptor, LDL receptor-related protein-1 (LRP1), considered as an inflammatory response regulator in macrophages and LDLR deficiency induces proinflammatory cytokine increase in LDLR<sup>-/-</sup> mice (Mantuano *et al*, 2016). Vitamin D3 supplementation could have a significant role to reduce the inflammatory response in LDLR<sup>-/-</sup> mice. In our previous work in our lab (published data) revealed that Vitamin D3 has a significant role in amelioration of transaminase elevations in WT and LDLR<sup>-/-</sup> fed a diabetogenic diet with or without admixed Vitamin D3 for 10 weeks (R. Kheder *et al*, 2017a). Additionally, Vitamin D3 corrects the hyperinsulinemia increase in the presence of Vitamin D3 supplemented to diabetogenic diet. The serum triglyceride and non-esterified, free fatty acid in LDLR<sup>+/+</sup> and LDLR<sup>-/-</sup> fed a diabetogenic diet without or with additional Vitamin D3 were significantly reduced on Vitamin D3 supplementation. In addition, Vitamin D3

reduced the levels of endotoxin and lipid peroxidation product, MDA, as inflammatory agents in the serum of WT and LDLR<sup>-/-</sup> fed a diabetogenic diet for 10 weeks without or with additional supplemented Vitamin D3 (R. Kheder *et al*, 2017a). The more important previous finding was that Vitamin D3 ameliorated the inflammatory response in LDLR<sup>+/+</sup> and LDLR<sup>-/-</sup> with Vitamin D3 supplementation (R. Kheder *et al*, 2017a). The exercising could influence the inflammatory cytokines production in LDLR<sup>-/-</sup> mice. It was found that the exercising has a significant effect in reducing the serum inflammatory cytokines in mice fed a high-fat diet with access to wheel exercising (R. K. Kheder, 2017b). Our results revealed that the serum inflammatory cytokines (TNF-alpha and IL-6) were significantly increased in LDLR deficient mice serum; this may indicate that LDLR<sup>-/-</sup> mice could exhibit an inflammatory response. In addition, the residual activity of classical and alternative pathways activation in LDLR<sup>-/-</sup> was significantly increased compared to control WT mice. In addition, our finding demonstrated that LDLR<sup>-/-</sup> mice receiving for 5 weeks Vitamin D3 supplementation or access to voluntary exercising normalised the levels of serum TNF-alpha and IL-6 in comparison to LDLR<sup>-/-</sup> mice (Figure 3-18). These results indicate that Vitamin D3 or exercising has an important effect of normalising the inflammatory cytokines production in LDLR<sup>-/-</sup> mice.

In conclusion, the *in vivo* investigations revealed that LDLR<sup>-/-</sup> as a hyperlipidemic model showed a significant increase in serum triglyceride level and significant elevation in the inflammatory response in terms of inflammatory cytokines and complement system activation. Therefore, the LDLR<sup>-/-</sup> mice have a significant increase in osteoclast activity and decrease in osteoblast activity. These results were likely to result in a bone mineral reduction in LDLR deficient mice. However, Vitamin D3 supplementation or access to wheel exercising were able to have a significant action to normalise the serum inflammatory cytokines levels in LDLR<sup>-/-</sup> mice for 5 weeks. In addition, Vitamin D3 supplementation or accessing to wheel exercising were shown to have a significant role in normalising the osteoclast and osteoblast in LDLR<sup>-/-</sup> to the activities in wildtype control mice. These results show the positive effect of Vitamin D3 supplementation or accessing to wheel exercise to normalise the bone mineral density compared to LDLR<sup>-/-</sup> mice. Moreover, the *in vitro* work revealed that Vitamin D3 addition to osteoclast or osteoblast cultures derived from LDLR<sup>-/-</sup> mice has a significant role to ameliorate the osteoclast resorptive activity and osteoblast mineral deposition activity. However, further *in vitro* investigation is needed to study the effect of mechanical stretching on osteoclasts and

osteoblasts derived from LDLR<sup>-/-</sup> mice. Ultimately, Vitamin D3 dietary supplementation or regular exercising have a significant action to ameliorate bone mineral density reduction induced by LDLR deficiency in mice (Figure 4-2).

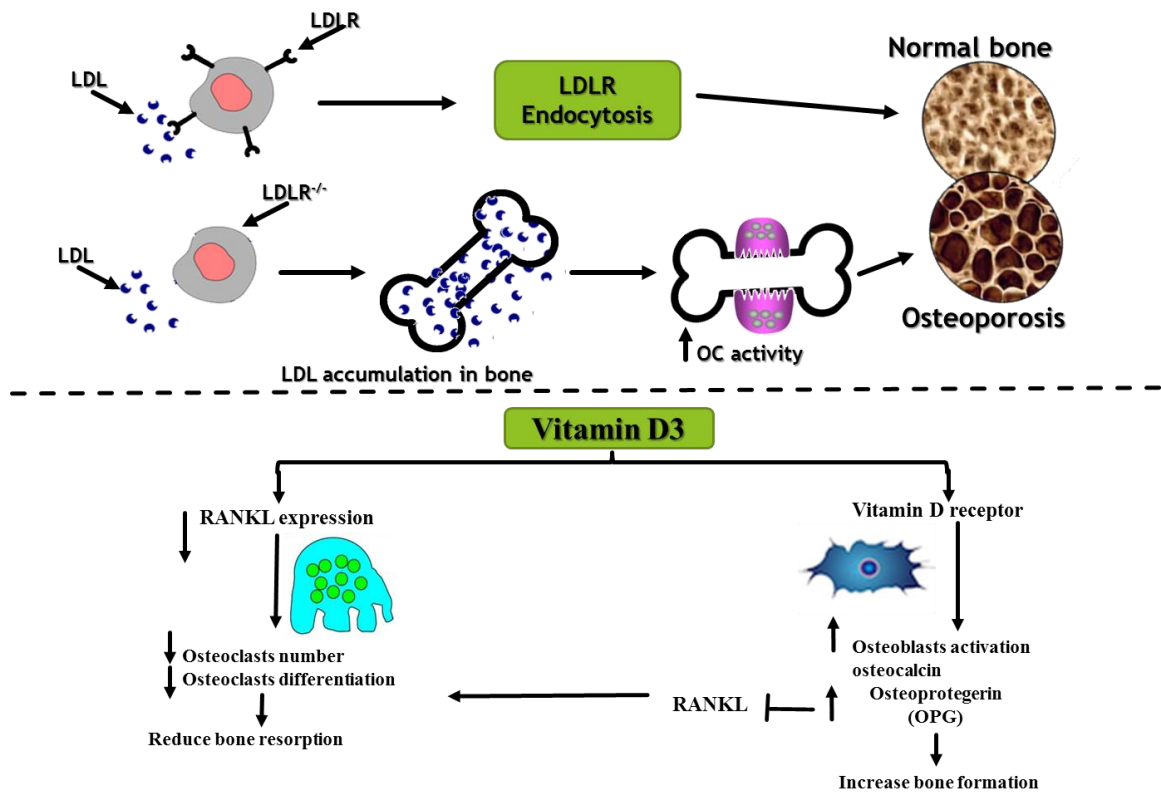


Figure 4-2: The effect of vitamin D3 on bone remodelling in LDLR deficient mice.

### 4.3 The effect of vitamin D3 and fatty acid on complement component production of the alternative pathway in murine osteoclasts.

The field of osteoimmunology is the functional connection between the immune system and bone at the anatomical, vascular, cellular, and molecular levels (Takayanagi, 2009). The receptor activator of the nuclear factor-kappa-B ligand (RANKL)/RANK/osteoprotegerin (OPG) pathway was identified as an essential molecular pathway that interacts between osteoblasts and osteoclasts (Fuller *et al*, 1998). It was shown that not only osteoblasts but also activated T lymphocytes, play an essential role in rheumatoid arthritis (RA) pathogenesis, and many other inflammatory cells could

produce RANKL, which stimulates the differentiation and activation of osteoclasts (Lacey *et al*, 1998). These findings have participated in developing osteoimmunology as a discipline.

The complement system has in direct and indirect contact with the bone formation and resorption. The complement proteins may have an influence on osteoclast and osteoblast activities (Huber-Lang, Kovtun and Ignatius, 2013). Various studies mentioned that the complement system has a crucial role in bone homeostasis. It was reported that inhibiting complement C3 by the anti-C3 antibody led to down-regulation of mRNA RANKL expression and decreased numbers of osteoclasts in non-human primates (Maekawa *et al*, 2016). In addition, C3 produced by stromal cells in response to 1 alpha,25-(OH)<sub>2</sub>D<sub>3</sub> was involved in osteoclast development by potentiating M-CSF-dependent proliferation of bone marrow cells and inducing osteoclast differentiation (Jin *et al*, 1992). In addition to C3 receptors, C3aR/C5aR that can also regulate OC differentiation, it was found that C3<sup>-/-</sup> BM cells exhibited a reduction in RANKL/OPG expression ratios, produced smaller amounts of macrophage colony-stimulating factor and interleukin-6 (IL-6), and generated significantly fewer OCs than wild-type (WT) BM cells (Tu *et al*, 2010). The complement components mediate the recruitment of mononuclear osteoclast precursors to the exposed mineralised bone surface; it was shown that C3 deposition on mineralised bone surfaces mediates the recruitment of mononuclear osteoclasts to this site as the mononuclear osteoclasts fuse to form the multinucleate osteoclast (Mangham, Scoones and Drayson, 1993). In addition, the complement C3 and its anaphylatoxin (C3a) was detected in osteoclast conditioned media (Matsuoka *et al*, 2014), that binds to its receptors, C3aR, that are highly expressed on osteoblast and osteoclast (Huber-Lang, Ignatius and Brenner, 2015). The C5aR has an essential role in osteoclasts and osteoblasts activity. C5aR activation by C5a induced strong chemotactic activity in osteoblasts especially during fracture healing (Ignatius *et al*, 2011b). This indicates that complement components or anaphylatoxins and their receptors actively participated in bone cell activation, both osteoclast and osteoblast.

This part of the project highlights that complement components play an essential role in homeostasis, away from its better-documented role in the innate immune response. One study investigates the fifth complement protein production and its cleavage to C5a by human osteoclasts differentiated from the human peripheral blood mononuclear cell (PBMC) (Ignatius *et al*, 2011a), but not in murine osteoclast differentiated from bone

marrow. Therefore, the C5/C5a was detected by Western blotting and ELISA, and the C5 gene expression was analysed in murine osteoclasts to investigate whether *in vitro* differentiated murine osteoclasts could express or produce C5 and cleave complement C5 to its anaphylatoxin C5a. There are various immune cells producing complement C5 like mast cells, monocytes, macrophages, dendritic cells, natural killer cells and B and T lymphocytes (Lubbers *et al*, 2017). In addition, it was found that the human osteoblast and osteoclast were able to produce the complement C3 while the complement C5 was produced by osteoblasts but not osteoclasts (Ignatius *et al*, 2011a). Moreover, it was claimed that human osteoclasts could cleave complement C5 by a specific serine protease located on osteoclasts cell membrane (Schoengraf *et al*, 2013). For the first time, our finding showed that murine osteoclasts did not express the complement C5. These findings were consistent with Ignatius *et al*. (2011a). Moreover, the ELISA analysis presented that there was no expression for C5 or C5a protein in murine osteoclasts supernatant but there was an expression in J774 macrophages supernatant as a positive control (Figure 3-22). In addition, to investigate whether murine osteoclasts incubated with purified C5 could cleave C5 to C5a; the rabbit polyclonal C5a antibody was used to detect the cleaved C5a and un-cleaved C5. The result revealed that murine osteoclast cell cultures had not expressed the C5a in the Western blotting analysis (Figure 3-21). This result was inconsistent with Ignatius *et al*. (2011a) who showed that human osteoclasts were able to cleave C5 to its C5a.

Since osteoclasts were derived from monocyte/macrophage lineage (Miron and Bosshardt, 2016), and the complement C5 was expressed by different immune cells like macrophages (Lubbers *et al*, 2017), the complement C5 gene expression was analysed in murine osteoclasts using PCR and qPCR. Our findings found a novel result that C5 was not expressed in murine osteoclasts although it was expressed in J774 cell line and mouse liver as a positive control (Figure 3-23). This result was consistent with Ignatius *et al*. (2011a) who showed that C5 could be produced by human osteoblasts but not osteoclasts, however, its expression in murine osteoclasts has been not analysed.

RANKL is the critical cytokine which is responsible for macrophages fusion for osteoclasts formation (Fuller *et al*, 1998). Therefore, it was hypothesised that RANKL could play a role in C5 downregulation in murine osteoclasts. The macrophage J774 cell line was treated with or without RANKL to investigate whether RANKL could influence C5 gene expression on osteoclasts during their differentiation. Our results showed for the

first time that C5 gene expression was downregulated in J774 cell line after treating with RANKL compared to untreated cells (Figure 3-24). Therefore, a novel finding was that unlike human osteoclasts, the murine osteoclasts did not cleave C5 to its anaphylatoxin and did not produce or express C5, this possibly due to the RANKL has a role in C5 gene suppression during murine osteoclast differentiation.

Moreover, the way by which the osteoclasts could have an action in alternative pathway activation has not investigated. The osteoclasts were generated from monocyte/macrophage lineage, which could be differentiated into osteoclasts by suitable bone microenvironment (Miron and Bosshardt, 2016; Udagawa *et al*, 1990). Macrophages are one of the immune cells which can produce different protein components of the complement system. It was found that macrophages have a significant role in producing most of the classical pathway components like C1q, C1r, C1s, C4 and C2 (Cole *et al*, 1980; Strunk *et al*, 1985). In addition, macrophages have significant participation in alternative pathway component secretion. It was proved that macrophages have an ability to produce C3, FB, FD, FP and C5 (Lubbers *et al*, 2017; de Ceulaer, Papazoglou and Whaley, 1980; Cole *et al*, 1980; Strunk *et al*, 1985). Therefore, it was proposed that murine osteoclasts are likely to have an essential role in complement system components production especially the alternative pathway components. Our findings showed for the first time that murine osteoclasts differentiated from mouse bone marrow expressed most of the alternative complement components genes like FB, FD, C3 and complement properdin but not C5. Therefore, it was difficult to measure the classical and alternative pathways activation *in vitro* because of the absence of C5 expression in murine osteoclasts as the principle of this measurement depends on the formation of C9, however, the complement activity could be measured *in vivo* because the C5 protein could be provided from different sources of cells. These novel findings could indicate that osteoclasts possibly have a part in alternative pathway activation and their participation in complement component productions.

The osteoclast stimulation by fatty acid with or without vitamin D3 could have a significant role in alternative pathway component gene expression. In various studies showed that a high-fat diet has an excessive effect on different gene expression. It has been reported that complement and coagulation cascade (69 genes) expression were increased by high-fat diet, this suggested that a high-fat diet has a significant effect on proinflammatory gene expression (Renaud *et al*, 2014). In addition, it was indicated that

fatty acid like palmitic acid have a direct role in inducing inflammatory gene expression (Glass and Olefsky, 2012). In contrast, Vitamin D3 could have an important anti-inflammatory role of regulating the inflammatory response. It has a significant anti-inflammatory action by reducing the inflammatory cytokine gene expression like TNF- $\alpha$ , IL-6 and MCP-1 (Yin and Agrawal, 2014; Calton *et al*, 2015). In addition, in this project, it was found that Vitamin D3 suppressed the detrimental effect of a high-fat diet *in vivo*. Moreover, it was found that Vitamin D3 *in vitro* suppressed the osteoclast resorptive activity induced by free fatty acid stimulation. Therefore, the level of gene expression of alternative pathway component was measured to investigate whether *in vitro* Vitamin D3 could normalise long chain fatty acid-induced expression of alternative pathway complement components in murine osteoclasts. Our finding showed for the first time that *in vitro* differentiated murine osteoclasts stimulated by fatty acid (palmitic and oleic acids) have an increase in alternative complement component gene expression e.g. complement factors D, B, P and C3. However, Vitamin D3 normalised the alternative components gene expression increase induced by fatty acid treatment in osteoclasts. It was found that the complement factors D, B, P and C3 were comparable to untreated osteoclasts' gene expression (Figure 3-30; Figure 3-31; Figure 3-32; Figure 3-33).

The interaction between fatty acid and vitamin D3 signals may be as follows: It was reported that fatty acid could activate the transcriptional factor NF-kB via TLR signalling pathway (Milanski *et al*, 2009). TLR-4 is expressed by osteoclasts and has a significant role in osteoclastogenesis (D. Wang *et al*, 2017). Therefore, it was proposed that fatty acid could influence the osteoclast differentiation and activation via TLR4 by activating the NF-kB pathway signalling which may increase the alternative complement components' gene expression (Boden *et al*, 2005; Baker, Hayden and Ghosh, 2011). TLR4 mediated increase in complement factor B and C3 has been shown for macrophages (Pope *et al*, 2010). In addition, it was found that fatty acid have a significant action to induce phosphorylated MAPK pathway activation that could enhance gene expression (Malhi *et al*, 2006; Gupta *et al*, 2012). However, a recent study showed that Vitamin D3 could inhibit the NF-kB pathway activation (Jeon and Shin, 2018; Janjetovic *et al*, 2009). Vitamin D3 may have an inhibiting role in the MAPK pathway (Meeker *et al*, 2014; Q. Wang *et al*, 2014). Therefore, the findings suggest that fatty acid may enhance osteoclast differentiation and activation through the NF-kB and MAPK pathways, and then increase

gene expression of complement factors D, B, P and C3, but Vitamin D3 may interfere with this pathway (Figure 4-3).

In summary, the murine osteoclasts' participation in complement system was investigated in this section. It was found that unlike human osteoclasts derived from the peripheral blood mononuclear cell (PBMC), the mouse osteoclasts were unable to cleave the complement C5 to its C5a. In addition, a novel finding was presented that mouse osteoclasts did not express the gene and produce the protein of the complement C5, also proposing that RANKL could downregulate C5 expression during the osteoclast differentiation process. However, the complement C5 could be provided by other stromal cells to allow MAC formation during complement activation in bone. Moreover, it was revealed that murine osteoclasts expressed most of the alternative pathway components like complement factor D, B, P and C3. In addition, our findings showed for the first time that fatty acid induced complement factor D, B, P and C3 overexpression in osteoclasts, but Vitamin D3 had a significant role to normalise complement factor D, B, P and C3 gene expression (Figure 4-3). This suggesting that Vitamin D3 could intercept fatty acid cellular signals in osteoclasts *in vitro*.

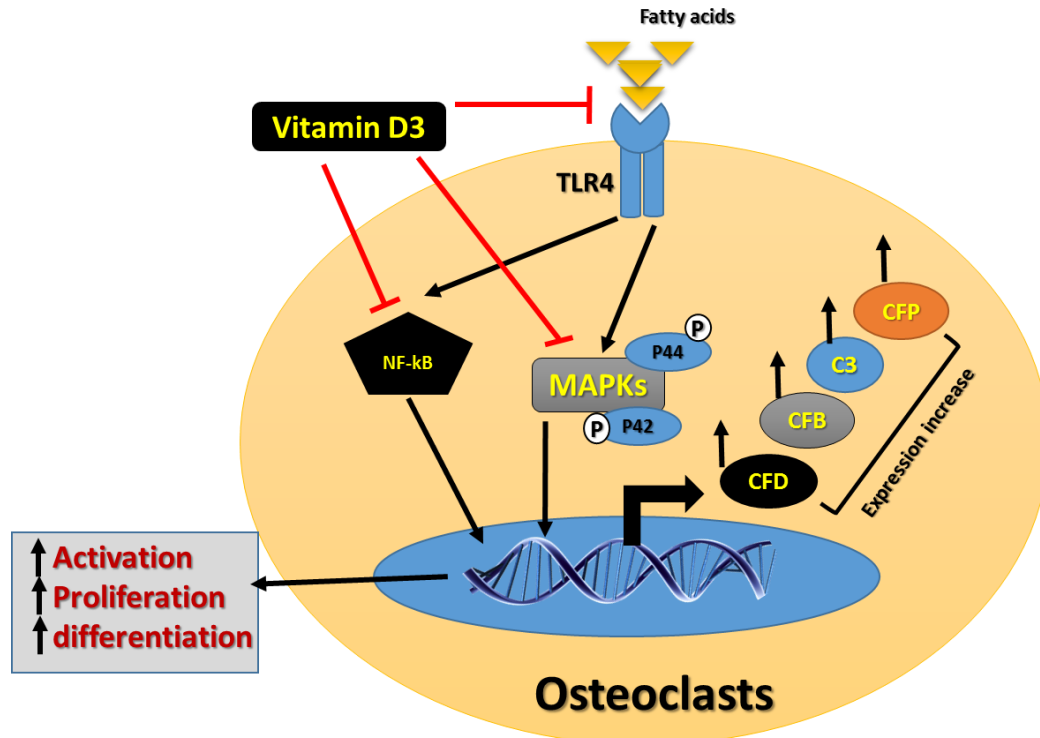


Figure 4-3: The interaction between Vitamin D3 and fatty acid stimulation of gene expression in osteoclasts.

## 5 Conclusion.

Complement properdin, the only positive regulator for the alternative complement system, and its gene absence was examined regarding bone mineral density. Previous work was carried out by Dupont *et al* (2014) showed that properdin-deficient mice had a skewing in macrophage activity, and since the osteoclasts are derived from the monocytes-macrophages lineage, it was proposed that absence of complement properdin could alter the bone remodelling activity. The main *in vivo* findings showed that the absence of complement properdin mice at 6 months old has no effects on bone mineral density compared to WT. The *in vitro* work revealed that there were no significant differences in differentiated osteoclast numbers, resorptive activity between properdin-deficient mice and WT. However, the absence of properdin showed there was a significant increase in bone mineral density, but at an older age (10 months old), this means that the absence of properdin could attenuate the osteoclasts activity but only at older ages.

Thereafter, further studies were performed to study the effect of vitamin D3 or exercising during high-fat diet feeding for 5 weeks. The effect of a high-fat diet for 5 weeks on bone mineral density was investigated. The results showed that bone mineral density was significantly reduced, and the levels of triglyceride increased in addition to significant alteration of bone remodelling activities (osteoclasts and osteoblasts). These changes could occur because of an increase in inflammatory cytokines due to high-fat diet intake for 5 weeks. Two interventions were applied to reduce the detrimental effects of a high-fat diet intake. Vitamin D3 on dietary supplementation or voluntary wheel cage exercising were combined with high-fat diet feeding for 5 weeks. These interventions have a significant role in normalising the bone mineral density reduction induced by normalising the osteoclasts and osteoblast activity *in vivo* and *in vitro*. This is showing the importance of Vitamin D3 or Exercise to keep the skeletal system healthy even during high-fat diet intake. Additionally, it was found that Vitamin D3 or exercising during a normal diet have a potentiating effect of increasing the bone mineral density by enhancing osteoblast activity and reducing osteoclast activity when these interventions have an anti-inflammatory effect.

The low-density lipoprotein receptor has an essential action in LDL uptake, and its absence increases the levels of lipoproteins in blood and accumulation in tissue. Lipoprotein accumulation could lead to an adverse effect on bone mineral density by

changing osteoclast and osteoblast activity balance and inducing an increase in inflammatory cytokine levels and complement system activation. Since Vitamin D3 or exercising have a positive effect on correcting bone mineral density during the high-fat diet, the effect of Vitamin D3 or exercising on bone mineral density reduction induced by LDLR<sup>-/-</sup> was examined *in vivo* and *in vitro*. The *in vivo* results revealed that Vitamin D3 supplementation or access to exercising has an important role to correct the bone mineral density reduction in LDLR<sup>-/-</sup> mice by enhancing osteoblast activity and reducing osteoclast activity, in addition to suppressing the inflammatory cytokine production (IL-6 and TNF- $\alpha$ ) and reducing the triglyceride serum level. The *in vitro* work showed that Vitamin D3 has a significant role in reducing or suppressing osteoclast resorptive activity and enhancing the bone mineral deposition by osteoblasts compared to LDLR<sup>-/-</sup> genotype. This suggests that Vitamin D3 or exercising could be beneficial to LDLR deficient families of humans that suffer from low bone mineral density.

To inspect whether murine osteoclasts could participate in complement alternative pathway component expression, the gene expression of CFD, CFB, CFP, C3 and C5 by osteoclasts was screened. The results showed that murine osteoclasts express CFD, CFB, CFP, C3 but not C5, suggesting that osteoclasts have a role in producing most of the alternative pathway components, and they could contribute in alternative pathway activation. Since the high-fat diet had a negative effect on bone mineral density by increased osteoclast activity but vitamin D3 could normalise the BMD, it was proposed the osteoclasts stimulation by fatty acid with or without Vitamin D3 as an *in vitro* model of high-fat diet could induce and alter alternative components expression. The results showed that the gene expression of CFD, CFB, CFP and C3 were excessively increased by osteoclasts treated with fatty acid compared to untreated osteoclasts, whilst *in vitro* addition of Vitamin D3 with fatty acid to differentiated osteoclasts expressed CFD, CFB, CFP and C3 genes. This could indicate that osteoclasts are likely to contribute to complement component production (CFD, CFB, CFP and C3). Vitamin D3 may have a role in curbing excessive complement component production by osteoclasts induced by fatty acid.

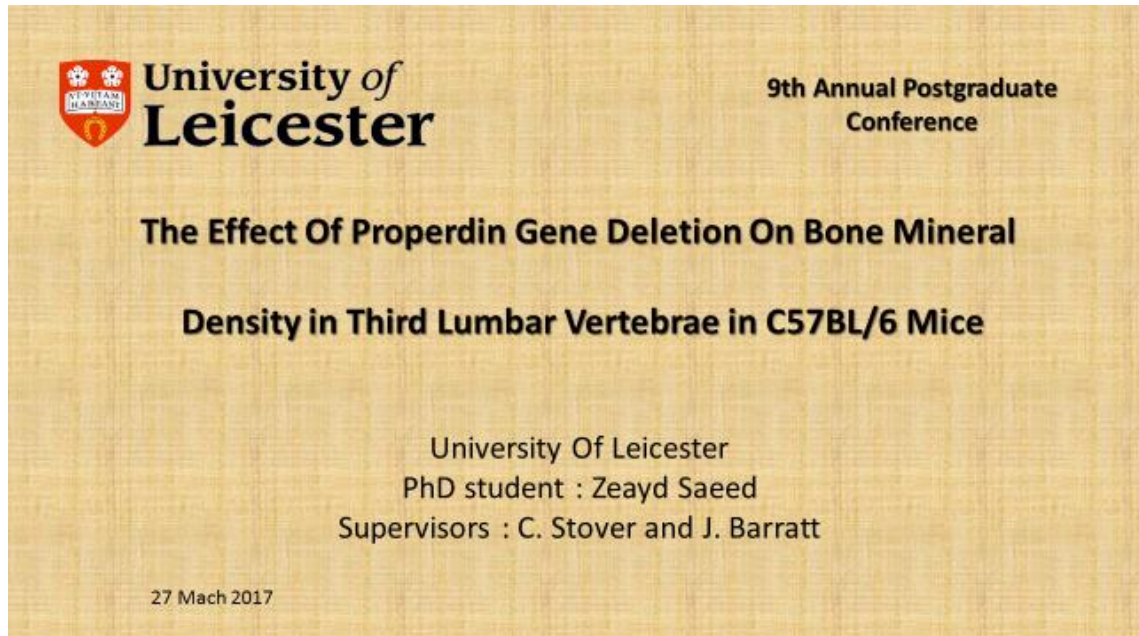
## 6 Future Plan:

- ❖ Providing further understanding to study the role of properdin gene deletion at older age (at or more than 10 months old mice) by *in vivo* measuring the role of complement properdin deficiency on bone mineral density using microcomputed tomography, then measuring the osteoclasts/osteoblasts activities. *In vitro* the osteoclasts activity could be measured by differentiated osteoclasts from PKO/WT and then measuring the number of osteoclasts and the resorptive activity by culturing them on hydroxyapatite well plates. Also, the osteoblasts activity could be measured by differentiating the osteoblasts from PKO/WT and then quantify the osteoblasts number and osteoblasts mineral deposition.
- ❖ In this thesis, it was found that vitamin D3 or exercising during high fat diet normalised the bone mineral density reduction induced by high fat diet in 5 weeks. The combination of Vitamin D3 and exercising during high fat diet could enhance or increase the bone mineral density whilst high fat diet feeding. This could be measured by feeding on high fat diet contains 11IU/g of vitamin D3 in additional to accessing to exercising for 5 weeks. Then, the bone mineral density by  $\mu$ -CT could be evaluated and then the bone remodelling could be assessed for both interventions.
- ❖ The osteoclast and osteoblast could be assessed *in vivo* and *in vitro* by differentiating the from LDLR<sup>-/-</sup> and applying them to mechanical stretching form one hour or overnight and then measuring the osteoclasts resorptive activity and osteoblasts mineral deposition.
- ❖ Identification the exact signalling pathway of Vitamin D3 or fatty acids that could interact with the gene expression or protein production of CFD, CFB, CFP and C3 by measuring the NF-kB, NFATc1, and different MAPKs signalling by western blotting or ELISA.
- ❖ Evaluate the role of osteoclast and osteoblast in genes and protein expression of complement classical and lectin pathways compounds, by identifying gene expression of complement classical and lectin pathways compounds expression in murine osteoclasts by differentiating osteoclast and quantify the gene expression by PCR or qPCR. Then, evaluation the role of Vitamin D3 on the gene expression with or without fatty acids stimulation.

## 7 Appendices

The talk's presentations and posters that were shared with other people like the following:

1- I have presented a talk presentation of the part from my project at the 9<sup>th</sup> annual postgraduate conference in University of Leicester, the presentation talk title is showing below.



2- I have presented a poster presentation of the part from my project in the “11<sup>th</sup> International Conference on Osteoporosis, Arthritis and Musculoskeletal disorder” held during December 04-05, 2017 in Madrid, Spain. In that conference, I have awarded the best poster presentation prize. The poster presentation copy and the prize certificates from the conference and congratulation letter from the head of the department are showing below.



## VITAMIN D OR EXERCISE WHILST ON HIGH FAT DIET NORMALISE BONE MINERAL DENSITY

Zeayd Saeed <sup>a,b</sup>, Justyna Janus <sup>a</sup>, Jonathan Barratt <sup>a</sup>, Cordula Stover <sup>a</sup>  
<sup>a</sup>University of Leicester, UK, <sup>b</sup> Al-Furat Al-Awsat Technical University, Iraq



---

### Introduction

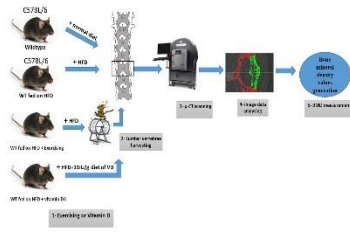
Diet induced obesity is a major health problem in developed and developing countries and affects not only cardiovascular but also skeletal health. Lipids have a direct reducing impact on bone mineral density by inhibiting osteoblast differentiation and enhancing osteoclast differentiation. Conversely, Vitamin D or exercise enhance the bone mineral microarchitecture through activating osteoblast activity and increasing the deposition of calcium.

### Hypothesis

We hypothesised that Vitamin D or exercising normalises the bone mineral density of mice receiving a high fat diet.

### Methods and Materials

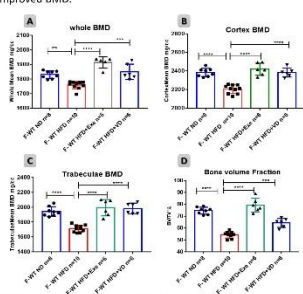
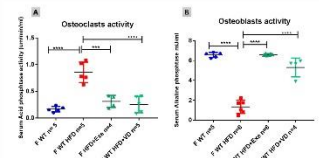
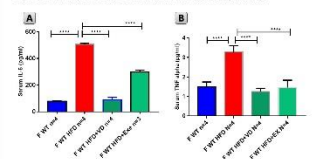
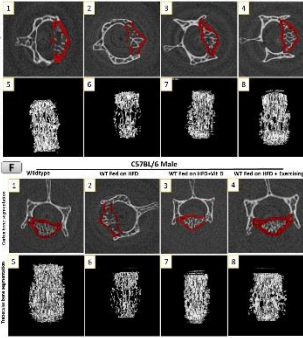
- ❖ **Experimental design:** C57/BL6 male and female 6-months-old mice received normal diet (ND) or high fat diet (HFD). The HFD groups received additional Vitamin D supplementation or had access to wheel exercising. The duration of study was 5 weeks. Percent of fat in ND is 4.8%, HFD 35.8%, Vitamin D in HFD 111U/g.
- ❖ **Microcomputed tomography (μ-CT):** The bodies of the 3rd lumbar vertebrae were scanned, then analysed to generate BMA values.
- ❖ **Osteoclast and osteoblasts activities measurements:** serum tartrate resistant acid phosphatase and alkaline phosphatase.
- ❖ **Inflammatory cytokines measurements:** TNF-α and IL-6



**Figure 1.** The experimental design to investigate the role of vitamin D or exercising in order to correct the high fat diet induced loss of bone mineral density.

### Results

After 5 weeks' high fat diet with or without access to exercising or additional supplement of dietary Vitamin D (111U/g), Bone Mineral Density (BMD) was reduced in HFD group compared to normal diet (ND), however, exercising or Vitamin D significantly improved BMD.

**Figure 2.** Bone microarchitecture was reduced during 5 weeks HFD feeding, but the exercising or Vitamin D normalised the whole, cortex, trabeculae BMDs and BV/TV (A, B, C and D). Cortex and trabecular segmentation (females, E, males, F) are represented by 3D images.

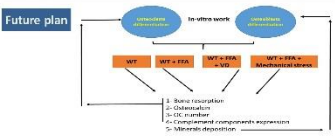
**Figure 3.** Osteoclast and Osteoblast activity: Osteoclast activity was increased and osteoblast activity was decreased when mice were fed HFD but their activities were corrected when the mice received vitamin D or exercised (IA and BI).

**Figure 4.** Cytokine measurements: Serum IL-6 and TNF-α were significantly increased in HFD group. Vitamin D normalised the levels. Exercising whilst on HFD normalised TNF-α, but not IL-6 because it can be produced during muscular contraction as a myokine.

### Conclusions

Vitamin D supplementation or additional exercise normalised within five weeks the bone mineral density in mice on a high fat diet: correction of cortex and trabeculae segmentations, normalisation of osteoblast and osteoclast activities. The inflammatory cytokines (IL-6 and TNF-α) also were normalised in HFD group receiving additional Vitamin D supplementation. The results were similar in males and females. We conclude that these two intervention modes may be of value to obese persons who are in the process of correcting their dietary habits.

### Future plan



---

### Acknowledgements:

- ❖ We thank the Higher Committee for Educational Development in Iraq (HCED) organisation for sponsoring this work of the project.
- ❖ We thank Justyna Janus - Imaging Technician- for her valuable contributions to my training on the Caliper Micro-CT machine and how to use it, and explain the safety conditions in the Core Biotechnology Services, University of Leicester.

### References

1. Vith, S., Liu, J., Yu, P., Srinivasan, S.R., Shi, L., Anand, S.V., Berhane, S., Corbin, L., Adhikari, L., and Wang, S. (2017) Acute effects of hyperglycemia on bone mineral density in youth. *Journal of Bone and Mineral Research*, 32(7), pp. 1361-1371.
2. Mittleman, B. and Parfitt, P.S. (1978) Osteoporosis: a new concept. *Journal of Bone and Mineral Research*, 3(1), pp. 1-7.
3. Li, S., Zou, Y., Li, J., Zhou, B., and Li, J. (2017) The effect of high fat diet on bone mineral density and bone microarchitecture in mice. *Journal of Cellular Biochemistry*, 142(4), pp. 1373-1379.
4. Kuo, K., Li, S., Zhou, B., and Li, J. (2017) The effect of high fat diet on bone mineral density and bone microarchitecture in mice. *Journal of Cellular Biochemistry*, 142(4), pp. 1373-1379.
5. Li, S., Zhou, B., Li, J., Zhou, B., and Li, J. (2017) The effect of high fat diet on bone mineral density and bone microarchitecture in mice. *Journal of Cellular Biochemistry*, 142(4), pp. 1373-1379.
6. Li, S., Zhou, B., Li, J., Zhou, B., and Li, J. (2017) The effect of high fat diet on bone mineral density and bone microarchitecture in mice. *Journal of Cellular Biochemistry*, 142(4), pp. 1373-1379.
7. Li, S., Zhou, B., Li, J., Zhou, B., and Li, J. (2017) The effect of high fat diet on bone mineral density and bone microarchitecture in mice. *Journal of Cellular Biochemistry*, 142(4), pp. 1373-1379.

**PULSUS**  
WWW.PULSUS.COM

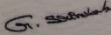
## Certificate of Recognition

PULSUS and the Editors of Journal of Clinical & Experimental Orthopaedics  
and Acta Rheumatologica wish to thank

*Prof/Dr/Mr/Ms. Zeayd Saeed*

*University of Leicester, UK*

for his Poster Presentation on  
*"Vitamin D or exercise whilst on high fat diet normalise bone mineral density"*  
at the "11<sup>th</sup> International Conference on Osteoporosis, Arthritis & Musculoskeletal Disorders"  
held during December 04-05, 2017 in Madrid, Spain

  
Srinu Babu Gedela  
CEO, Pulsus Group, UK

**PULSUS**  
WWW.PULSUS.COM

*Best Poster Award*

Awarded to

ZEAYD SAEED

for presenting the poster entitled:

VITAMIN D OR EXERCISE WHILST ON  
HIGH FAT DIET NORMALISE BONE MINERAL DENSITY

at the "10<sup>th</sup> International Conference on Arthroplasty"  
held during December 04-05, 2017 in Madrid, Spain

The award has been attributed in recognition of research paper quality, novelty and significance.

*G. Srinu Babu*

Srinu Babu Gedela  
CEO, Pulsus Group, UK



Department of Infection, Immunity  
and Inflammation  
Maurice Shock Building  
University Road  
Leicester LE1 7RH, UK

Head of Department and Professor of  
Respiratory Medicine  
**Professor Andrew Wardlaw**  
T +44 (0)116 2522951 (*Secretary*)  
F +44 (0)116 2525035

E [ajb64@le.ac.uk](mailto:ajb64@le.ac.uk) (*Secretary*)  
E [aw24@le.ac.uk](mailto:aw24@le.ac.uk)

7 February 2018

Dear Zeayd,

I would like to take this opportunity to congratulate you on receiving the award for Best Poster at the 10<sup>th</sup> International Conference on Arthroplasty. This is a great achievement and a credit to the department of which you should be very proud.

Yours sincerely

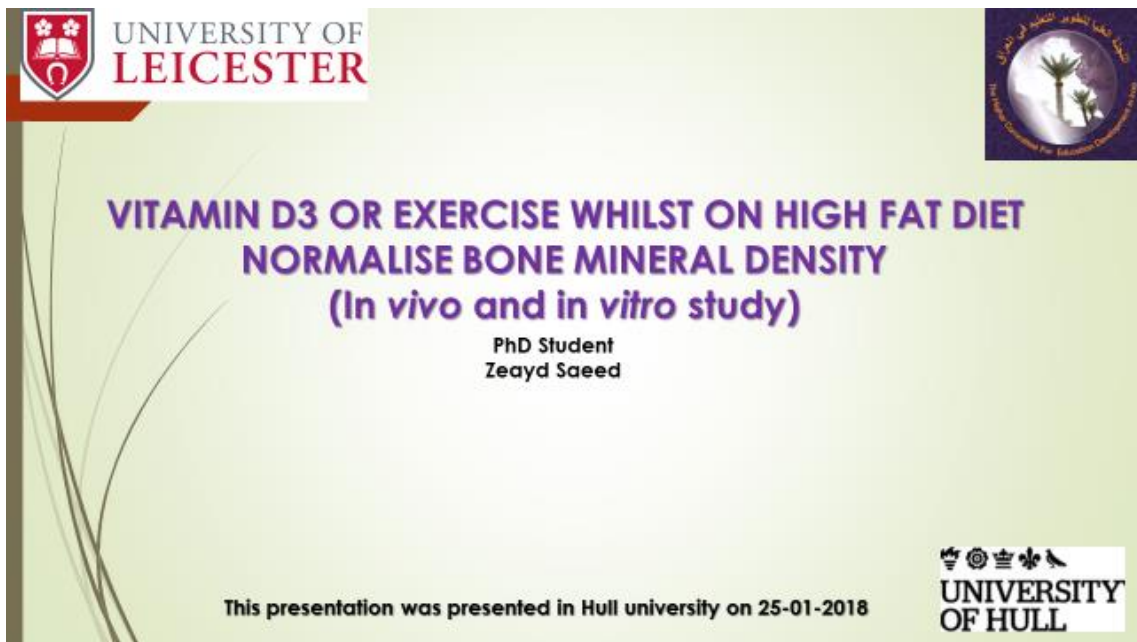
A handwritten signature in blue ink, appearing to read "Andrew Wardlaw".

Professor Andrew Wardlaw  
Head of Department

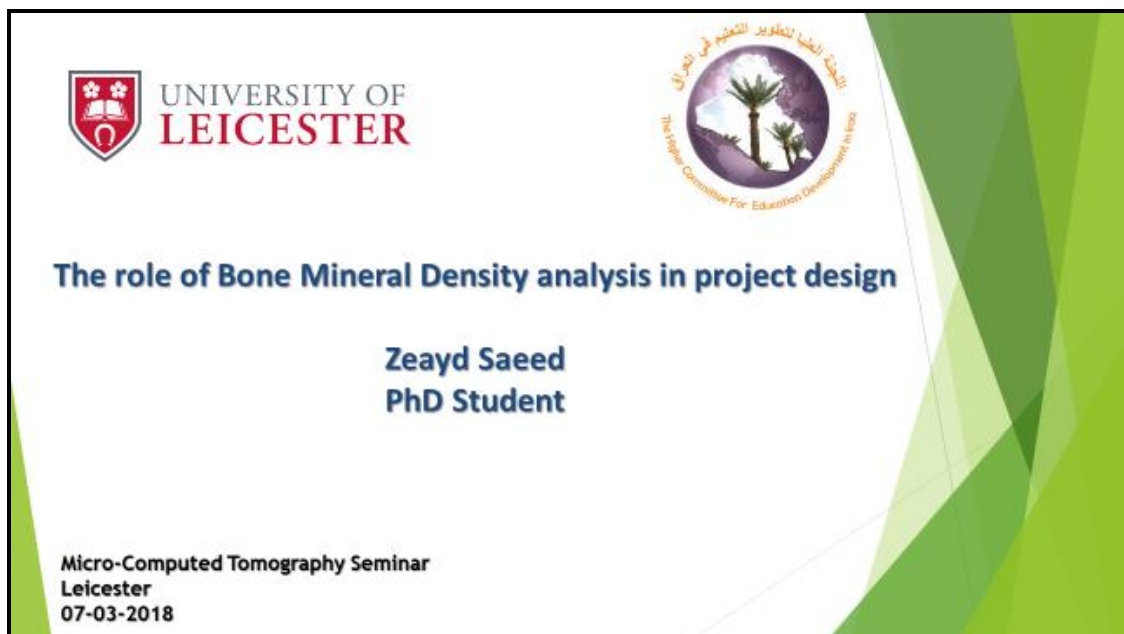
Cc: Dr Cordula Stover and Professor Jonathan Barratt



3- I have presented a talk presentation of the part from my project in a seminar in University of Hull, this talk included the *in vivo* and *in vitro* work, and the presentation talk title is showing below.



4- I have presented a talk presentation of the part from my project in the Micro-computed tomography seminar at the University of Leicester, the presentation talk title is showing below.



5- I have presented a poster presentation of the part from my project in the Complement UK Annual Conference, Manchester 2018, the presentation talk title is showing below.



**UNIVERSITY OF LEICESTER**

## Vitamin D3 normalises long chain fatty acid induced expression of alternative pathway complement components in osteoclasts.

Zeayd Saeed <sup>a,b</sup>, Cordula Stover <sup>a</sup>

<sup>a</sup>University of Leicester, UK, <sup>b</sup> Al-Furat Al-Awsat Technical University, Iraq



---

### Introduction

Diet induced obesity leads to a state of low grade inflammation. Complement is activated in hyperlipidemic serum. Complement activation positively influences osteoclast formation by direct and indirect effects and this may have substantive implications for decreased bone mineral density and increased fracture risk in obese individuals. Vitamin D3 apart from its actions as a regulator of minerals, also has an anti-inflammatory role.

### Hypothesis

In vitro addition of Vitamin D3 normalises the complement component production from differentiated osteoclasts stimulated by fatty acids.

### Materials and Methods

❖ **Experimental design:** Osteoclasts were differentiated from mouse bone marrow using MSCF and RANKL (20ng/ml each). Osteoclasts were stimulated by 40µM/ml of fatty acids (Oleic 2:1 palmitic) conjugated-BSA with or without 4µg/ml Vitamin D3 for 24hr.

❖ **Quantification of complement component expression level:** Total RNA was extracted from differentiated osteoclasts (untreated, FFA treatment, and FFA+ Vitamin D3 treatments) and quantitative reverse transcriptase chain reaction was done to measure the level of gene expression for the alternative pathway amplification loop components (CFD, CFB, CFP and C3).

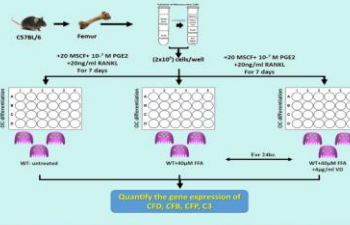
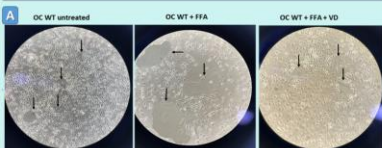


Figure 1. Experimental design of OC differentiation and stimulation by fatty acids and vitamin D3

### Results

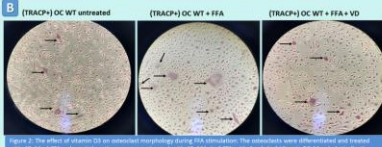
Morphologically, there is significant increase in OC size treated with FFA compared to WT and treated with VD. The level of gene expression for the alternative pathway components was significantly increased in osteoclasts treated with FFA comparing to untreated osteoclasts. Conversely, Vitamin D3 supplementation with FFA normalised or reduced gene expression of CFD, CFB, CFP and C3 by osteoclasts derived from mouse bone marrow.

**A**



(TRACP+) OC WT untreated (TRACP+) OC WT + FFA (TRACP+) OC WT + FFA + VD

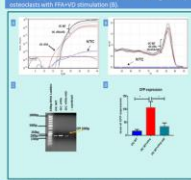
**B**



(TRACP-) OC WT untreated (TRACP-) OC WT + FFA (TRACP-) OC WT + FFA + VD

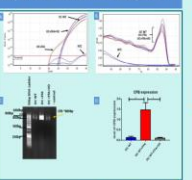
Figure 2. The effect of vitamin D3 on osteoclast morphology during FFA stimulation. The osteoclasts were differentiated and treated with 40µM of FFA and the other group was treated with 40µM of FFA and 4µg/ml of Vitamin D3. Morphologically, the osteoclasts were significantly enlarged in presence of FFA treatment only, but vitamin D3 compensation with FFA counteracted the same size (B). The TRACP+ osteoclast number were significantly increased by FFA stimulation but their number still comparable to osteoclasts with FFA+VD stimulation (B).

**3**



CFD expression

**4**



CFB expression

Figure 3. Vitamin D3 normalises the excessive complement component expression induced by free fatty acids.

**5**



CFP expression

**6**



C3 expression

Figure 4. Vitamin D3 normalises the excessive complement factor 3 expression induced by free fatty acids.

### Conclusion

Osteoclasts are likely to contribute to complement component production CFD, CFB, CFP and C3. Vitamin D3 may have role to curb excessive complement component production by osteoclasts induced by fatty acids.

### References

- Kelly, K.A. and Gimble, J.M. (1998) 1, 25-Dihydroxy vitamin D3 inhibits adipocyte differentiation and gene expression in murine bone marrow stromal cell clones and primary cultures. *Endocrinology*, 133(5), pp. 2622-2628.
- Boudreau, G.D. (2006) Regulation of osteoclast differentiation. *Annals of the New York Academy of Sciences*, 1082(1), pp. 220-226.
- Marcellino, D. and Landis, J.D. (2002) Complement: more than a "guard against invading pathogens?". *Trends in Immunology*, 23(10), pp. 485-493.
- Chapoy, M.C., Anic, M.E., Dubouat, E., Broly, J., Couzou, B., Arnaud, S., Delmas, P.D. and Maziere, P.J. (1992) Vitamin D3 and calcium to prevent hip fractures in elderly women. *New England Journal of Medicine*, 327(23), pp. 2637-2642.
- Harada, T., Mizoguchi, T., Kikuyoshi, T., Nakamoto, Y., Tamaki, S., Saito, S., Nakahara, F., Saito, H., Yoshida, H. and Otagawa, H. (2012) Daily administration of ethacrynic acid (ESA-711), an active vitamin D analog, increases bone mineral density by suppressing RANKL expression in mouse trabecular bone. *Journal of Bone and Mineral Research*, 27(2), pp. 461-473.

---

**Acknowledgements:** We thank the Higher Committee for Educational Development in Iraq (HCED) organisation for sponsoring this work of the project.

The Complement UK Annual Conference, Manchester, 2018



## Certificate of Attendance

This certificate confirms that:

**Zeayd Saeed**

Attended the

### **Complement UK Symposium & Training Course**

held on

Monday 26<sup>th</sup> & Tuesday 27<sup>th</sup> March 2018

at

**The University of Manchester**

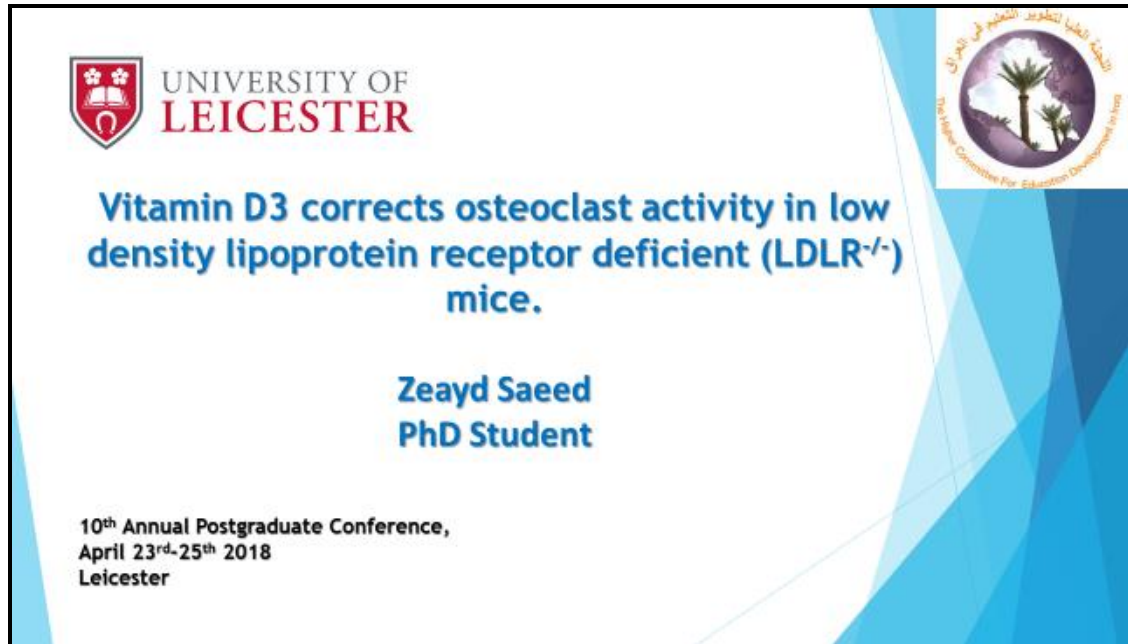
**Course Organiser's Signature**



**March 26<sup>th</sup> 2018**



6- I have presented a talk presentation of the part from my project at the 10<sup>th</sup> annual postgraduate conference in University of Leicester, the presentation talk title is showing below.



 UNIVERSITY OF  
**LEICESTER**

**Vitamin D3 corrects osteoclast activity in low density lipoprotein receptor deficient (LDLR<sup>-/-</sup>) mice.**

**Zeayd Saeed  
PhD Student**

10<sup>th</sup> Annual Postgraduate Conference,  
April 23<sup>rd</sup>-25<sup>th</sup> 2018  
Leicester



## 8 References

### Bibliography

- Ajjola, O.A., Dong, C., Herderick, E.E., Ma, Q., Goldschmidt-Clermont, P.J. and Yan, Z. (2009) 'Voluntary Running suppresses proinflammatory cytokines and bone marrow endothelial progenitor cell levels in apolipoprotein-E-deficient mice', *Antioxidants & redox signaling*, 11(1), pp. 15-23.
- Alex, S., Boss, A., Heerschap, A. and Kersten, S. (2015) 'Exercise training improves liver steatosis in mice', *Nutrition & metabolism*, 12(1), pp. 29.
- Ali, A.A., Weinstein, R.S., Stewart, S.A., Parfitt, A.M., Manolagas, S.C. and Jilka, R.L. (2005) 'Rosiglitazone causes bone loss in mice by suppressing osteoblast differentiation and bone formation', *Endocrinology*, 146(3), pp. 1226-1235.
- Almeida, M., Han, L., Martin-Millan, M., Plotkin, L.I., Stewart, S.A., Roberson, P.K., Kousteni, S., O'Brien, C.A., Bellido, T., Parfitt, A.M., Weinstein, R.S., Jilka, R.L. and Manolagas, S.C. (2007) 'Skeletal involution by age-associated oxidative stress and its acceleration by loss of sex steroids', *The Journal of biological chemistry*, 282(37), pp. 27285-27297.
- Alper, C.A., Johnson, A.M., Birtch, A.G. and Moore, F.D. (1969) 'Human C<sup>3</sup>: evidence for the liver as the primary site of synthesis', *Science (New York, N.Y.)*, 163(3864), pp. 286-288.
- Andrades, J.A., Nimni, M.E., Becerra, J., Eisenstein, R., Davis, M. and Sorgente, N. (1996) 'Complement proteins are present in developing endochondral bone and may mediate cartilage cell death and vascularization', *Experimental cell research*, 227(2), pp. 208-213.
- André, D.M., Calixto, M.C., Sollon, C., Alexandre, E.C., Tavares, E.B., Naime, A.C., Anhê, G.F. and Antunes, E. (2017) 'High-fat diet-induced obesity impairs insulin signaling in lungs of allergen-challenged mice: Improvement by resveratrol', *Scientific reports*, 7(1), pp. 17296.
- Anh, D., Dimai, H., Hall, S. and Farley, J. (1998) 'Skeletal alkaline phosphatase activity is primarily released from human osteoblasts in an insoluble form, and the net release is inhibited by calcium and skeletal growth factors', *Calcified tissue international*, 62(4), pp. 332-340.
- Aspinall, V. and O'Reilly, M. (2004) 'The Endocrine System', *Introduction to Veterinary Anatomy and Physiology. Butterworth Heinemann, St Louis*, , pp. 82-83.
- Assuma, R., Oates, T., Cochran, D., Amar, S. and Graves, D.T. (1998) 'IL-1 and TNF antagonists inhibit the inflammatory response and bone loss in experimental periodontitis', *Journal of immunology (Baltimore, Md.: 1950)*, 160(1), pp. 403-409.

- Baker, R.G., Hayden, M.S. and Ghosh, S. (2011) 'NF- $\kappa$ B, inflammation, and metabolic disease', *Cell metabolism*, 13(1), pp. 11-22.
- Barnum, S.R. and Volanakis, J.E. (1985) 'In vitro biosynthesis of complement protein D by U937 cells', *Journal of immunology (Baltimore, Md.: 1950)*, 134(3), pp. 1799-1803.
- Bartelt, A., Behler-Janbeck, F., Beil, F.T., Koehne, T., Müller, B., Schmidt, T., Heine, M., Ochs, L., Yilmaz, T. and Dietrich, M. (2018) 'Lrp1 in osteoblasts controls osteoclast activity and protects against osteoporosis by limiting PDGF-RANKL signaling', *Bone research*, 6(1), pp. 4.
- Bergdolt, S., Kovtun, A., Hägele, Y., Liedert, A., Schinke, T., Amling, M., Huber-Lang, M. and Ignatius, A. (2017) 'Osteoblast-specific overexpression of complement receptor C5aR1 impairs fracture healing', *PloS one*, 12(6), pp. e0179512.
- Bertoli, S., Striuli, L., Testolin, G., Cardinali, S., Veggiotti, P., Salvatori, G.C. and Tagliabue, A. (2002) 'Nutritional status and bone mineral mass in children treated with ketogenic diet', *Recenti progressi in medicina*, 93(12), pp. 671-675.
- Bharadwaj, S., Naidu, A., Betageri, G., Prasadarao, N. and Naidu, A. (2009) 'Milk ribonuclease-enriched lactoferrin induces positive effects on bone turnover markers in postmenopausal women', *Osteoporosis International*, 20(9), pp. 1603-1611.
- Bieghs, V., Van Gorp, P.J., Wouters, K., Hendriks, T., Gijbels, M.J., van Bilsen, M., Bakker, J., Binder, C.J., Lütjohann, D. and Staels, B. (2012) 'LDL receptor knock-out mice are a physiological model particularly vulnerable to study the onset of inflammation in non-alcoholic fatty liver disease', *PloS one*, 7(1), pp. e30668.
- Birbrair, A. and Frenette, P.S. (2016) 'Niche heterogeneity in the bone marrow', *Annals of the New York Academy of Sciences*, 1370(1), pp. 82-96.
- Blair, H.C., Zaidi, M. and Schlesinger, P.H. (2002) 'Mechanisms balancing skeletal matrix synthesis and degradation', *The Biochemical journal*, 364(Pt 2), pp. 329-341.
- Boden, G., She, P., Mozzoli, M., Cheung, P., Gumireddy, K., Reddy, P., Xiang, X., Luo, Z. and Ruderman, N. (2005) 'Free fatty acid produce insulin resistance and activate the proinflammatory nuclear factor-kappaB pathway in rat liver', *Diabetes*, 54(12), pp. 3458-3465.
- Bostrom, R.D. and Mikos, A.G. (1997) 'Tissue engineering of bone', in Anonymous *Synthetic biodegradable polymer scaffolds*. Springer, pp. 215-234.
- Boutahar, N., Guignandon, A., Vico, L. and Lafage-Proust, M.H. (2004) 'Mechanical strain on osteoblasts activates autophosphorylation of focal adhesion kinase and proline-rich tyrosine kinase 2 tyrosine sites involved in ERK activation', *The Journal of biological chemistry*, 279(29), pp. 30588-30599.

- Burstone, M. (1958) 'Histochemical comparison of naphthol AS-phosphates for the demonstration of phosphatases', *Journal of the National Cancer Institute*, 20(3), pp. 601-615.
- Calder, P.C., Ahluwalia, N., Brouns, F., Buetler, T., Clement, K., Cunningham, K., Esposito, K., Jönsson, L.S., Kolb, H. and Lansink, M. (2011) 'Dietary factors and low-grade inflammation in relation to overweight and obesity', *British Journal of Nutrition*, 106(S3), pp. S1-S78.
- Calton, E.K., Keane, K.N., Newsholme, P. and Soares, M.J. (2015) 'The impact of vitamin D levels on inflammatory status: a systematic review of immune cell studies', *PloS one*, 10(11), pp. e0141770.
- Cao, J.J., Sun, L. and Gao, H. (2010) 'Diet-induced obesity alters bone remodeling leading to decreased femoral Trabecular bone mass in mice', *Annals of the New York Academy of Sciences*, 1192(1), pp. 292-297.
- Cao, J.J., Gregoire, B.R. and Gao, H. (2009) 'High-fat diet decreases cancellous bone mass but has no effect on cortical bone mass in the tibia in mice', *Bone*, 44(6), pp. 1097-1104.
- Carvalho, J.T.G., Schneider, M., Cuppari, L., Grabulosa, C.C., Aoike, D.T., Redublo, B.M.Q., Batista, M.C., Cendoroglo, M., Moyses, R.M. and Dalboni, M.A. (2017) 'Cholecalciferol decreases inflammation and improves vitamin D regulatory enzymes in lymphocytes in the uremic environment: A randomized controlled pilot trial', *PloS one*, 12(6), pp. e0179540.
- Chapuy, M.C., Arlot, M.E., Duboeuf, F., Brun, J., Crouzet, B., Arnaud, S., Delmas, P.D. and Meunier, P.J. (1992) 'Vitamin D3 and calcium to prevent hip fractures in elderly women', *New England journal of medicine*, 327(23), pp. 1637-1642.
- Cole, F.S., Matthews, W.J., Jr, Marino, J.T., Gash, D.J. and Colten, H.R. (1980) 'Control of complement synthesis and secretion in bronchoalveolar and peritoneal macrophages', *Journal of immunology (Baltimore, Md.: 1950)*, 125(3), pp. 1120-1124.
- Collins, S., Martin, T.L., Surwit, R.S. and Robidoux, J. (2004) 'Genetic vulnerability to diet-induced obesity in the C57BL/6J mouse: physiological and molecular characteristics', *Physiology & Behavior*, 81(2), pp. 243-248.
- Constantinou, C., Mpatsoulis, D., Natsos, A., Petropoulou, P.I., Zvintzou, E., Traish, A.M., Voshol, P.J., Karagiannides, I. and Kypreos, K.E. (2014) 'The low density lipoprotein receptor modulates the effects of hypogonadism on diet-induced obesity and related metabolic perturbations', *Journal of lipid research*, 55(7), pp. 1434-1447.
- Cornish, J., MacGibbon, A., Lin, J., Watson, M., Callon, K.E., Tong, P., Dunford, J.E., van der Does, Y., Williams, G.A. and Grey, A.B. (2008) 'Modulation of osteoclastogenesis by fatty acid', *Endocrinology*, 149(11), pp. 5688-5695.

- Cortez, M., Carmo, L.S., Rogero, M.M., Borelli, P. and Fock, R.A. (2013) 'A high-fat diet increases IL-1, IL-6, and TNF- $\alpha$  production by increasing NF- $\kappa$ B and attenuating PPAR- $\gamma$  expression in bone marrow mesenchymal stem cells', *Inflammation*, 36(2), pp. 379-386.
- Daha, M.R. and van Kooten, C. (2000) 'Is there a role for locally produced complement in renal disease?', *Nephrology Dialysis Transplantation*, 15(10), pp. 1506-1509.
- Dall'Aglio, E., Chang, F., Chang, H., Stern, J. and Reaven, G. (1983) 'Effect of exercise and diet on triglyceride metabolism in rats with moderate insulin deficiency', *Diabetes*, 32(1), pp. 46-50.
- de Ceulaer, C., Papazoglou, S. and Whaley, K. (1980) 'Increased biosynthesis of complement components by cultured monocytes, synovial fluid macrophages and synovial membrane cells from patients with rheumatoid arthritis', *Immunology*, 41(1), pp. 37-43.
- Diascro, D.D., Vogel, R.L., Johnson, T.E., Witherup, K.M., Pitzemberger, S.M., Rutledge, S.J., Prescott, D.J., Rodan, G.A. and Schmidt, A. (1998) 'High Fatty Acid Content in Rabbit Serum Is Responsible for the Differentiation of Osteoblasts Into Adipocyte-like Cells', *Journal of Bone and Mineral Research*, 13(1), pp. 96-106.
- Dixon, J.B. (2010) 'The effect of obesity on health outcomes', *Molecular and cellular endocrinology*, 316(2), pp. 104-108.
- Doerner, S.K., Reis, E.S., Leung, E.S., Ko, J.S., Heaney, J.D., Berger, N.A., Lambris, J.D. and Nadeau, J.H. (2016) 'High-Fat Diet-Induced Complement Activation Mediates Intestinal Inflammation and Neoplasia, Independent of Obesity', *Molecular cancer research : MCR*, 14(10), pp. 953-965.
- Drosatos-Tampakaki, Z., Drosatos, K., Siegelin, Y., Gong, S., Khan, S., Van Dyke, T., Goldberg, I.J., Schulze, P.C. and Schulze-Späte, U. (2014) 'Palmitic Acid and DGAT1 Deficiency Enhance Osteoclastogenesis, while Oleic Acid-Induced Triglyceride Formation Prevents It', *Journal of Bone and Mineral Research*, 29(5), pp. 1183-1195.
- Dupont, A., Mohamed, F., Salehen, N., Glenn, S., Francescut, L., Adib, R., Byrne, S., Brewin, H., Elliott, I., Richards, L., Dimitrova, P., Schwaeble, W., Ivanovska, N., Kadioglu, A., Machado, L.R., Andrew, P.W. and Stover, C. (2014) 'Septicaemia models using *Streptococcus pneumoniae* and *Listeria monocytogenes*: understanding the role of complement properdin', 203(4), pp. pp 257–271.
- Dutta, S. and Sengupta, P. (2016) 'Men and mice: relating their ages', *Life Sciences*, 152, pp. 244-248.
- Ehrlich, P. and Lanyon, L. (2002) 'Mechanical strain and bone cell function: a review', *Osteoporosis International*, 13(9), pp. 688-700.
- Ehrnthaller, C., Huber-Lang, M., Recknagel, S., Bindl, R., Redeker, S., Rapp, A., Gebhard, F. & Ignatius, A. (2013) 'The role of complement in bone healing:

- Fracture healing in C3 and C5-deficient mice', *Orthopaedic Proceedings* The British Editorial Society of Bone & Joint Surgery, pp. 59.
- Farhi, D. (ed.) (2009) *Pathology of bone marrow and blood cells*. 2nd ed. edn. Philadelphia: Wolters Kluwer Health/Lippincott Williams & Wilkins.
- Fearon, D.T. and Austen, K.F. (1975) 'Properdin: binding to C3b and stabilization of the C3b-dependent C3 convertase', *The Journal of experimental medicine*, 142(4), pp. 856-863.
- Febbraio, M.A. and Pedersen, B.K. (2005) 'Contraction-induced myokine production and release: is skeletal muscle an endocrine organ?', *Exercise and sport sciences reviews*, 33(3), pp. 114-119.
- Fischer, V., Haffner-Luntzer, M., Prystaz, K., Vom Scheidt, A., Busse, B., Schinke, T., Amling, M. and Ignatius, A. (2017) 'Calcium and vitamin-D deficiency marginally impairs fracture healing but aggravates posttraumatic bone loss in osteoporotic mice', *Scientific Reports*, 7(1), pp. 7223.
- Fuller, K., Wong, B., Fox, S., Choi, Y. and Chambers, T.J. (1998) 'TRANCE is necessary and sufficient for osteoblast-mediated activation of bone resorption in osteoclasts', *The Journal of experimental medicine*, 188(5), pp. 997-1001.
- Gala, J., Di, M. and de la Piedra, C. (2001) 'Short-and long-term effects of calcium and exercise on bone mineral density in ovariectomized rats', *British Journal of Nutrition*, 86(4), pp. 521-527.
- Gardiner, E.M., Baldock, P.A., Thomas, G.P., Sims, N.A., Henderson, N.K., Hollis, B., White, C.P., Sunn, K.L., Morrison, N.A., Walsh, W.R. and Eisman, J.A. (2000) 'Increased formation and decreased resorption of bone in mice with elevated vitamin D receptor in mature cells of the osteoblastic lineage', *FASEB journal : official publication of the Federation of American Societies for Experimental Biology*, 14(13), pp. 1908-1916.
- Gdyczynski, C.M., Manbachi, A., Hashemi, S., Lashkari, B. and Cobbold, R.S.C. (2014) 'On estimating the directionality distribution in pedicle Trabecular bone from micro-CT images', *Physiological Measurement*, 35(12), pp. 2415.
- Gharavi, N. (2002) 'Role of lipids in osteoporotic bone loss', *Nutrition Bytes*, 8(2).
- Glass, C.K. and Olefsky, J.M. (2012) 'Inflammation and lipid signaling in the etiology of insulin resistance', *Cell metabolism*, 15(5), pp. 635-645.
- Gold, A.M. (1967) '[83] Sulfonylation with sulfonyl halides', in Anonymous *Methods in enzymology*. Elsevier, pp. 706-711.
- Goldring, S.R. (2002) 'Bone and joint destruction in rheumatoid arthritis: what is really happening?', *The Journal of rheumatology. Supplement*, 65, pp. 44-48.
- Gomez, S. (2002) 'Crisóstomo Martínez, 1638–1694', *Endocrine*, 17(1), pp. 3-4.

- Grados, F., Brazier, M., Kamel, S., Duver, S., Heurtebize, N., Maamer, M., Mathieu, M., Garabédian, M., Sebert, J. and Fardellone, P. (2003) 'Effects on bone mineral density of calcium and vitamin D supplementation in elderly women with vitamin D deficiency', *Joint Bone Spine*, 70(3), pp. 203-208.
- Guo, Y., Wang, Y., Liu, Y., Wang, H., Guo, C., Zhang, X. and Bei, C. (2015) 'Effect of the same mechanical loading on osteogenesis and osteoclastogenesis in vitro', *Chinese Journal of Traumatology*, 18(3), pp. 150-156.
- Gupta, S., Knight, A.G., Gupta, S., Keller, J.N. and Bruce-Keller, A.J. (2012) 'Saturated long-chain fatty acid activate inflammatory signaling in astrocytes', *Journal of neurochemistry*, 120(6), pp. 1060-1071.
- Hall, J. (ed.) (2011) *Textbook of Medical Physiology*. 12th ed. edn. Philadelphia: Elsevier.
- Hall, S.J. (ed.) (2007) *Basic Biomechanics with OLC*. 5th ed., Revised. ed. edn. Burr Ridge: McGraw-Hill Higher Education.
- Harada, S., Mizoguchi, T., Kobayashi, Y., Nakamichi, Y., Takeda, S., Sakai, S., Takahashi, F., Saito, H., Yasuda, H. and Udagawa, N. (2012) 'Daily administration of eldcalcitol (ED-71), an active vitamin D analog, increases bone mineral density by suppressing RANKL expression in mouse Trabecular bone', *Journal of Bone and Mineral Research*, 27(2), pp. 461-473.
- Hardy, R. and Cooper, M.S. (2009) 'Bone loss in inflammatory disorders', *The Journal of endocrinology*, 201(3), pp. 309-320.
- Hillian, A.D., McMullen, M.R., Sebastian, B.M., Roychowdhury, S., Kashyap, S.R., Schauer, P.R., Kirwan, J.P., Feldstein, A.E. and Nagy, L.E. (2013) 'Mice lacking C1q are protected from high fat diet-induced hepatic insulin resistance and impaired glucose homeostasis', *The Journal of biological chemistry*, 288(31), pp. 22565-22575.
- Hirasawa, H., Tanaka, S., Sakai, A., Tsutsui, M., Shimokawa, H., Miyata, H., Moriwaki, S., Niida, S., Ito, M. and Nakamura, T. (2007) 'ApoE Gene Deficiency Enhances the Reduction of Bone Formation Induced by a High-Fat Diet Through the Stimulation of p53-Mediated Apoptosis in Osteoblastic Cells', *Journal of Bone and Mineral Research*, 22(7), pp. 1020-1030.
- Hoe, E., Nathanielsz, J., Toh, Z.Q., Spry, L., Marimla, R., Balloch, A., Mulholland, K. and Licciardi, P.V. (2016) 'Anti-inflammatory effects of vitamin D on human immune cells in the context of bacterial infection', *Nutrients*, 8(12), pp. 806.
- Holtrop, M.E. and King, G.J. (1977) 'The ultrastructure of the osteoclast and its functional implications', *Clinical orthopaedics and related research*, (123)(123), pp. 177-196.
- HONG, M.H., JIN, C.H., SATO, T., ISHIMI, Y., ABE, E. and SUDA, A.T. (1991) 'Transcriptional Regulation of the Production of the Third Component of

- Complement (C3) by  $\alpha$ , 25-Dihydroxyvitamin D3 in Mouse Marrow-Derived Stromal Cells (ST2) and Primary Osteoblastic Cells', *Endocrinology*, 129(5), pp. 2774-2779.
- Horlick, M., Wang, J., Pierson, R.N., Jr and Thornton, J.C. (2004) 'Prediction models for evaluation of total-body bone mass with dual-energy X-ray absorptiometry among children and adolescents', *Pediatrics*, 114(3), pp. e337-45.
- Hou, J., Zernicke, R. and Barnard, R. (1990) 'High fat-sucrose diet effects on femoral neck geometry and biomechanics', *Clinical Biomechanics*, 5(3), pp. 162-168.
- Hourcade, D.E. (2006) 'The Role of Properdin in the Assembly of the Alternative Pathway C3 Convertases of Complement', *Journal of Biological Chemistry*, 281(4), pp. 2128-2132.
- Hsieh, Y., Robling, A.G., Ambrosius, W.T., Burr, D.B. and Turner, C.H. (2001) 'Mechanical loading of diaphyseal bone in vivo: the strain threshold for an osteogenic response varies with location', *Journal of Bone and Mineral Research*, 16(12), pp. 2291-2297.
- Huber-Lang, M., Ignatius, A. and Brenner, R.E. (2015) 'Role of complement on broken surfaces after trauma', in Anonymous *Immune Responses to Biosurfaces*. Springer, pp. 43-55.
- Huber-Lang, M., Kovtun, A. & Ignatius, A. (2013) 'The role of complement in trauma and fracture healing', *Seminars in immunology* Elsevier, pp. 73.
- Hui, S.L., Slemenda, C.W. and Johnston, C.C., Jr (1988) 'Age and bone mass as predictors of fracture in a prospective study', *The Journal of clinical investigation*, 81(6), pp. 1804-1809.
- Ignatius, A., Schoengraf, P., Kreja, L., Liedert, A., Recknagel, S., Kandert, S., Brenner, R.E., Schneider, M., Lambris, J.D. and Huber-Lang, M. (2011a) 'Complement C3a and C5a modulate osteoclast formation and inflammatory response of osteoblasts in synergism with IL-1 $\beta$ ', *Journal of cellular biochemistry*, 112(9), pp. 2594-2605.
- Ignatius, A., Ehrnthaller, C., Brenner, R.E., Kreja, L., Schoengraf, P., Lisson, P., Blakytyn, R., Recknagel, S., Claes, L., Gebhard, F., Lambris, J.D. and Huber-Lang, M. (2011b) 'The anaphylatoxin receptor C5aR is present during fracture healing in rats and mediates osteoblast migration in vitro', *The Journal of trauma*, 71(4), pp. 952-960.
- Inzana, J.A., Kung, M., Shu, L., Hamada, D., Xing, L.P., Zuscik, M.J., Awad, H.A. and Mooney, R.A. (2013) 'Immature mice are more susceptible to the detrimental effects of high fat diet on cancellous bone in the distal femur', *Bone*, 57(1), pp. 174-183.
- Ishimi, Y., Miyaura, C., Jin, C.H., Akatsu, T., Abe, E., Nakamura, Y., Yamaguchi, A., Yoshiki, S., Matsuda, T. and Hirano, T. (1990) 'IL-6 is produced by osteoblasts and

- induces bone resorption', *Journal of immunology (Baltimore, Md.: 1950)*, 145(10), pp. 3297-3303.
- Janjetovic, Z., Zmijewski, M.A., Tuckey, R.C., DeLeon, D.A., Nguyen, M.N., Pfeffer, L.M. and Slominski, A.T. (2009) '20-Hydroxycholecalciferol, product of vitamin D3 hydroxylation by P450scc, decreases NF- $\kappa$ B activity by increasing I $\kappa$ B $\alpha$  levels in human keratinocytes', *PloS one*, 4(6), pp. e5988.
- Jeon, S. and Shin, E. (2018) 'Exploring vitamin D metabolism and function in cancer', *Experimental & molecular medicine*, 50(4), pp. 20.
- Jilka, R.L. (2013) 'The relevance of mouse models for investigating age-related bone loss in humans', *Journals of Gerontology Series A: Biomedical Sciences and Medical Sciences*, 68(10), pp. 1209-1217.
- Jin, C.H., Shinki, T., Hong, M.H., Sato, T., Yamaguchi, A., Ikeda, T., Yoshiki, S., Abe, E. and Suda, T. (1992) '1 alpha,25-dihydroxyvitamin D3 regulates in vivo production of the third component of complement (C3) in bone', *Endocrinology*, 131(5), pp. 2468-2475.
- Karaca, I. and Ugar, D. (1999) 'MINI-REVIEW: WHAT DO WE KNOW ABOUT SERUM ALKALINE PHOSPHATASE ACTIVITY ASA BIOCHEMICAL BONE FORMATION MARKER?', *Biochemical archives*, 15(1), pp. 1-4.
- Kheder, R.K. (2017b) *Immune modulation in the prevention of pathologies relating to diet-induced obesity*, PhD thesis, Department of infection, immunity and inflammation(University of Leicester, UK).
- Kheder, R., Hobkirk, J., Saeed, Z., Janus, J., Carroll, S., Browning, M.J. and Stover, C. (2017a) 'Vitamin D3 supplementation of a high fat high sugar diet ameliorates prediabetic phenotype in female LDLR $^{-/-}$  and LDLR / mice', *Immunity, inflammation and disease*, 5(2), pp. 151-162.
- Khosla, S. (2001) 'Minireview: the OPG/RANKL/RANK system', *Endocrinology*, 142(12), pp. 5050-5055.
- Kirstein, B., Chambers, T.J. and Fuller, K. (2006) 'Secretion of tartrate-resistant acid phosphatase by osteoclasts correlates with resorptive behavior', *Journal of cellular biochemistry*, 98(5), pp. 1085-1094.
- Kotimaa, J.P., van Werkhoven, M.B., O'Flynn, J., Klar-Mohamad, N., van Groningen, J., Schilders, G., Rutjes, H., Daha, M.R., Seelen, M.A. and van Kooten, C. (2015) 'Functional assessment of mouse complement pathway activities and quantification of C3b/C3c/iC3b in an experimental model of mouse renal ischaemia/reperfusion injury', *Journal of immunological methods*, 419, pp. 25-34.
- Kovtun, A., Bergdolt, S., Hägele, Y., Matthes, R., Lambris, J.D., Huber-Lang, M. and Ignatius, A. (2017) 'Complement receptors C5aR1 and C5aR2 act differentially during the early immune response after bone fracture but are similarly involved in bone repair', *Scientific reports*, 7(1), pp. 14061.

- Lac, G., Cavalie, H., Ebal, E. and Michaux, O. (2008) 'Effects of a high fat diet on bone of growing rats. Correlations between visceral fat, adiponectin and bone mass density', *Lipids in health and disease*, 7(1), pp. 16.
- Lacey, D., Timms, E., Tan, H., Kelley, M., Dunstan, C., Burgess, T., Elliott, R., Colombero, A., Elliott, G. and Scully, S. (1998) 'Osteoprotegerin ligand is a cytokine that regulates osteoclast differentiation and activation', *Cell*, 93(2), pp. 165-176.
- Lee, N.K., Sowa, H., Hinoi, E., Ferron, M., Ahn, J.D., Confavreux, C., Dacquin, R., Mee, P.J., McKee, M.D. and Jung, D.Y. (2007) 'Endocrine regulation of energy metabolism by the skeleton', *Cell*, 130(3), pp. 456-469.
- Li, K., Zernicke, R.F., Barnard, R.J. and Li, A.F. (1990) 'Effects of a high fat-sucrose diet on cortical bone morphology and biomechanics', *Calcified tissue international*, 47(5), pp. 308-313.
- Li, D., Zou, L., Feng, Y., Xu, G., Gong, Y., Zhao, G., Ouyang, W., Thurman, J.M. and Chao, W. (2016) 'Complement Factor B Production in Renal Tubular Cells and Its Role in Sodium Transporter Expression During Polymicrobial Sepsis', *Critical Care Medicine*, 44(5), pp. e289-99.
- Li, K., Anderson, K.J., Peng, Q., Noble, A., Lu, B., Kelly, A.P., Wang, N., Sacks, S.H. and Zhou, W. (2008) 'Cyclic AMP plays a critical role in C3a-receptor-mediated regulation of dendritic cells in antigen uptake and T-cell stimulation', *Blood*, 112(13), pp. 5084-5094.
- Lips, P. (2006) 'Vitamin D physiology', *Progress in biophysics and molecular biology*, 92(1), pp. 4-8.
- Lipscombe, L.L., Jamal, S.A., Booth, G.L. and Hawker, G.A. (2007) 'The risk of hip fractures in older individuals with diabetes: a population-based study', *Diabetes care*, 30(4), pp. 835-841.
- Lubbers, R., van Essen, M., van Kooten, C. and Trouw, L. (2017) 'Production of complement components by cells of the immune system', *Clinical & Experimental Immunology*, 188(2), pp. 183-194.
- Maekawa, T., Briones, R.A., Resuello, R.R., Tuplano, J.V., Hajishengallis, E., Kajikawa, T., Koutsogiannaki, S., Garcia, C.A., Ricklin, D. and Lambris, J.D. (2016) 'Inhibition of pre-existing natural periodontitis in non-human primates by a locally administered peptide inhibitor of complement C3', *Journal of clinical periodontology*, .
- Malhi, H., Bronk, S.F., Werneburg, N.W. and Gores, G.J. (2006) 'Free fatty acid induce JNK-dependent hepatocyte lipoapoptosis', *The Journal of biological chemistry*, 281(17), pp. 12093-12101.

- Mangham, D.C., Scoones, D.J. and Drayson, M.T. (1993) 'Complement and the recruitment of mononuclear osteoclasts', *Journal of clinical pathology*, 46(6), pp. 517-521.
- Mantuano, E., Brifault, C., Lam, M.S., Azmoon, P., Gilder, A.S. and Gonias, S.L. (2016) 'LDL receptor-related protein-1 regulates NFkappaB and microRNA-155 in macrophages to control the inflammatory response', *Proceedings of the National Academy of Sciences of the United States of America*, 113(5), pp. 1369-1374.
- Marx, R.E., Cillo, J.E., Jr and Ulloa, J.J. (2007) 'Oral bisphosphonate-induced osteonecrosis: risk factors, prediction of risk using serum CTX testing, prevention, and treatment', *Journal of oral and maxillofacial surgery : official journal of the American Association of Oral and Maxillofacial Surgeons*, 65(12), pp. 2397-2410.
- Matsuoka, K., Park, K., Ito, M., Ikeda, K. and Takeshita, S. (2014) 'Osteoclast-Derived Complement Component 3a Stimulates Osteoblast Differentiation', *Journal of Bone and Mineral Research*, 29(7), pp. 1522-1530.
- Maurer, L., Tang, H., Haumesser, J.K., Altschüler, J., Kühn, A.A., Spranger, J. and Riesen, C. (2017) 'High-fat diet-induced obesity and insulin resistance are characterized by differential beta oscillatory signaling of the limbic cortico-basal ganglia loop', *Scientific Reports*, 7(1), pp. 15555.
- McCabe, L.R., Irwin, R., Tekalur, A., Evans, C., Schepper, J.D., Parameswaran, N. and Ciancio, M. (2018) 'Exercise prevents high fat diet-induced bone loss, marrow adiposity and dysbiosis in male mice', *Bone*, .
- Meeker, S., Seamons, A., Paik, J., Treuting, P.M., Brabb, T., Grady, W.M. and Maggio-Price, L. (2014) 'Increased dietary vitamin D suppresses MAPK signaling, colitis, and colon cancer', *Cancer research*, 74(16), pp. 4398-4408.
- Meissner, M., Lombardo, E., Havinga, R., Tietge, U.J., Kuipers, F. and Groen, A.K. (2011) 'Voluntary wheel running increases bile acid as well as cholesterol excretion and decreases atherosclerosis in hypercholesterolemic mice', *Atherosclerosis*, 218(2), pp. 323-329.
- Milanski, M., Degasperi, G., Coope, A., Morari, J., Denis, R., Cintra, D.E., Tsukumo, D.M., Anhe, G., Amaral, M.E., Takahashi, H.K., Curi, R., Oliveira, H.C., Carvalheira, J.B., Bordin, S., Saad, M.J. and Velloso, L.A. (2009) 'Saturated fatty acid produce an inflammatory response predominantly through the activation of TLR4 signaling in hypothalamus: implications for the pathogenesis of obesity', *The Journal of neuroscience : the official journal of the Society for Neuroscience*, 29(2), pp. 359-370.
- Miron, R.J. and Bosshardt, D.D. (2016) 'OsteoMacs: Key players around bone biomaterials', *Biomaterials*, 82, pp. 1-19.
- Mödinger, Y., Löffler, B., Huber-Lang, M. & Ignatius, A. (2018) 'Complement involvement in bone homeostasis and bone disorders', *Seminars in immunology* Elsevier.

- Mori, T., Okimoto, N., Sakai, A., Okazaki, Y., Nakura, N., Notomi, T. and Nakamura, T. (2003) 'Climbing exercise increases bone mass and Trabecular bone turnover through transient regulation of marrow osteogenic and osteoclastogenic potentials in mice', *Journal of bone and mineral research*, 18(11), pp. 2002-2009.
- Moseti, D., Regassa, A. and Kim, W. (2016) 'Molecular regulation of adipogenesis and potential anti-adipogenic bioactive molecules', *International journal of molecular sciences*, 17(1), pp. 124.
- Mueller, C.G. and Hess, E. (2012) 'Emerging functions of RANKL in lymphoid tissues', *Frontiers in immunology*, 3, pp. 261.
- Navab, M., Ananthramaiah, G.M., Reddy, S.T., Van Lenten, B.J., Ansell, B.J., Fonarow, G.C., Vahabzadeh, K., Hama, S., Hough, G., Kamranpour, N., Berliner, J.A., Lusis, A.J. and Fogelman, A.M. (2004) 'The oxidation hypothesis of atherogenesis: the role of oxidized phospholipids and HDL', *Journal of lipid research*, 45(6), pp. 993-1007.
- Numan, M.S., Amiable, N., Brown, J.P. and Michou, L. (2015) 'Paget's disease of bone: an osteoimmunological disorder?', *Drug design, development and therapy*, 9, pp. 4695-4707.
- Oh, S., Sul, O., Kim, Y., Kim, H., Yu, R., Suh, J. and Choi, H. (2010) 'Saturated fatty acid enhance osteoclast survival', *Journal of lipid research*, 51(5), pp. 892-899.
- Okayasu, M., Nakayachi, M., Hayashida, C., Ito, J., Kaneda, T., Masuhara, M., Suda, N., Sato, T. and Hakeda, Y. (2012) 'Low-density lipoprotein receptor deficiency causes impaired osteoclastogenesis and increased bone mass in mice because of defect in osteoclastic cell-cell fusion', *The Journal of biological chemistry*, 287(23), pp. 19229-19241.
- Orimo, H. (2010) 'The mechanism of mineralization and the role of alkaline phosphatase in health and disease', *Journal of Nippon Medical School*, 77(1), pp. 4-12.
- Ornoy, A., Goodwin, D., Noff, D. and Edelstein, S. (1978) '24, 25-Dihydroxyvitamin D is a metabolite of vitamin D essential for bone formation', *Nature*, 276(5687), pp. 517.
- Owen, T.A., ARONOW, M.S., Barone, L.M., BETTENCOURT, B., Stein, G.S. and Lian, J.B. (1991) 'Pleiotropic effects of vitamin D on osteoblast gene expression are related to the proliferative and differentiated state of the bone cell phenotype: dependency upon basal levels of gene expression, duration of exposure, and bone matrix competency in normal rat osteoblast cultures', *Endocrinology*, 128(3), pp. 1496-1504.
- Parhami, F., Tintut, Y., Beamer, W.G., Gharavi, N., Goodman, W. and Demer, L.L. (2001) 'Atherogenic High-Fat Diet Reduces Bone Mineralization in Mice', *Journal of Bone and Mineral Research*, 16(1), pp. 182-188.

- Parhami, F., Garfinkel, A. and Demer, L.L. (2000) 'Role of Lipids in Osteoporosis', *Arteriosclerosis, Thrombosis, and Vascular Biology: Journal of the American Heart Association*, 20(11), pp. 2346-2348.
- Pathak, J.L., Bravenboer, N., Luyten, F.P., Verschueren, P., Lems, W.F., Klein-Nulend, J. and Bakker, A.D. (2015) 'Mechanical loading reduces inflammation-induced human osteocyte-to-osteoclast communication', *Calcified tissue international*, 97(2), pp. 169-178.
- Patkova, J.; Andel, M.; Trnka, J. (2014) Palmitate-induced cell death and mitochondrial respiratory dysfunction in myoblasts are not prevented by mitochondria-targeted antioxidants, *Cell. Physiol. Biochem.*, 33, 5, 1439-1451, S. Karger AG, Basel, Germany.
- Patsch, J.M., Kiefer, F.W., Varga, P., Pail, P., Rauner, M., Stupphann, D., Resch, H., Moser, D., Zysset, P.K., Stulnig, T.M. and Pietschmann, P. (2011) 'Increased bone resorption and impaired bone microarchitecture in short-term and extended high-fat diet-induced obesity', *Metabolism: clinical and experimental*, 60(2), pp. 243-249.
- Pearson, G., Robinson, F., Beers Gibson, T., Xu, B., Karandikar, M., Berman, K. and Cobb, M.H. (2001) 'Mitogen-activated protein (MAP) kinase pathways: regulation and physiological functions', *Endocrine reviews*, 22(2), pp. 153-183.
- Peterson, B.R. (2005) 'Synthetic mimics of mammalian cell surface receptors: prosthetic molecules that augment living cells', *Organic & biomolecular chemistry*, 3(20), pp. 3607-3612.
- Pfluger, P.T., Herranz, D., Velasco-Miguel, S., Serrano, M. and Tschop, M.H. (2008) 'Sirt1 protects against high-fat diet-induced metabolic damage', *Proceedings of the National Academy of Sciences of the United States of America*, 105(28), pp. 9793-9798.
- Phieler, J., Chung, K.J., Chatzigeorgiou, A., Klotzsche-von Ameln, A., Garcia-Martin, R., Sprott, D., Moisdou, M., Tzanavari, T., Ludwig, B., Baraban, E., Ehrhart-Bornstein, M., Bornstein, S.R., Mziaut, H., Solimena, M., Karalis, K.P., Economopoulou, M., Lambris, J.D. and Chavakis, T. (2013) 'The complement anaphylatoxin C5a receptor contributes to obese adipose tissue inflammation and insulin resistance', *Journal of immunology (Baltimore, Md.: 1950)*, 191(8), pp. 4367-4374.
- Pietrzak, W.S. (2008) 'Bioabsorbable polymer applications in musculoskeletal fixation and healing', in Anonymous *Musculoskeletal Tissue Regeneration*. Springer, pp. 509-529.
- Pirih, F., Lu, J., Ye, F., Bezouglaia, O., Atti, E., Ascenzi, M., Tetradis, S., Demer, L., Aghaloo, T. and Tintut, Y. (2012) 'Adverse effects of hyperlipidemia on bone regeneration and strength', *Journal of Bone and Mineral Research*, 27(2), pp. 309-318.

- Pittenger, M.F., Mackay, A.M., Beck, S.C., Jaiswal, R.K., Douglas, R., Mosca, J.D., Moorman, M.A., Simonetti, D.W., Craig, S. and Marshak, D.R. (1999) 'Multilineage potential of adult human mesenchymal stem cells', *Science (New York, N.Y.)*, 284(5411), pp. 143-147.
- Pobanz, J.M., Reinhardt, R.A., Koka, S. and Sanderson, S.D. (2000) 'C5a modulation of interleukin-1 $\beta$ -induced interleukin-6 production by human osteoblast-like cells', *Journal of periodontal research*, 35(3), pp. 137-145.
- Pope, M.R., Hoffman, S.M., Tomlinson, S. and Fleming, S.D. (2010) 'Complement regulates TLR4-mediated inflammatory responses during intestinal ischemia reperfusion', *Molecular immunology*, 48(1), pp. 356-364.
- Raggatt, L.J. and Partridge, N.C. (2010) 'Cellular and molecular mechanisms of bone remodeling', *The Journal of biological chemistry*, 285(33), pp. 25103-25108.
- Renaud, H.J., Cui, J.Y., Lu, H. and Klaassen, C.D. (2014) 'Effect of Diet on Expression of Genes Involved in Lipid Metabolism, Oxidative Stress, and Inflammation in Mouse Liver—Insights into Mechanisms of Hepatic Steatosis', *PloS one*, 9(2), pp. e88584.
- Rodan, G.A. and Jack, M.T. (1981) 'Role of Osteoblasts in Hormonal Control of Bone Resorption-- A Hypothesis', *Calcified Tissue International*, 33, pp. 349-351.
- Rousseau, S., Dolado, I., Beardmore, V., Shpiro, N., Marquez, R., Nebreda, A.R., Arthur, J.S.C., Case, L.M., Tessier-Lavigne, M. and Gaestel, M. (2006) 'CXCL12 and C5a trigger cell migration via a PAK1/2-p38 $\alpha$  MAPK-MAPKAP-K2-HSP27 pathway', *Cellular signalling*, 18(11), pp. 1897-1905.
- Rubin, C., Turner, A.S., Müller, R., Mitra, E., McLeod, K., Lin, W. and Qin, Y. (2002) 'Quantity and quality of Trabecular bone in the femur are enhanced by a strongly anabolic, noninvasive mechanical intervention', *Journal of bone and mineral research*, 17(2), pp. 349-357.
- Rubin, R., Strayer, D.S. and Rubin, E. (2008) *Rubin's pathology: clinicopathologic foundations of medicine*. Lippincott Williams & Wilkins.
- Sage, A.P., Lu, J., Atti, E., Tetradis, S., Ascenzi, M., Adams, D.J., Demer, L.L. and Tintut, Y. (2011) 'Hyperlipidemia induces resistance to PTH bone anabolism in mice via oxidized lipids', *Journal of Bone and Mineral Research*, 26(6), pp. 1197-1206.
- Sahu, A. and Lambris, J.D. (2001) 'Structure and biology of complement protein C3, a connecting link between innate and acquired immunity', *Immunological reviews*, 180(1), pp. 35-48.
- Sakiyama, H., Inaba, N., Toyoguchi, T., Okada, Y., Matsumoto, M., Moriya, H. and Ohtsu, H. (1994) 'Immunologicalization of complement C1s and matrix metalloproteinase 9 (92kDa gelatinase/type IV collagenase) in the primary

- ossification center of the human femur', *Cell and tissue research*, 277(2), pp. 239-245.
- Sakiyama, H., Nakagawa, K., Kuriwa, K., Imai, K., Okada, Y., Tsuchida, T., Moriya, H. and Imajoh-Ohmi, S. (1997) 'Complement C1s, a classical enzyme with novel functions at the endochondral ossification center: immunohistochemical staining of activated C1s with a neoantigen-specific antibody', *Cell and tissue research*, 288(3), pp. 557-565.
- Salehpour, A., Hosseiniapanah, F., Shidfar, F., Vafa, M., Razaghi, M., Dehghani, S., Hoshiarrad, A. and Gohari, M. (2012) 'A 12-week double-blind randomized clinical trial of vitamin D 3 supplementation on body fat mass in healthy overweight and obese women', *Nutrition journal*, 11(1), pp. 78.
- Salem, G.J., Zernicke, R.F. and Barnard, R.J. (1992) 'Diet-related changes in mechanical properties of rat vertebrae', *The American Journal of Physiology*, 262(2 Pt 2), pp. R318-21.
- Sato, T., Abe, E., Jin, C.H., Hong, M., Katagiri, T., Kinoshita, T., Amizuka, N., Ozawa, H. and Suda, T. (1993) 'The biological roles of the third component of complement in osteoclast formation', *Endocrinology*, 133(1), pp. 397-404.
- Sato, T., Hong, M.H., Jin, C.H., Ishimi, Y., Udagawa, N., Shinki, T., Abe, E. and Suda, T. (1991) 'The specific production of the third component of complement by osteoblastic cells treated with 1 $\alpha$ , 25-dihydroxyvitamin D3', *FEBS letters*, 285(1), pp. 21-24.
- Schmidt-Nielsen, K. (1984) *Scaling: why is animal size so important?* Cambridge University Press.
- Schoengraf, P., Lambris, J.D., Recknagel, S., Kreja, L., Liedert, A., Brenner, R.E., Huber-Lang, M. and Ignatius, A. (2013) 'Does complement play a role in bone development and regeneration?', *Immunobiology*, 218(1), pp. 1-9.
- Schraufstatter, I.U., Discipio, R.G., Zhao, M. and Khaldoyanidi, S.K. (2009) 'C3a and C5a are chemotactic factors for human mesenchymal stem cells, which cause prolonged ERK1/2 phosphorylation', *Journal of immunology (Baltimore, Md.: 1950)*, 182(6), pp. 3827-3836.
- Schwaeble, W.J. and Reid, K.B. (1999) 'Does properdin crosslink the cellular and the humoral immune response?', *Immunology today*, 20(1), pp. 17-21.
- Sergeev, I.N. and Song, Q. (2014) 'High vitamin D and calcium intakes reduce diet-induced obesity in mice by increasing adipose tissue apoptosis', *Molecular nutrition & food research*, 58(6), pp. 1342-1348.
- Serra, A.J., Santos, M.H., Bocalini, D.S., Antônio, E.L., Levy, R.F., Santos, A.A., Higuchi, M.L., Silva Jr, J.A., Magalhães, F.C. and Baraúna, V.G. (2010) 'Exercise training inhibits inflammatory cytokines and more than prevents myocardial

- dysfunction in rats with sustained  $\beta$ -adrenergic hyperactivity', *The Journal of physiology*, 588(13), pp. 2431-2442.
- Shu, L., Beier, E., Sheu, T., Zhang, H., Zuscik, M.J., Puzas, E.J., Boyce, B.F., Mooney, R.A. and Xing, L. (2015) 'High-fat diet causes bone loss in young mice by promoting osteoclastogenesis through alteration of the bone marrow environment', *Calcified tissue international*, 96(4), pp. 313-323.
- Sims, N.A. and Martin, T.J. (2014) 'Coupling the activities of bone formation and resorption: a multitude of signals within the basic multicellular unit', *BoneKEY reports*, 3.
- Smith, E.E., Ferguson, V.L., Simske, S.J., Gayles, E.C. and Pagliassotti, M.J. (2000) 'Effects of high fat or high sucrose diets on rat femora mechanical and compositional properties', *Biomedical sciences instrumentation*, 36, pp. 385-390.
- Smith, J.K., Chi, D.S., Krish, G., Reynolds, S. and Cambron, G. (1990) 'Effect of exercise on complement activity', *Annals of Allergy*, 65(4), pp. 304-310.
- Standring, S. and Wigley, C. (2005) 'Functional anatomy of the musculoskeletal system', *Gray's Anatomy The Anatomical Basis of Clinical Practice.39th ed.Elsevier Churchill Livingstone*, , pp. 83-136.
- Steele, D.G. and Bramblett, C.A. (1988) *The anatomy and biology of the human skeleton*. Texas A&M University Press.
- Strunk, R.C., Cole, F.S., Perlmutter, D.H. and Colten, H.R. (1985) 'gamma-Interferon increases expression of class III complement genes C2 and factor B in human monocytes and in murine fibroblasts transfected with human C2 and factor B genes', *The Journal of biological chemistry*, 260(28), pp. 15280-15285.
- Suzuki, N., Yoshimura, Y., Deyama, Y., Suzuki, K. and Kitagawa, Y. (2008) 'Mechanical stress directly suppresses osteoclast differentiation in RAW264.7 cells', *International journal of molecular medicine*, 21(3), pp. 291-296.
- Takayanagi, H. (2009) 'Osteoimmunology and the effects of the immune system on bone', *Nature Reviews Rheumatology*, 5(12), pp. 667.
- Tanaka, T., Oyama, T., Sugie, S. and Shimizu, M. (2016) 'Different Susceptibilities between Apoe- and Ldlr-Deficient Mice to Inflammation-Associated Colorectal Carcinogenesis', *International Journal of Molecular Sciences*, 17(11), pp. 1806.
- Tang, L., Lin, Z. and Li, Y.M. (2006) 'Effects of different magnitudes of mechanical strain on Osteoblasts in vitro', *Biochemical and biophysical research communications*, 344(1), pp. 122-128.
- Teitelbaum, S.L. (2000) 'Bone resorption by osteoclasts', *Science (New York, N.Y.)*, 289(5484), pp. 1504-1508.

- Tevlin, R., McArdle, A., Chan, C.K., Pluvinae, J., Walmsley, G.G., Wearda, T., Marecic, O., Hu, M.S., Paik, K.J. and Senarath-Yapa, K. (2014) 'Osteoclast derivation from mouse bone marrow', *JoVE (Journal of Visualized Experiments)*, (93), pp. e52056-e52056.
- Tintut, Y., Morony, S. and Demer, L.L. (2004) 'Hyperlipidemia promotes osteoclastic potential of bone marrow cells ex vivo', *Arteriosclerosis, Thrombosis, and Vascular Biology*, 24(2), pp. e6-10.
- Toyoguchi, T., Yamaguchi, K., Nakagawa, K., Fukusawa, T., Moriya, H. and Sakiyama, H. (1996) 'Change of complement C1s synthesis during development of hamster cartilage', *Cell and tissue research*, 285(2), pp. 199-204.
- Tsukamoto, H., Ueda, A., Nagasawa, K., Tada, Y. and Niho, Y. (1990) 'Increased production of the third component of complement (C3) by monocytes from patients with systemic lupus erythematosus', *Clinical & Experimental Immunology*, 82(2), pp. 257-261.
- Tu, Z., Bu, H., Dennis, J.E. and Lin, F. (2010) 'Efficient osteoclast differentiation requires local complement activation', *Blood*, 116(22), pp. 4456-4463.
- Udagawa, N., Takahashi, N., Akatsu, T., Tanaka, H., Sasaki, T., Nishihara, T., Koga, T., Martin, T.J. and Suda, T. (1990) 'Origin of osteoclasts: mature monocytes and macrophages are capable of differentiating into osteoclasts under a suitable microenvironment prepared by bone marrow-derived stromal cells', *Proceedings of the National Academy of Sciences of the United States of America*, 87(18), pp. 7260-7264.
- Väänänen, H.K. and Härkönen, P.L. (1996) 'Estrogen and bone metabolism', *Maturitas*, 23, pp. S65-S69.
- Vaananen, H.K., Zhao, H., Mulari, M. and Halleen, J.M. (2000) 'The cell biology of osteoclast function', *Journal of cell science*, 113 ( Pt 3)(Pt 3), pp. 377-381.
- Van Der Heijden, Roel A, Bijzet, J., Meijers, W.C., Yakala, G.K., Kleemann, R., Nguyen, T.Q., De Boer, R.A., Schalkwijk, C.G., Hazenberg, B.P. and Tietge, U.J. (2015) 'Obesity-induced chronic inflammation in high fat diet challenged C57BL/6J mice is associated with acceleration of age-dependent renal amyloidosis', *Scientific reports*, 5, pp. 16474.
- van Driel, M., Koedam, M., Buurman, C., Roelse, M., Weyts, F., Chiba, H., Uitterlinden, A., Pols, H. and Van Leeuwen, J. (2006) 'Evidence that both 1 $\alpha$ , 25-dihydroxyvitamin D3 and 24-hydroxylated D3 enhance human osteoblast differentiation and mineralization', *Journal of cellular biochemistry*, 99(3), pp. 922-935.
- Verdeguer, F., Castro, C., Kubicek, M., Pla, D., Vila-Caballer, M., Vinué, Á, Civeira, F., Pocoví, M., Calvete, J.J. and Andrés, V. (2007) 'Complement regulation in murine and human hypercholesterolemia and role in the control of macrophage and smooth muscle cell proliferation', *Cardiovascular research*, 76(2), pp. 340-350.

- Wada, T., Nakashima, T., Hiroshi, N. and Penninger, J.M. (2006) 'RANKL–RANK signaling in osteoclastogenesis and bone disease', *Trends in molecular medicine*, 12(1), pp. 17-25.
- Wang, L., Chai, Y., Li, C., Liu, H., Su, W., Liu, X., Yu, B., Lei, W., Yu, B. and Crane, J.L. (2018) 'Oxidized phospholipids are ligands for LRP6', *Bone research*, 6(1), pp. 22.
- Wang, D., Gilbert, J.R., Taylor, G.M., Sodhi, C.P., Hackam, D.J., Losee, J.E., Billiar, T.R. and Cooper, G.M. (2017) 'TLR4 Inactivation in Myeloid Cells Accelerates Bone Healing of a Calvarial Defect Model in Mice', *Plastic and Reconstructive Surgery*, 140(2), pp. 296e-306e.
- Wang, Q., He, Y., Shen, Y., Zhang, Q., Chen, D., Zuo, C., Qin, J., Wang, H., Wang, J. and Yu, Y. (2014) 'Vitamin D inhibits COX-2 expression and inflammatory response by targeting thioesterase superfamily member 4', *The Journal of biological chemistry*, 289(17), pp. 11681-11694.
- Ward, W.E., Kim, S. and Bruce, W.R. (2003) 'A western-style diet reduces bone mass and biomechanical bone strength to a greater extent in male compared with female rats during development', *British Journal of Nutrition*, 90(3), pp. 589-595.
- Watkins, B.A., Li, Y., Lippman, H.E. and Feng, S. (2003) 'Modulatory effect of omega-3 polyunsaturated fatty acid on osteoblast function and bone metabolism', *Prostaglandins, leukotrienes and essential fatty acid*, 68(6), pp. 387-398.
- White, R.T., Damm, D., Hancock, N., Rosen, B.S., Lowell, B.B., Usher, P., Flier, J.S. and Spiegelman, B.M. (1992) 'Human adiponin is identical to complement factor D and is expressed at high levels in adipose tissue', *The Journal of biological chemistry*, 267(13), pp. 9210-9213.
- Williamson, L., Hayes, A., Hanson, E.D., Pivonka, P., Sims, N.A. and Gooi, J.H. (2017) 'High dose dietary vitamin D3 increases bone mass and strength in mice', *Bone reports*, 6, pp. 44-50.
- Winzenberg, T., Powell, S., Shaw, K.A. and Jones, G. (2011) 'Effects of vitamin D supplementation on bone density in healthy children: systematic review and meta-analysis', *BMJ (Clinical research ed.)*, 342, pp. c7254.
- Wong, S.K., Chin, K., Suhaimi, F.H., Ahmad, F. and Ima-Nirwana, S. (2016) 'The relationship between metabolic syndrome and osteoporosis: a review', *Nutrients*, 8(6), pp. 347.
- Wuelling, M. and Vortkamp, A. (2010) 'Transcriptional networks controlling chondrocyte proliferation and differentiation during endochondral ossification', *Pediatric nephrology*, 25(4), pp. 625-631.
- Yamaguchi, K., Sakiyama, H., Matsumoto, M., Moriya, H. and Sakiyama, S. (1990) 'Degradation of type I and II collagen by human C1s', *FEBS letters*, 268(1), pp. 206-208.

- Yasuda, H., Shima, N., Nakagawa, N., Yamaguchi, K., Kinosaki, M., Mochizuki, S., Tomoyasu, A., Yano, K., Goto, M., Murakami, A., Tsuda, E., Morinaga, T., Higashio, K., Udagawa, N., Takahashi, N. and Suda, T. (1998) 'Osteoclast differentiation factor is a ligand for osteoprotegerin/osteoclastogenesis-inhibitory factor and is identical to TRANCE/RANKL', *Proceedings of the National Academy of Sciences of the United States of America*, 95(7), pp. 3597-3602.
- Yin, K. and Agrawal, D.K. (2014) 'Vitamin D and inflammatory diseases', *Journal of inflammation research*, 7, pp. 69-87.
- Yoshizawa, T., Handa, Y., Uematsu, Y., Takeda, S., Sekine, K., Yoshihara, Y., Kawakami, T., Arioka, K., Sato, H., Uchiyama, Y., Masushige, S., Fukamizu, A., Matsumoto, T. and Kato, S. (1997) 'Mice lacking the vitamin D receptor exhibit impaired bone formation, uterine hypoplasia and growth retardation after weaning', *Nature genetics*, 16(4), pp. 391-396.
- Young, B. (2006) 'Wheater's functional histology: a text and colour atlas., 5th edn. Churchill Livingstone Elsevier', .
- Yu, H., Kim, J., Kim, H., Lewis, M.P. and Wall, I. (2016) 'Impact of mechanical stretch on the cell behaviors of bone and surrounding tissues', *Journal of tissue engineering*, 7, pp. 2041731415618342.
- Yuan, R., Tsaih, S., Petkova, S.B., De Evsikova, C.M., Xing, S., Marion, M.A., Bogue, M.A., Mills, K.D., Peters, L.L. and Bult, C.J. (2009) 'Aging in inbred strains of mice: study design and interim report on median lifespans and circulating IGF1 levels', *Aging cell*, 8(3), pp. 277-287.
- Zernicke, R., Salem, G., Barnard, R. and Schramm, E. (1995) 'Long-term, high-fat-sucrose diet alters rat femoral neck and vertebral morphology, bone mineral content, and mechanical properties', *Bone*, 16(1), pp. 25-31.
- Zhang, L., Chen, X., Wu, J., Yuan, Y., Guo, J., Biswas, S., Li, B. and Zou, J. (2017) 'The effects of different intensities of exercise and active vitamin D on mouse bone mass and bone strength', *Journal of bone and mineral metabolism*, 35(3), pp. 265-277.
- Zhang, N., Zhang, Y., Lin, J., Qiu, X., Chen, L., Pan, X., Lu, Y., Zhang, J., Wang, Y. and Li, D. (2017) 'Low-density lipoprotein receptor deficiency impaired mice osteoblastogenesis in vitro', *Bioscience trends*, 11(6), pp. 658-666.